

4-20-2018

Development of Rules of Attraction for Intercalated Guest Molecules Inside of a Hydrogen Bonded Framework

Matthew Fischer
fischermatt80@yahoo.com

Follow this and additional works at: <https://irl.umsl.edu/dissertation>

 Part of the [Analytical Chemistry Commons](#), [Inorganic Chemistry Commons](#), and the [Materials Chemistry Commons](#)

Recommended Citation

Fischer, Matthew, "Development of Rules of Attraction for Intercalated Guest Molecules Inside of a Hydrogen Bonded Framework" (2018). *Dissertations*. 731.
<https://irl.umsl.edu/dissertation/731>

This Dissertation is brought to you for free and open access by the UMSL Graduate Works at IRL @ UMSL. It has been accepted for inclusion in Dissertations by an authorized administrator of IRL @ UMSL. For more information, please contact marvinh@umsl.edu.

Development of Rules of Attraction for Intercalated Guest Molecules Inside of a
Hydrogen Bonded Framework.

By

Matthew Joseph Fischer, Sr

M.Sc., Chemistry, Saint Louis University, 2006

B.A. Chemistry, Saint Louis University, 2003

A DISSERTATION

Submitted to The Graduate School at the

UNIVERSITY OF MISSOURI – ST. LOUIS

In Partial Fulfillment of the Requirements for the Degree

DOCTOR OF PHILOSOPHY

in

CHEMISTRY

with an emphasis in Inorganic Chemistry

May 2018

Advisory Committee

Alicia M. Beatty, Ph.D.
Chairperson

George Gokel, Ph.D.

Stephen Holmes, PhD

James Chickos, PhD

Abstract

Development of Rules of Attraction for Intercalated Guest Molecules Inside of a
Hydrogen Bonded Framework.

(May 2018)

Matthew Joseph Fischer, Sr

M.Sc., Chemistry, Saint Louis University, 2006

B.A. Chemistry, Saint Louis University, 2003

Chair of Committee: Dr. Alicia M. Beatty

Supramolecular chemistry has synthesized large and small molecules which host guest molecules for several decades. What started as a way to mimic of enzymes in nature, has exploded into a sea of materials such as porous coordination polymers, low-density metal-organic frameworks, inclusion compounds, and hydrogen bonded frameworks. We previously designed a layered framework consisting of a metal complex with coordinate covalent ligands. These ligands have peripheral carboxylic acid groups which hydrogen bond to organic pillars containing terminal amines. The layered structure is separated by these pillars, which are closed-packed, creating 1-dimensional channels able to co-crystallize molecules. There is interest in selectively binding molecules for separation, catalysis, molecular recognition or transport. How do guests selectively co-crystallize into the framework? Do properties of guest molecules such as size, shape or electronics dictate preference? By establishing a set of selectivity rules, potential applications appear.

In our pursuit, we devised a new way of coupling a thermogravimetric analyzer to a mass spectrometer using solid-phase microextraction fibers. These two instruments can be used together for a fraction existing coupling cost.

By testing guests of different size and shape, we found large guest molecules will co-crystallize over smaller ones. If a guest is too large, the selectivity can become concentration dependent. Maintaining the size difference between two molecules, we changed to geometric isomers. The framework lost selectivity due to poor guest co-crystallization and low guest inclusion rates.

Next, we tested guest molecules whose size and shape was similar but had different electronics. Aromatic guests with electron donating substituents were preferred over those with electron withdrawing groups. The framework could detect subtle changes in the electronic structure, *e.g.*, substituting chloro- for a methyl. Guests containing anchor points, σ -hole, were showed preference. Selectivity correlated to physical properties such as boiling point and density of the guests containing electron withdrawing substituents.

Finally, we focused on single co-crystallized guests tested by thermogravimetric analysis, gas chromatography, and powder x-ray diffraction. The preferred guests in the previous study contained electron donating groups and high occupancy. Outliers such as iodobenzene were preferred in competition but had low concentrations as a single guest.

Dedication

This dissertation is dedicated to family, especially my beautiful wife, Jenny.

Without her patience and love, I would not be the man I am today. I thank her for just being her because that is all I have ever wanted. She has always believed in me, and I thank her. To my beautiful children; Isabelle, Matthew Jr., Joseph, Marielle, and Ivette, I thank you as well. For all those late nights and kind words. My children will always be my greatest achievement. To my parents, Robert and Sharon Fischer, I thank you for all the love and support you have given me. For all the times you pushed me forward, thank you. To my mother and father-in-law, Kenneth and Sandy Suetterlin, thank you for all the support and guidance throughout the years. To all my siblings, thank you for all the years of encouragement and support. Most of all, I thank God for all His gifts, they are indeed cherished.

Acknowledgments

I would like to thank my advisor, Dr. Alicia M. Beatty. She provided me an opportunity, and I have never looked back. Dr. Beatty has been an amazing mentor who has guided me and pushed me to be the best chemist that I can be. Her constant encouragement and patience have helped me go beyond the person I was and challenged me to be even more than I thought possible. I would like to thank her for her strength and friendship. I owe her so much and hope to continue her passion and curiosity for science.

I would like to thank the members of my dissertation committee, Dr. George Gokel, Dr. Stephen Holmes, and Dr. James Chickos. Each member has offered great insights during the journey to my Ph.D. Dr. Gokel was an excellent instructor during my time in class with him, and I thank him for that. I also thank him for his words of encouragement. I would like to thank Dr. Holmes for working with me through the years. I would not have been able to do this without his support. I would also like to thank Dr. Chickos for his advice when I came to see him. I do not know if he knows how much our short conversation helped.

For all his time and efforts, I would especially like to thank Joseph Kramer. Joe and I spent some long hours next to the GCMS, especially when it was not running. Joe was one of the first people I met at the university. He did not know me but immediately helped me as if we had known each other for years. I thank him for his guidance and constant can do spirit.

A special thanks to Dr. Nigam Rath. Dr. Rath has been helping me with crystallography since 2006 when I attended St. Louis University and Novus International. Dr. Rath has always been there throughout my journey. I thank him for his support.

A special thanks to my employer, Novus International. My friends and colleagues at Novus have always provided me with such fervent support. Novus offered me the flexibility to work full-time while still pursuing my Ph.D. I would not have been able to this without them.

Lastly, I would like to thank my group members from the Beatty Lab. We took this journey together, and I thank Stephanie and Carl for their support and guidance.

Table of Contents

Abstract	i
Dedication	iii
Acknowledgments.....	iv
Table of Figures	ix
Table of Tables	xiv
Chapter 1.....	1
1.1 Background.....	2
1.2 Porous Solid-State Materials.....	4
1.3 Hydrogen Bonded Materials	7
1.6 Analysis of Host-Guest Materials	15
1.7 Size and Shape Molecular Separation by Host-Guest Materials	18
1.8 Electron Factors for Host-Guest Molecular Separation	21
1.9 Proposed Work.....	23
1.10 References.....	25
Chapter 2.....	41
2.1 Abstract.....	42
2.2 Background.....	42
2.3 Introduction.....	49
2.4 Experimental	49
2.4.2 Chromatographic Methods.....	51
2.4.3 SPME Coupled TGA	51
2.5 Results and Discussion	53
2.6 Conclusions.....	58
2.7 References.....	60
Chapter 3.....	65
3.1 Abstract.....	66
3.2 Introduction.....	66
3.2.1 Guest Molecule Separation Using Host Materials	68
3.2.1.1 The Separation of Gaseous Species Using Host-Guest Materials.....	69
3.2.1.2 Host-Guest Materials Capable of Small Molecule Separation.....	70
3.2.1.3 Large Molecule Host-Guest Separation.....	72
3.2.1.4 The Separation of Guest Molecules Based on Size and Shape	73

3.3 Background Work.....	74
3.4 Current Work.....	76
3.5 Experimental.....	77
3.5.1 Synthesis of 1•guest.....	79
3.6 Results.....	80
3.6.1 Guest Preference: Size.....	81
3.6.2 Guest Preference: Shape.....	87
3.7 Discussion.....	92
3.8 Conclusions.....	97
3.9 References.....	100
Chapter 4.....	109
4.1.1 Abstract.....	110
4.1.2 Background.....	110
4.2.1 Experimental Procedures.....	114
4.2.2 Synthesis of 1•guest.....	115
4.2.3 Chromatographic Methods.....	115
4.3 Results and Discussion.....	116
4.3.1 Calculation of Electrostatic Potential for Guest Molecules.....	116
4.3.2 Electron withdrawing versus donating in para-substituted aromatics.....	122
4.3.3 p-xylene vs. p-chlorotoluene.....	123
4.3.4 Varying Guest Electronics to Probe Sensitivity of Framework Selectivity.....	125
4.3.5 Using the Properties of the Guest Molecules to Understand the Order of Selectivity.....	136
4.4 Conclusions.....	143
4.5 References.....	147
Chapter 5.....	151
5.1 Abstract.....	152
5.2 Background.....	153
5.3.1 Experimental.....	157
5.3.2 Synthesis of 1•guest.....	157
5.3.3 Thermogravimetric Analysis Studies.....	158
5.3.4 Chromatographic Methods.....	159
5.3.6. Powder x-ray diffraction.....	161
5.3.7. Temperature-dependent powder x-ray diffraction.....	161

5.3.8. Approximating Energy of Activation for Guest Loss	161
5.4 Results and Discussion	162
5.5 Thermogravimetric Analysis of Single Guest.....	164
5.6 Guest Quantitation by Gas Chromatography	165
5.7 Comparison of Guest Loss by Gas Chromatography and Thermogravimetric Analysis	167
5.8 Tracking Guest Evolution by Powder X-ray Diffraction.....	171
5.9 Approximation of Activation Energy	174
5.10. Conclusions.....	178
5.5 References.....	182
Chapter 6.....	185
6.1 Final Conclusions.....	186
Appendix I – Powder Pattern Data	192
Appendix II – Thermogravimetric Analysis Data.....	217
Appendix III – Supplemental Figures for Chapter 5.....	263

Table of Figures

Figure 1.1.1 Representations of host molecules from (I) Pedersen, (II) Cram and (III) Lehn ¹⁻³	2
Figure 1.1.2 Examples of organic-based host structures. I) carcerand, II) alpha-cyclodextrin, III) rotaxane, IV) pillarene, V) molecular tweezers, VI) catenane, VII) molecular capsule ⁶	3
Figure 1.1.3. Coordination cluster, M ₄ L ₆ by Raymond <i>et al.</i> 4c.....	4
Figure 1.1.4. Lin <i>et al.</i> chiral organometallic triangle. ⁹	4
Figure 1.2.1 ZSM-5 zeolite is a catalyst used for the industrial isomerization reaction converting meta-xylene to <i>p</i> -xylene ¹⁵	4
Figure 1.2.2 Structural change through photodimerization of a porous coordination polymer can influence the gas sorption isotherms ²⁶	6
Figure 1.2.3 MOF-5, Zn ₄ (O)(BDC) ₃ , framework, where the yellow sphere is indicative of the large internal cavity space which has a diameter of 18.5Å. ³⁰	6
Figure 1.3.1 Ring motif which uses the 1 st rule of hydrogen bonding. “All good proton donors and acceptors are used in hydrogen bonding.” ³⁵	7
Figure 1.3.2 Examples of homomeric and heteromeric hydrogen bonding ^{32c}	8
Figure 1.3.3 Hydrogen bonded dimer of benzoic acid, 0-D ³⁸	9
Figure 1.3.4 1-D terephthalic acid chain formed in the solid state ³⁹	10
Figure 1.3.5 1-D isophthalic acid zig-zag motif. ⁴⁰	10
Figure 1.3.6 Trimesic acid 2-D honeycomb structure. ⁴¹	11
Figure 1.3.7 Zaworotko’s trimesic acid and 4,4’-bipyridine expanded honeycomb design. ⁴¹	11
Figure 1.4.1 Depiction of the guanidinium-sulfonate layer. 1) Layer from above. 2) Representation of the bilayer and single layered structures ^{32a}	12
Figure 1.4.2 Hydrogen-bonded layered brick structure where pillars, with terminal sulfonates, separate the guanidinium layers ⁴³	13
Figure 1.5.1 Strong donor/acceptor groups such as 1) -COOH, 2) -COHNR amido and 3) -OH ⁴⁵	14

Figure 1.5.2 Representation of typical pillared-layer framework structures formed of the anionic metal complex [Co(en)(ox) ₂] ⁻ and the cationic bipyridinium pillars (H ₂ bpy) ²⁺ and (H ₂ bppe) ²⁺ . ⁴⁸	15
Figure 1.7.1 Using the minimum dimensions of benzene to determine whether it will fit into a pore. ⁷⁶	19
Figure 1.7.2 Effect of size and shape of xylene isomers and mesitylene molecules on their entry and diffusion through H-ZSM-5. ⁷⁸	20
Figure 1.7.3 Representation of the organic building block (tecton) used to make (a) which can separate C ₂ H ₂ and C ₂ H ₄ . Yellow spheres mark the permanent pores ^{42p}	21
Figure 1.8.1 Calculated electrostatic potentials for diacetoxy substituted benzo[k]fluoroanthene clip (1a) and guest molecules anthra-9,10-quinone (AQ), 1,8-dinitroanthra-9,10-quinone (1,8-DNAQ), 1,5-dinitroanthra-9,10-quinone (1,5-DNAQ) and 9-dicyanomethylene-2,4,7-trinitrofluorene (TNF). Red areas have higher electron density, and blue areas have low electron density. ⁸⁰	22
Figure 1.8.2 Electrostatic potential maps over the 18-6 crown ether and methylsulfonamide. ⁸¹	23
Figure 1.9.1 Charge-assisted hydrogen-bonded framework from the Beatty lab, 1	23
Figure 2.2.1 Representation of the zinc complex plus dimethylbenzidine which forms the layers and pillars of the framework, 1	43
Figure 2.2.2 Diagram of one-directionality of the channels within the hydrogen bonded framework where the guest molecules reside.....	43
Figure 2.4.3.1 TGA plot of Zn(HPDCA) ₂ *(H ₂ O) ₂ plus o-tolidine framework containing toluene guest from 40°C to 550°C at a heating rate of 10°C/min.....	52
Figure 2.5.1 Plot of toluene guest TGA weight versus peak area.....	54
Figure 3.2.1 Guanidinium sulfonate charge-assisted hydrogen bonded frameworks where terminal sulfonates form pillars separating guanidium layers, Ward <i>et al.</i> ²	67
Figure 3.2.2 Permanently porous material, {[Ni(tame) ₂] ₁ (PES) ₂ } ₃	67
Figure 3.2.1.1 Representation with framework flexibility and selective guest accommodation (left). Strategically designed flexible ligand (right). ¹⁹	71

Figure 3.2.1.2 The MOF, ([In(OH)(OBA)]·DMF, H ₂ OBA = 4,4'-oxybis(benzoic acid), JUC-77. Vapor adsorption and desorption with benzene (red circles, adsorption, red open circles desorption), adsorption of toluene (purple triangles), adsorption of <i>p</i> -xylene (blue rhombus), adsorption of <i>o</i> -xylene (star), and adsorption of <i>m</i> -xylene ⁴⁰	71
Figure 3.2.1.3 Selective binding of guest molecules in cucurbit[n]urils. ²⁷	72
Figure 3.3.1 View of 1 (framework). One-Dimensional channels formed by layers of zinc (II) complex and di-ammonium pillars. The view from the side shows the channels being closed off.....	75
Figure 3.4.1 Summary of guest molecules used in the studies.....	77
Figure 3.5.1. The mole fraction of guest molecules across each competition.....	78
Figure 3.5.2 Selectivity profiles for a two-guest competition study. A) Represents no selectivity between guest A and B. B) Depicts a significant preference for guest A. C) Shows a selectivity which is concentration dependent as selectivity starts with guest B and moves to guest A.....	79
Figure 3.6.1.1 Competition study between benzene versus phenol.....	82
Figure 3.6.1.2 Competition between benzene versus toluene, toluene was shown to be preferred over benzene.....	83
Figure 3.6.1.3 Competition between <i>p</i> -xylene versus fluorobenzene, <i>p</i> -xylene was shown to be preferred over fluorobenzene.....	84
Figure 3.6.1.4 Competition between toluene versus 1,4-di-fluorobenzene, 1 was selective towards toluene.	85
Figure 3.6.1.5 Competition between <i>p</i> -xylene versus 1,4-fluorobenzene, 1 was selective towards <i>p</i> -xylene.....	86
Figure 3.6.1.6 Competition between <i>p</i> -diethylbenzene versus 1,4-difluorobenzene, 1 had a concentration-dependent selectivity towards <i>p</i> -diethylbenzene.....	87
Figure 3.6.2.1 Competition between <i>m</i> -xylene versus fluorobenzene, 1 shows selectivity towards <i>m</i> -xylene.....	88
Figure 3.6.2.2 Competition study of <i>p</i> -xylene versus <i>p</i> -diethylbenzene, 1 was selective to <i>p</i> -xylene.....	89
Figure 3.6.2.3 Competition study of <i>m</i> -xylene versus <i>m</i> -diethylbenzene, 1 is selective towards <i>m</i> -diethylbenzene.....	90

Figure 3.6.2.4 Competition study of <i>o</i> -xylene versus <i>o</i> -diethylbenzene, 1 was selective towards <i>o</i> -diethylbenzene.....	91
Figure 4.1.2.1 B3LYP/6-31G* electrostatic potentials (ESPs) at the ring centers of <i>para</i> -substituted <i>meta</i> -xylenes correlate well with Hammett <i>meta</i> -substituent constants that have previously been used in structure-activity relationships describing aromatic stacking interactions. ¹¹	112
Figure 4.1.2.2 Schematic representation of the effect of substituents on stacking interactions. ¹⁶	113
Figure 4.3.1.1 Electrostatic potential maps of <i>p</i> -dichlorobenzene, <i>p</i> -chlorotoluene, and <i>p</i> -xylene, legend units are in kJ·mol ⁻¹	117
Figure 4.3.1.2 Calculated guest electrostatic potential maps; guests with electron donating substituents were preferred with a few outliers such as iodobenzene and bromobenzene.....	119
Figure 4.3.1.3 Calculated ESP map of the <i>o</i> -tolidine pillar, salted with isonicotinat....	120
Figure 4.3.1.4 Zn (II) coordination complex, forms the layers of 1	121
Figure 4.3.2.1 Competition study of <i>p</i> -xylene versus <i>p</i> -dichlorobenzene, 1 was selective for <i>p</i> -xylene.....	123
Figure 4.3.3.1 Competition study of <i>p</i> -xylene versus <i>p</i> -chlorotoluene, 1 was selective for <i>p</i> -xylene.....	123
Figure 4.3.4.1 Guest competition study with benzene used as the control; all guests were preferred over benzene.....	127
Figure 4.3.4.2 Guest competition study with fluorobenzene used as the control; all guests, except benzene, were preferred over fluorobenzene.....	128
Figure 4.3.4.3 Guest competition study with nitrobenzene used as the control; N,N-DMA, ethylbenzene, benzene, iodobenzene, chlorobenzene, and bromobenzene were preferred over nitrobenzene.....	129
Figure 4.3.4.4 Guest competition study with chlorobenzene used as the control; N,N-DMA, toluene, ethylbenzene, iodobenzene, and bromobenzene were preferred over chlorobenzene.....	130
Figure 4.3.4.5 Guest competition study with toluene used as the control; ethylbenzene, iodobenzene, bromobenzene, and nitrobenzene were preferred over toluene.....	131

Figure 4.3.4.6 Guest competition study with bromobenzene used as the control; iodobenzene was preferred over bromobenzene.....	132
Figure 4.3.4.7. Guest competition study with N,N-DMA used as the control; only toluene, iodobenzene, and bromobenzene were preferred over N,N-DMA.....	133
Figure 4.3.4.8 Guest competition study with ethylbenzene used as the control; N,N-DMA, and bromobenzene were preferred over ethylbenzene.....	134
Figure 4.3.4.9 Guest competition study with iodobenzene used as the control; ethylbenzene was preferred over iodobenzene.....	135
Figure 4.3.5.1 Comparison plot of guest mean peak area versus σ -para value.....	137
Figure 4.3.5.2 Comparison plot of mean peak area vs. guest density (g/cc).....	138
Figure 4.3.5.3 Comparison of mean peak area versus density (g/cc), electron withdrawing only.....	139
Figure 4.3.5.4 Comparison of mean peak area vs. guest volume (\AA^3).....	140
Figure 4.3.5.5 Comparison of mean peak area versus boiling point ($^{\circ}\text{C}$).....	141
Figure 4.3.5.6 Comparison of mean peak area versus functional group σ -hole/tip ESP value.....	142
Figure 5.2.1 Example TGA plot using multiple heating ramp rates to study guest evolution of N,N-dimethylaniline from 1; the α -level is calculated at a point of 3% mass loss.....	153
Figure. 5.3.3.1. TGA plot of each guest containing sample.....	158
Figure. 5.3.3.2. TGA plot of toluene guest within 1•framework.....	159
Figure. 5.7.1 Comparison plot of the guest, toluene evolving from the host framework, the TGA and GC evolution data are overlaid to show a similar profile.....	168
Figure. 5.7.2 Comparison plot of the guest, ethylbenzene, evolving from the host framework, the TGA and GC evolution data are overlaid.....	170
Figure. 5.8.1. Temperature-dependent powder x-ray diffraction, toluene has filled the framework as can be seen at 25°C , by 40°C the framework is beginning to evolve guest molecule.....	172
Figure. 5.9.1. Arrhenius plot used to approximate the activation energy (E_a) required to evolve N,N-dimethylaniline from the framework.....	174

Table of Tables

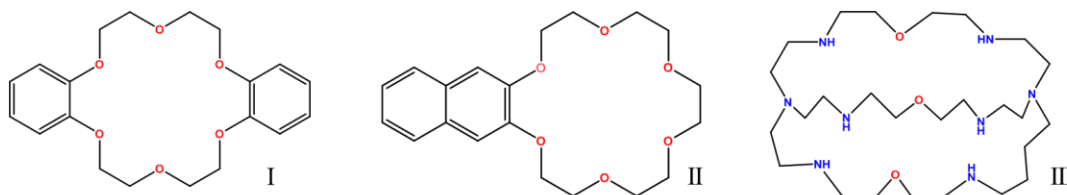
Table 2.5.1 Measured peak areas for 1-toluene detection during step-wise temperature gradient.....	54
Table 2.5.2 Measured data for 1-toluene from the TGA and GCMS using 85 μ m PA SPME fiber.....	56
Table 3.6.1 Reproducibility experiment where 1,4-difluorobenzene (0.9 χ) was in competition with <i>p</i> -diethylbenzene (0.1 χ).....	81
Table 3.7.1 TGA analysis of co-crystallized single guests in 1.....	96
Table 4.3.5.1 Ranked Guest Peak Area Percent Average.....	137
Table 5.5.1 Thermogravimetric analysis of co-crystallized single guests within the host framework.....	165
Table 5.6.1 Comparison of TGA recovery vs. GC recovery results for co-crystallized single guest molecules, in many cases the GC values were lower.....	166
Table 5.7.1 Onset temperatures for guest evolution, the comparison between onset temperature from TGA and first detection temperature in the GC.....	169
Table 5.8.1. Onset temperatures for guest evolution, the comparison between onset temperature from TGA, first detection temperature in the GC, and powder x-ray diffraction.....	173
Table 5.9.1. Onset temperatures for guest evolution, the comparison between onset temperature from TGA, first detection temperature in the GC, onset temperatures from powder x-ray diffraction, and approximated activation energy, E_a , for guest loss.....	176

Chapter 1

Introduction

1.1 Background

Supramolecular chemists have explored a myriad of materials over the course of several decades when it comes to designing molecular architectures which have host-guest properties. In 1967, Charles Pedersen synthesized organic based crown ethers while at the American du Pont de Nemours company.¹ D.J. Cram and Jean-Marie Lehn expanded into a more 3-D approach.² For their work, Pedersen, Cram, and Lehn shared the Nobel Prize in Chemistry in 1987. Cram stated that host structures could be “designed and synthesized which contain enforced cavities large enough to complex and even surround simple in



organic or organic guest compounds” (Figure 1.1.2).³

Figure 1.1.2 Representations of host molecules from (I) Pedersen, (II) Cram and (III) Lehn¹⁻³

The host/guest pairs bind through non-covalent interactions such as hydrogen bonding, Van der Waals forces, and hydrophobic interactions.⁴ Organic materials that can act as hosts,^{5a} such as cucurbiturils,^{5b} macrocycles and polyethers,^{5c} pillarenes,^{5d} molecular tweezers,^{5e} rotaxanes,^{5f} carcerands,^{5g} fullerenes,^{5h} calixarene,⁵ⁱ cyclodextrins,^{5j} cavitands,^{5k} spherands,^{5l} and capsules^{5m} have been carefully made to bind organic molecules, ions or metal ions (Figure 1.1.2).

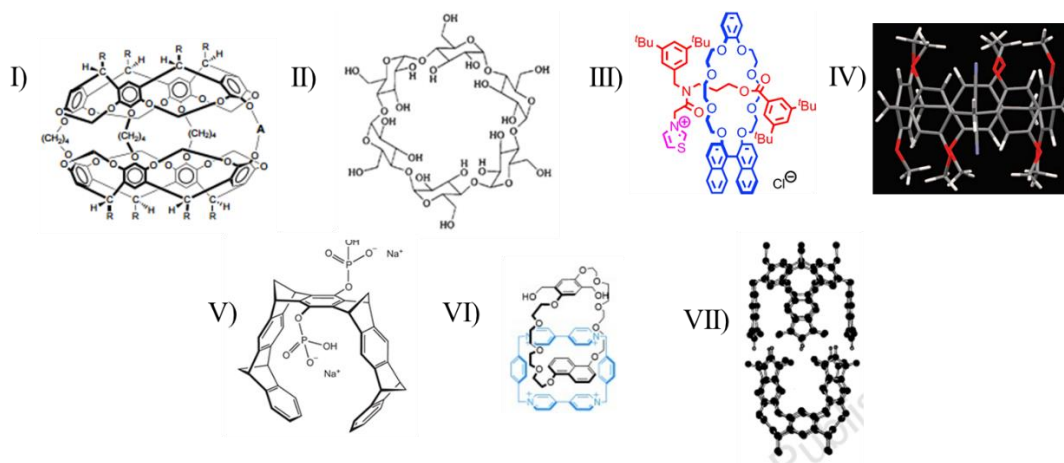


Figure 1.1.2 Examples of organic-based host structures. I) carcerand, II) alpha-cyclodextrin, III) rotaxane, IV) pillarene, V) molecular tweezers, VI) catenane, VII) molecular capsule⁶

Raymond and others have performed numerous studies on high-symmetry coordination clusters which include M_2L_3 helicates and mesocates, M_4L_6 and M_4L_4 tetrahedra, M_6L_6 and M_8L_8 cylinders and M_8L_6 octahedra (Figure 1.1.3).^{7,8}

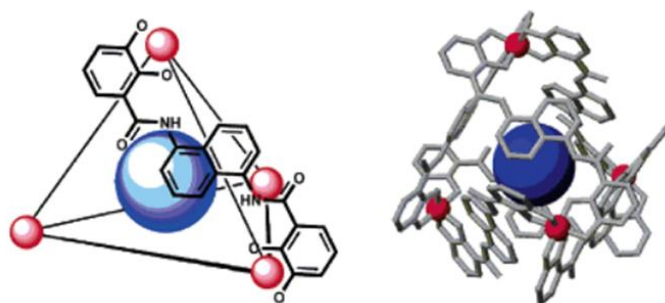


Figure 1.1.3. Coordination cluster, M_4L_6 by Raymond *et al.*^{4c}

These can host both neutral and cationic guest molecules in solution.^{7,8} The featured coordination cluster in Figure 1.1.3 can bind guests in aqueous solution. It is selective towards the size and shape of the guest. Lin *et al.* provided the first example of a chiral organometallic triangle for asymmetric catalysis which had >95% conversion at room

temperature (Figure 1.1.4).⁹ The materials described offer a variety of possibilities, but their host-guest interactions occur in solution.

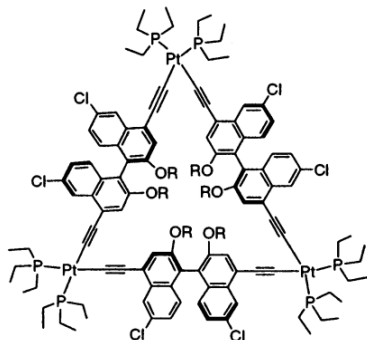


Figure 1.1.4. Lin *et al.* chiral organometallic triangle.⁹

1.2 Porous Solid-State Materials

Solid state materials which have host-guest properties are essential in many industrial applications. A well-known example is zeolites.¹⁰ These porous materials have several different uses such as the separation of n-alkane mixtures,¹¹ adsorption of pollutants from water supplies,¹² and catalysis for ethylation under non-isomerizing conditions¹³, but their pores and channels are of limited size (Figure 1.2.1).¹⁴

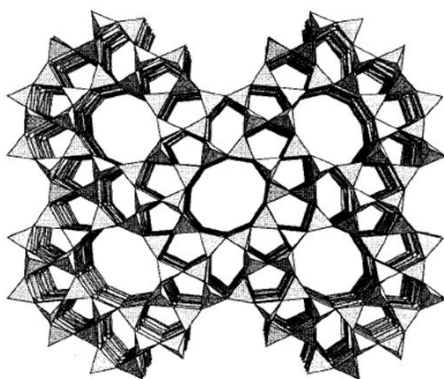


Figure 1.2.1 ZSM-5 zeolite is a catalyst used for the industrial isomerization reaction converting meta-xylene to *p*-xylene¹⁵

The number of natural zeolites includes over 230 framework types; however,¹⁶ synthetic zeolites expanded the variety of zeolites, and their pore structure, which increased their functionality.¹⁷ Close mimics to zeolites are porous coordination polymers.¹⁸ In 1964, J.C. Bailar described porous coordination polymers as “an infinite array of coordination complexes in which metal ions are bridged by multidentate ligands”.¹⁹ A variety of synthetic approaches were adopted to increase the functionality of porous coordination polymers. The strategy has given way to numerous structures and geometries. The previously described structures carry a charge and therefore have counter ions which can reside in the pore and channels. If the pore size is large enough, and under the right conditions, the anion guests can exchange.²⁰

Due to the many synthetic design strategies, functional porous coordination polymers have been made to be selective towards certain gases and capable of separating gas mixtures such as CO₂, N₂, O₂ and CO.^{21, 22, 23} Larger molecules can absorb into porous coordination polymers such as solvents and small aromatic molecules.^{24,25} Kitagawa *et al.* created a coordination polymer which can undergo [2+2] photo-dimerization changing the structure and affecting the gas sorption properties (Figure 1.2.2).^{26,27,28,29}

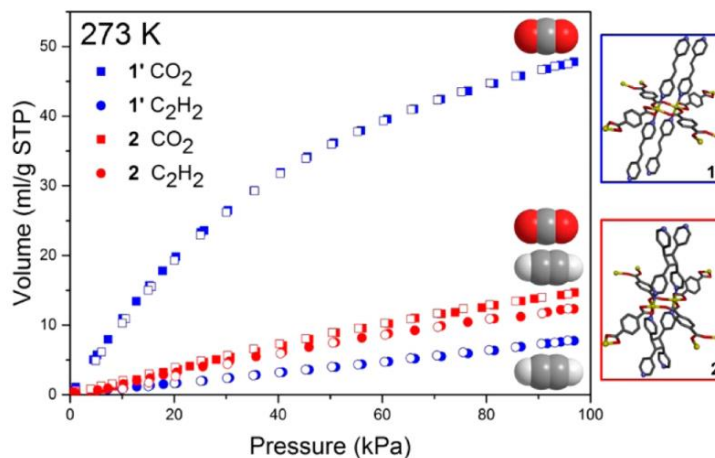


Figure 1.2.2 Structural change through photodimerization of a porous coordination polymer can influence the gas sorption isotherms.²⁶

In 1998, Yaghi *et al.* developed the metal-organic framework (MOF) as the next step from zeolites and was a subset of porous coordination polymers.^{30,19} MOFs made from metal centers connected by dicarboxylate linkers form large pore materials.^{30, 19} These opened a new avenue of porous materials that have a high internal surface area and do not collapse upon guest removal (Figure 1.2.3).

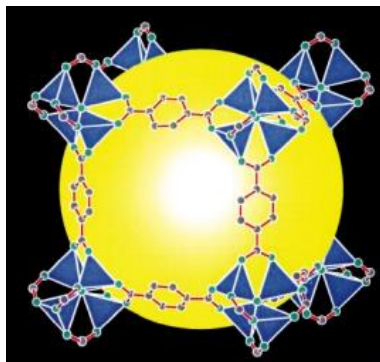


Figure 1.2.3 MOF-5, Zn₄(O)(BDC)₃, framework, where the yellow sphere is indicative of the large internal cavity space which has a diameter of 18.5Å.³⁰

Guest molecules of dimethylformamide and chlorobenzene become trapped during the synthesis of MOF-5. Due to their mobility, these guests exchange with chloroform. The guests can be removed entirely without the collapse of MOF-5. MOFs typically lack small molecule selectivity. The pores usually are too large for guest selectivity. Compared to porous zeolites, there are several thousand metal-organic framework structures already discovered.³¹ However, what about other methods for creating functional host-guest materials which did not rely solely on covalent bonds to hold them together or to “enforce cavities”?

1.3 Hydrogen Bonded Materials

Hydrogen bonds are best known for holding DNA in its famous double-helix.³³ Chemists have looked at how the hydrogen bond can play a significant role in designing larger structured materials.³² Etter further described hydrogen-bonding patterns for organic compounds stating that the “consequences of directed and selective hydrogen-bond interactions on a set of molecules” “are to a solid state-chemist what a new synthesis is to a solution chemist, *i.e.*, the formation of a new chemical species.”³⁴ She went onto to describe eight rules for hydrogen-bonding in an organic structure.³⁵ Crystal packing patterns demonstrate these rules (Figure 1.3.1).³⁵

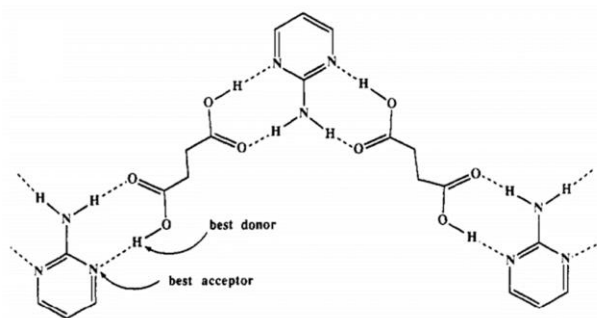


Figure 1.3.1 Ring motif which uses the 1st rule of hydrogen bonding. “All good proton donors and acceptors are used in hydrogen bonding.”³⁵

As can be seen in Figure 1.3.1, self-assembly occurs through the combination of the best donor and the best acceptor. The first three, termed ‘General Rules’ by Etter, are as follows:

- 1) All good proton donors and acceptors are used in hydrogen bonding³⁵
- 2) Six-membered-ring intramolecular hydrogen bonds form in preference to intermolecular hydrogen bonds³⁵
- 3) The best proton donors and acceptors remaining after intramolecular hydrogen-bond formation form intermolecular hydrogen bonds to one another³⁵

These patterns are seen through-out self-assembled hydrogen bonded materials and are useful in numerous pathways to crafting new materials.³⁶ Examples of these synthons can be seen in Figure 1.3.2.^{32c, 32d}

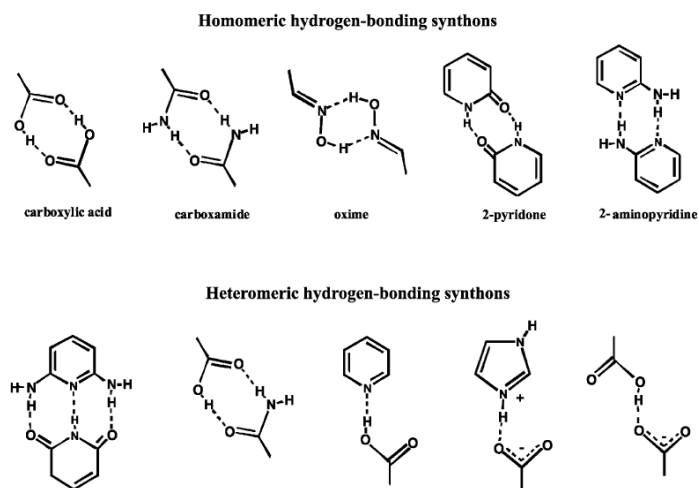


Figure 1.3.2 Examples of homomeric and heteromeric hydrogen bonding synthons ^{32c}

Homomeric synthons are those which hydrogen bond to the same functional group synthon, *e.g.*, carboxylic acid to carboxylic acid. Heteromeric synthons are those which hydrogen bond between two different synthons such as pyridine and a carboxylic acid group. Hydrogen-bonded synthons are part of molecular tectons. “Molecular tectons are molecules whose interactions are dominated by specific attractive forces that induce the assembly of aggregates with control geometries”.^{36d,37} Combining the idea of synthons with molecular tectons, Wuest generated porous hydrogen-bonded networks where the robustness of the material increased.³⁷

Based on the rules set forth by Etter for hydrogen bonding, hydrogen bonded assemblies, motifs, and structures begin to arise with dimensionality. The beginning starts at zero or the 0-D structure. A 0-D structure would be a dimer where the two homomeric or heteromeric synthons align. An example of this would be a dimer of benzoic acid where the carboxylic acid groups are hydrogen bonded to each other (Figure 1.3.3).³⁸

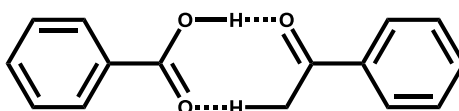


Figure 1.3.3 Hydrogen bonded dimer of benzoic acid, 0-D³⁸

A 1-D hydrogen bonded motifs form when synthons capable of hydrogen bonding are on opposing sides of a molecular tectons. An example would be a 1-D hydrogen bonded chain of terephthalic acid. The two carboxylic acid groups are 180° from each other on the aromatic ring. In the solid state, the carboxylic acid groups align just like the benzoic dimer in Figure 1.1.12 but form a long chain (Figure 1.3.4).³⁹

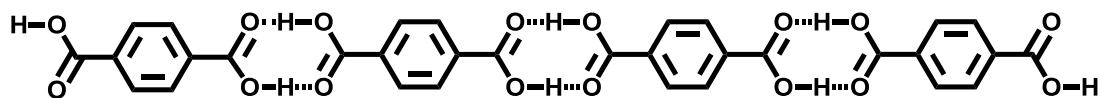


Figure 1.3.4 1-D terephthalic acid chain formed in the solid state.³⁹

The 1-D structure will adjust to a zig-zag pattern, by placing the carboxylic acid groups at the 1 and 3-position around the aromatic ring making a 120° angle. The molecular tecton, isophthalic acid, creates a repeating 1-D zig-zag pattern discovered by Deriseen *et al.*

(Figure 1.3.5).⁴⁰

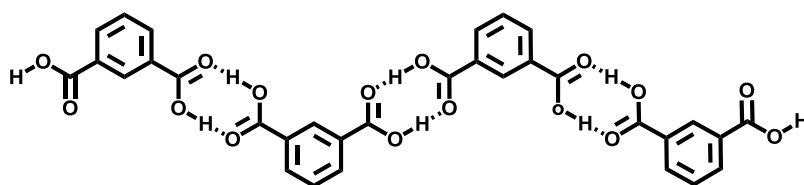


Figure 1.3.5 1-D isophthalic acid zig-zag motif.⁴⁰

More complex, 2-D structures form from molecular tectons which allow for hydrogen bonding in two dimensions. Trimesic acid contains three carboxylic acid synthons at 90° from each other. By adding this third carboxylic acid substituent, a 2-D structure of trimesic acid is formed. In the solid state, trimesic acid has been discovered to form a 2-D honeycomb network (Figure 1.3.6).⁴¹

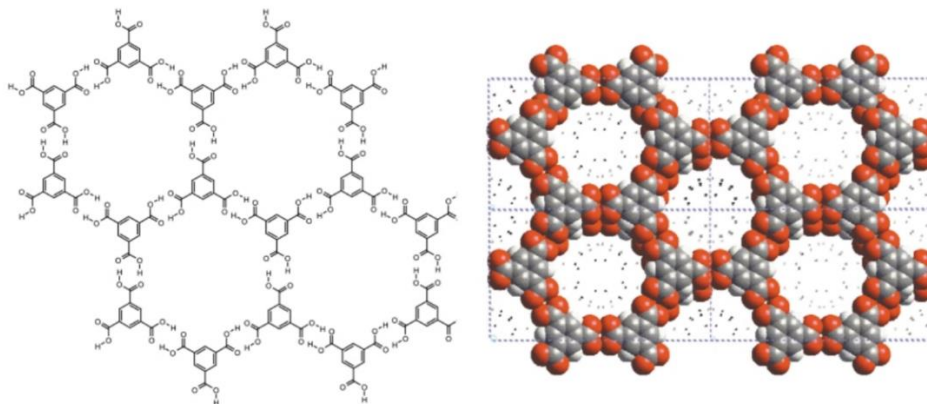


Figure 1.3.6 Trimesic acid 2-D honeycomb structure.⁴¹

Michael Zaworotko added another tecton to Figure 1.1.15, in this case, 4,4'-bipyridine, and demonstrated the honeycomb motif could expand in size.⁴¹ Expanding the pore size of the honeycomb demonstrates that not only can self-assembled hydrogen bonded structures be generated, but they can be tuned as well (Figure 1.3.7).⁴¹

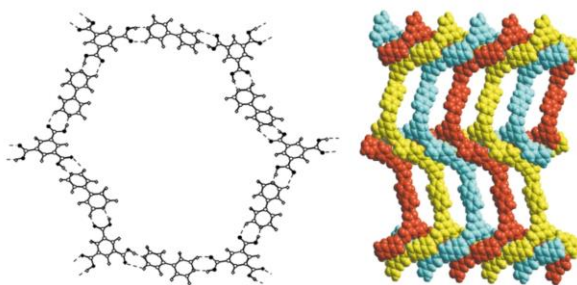


Figure 1.3.7 Zaworotko's trimesic acid and 4,4'-bipyridine expanded honeycomb design.⁴¹

1.4 Organic Solids with Host-Guest Properties

In 1994, Etter and Ward published a series of structures containing guanidinium and arenesulfonates.^{32a} These structures used directed hydrogen bonds between the six guanidinium protons and the six lone electron pairs of the sulfonate oxygen atoms. The self-assembled structures contained two-dimensional hydrogen-bonded sheets. These sheets have a third dimension by assembling into single layers or bilayers (Figure 1.4.1).^{32a}

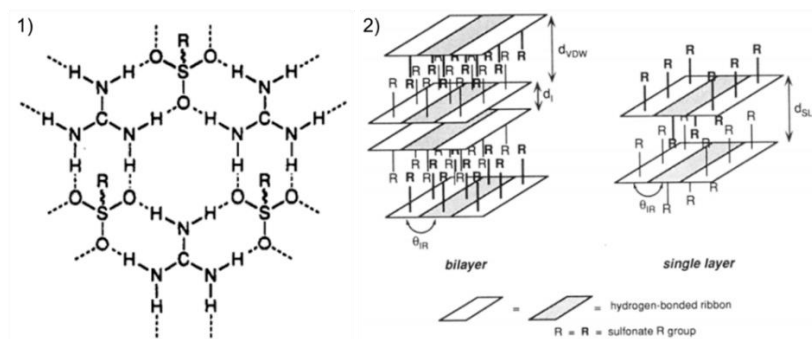


Figure 1.4.1 Depiction of the guanidinium-sulfonate layer. 1) Layer from above. 2) Representation of the bilayer and single layered structures^{32a}

In the depiction, d_I is the ionic spacing, d_{VDW} is the Van der Waals spacing and d_{SL} is spacing in single layer salts.^{29a} The inter-ribbon dihedral angle, θ_{IR} , measures the dihedral angle between the ribbons since the sheets tend to pucker to allow closer packing of the R groups.^{32a}

Ward *et al.* have published several iterations of the layered guanidinium sulfonate host framework and found it capable of capturing guest molecules.^{42a, 42i} Using the same approach, but now using sulfonates as pillars, yielded a simple brick structure (Figure 1.4.2).

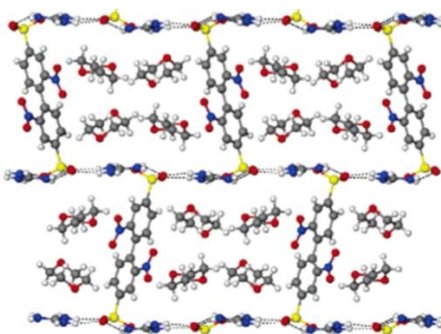


Figure 1.4.2 Hydrogen-bonded layered brick structure where pillars, with terminal sulfonates, separate the guanidinium layers ⁴³

In this soft framework, the guanidinium bilayer structures are separated by pillars containing terminal sulfonates.⁴³ This created space within the structure for guest molecules. Guest molecules co-crystallize in these systems during synthesis. Once the guests leave the space, the cavity collapses.⁴³ By changing the type of sulfonate pillars, not only could the distance between the layers be changed but the framework could be retained and can undergo guest exchange.^{42b} Using this concept, Ward *et al.* have made over 300 compounds.^{42c} The host material can capture a laser dye, coumarin, and depending on the framework structure create a blue or red shift in the emission spectra.^{42d} The guanidinium chemistry has been used to make supramolecular cylinders,^{42e, 42i} frameworks which change shape based on host-guest interactions,^{42f} and layer separation was increased or decreased by simply changing the pillar molecule.^{42g, 42h, 42j, 42k, 42n, 44} Hydrogen bonded materials can be used to separate molecules from solution, act as catalysts, and the separation of gases.⁴² Supramolecular organic frameworks can absorb and store carbon dioxide, methane, and nitrogen.^{42p, 42r} Hydrogen-bonded systems can undergo dynamic processes and be thermally stable.⁴⁴

1.5 Hydrogen Bonded Frameworks Containing Metals

It was stated earlier, that “all good proton donors and acceptors are used in hydrogen bonding”.³⁵ This is also true for pure organic species which are part of metal-coordinated ligands. These contain terminal synthons which can hydrogen bond (Figure 1.5.1).⁴⁵

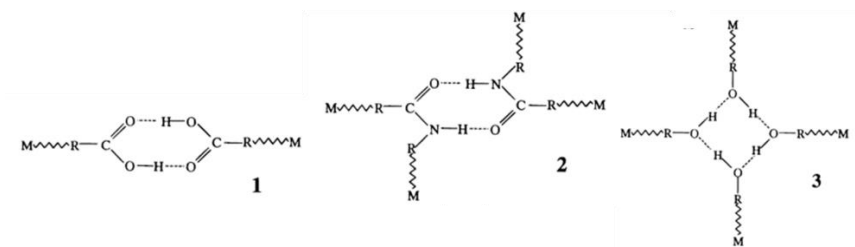


Figure 1.5.1 Strong donor/acceptor groups such as 1) -COOH, 2) -COHNR amido and 3) -OH⁴⁵

For crystal engineers, this makes available new tecton building blocks which could be used to build robust structures with pores, and channels.^{45, 46, 47} These structures are less densely packed making them capable of guest inclusion.⁴⁶ The increased stability of these frameworks comes from the addition of charge-assisted hydrogen bonds between the building units (Figure 1.5.2).

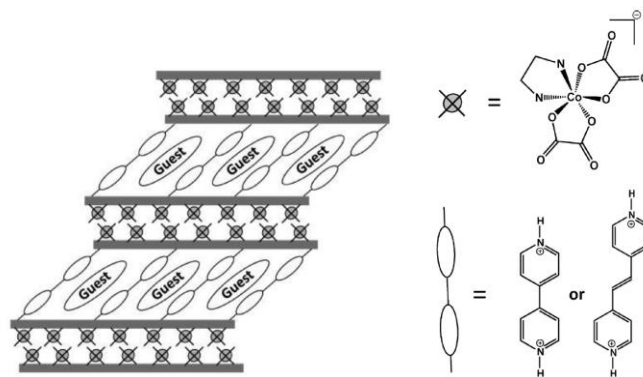


Figure 1.5.2 Representation of typical pillared-layer framework structures formed of the anionic metal complex $[\text{Co}(\text{en})(\text{ox})_2]^-$ and the cationic bipyridinium pillars $(\text{H}_2\text{bpy})^{2+}$ and $(\text{H}_2\text{bpye})^{2+}$.⁴⁸

As can be seen from the figure, the protonated bipyridine carries a positive charge and creates the charge-assisted hydrogen bond to the anionic cobalt complex.⁴⁸ This soft framework demonstrates that using hydrogen bonding to assemble a structure allows for structural flexibility which can accommodate guest molecules.⁴⁸ Once the guest containing frameworks assemble, it becomes necessary to determine effective and efficient means of analysis.

1.6 Analysis of Host-Guest Materials

Many techniques are used to determine the identify guest molecules in host-guest crystalline materials. These techniques include nuclear magnetic resonance (NMR), thermogravimetric analysis (TGA), single crystal x-ray diffraction (SCXRD), powder x-ray diffraction (PXRD), gas chromatography (GC), differential scanning calorimetry (DSC), and spectroscopic methods.

NMR is a useful technique for identifying the presence of guest molecules within a host material. It will also identify the interaction between the guest and host. Proton

NMR has probed host-guest interactions and mapped the magnetic interior of the host material.⁴⁹ The guests can be identified by proton NMR if the crystals are soluble.⁵⁰ There have also been deuterium NMR studies used for characterization as well as ^1H - ^{13}C heteronuclear correlation NMR to confirm host-guest interaction at the atomic level.^{51,52} ^{113}Cd NMR probed the structural dynamics of a flexible framework which shows high selectivity towards O_2 over N_2 .⁵³ A combination of ^1H NMR and cyclic voltammetry was able to distinguish when redox active guest molecules were present.⁵⁴

Thermogravimetric analysis (TGA) is a common technique for analyzing host-guest systems. The loss in mass equates to a guest loss, solvent loss or water loss.⁵⁵ TGA is a useful analytical tool for these systems as it identifies what temperature the guest evolves from the host material compared to the degradation temperature of the host.⁵⁶ Others have reported that a combination of TGA and DSC can be used to determine the guest kinetics of desorption from the host framework.⁵⁷ Schatz *et al.* qualitatively measured the binding strength of the guest molecule in the crystal lattice of a calixarene by comparing the temperature of a guest loss against the known boiling point of the guest.⁵⁸ Studies with calixarenes qualitatively estimated their binding strength to guest molecules within the crystal lattice.⁵⁸

Another common but powerful tool used to look at the relationship between the host and its guest is single crystal x-ray diffraction (SCXRD).⁵⁹ It makes it possible not only to visualize the host structure but also the orientation of the guest within the host.^{42a} When crystalizing a host material using a variety of tectons, it gives a clear picture of how the material has changed and how that affects the guest molecule orientation.^{42k} It can elucidate how guests pack within the channels or cavities of the host material, such as

polar guests lining up in a head-to-tail fashion.⁶⁰ When designing functional materials, such as liquid crystals, single crystal XRD affords the opportunity to look at how the molecules pack together providing information for planning the next series of experiments.⁶¹

Powder x-ray (PXRD) diffraction can identify structural features of a host material and how that structure changes by adding or removing guest molecules. Powder x-ray diffraction provides crucial structure information in this field,⁶² and a PXRD scan finishes in a fraction of the time. Bharajwaj used PXRD to observe structural changes in a diamondoid three-dimensional MOF as it lost guest molecules.⁶¹ Using PXRD, the Beatty group observes a contraction between the hydrophilic layers of a hydrogen bonded framework which is a result of the guest loss.⁶³ Time-resolved powder x-ray diffraction coupled with gravimetric sorption analysis is used to observe the uptake and release of guest molecules.⁶⁴ Arriortua *et al.* performed thermodiffraction studies to show coordinated water loss at different temperatures, which translated to crystal structure transformations stemming from the reduction of interlayer distances while reducing crystallinity.⁶⁵ *In situ* synchrotron x-ray powder diffraction patterns have revealed how a porous coordination polymer can have a shrinkable framework and have elucidated previously unrecognizable structural features.⁶⁶

A precise method for analyzing guest molecules is gas chromatography. This analytical method detects guest molecules with specificity since the guest molecules elution times are known. A standard curve of the guest molecule will allow for unknown concentrations of that guest to be calculated from a sample. Nassimbeni *et al.* analyzed the selectivity of a clathrate towards THF and ethanol. The competition studies

performed using GC analysis showed that THF was preferentially enclatharated.⁶⁷ In many cases, a crystal was formed from a solution containing two potential guest molecules; dissolved in organic solvent and injected into a gas chromatograph to determine the selectivity of the host.⁶⁸ The guest concentration can also be determined by analyzing the growth solution by gas chromatography.⁶⁹ Plotting the results of several experiments generates a selectivity curve for that host against the two guest molecules.⁶⁸

The relationship between host and guest has been explored using differential scanning calorimetry (DSC). DSC can be used to calculate desorption kinetics of a guest molecule as it leaves the host.⁵⁷ Exotherms in a DSC curve can signify molecule release from the host, especially in tandem with TGA data.⁶⁵ In some cases, the DSC curve will show an endotherm for guest loss, followed by another which signifies melting of the host.⁷⁰

Spectroscopy has been used to understand the interaction between the guest and its host. UV-Vis titration experiments can monitor host-guest complex formation.⁷¹ Fluorescence measurements have demonstrated the use of host-guest materials chemical sensing.⁷² Fluorescence from a host-guest exciplex, where the guest is mechanically trapped, help understand concepts such as energy transfer as it relates to donor-acceptor distance.⁷³ There is even a case where visible color changes have been used to identify different guests occupying the host material.⁷⁴

1.7 Size and Shape Molecular Separation by Host-Guest Materials

For a host molecule or structure to uptake, separate or co-crystallize guest molecules, the guest must fit in the host. Therefore, the size and shape of guest can be

important to host selectivity. The laws of attraction also apply; the electronic nature of the guest molecule must fit that of the host structure or molecule.

Size is important when a molecule is trying to pass through a channel or pore. Many studies have looked at how the guest's size and shape play a role in the host-guest relationship.⁷⁵ The dimensions of a molecule can become immensely important when determining if it will be taken up by a host. Critical dimensions are calculated for molecules to determine if they will be absorbed by zeolites.⁷⁶ The critical dimension of a molecule will also depend on the shape of the opening in the host material (Figure 1.7.1).

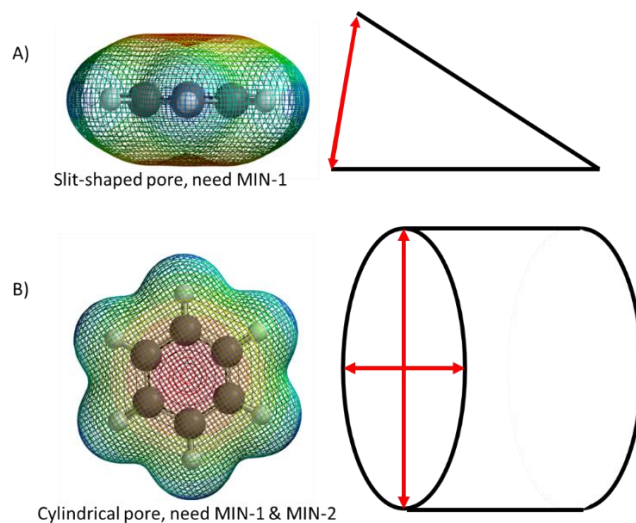


Figure 1.7.1 Using the minimum dimensions of benzene to determine whether it will fit into a pore.⁷⁶

For a slit-shaped pore, there is only one minimum dimension which must be met (MIN-1).⁷⁶ A cylindrical pore requires two minimum dimensions (MIN-1 & MIN-2).⁷⁶ In zeolites where the cavities are particularly rigid, the size and shape of the guest molecule controls the absorption process.⁷⁷ In ZSM-5, normal alkanes and simple aromatic hydrocarbons pass through.⁷⁷ The openings in ZSM-5 have such narrow openings that molecules must be the correct size, or they will not pass through. The size of the pore is

why ZSM-5 can differentiate between *p*-xylene and *o*-xylene.⁷⁸ The size and shape of a guest make a difference as to how it interacts with a host (Figure 1.7.2).

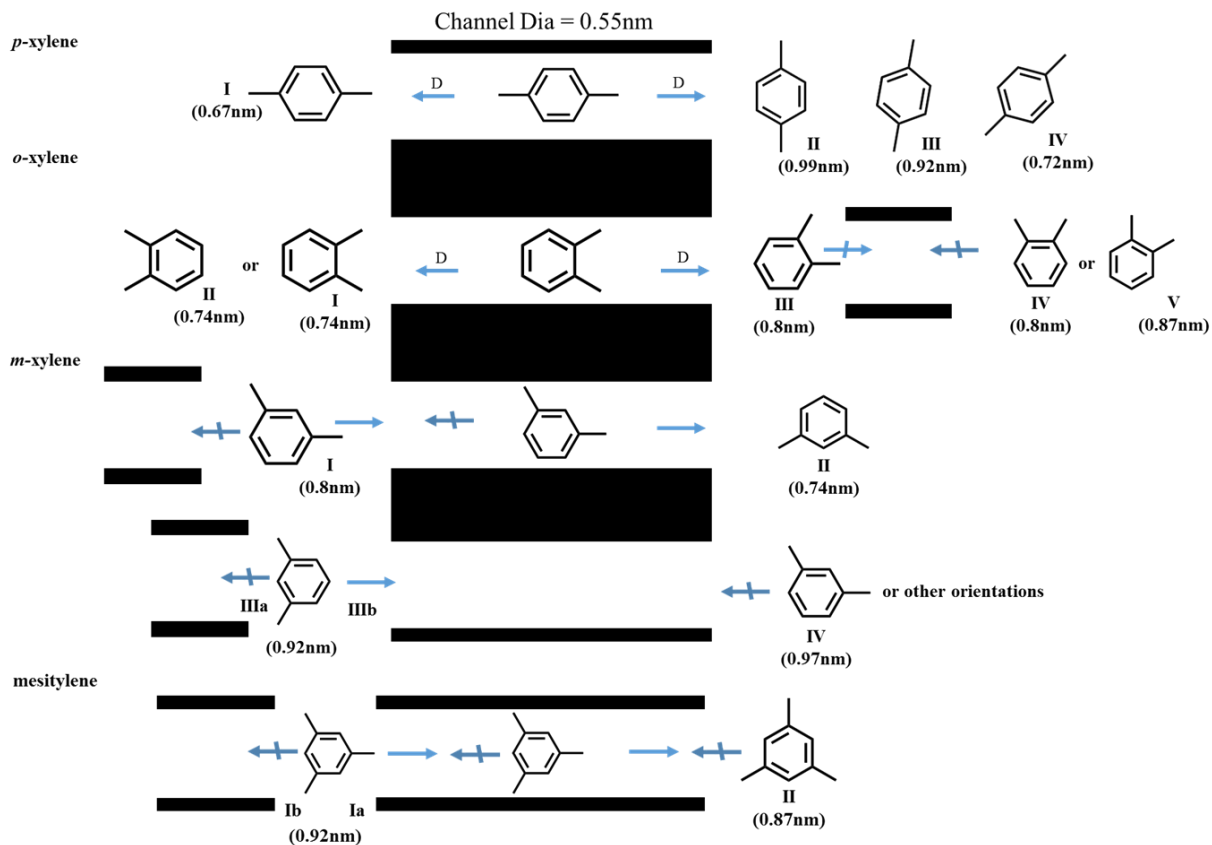


Figure 1.7.2 Effect of size and shape of xylene isomers and mesitylene molecules on their entry and diffusion through H-ZSM-5.⁷⁸

Xylene isomers though similar, interact differently with the same channel. Figure 1.18 describes how each of the guests can only enter the channel when in the most favorable conformation. A single → means the *p*-xylene, as I, can pass through linearly in both directions. *O*-xylene in I and II can pass through but have a larger critical dimension (0.74 nm) than *p*-xylene (0.67 nm). *O*-xylene in III, IV and V cannot pass through. Mesitylene is almost completely occluded.

Directed hydrogen-bonding provides a pathway to assemble functional host-guest materials. For example, Chen *et al.* constructed this microporous hydrogen bonded frameworks to separate ethyne from ethylene gas mixtures as they pass through the porous material at different pressures and temperatures (Figure 1.7.3).^{42p}

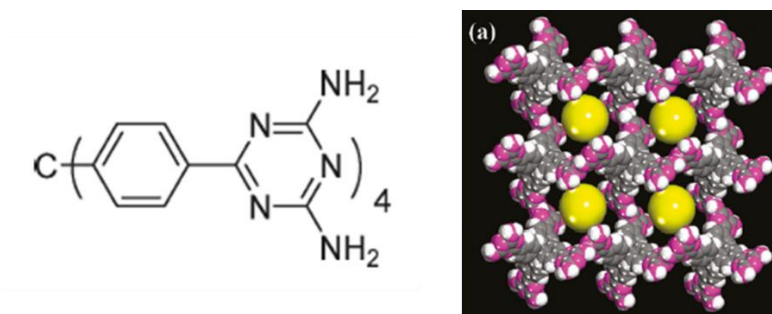


Figure 1.7.3 Representation of the organic building block (tecton) used to make (a) which can separate C₂H₂ and C₂H₄. Yellow spheres mark the permanent pores ^{42p}

1.8 Electron Factors for Host-Guest Molecular Separation

Just as size and shape are important so can the electronic nature of guest. DFT and *ab initio* molecular dynamics studies can describe how the guest molecules may interact with a host. In one example, these techniques estimated the stability of argon as a guest molecule.⁷⁹ Calculating the electronic nature of the guest molecule can indicate how it might fit with the host (Figure 1.8.1).

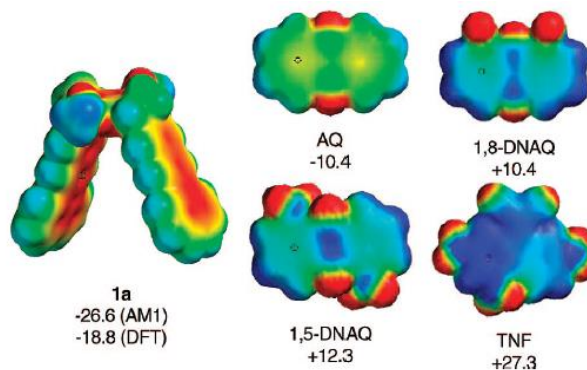


Figure 1.8.1 Calculated electrostatic potentials for diacetoxy substituted benzo[k]fluoroanthrene clip (**1a**) and guest molecules anthra-9,10-quinone (AQ), 1,8-dinitroanthra-9,10-quinone (1,8-DNAQ), 1,5-dinitroanthra-9,10-quinone (1,5-DNAQ) and 9-dicyanomethylene-2,4,7-trinitrofluorene (TNF). Red areas have higher electron density, and blue areas have low electron density.⁸⁰

Calculating the electrostatic potential of the host and guest molecules can provide a guide as to why certain guest show preference over others.⁸⁰ From Figure 1.1.24, the interior of **1a** has a high level of electron density as seen by the red/orange areas.⁸⁰ The TNF molecule, with its low level of electron density, is the most stable inside of molecular tweezers (**1a**) (Figure 1.8.1).⁸⁰ The negative cavity fits well with the positively polarized guest molecule.⁸⁰ By comparison, AQ is weakly bound within **1a** (Figure 1.8.1).⁸⁰ Calculating these interactions and visualizing the electrostatic potential maps allows one to see just how the host and guest are interacting (Figure 1.8.2).⁸¹ These types of interactions are especially applicable when investigating how enzymes bind to small molecules and it was found that the electrostatic surface potential of a guest molecule needs to be considered.⁸²

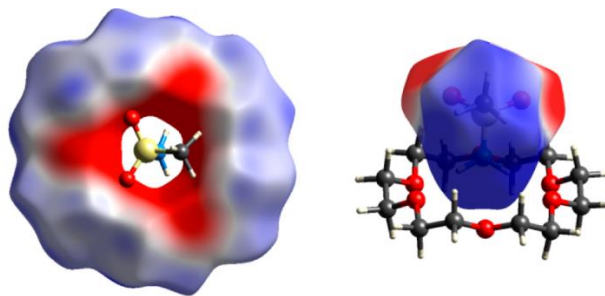


Figure 1.8.2 Electrostatic potential maps over the 18-6 crown ether and methylsulfonamide.⁸¹

1.9 Proposed Work

Our research will be primarily focused on a charge-assisted hydrogen bonded framework synthesized in the Beatty Lab (Figure 1.8.1).⁶³

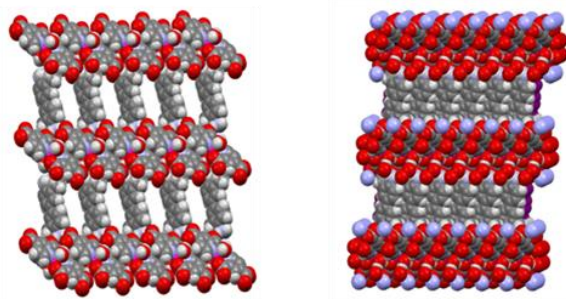


Figure 1.9.1 Charge-assisted hydrogen-bonded framework from the Beatty lab, 1

This material is comprised of a metal coordination complex, where each of the ligands contains a terminal carboxylic acid functional group. The structure allows for hydrogen bonding with organic pillar molecules containing terminal amines. The pillars separate the layers of the metal complex to form a hydrogen bonded framework. The pillars are arranged in a louvered fashion and are closed packed. This physical characteristic of the framework creates a one-dimensional channel which has been shown to host small organic guest molecules.

This research explores what influences the type of guest that occupies the channels inside **1**. By developing this understanding, we are determined to establish a set of guidelines or rules to hypothesize the guest molecules which will preferentially co-crystallize within this framework. To perform this work, we will place potential guest molecules in a series of competition reactions. By pitting one molecule against another, the framework will begin to provide clues as to what aspects are critical the selection process. We will focus on three specific areas to draw our conclusions:

- 1) By varying the size and shape of guest molecules, can we draw a conclusion about the influence these parameters have on the framework's selectivity?
- 2) For a pair of guest molecules, if the size and shape is kept as close as possible, can the selectivity of the framework be influenced by the electronic nature of the guest molecule?
- 3) Once the clues of the nature of the framework's selectivity begin to fall into place, is it possible to use single co-crystallized guest molecules to explain the patterns or trends observed in the competition studies?

To further understand what influences the guests occupying the channels inside **1**, we investigated the size, shape and electronic nature of small aromatic molecules and whether our framework can separate them.

1.10 References

- 1) Pedersen, C.J. *J. Am. Chem. Soc.* **1967**, *89*, 2495-2496; Pedersen, C.J. *J. Am. Chem. Soc.* **1967**, *89*, 7017-7036; Pedersen, C.J. *J. Am. Chem. Soc.* **1970**, *92*, 391-394
- 2) Cram, D.J.; Helgeson, R.C.; Sousa, L.R.; Timko, J.M.; Newcomb, M.; Moreau, P.; de Jong, F.; Gokel, G.W.; Hoffman, D.H.; Domeier, L.A.; Peacock, S.C.; Madan, K.; Kaplan, L. *Pure Appl. Chem.* **1975**, *43*, 327-349; Kyba, E.P.; Helgeson, R.C.; Madan, K.; Gokel, G.W.; Tarnowski, T.L.; Moore, S.S.; Cram, D.J. *J. Am. Chem. Soc.* **1977**, *99*, 2564-2571; Lingenfelter, D.S.; Helgeson, R.C.; Cram, D.J. *J. Org. Chem.* **1981**, *46*, 393-406; Lehn, J.M.; Sonveaux, E.; Willard, A.K. *J. Am. Chem. Soc.* **1978**, *100*, 4914-4916; Kauffmann, E.; Dye, J.L.; Lehn, J.M.; Popov, A.I. *J. Am. Chem. Soc.* **1980**, *102*, 2274-2278; Smith, P.B.; Dye, J.L.; Cheney, J.; Lehn, J.M. *J. Am. Chem. Soc.* **1981**, *103*, 6044-6048; Kotzyba-Hibert, F.; Lehn, J.M.; Saigo, K. *J. Am. Chem. Soc.* **1981**, *103*, 4266-4268; Graf, E.; Kintzinger, J.P.; Lehn, J.M.; LeMoigne, J. *J. Am. Chem. Soc.* **1982**, *104*, 1672-1678; Cram, D.J.; Cram, J.M. *Science* **1974**, *183*, 803-809
- 3) Cram, D.J. *Science* **1983**, *219*, 1177-1183
- 4) Oshovsky, G.V.; Reinhoudt, D.N.; Verboom, W. *Angewandte Chemie Int. Ed.* **2007**, *46*, 2366-2393; Biroš, S.M.; Ullrich, E.C.; Hof, F.; Trembleau, L.; Rebek, J. *J. Am. Chem. Soc.* **2004**, *126*, 2870-2876; Biroš, S.M.; Bergman, R.G.; Raymond, K.N. *J. Am. Chem. Soc.* **2007**, *129*, 12094-12095; Marmur, A. *J. Am. Chem. Soc.* **2000**, *122*, 2120-2121; Tanford, C. *Science*, **1978**, *200*, 1012-1018
- 5a) Cram, D.J. *Angewandte Chemie Int. Ed.* **1988**, *27*, 1009-1020

- 5b) MacGillivray, L.R.; Atwood, J.L.; Ko, Y.H.; Kim, K.; Kang, J.; Chun, H.; Lee, J.W.; Sakamoto, S.; Yamaguchi, K.; Fettinger, J.C.; Kim, K. *J. Am. Chem. Soc.* **2004**, *126*, 1932-1933; Ni, X.; Chen, S.; Yang, Y.; Tao, Z. *J. Am. Chem. Soc.* **2016**, *138*, 6177-6183; Lagona, J.; Mukhopadhyay, P.; Chakrabarti, S.; Isaacs, L. *Angewandte Chemie Int. Ed.* **2005**, *44*, 4844-4870; Marquez, C.; Hudgins, R.R.; Nau, W.M. *J. Am. Chem. Soc.* **2004**, *126*, 5806-5816
- 5c) Omoto, K.; Tashiro, S.; Kuritani, M.; Shionoya, M. *J. Am. Chem. Soc.* **2014**, *136*, 17946-17949; Timko, J.M.; Helgeson, R.; Cram, D.J. *J. Am. Chem. Soc.* **1978**, *100*, 2828-2834; Seel, C.; Vogtle, F. *Angewandte Chemie Int. Ed.* **1991**, *103*, 433-436; Ito, S.; Takata, H.; Ono, K.; Iwasawa, N. *Angew. Chem., Int. Ed.* **2013**, *52*, 11045-11048; Yang, J.; Dewal, M.B.; Profeta, S.; Smith, M.D.; Li, Y.; Shimizu, L.S. *J. Am. Chem. Soc.* **2008**, *130*, 612-621; Kyba, E.P.; Helgeson, R.C.; Madan, K.; Gokel, G.W.; Tarnowski, T.L.; Moore, S.S.; Cram, D.J. *J. Am. Chem. Soc.* **1977**, *99*, 2564-2571
- 5d) Ogoshi, T.; Sueto, R.; Yoshikoshi, K.; Sakata, Y.; Akine, S.; Yamagishi, T. *Angewandte Chemie Int. Ed.* **2015**, *54*, 9849-9852; Yu, G.; Xue, M.; Zhang, Z.; Li, J.; Han, C.; Huang, F. *J. Am. Chem. Soc.* **2012**, *134*, 13248-13251
- 5e) Brown, S.P.; Schaller, T.; Seelbach, U.P.; Koziol, F.; Ochsenfeld, C.; Klarner, F.; Spiess, H.W. *Angew. Chem., Int. Ed.* **2001**, *40*, 717-720
- 5f) Dvornikovs, V.; House, B.E.; Kaetzel, M.; Dedman, J.R.; Smithrud, D.B. *J. Am. Chem. Soc.* **2003**, *125*, 8290-8301; Wang, X.; Bao, X.; McFarland-Mancini, M.; Isaacsohn, I.; Drew, A.F.; Smithrud, D.B. *J. Am. Chem. Soc.* **2007**, *129*, 7284-7293

- 5g) Cram, D.J.; Tanner, M.E.; Thomas, R. *Angew. Chem., Int. Ed.* **1991**, *30*, 1024-1027;
Jankowska, K.I.; Pagba, C.V.; Piatnitski Chekler, E.L.; Deshayes, K.; Piotrowiak,
P. J. Am. Chem. Soc. **2010**, *132*, 16423-16431
- 5h) Ouchi, A.; Tashiro, K.; Yamaguchi, K.; Tsuchiya, T.; Akasaka, T.; Aida, T. *Angew.
Chem., Int. Ed.* **2006**, *45*, 3542-3546
- 5i) Sawada, T.; Hisada, H.; Fujita, M. *J. Am. Chem. Soc.* **2014**, *136*, 4449-4451
- 5j) Auletta, T.; De Jong, M.R.; Mulder, A.; Van Veggel, F.C.J.M.; Huskens, J.;
Reinhoudt, D.N.; Zou, S.; Zapotoczny, S.; Schoenherr, H.; Vancso, G.J.; Kuipers,
L. J. Am. Chem. Soc. **2004**, *126*, 1577-1584; Zhou, H.; Yamada, T.; Kimizuka, N.
J. Am. Chem. Soc. **2016**, *138*, 10502-10507; Wenz, G. *Angewandte Chemie Int.
Ed.*, **1994**, *33*, 803-822; Li, H.; Li, F.; Zhang, B.; Zhou, X.; Yu, F.; Sun, L. *J. Am.
Chem. Soc.* **2015**, *137*, 4332-4335
- 5k) Schramm, M.P.; Hooley, R.J.; Rebek, J. *J. Am. Chem. Soc.* **2007**, *129*, 9773-9779;
Zhang, K.; Ajami, D.; Gavette, J.V.; Rebek, J. *J. Am. Chem. Soc.* **2014**, *136*, 5264-
5266; Butterfield, S.M.; Rebek, J. *J. Am. Chem. Soc.* **2006**, *128*, 15366-15367;
Kobayashi, K.; Ishii, K.; Sakamoto, S.; Shirasaka, T.; Yamaguchi, K. *J. Am. Chem.
Soc.* **2003**, *125*, 10615-10625
- 5l) Cram, D.J.; Dicker, I.B.; Lauer, M.; Knobler, C.B.; Trueblood, K.N. *J. Am. Chem.
Soc.* **1984**, *106*, 7150-7167
- 5m) Tiefenbacher, K.; Ajami, D.; Rebek, J. *Angew. Chem., Int. Ed.*, **2011**, *50*,
12003-12007; Shivanyuk, A.; Rebek, J. *Angew. Chem., Int. Ed.* **2003**, *42*, 684-686

- 6) Yoon, J.; Knobler, C.B.; Maverick, E.F.; Cram, D.J. *Chem. Commun.*, **1997**, 1303-1304; Biwer, A.; Antranikian, G.; Heinzle, E. *Appl Microbiol Biotechnol*, **2002**, *59*, 609-617; Neal, E.; Goldup, S.M. *Chem. Commun.*, **2014**, *50*, 5128-5142; Ogoshi, T.; Kanai, S.; Fujinami, S.; Yamagishi, T.; Nakamoto, Y. *J. Am. Chem. Soc.* **2008**, *130*, 5022-5023; Bier, D.; Rose, R.; Bravo-Rodriguez, K.; Bartel, M.; Ramirez-Angueta, J.M.; Dutt, S.; Wilch, C.; Klarner, F.G.; Sanchez-Garcia, E.; Schrader, T.; Ottman, C. *Nature Chemistry*, **2013**, *5*, 234-239; Hamers, C.; Raymo, F.M.; Stoddart, J.F. *Eur. J. Org. Chem.*, **1998**, 2109-2117; Heinz, T.; Rudkevich, D.M.; Rebek Jr., J. *Nature*, **1998**, *394*, 764-766
- 7) Mugridge, J.S.; Szigethy, G.; Bergman, R.G.; Raymond, K.N. *J. Am. Chem. Soc.*, **2010**, *132*, 16256-16264; Mugridge, J.S.; Zahl, A.; van Eldik, R.; Bergman, R.G.; Raymond, K.N. *J. Am. Chem. Soc.*, **2013**, *135*, 4299-4306; Mugridge, J.S.; Bergman, R.G.; Raymond, K.N. *J. Am. Chem. Soc.*, **2012**, *134*, 2057-2066; Mugridge, J.S.; Bergman, R.G.; Raymond, K.N. *J. Am. Chem. Soc.*, **2011**, *133*, 11205-11212
- 8) Turega, S.; Cullen, W.; Whitehead, M.; Hunter, C.A.; Ward, M.D. *J. Am. Chem. Soc.*, **2014**, *136*, 8475-8483; Cullen, W.; Hunter, C.; Ward, M.D. *Inorganic Chemistry*, **2015**, *54*, 2626-2637; Turega, S.; Whitehead, M.; Hall, B.R.; Meijer, A.J.H.M.; Hunter, C.A.; Ward, M.D. *Inorg. Chem.*, **2013**, *52*, 1122-1132; Ward, M.D.; Hunter, C.; Williams, N.H. *Chemistry Letters*, **2017**, *46*, 2-9
- 9) Lee, S.J.; Hu, A.; Lin, W. *J. Am. Chem. Soc.* **2002**, *124*, 12948-12949
- 10) Wagner, P.; Nakagawa, Y.; Lee, G.S.; Davis, M.E.; Elomari, S.; Medrud, R.C.; Zones, S.I. *J. Am. Chem. Soc.* **2000**, *122*, 263-273; Wang, H.; Huang, Y.

- Langmuir* **2009**, *25*, 8042-8050; Erdem, O.F.; Michel, D. *J. Phys. Chem. B*, **2005**, *109*, 12054-12061; Han, D.; Woo, A.; Nam, I.; Hong, S.B. *J. Phys. Chem. B*, **2002**, *106*, 6206-6120; Paik, W.C.; Shin, C.H.; Lee, J.M.; Ahn, B.J.; Hong, S.B. *J. Phys. Chem. B*, **2001**, *105*, 9994-10000; Zaborowski, E.; Zimmermann, H.; Vega, S. *J. Am. Chem. Soc.* **1998**, *120*, 8113-8123
- 11) Denayer, J. F. M.; De Meyer, K.; Martens, J. A.; Baron, G. V. *Angew. Chem., Int. Ed.* **2003**, *42*, 2774-2777; Denayer, J. F. M.; De Jonckheere, B.; Hloch, M.; Marin, G. B.; Vanbutsele, G.; Martens, J. A.; Baron, G. V. *J. Cat.* **2002**, *210*, 445-452
- 12) Kamble, S. P.; Mangrulkar, P. A.; Bansiwala, A. K.; Rayalu, S. S. *Chemical Engineering Journal*, **2008**, *128*, 73-83
- 13) Coughlan, B.; Carroll, W. M.; Nunan, J. J. *Chem. Soc., Faraday Trans. 1* **1983**, *79*, 327-342
- 14) Riedmann, R.A.; Purtschert, R. *Separation and Purification Technology* **2016**, *170*, 217-233; Palagin, D.; Sushkevich, V.L.; Ivanova, I.I. *J. Phys. Chem. C*, **2016**, *120*, 23566-23575; Xu, Z.; Michos, I.; Cao, Z.; Jing, W.; Gu, X.; Hinkle, K.; Murad, S.; Dong, J. *J. Phys. Chem. C*, **2016**, *120*, 26386-26392; Arefi Pour, A.; Sharifnia, S.; Neishabouri Salehi, R.; Ghodrati, M. *Journal of Natural Gas Science and Engineering* **2016**, *36*, 630-643; Sanchez-Castillo, M.A.; Agarwal, N.; Bartsch, A.; Cortright, R.D.; Madon, R.J.; Dumesic, J.A. *Journal of Catalysis* **2003**, *218*, 88-103; Yaluris, G.; Rekoske, J.E.; Aparicio, L.M.; Madon, R.J.; Dumesic, J.A. *Journal of Catalysis* **1995**, *153*, 65-75; Weeks, T.J.; Angell, C.L.; Ladd, I.R.; Bolton, A.P. *Journal of Catalysis* **1974**, *33*, 256-264; Sun, H.; Wu, D.;

- Guo, X.; Shen, B.; Liu, J. ; Navrotsky, A. *J. Phys. Chem. C*, **2014**, *118*, 25590-25596; Lee, J.J.; Sobolev, A.N.; Turner, M.J.; Fuller, R.O.; Iversen, B.B.; Koutsantonis, G.A.; Spackman, M.A. *Cryst. Growth Des.* **2014**, *14*, 1296-1306; Sivasankar, N.; Vasudevan, S. *J. Phys. Chem. B*, **2005**, *109*, 15417-15421; Boulfelfel, S.E.; Ravikovitch, P.I.; Sholl, D.S. *J. Phys. Chem. C*, **2015**, *119*, 15643-15653; Blanco, C.; Auerbach, S.M. *J. Am. Chem. Soc.* **2002**, *124*, 6250-6251; Santander, J.E.; Conner, W.C.; Jobic, H.; Auerbach, S.M. *J. Phys. Chem. C*, **2009**, 13776-13781; Blanco, C.; Auerbach, S. *J. Phys. Chem. B*, **2003**, *107*, 2490-2499; Ozin, G.; Kuperman, A.; Stein, A. *Angewandte Chemie* **1989**, *28*, 359-376; Comotti, A.; Bracco, S.; Valsesia, P.; Beretta, M.; Sozzani, P. *Angewandte Chemie Int. Ed.* **2010**, *49*, 1760-1764; Croissant, J.G.; Fatieiev, Y.; Julfakyan, K.; Lu, J.; Emwas, A.; Anjum, D.H.; Omar, H.; Tamanoi, F.; Zink, J.I.; Khashab, N.M. *Chemistry Eur. J.* **2016**, *22*, 14806-14811
- 15) Cheetham, A.; Ferey, G.; Loiseau, T. *Angew. Chem. Int. Ed.* **1999**, *38*, 3268-3292
- 16) International Zeolite Association, Database of Zeolite Structures (include web address)
- 17) Moliner, M.; Martinez, C.; Corma, A. *Chem. Mater.* **2014**, *26*, 246-258; Zones, S. I.; Hwang, S.; Olmstead, M.M.; Teat, S.J.; Jackowski, A.; Burton, A.W.; Kim, C. *J. Phys. Chem. C*, **2010**, *114*, 8899-8904; Smeets, S.; McCusker, L.B.; Baerlocher, C.; Elomari, S.; Xie, D.; Zones, S.I. *J. Am. Chem. Soc.* **2016**, *138*, 7099-7106; Hong, S.B.; Cambor, M.A.; Davis, M.E. *J. Am. Chem. Soc.* **1997**, *119*, 761-770

- 18) Batten, S.R.; Turner, D.R.; Neville, S.M. *Coordination Polymers: Design, Analysis and Application*. The Royal Society of Chemistry, Thomas Graham House Cambridge, Cambridge CB4 0WF, UK 2009
- 19) Desiraju, G.R.; Vittal, J.J.; Ramanan, A. *Crystal Engineering, A Textbook*. World Scientific Publishing Company. Pte. Ltd., **2011**
- 20) Yaghi, O.; Li, H.; Davis, C.; Richardson, D.; Groy, T. *Acc. Chem. Res.* **1998**, *31*, 474-484
- 21) Duan, J.; Higuchi, M.; Krishna, R.; Kiyonaga, T.; Tsutsumi, Y.; Sato, Y.; Kubota, Y.; Takata, M.; Kitagawa, S. *Chemical Science* **2014**, *5*, 660-666
- 22) Roy, S.; Chakraborty, A.; Tapas, K. *Coordination Chemistry Reviews* **2014**, *273-274*, 139-164
- 23) Sato, H.; Kosaka, W.; Matsuda, R.; Hori, A.; Hijikata, Y.; Belosludov, R. V.; Sakaki, S.; Takata, M.; Kitagawa, S. *Science* **2014**, *343*, 167-170
- 24) Biradha, K.; Fujita, M. *Crystal Design: Structure and Function*; Desiraju, G. R., Ed.; John Wiley & sons: 2003
- 25) Biradha, K.; Fujita, M. *Journal of Inclusion Phenomena and Macrocyclic Chemistry* **2001**, *49*, 201-208
- 26) Foo, M. L.; Matsuda, R.; Hijikata, Y.; Krishna, R.; Sato, H.; Horike, S.; Hori, A.; Duan, J.; Sato, Y.; Kubota, Y.; Takata, M.; Kitagawa, S. *J. Am. Chem. Soc.* **2016**, *138*, 3022-3030
- 27) Kishida, K.; Watanabe, Y.; Horike, S.; Watanabe, Y.; Okumura, Y.; Hijikata, Y.; Sakaki, S.; Kitagawa, S. *Eur.J.Inorg.Chem.* **2014**, 2747-2752

- 28) Kishida, K.; Horike, S.; Watanabe, Y.; Tahara, M.; Inubushi, Y.; Kitagawa, S.
Chemistry - An Asian Journal **2014**, *9*, 1643-1647
- 29) Duan, J.; Higuchi, M.; Foo, M.; Horike, S.; Rao, Koya P.; Kitagawa, S. *Inorganic Chemistry* **2013**, *52*, 8244-8249
- 30) Li, H.; Eddaoudi, M.; Groy, T.L.; Yaghi, O.M. *J. Am. Chem. Soc.* **1998**, *120*, 8571-8572; Li, H.; Eddaoudi, M.; O’Keeffe, M.; Yaghi, O.M. *Nature* **1999**, *402*, 276-279
- 31) Suzuki, T.; Kotani, R.; Kondo, A.; Maeda, K. *J. Phys. Chem. C*, **2016**, *120*, 21571-21579; Peterson, V.K.; Southon, P.D.; Halder, G.J.; Price, D.J.; Bevitt, J.J.; Kepert, C.J. *Chem. Mater.*, **2014**, *26*, 4712-4723; Li, J.; Fu, H.; Zhang, J.; Zheng, L.; Tao, J. *Inorg. Chem.*, **2015**, *54*, 3093-3095; Millange, F.; Guillou, N.; Medina, M. E.; Ferey, G.; Carlin-Sinclair, A.; Golden, K. M.; Walton, R. I. *Chem. Mater.*, **2010**, *22*, 4237-4245; Ling, S.; Walton, R. I.; Slater, B. *Molecular Simulation*, **2015**, *41*, 1348-1356; El Osta, R.; Carlin-Sinclair, A.; Guillou, N.; Walton, R. I.; Vermoortele, F.; Maes, M.; de Vos, D.; Millange, F. *Chem. Mater.*, **2012**, *24*, 2781-2791; Sumida, K.; Foo, M.L.; Horike, S.; Long, J.R. *Eur. J. Inorg. Chem.* **2010**, 3739-3744; Geier, S.J.; Mason, J.A.; Bloch, E.D.; Queen, W.L.; Hudson, M.R.; Brown, C.M.; Long, J.R. *Chem. Sci.* **2013**, *4*, 2054-2061; Krishna, R.; Long, J.R. *J. Phys. Chem. C*, **2011**, *115*, 12941-12950; Levine, D.J.; Runcevski, T.; Kapelewski, M.T.; Keitz, B.K.; Oktawiec, J.; Reed, D.A.; Mason, J.A.; Jiang, H.Z.H.; Colwell, K.A.; Legendre, C.M.; FitzGerald, S.A.; Long, J.R. *J. Am. Chem. Soc.*, **2016**, *138*, 10143-10150; Herm, Z.R.; Bloch, E.D.; Long, J.R. *Chem. Mater.*, **2014**, *26*, 323-338; Bloch, E.D.; Queen, W.L.; Krishna, R.; Zadrozny,

- J.M.; Brown, C.M.; Long, J.R. *Science*, **2012**, 335, 1606-1610; Li, J.; Sculley, J.; Zhou, H. *Chem. Rev.*, **2012**, 112, 869-932; Li, B.; Ma, D.; Li, Y.; Zhang, Y.; Li, G.; Shi, Z.; Feng, S.; Zaworotko, M.J. *Chem. Mater.*, **2016**, 28, 4781-4786
- 32) Russell, V.A.; Etter, M.C; Ward, M.D. *J. Am. Chem. Soc.*, **1994**, 116, 1941-1952; Adachi, T.; Ward, M.D. *Acc. Chem. Res.*, **2016**, Beatty, A.M. *Coordination Chemistry Reviews*, **2003**, 246, 131-143; Desiraju, G.R. *Angew. Chem., Int. Ed.*, **1995**, 34, 2311-2327
- 33) Watson, J.D.; Crick, F.H.C. *Nature*, **1953**, 171,737-738
- 34) Etter, M.C. *Acc. Chem. Res.* **1990**, 23, 120-126
- 35) Etter, M.C. *J. Phys. Chem.* **1991**, 95, 4601-4610
- 36) Beatty, A. M. *CrystEngComm*. **2001**, 3, 243-255; Aakeroy, C. B.; Beatty, A. M. *Australian Journal of Chemistry* **2001**, 54, 409-421; Bacchi, A.; Carcelli, M.; Pelagatti, P. *Crystallography Reviews* **2012**, 18, 253-279; Brunet, P.; Simard, M.; Wuest, J.D. *J. Am. Chem. Soc.* **1997**, 119, 2737-2738; Kerckhoffs, J.M.C.A.; Ten Cate, M.G.J.; Mateos-Timoneda, M.A.; Van Leeuwen, F.W.B.; Snellink-Rueel, B.; Spek, A.L.; Kooijman, H.; Crego-Calama, M.; Reinhoudt, D.N. *J. Am. Chem. Soc.*, **2005**, 127, 12697-12708; Tanaka, T.; Tasaki, T.; Aoyama, Y. *J. Am. Chem. Soc.*, **2002**, 124, 12453-12462; Lee, S.; Kariuki, B.M.; Harris, K.D.M. *Angewandte Chemie, Int. Ed.*, **2002**, 41, 2181-2184, Wuest, J.D. *Chem. Commun.* **2005**, 5830-5837; Saied, O.; Maris, T.; Wuest, J.D. *J. Am. Chem. Soc.* **2003**, 125, 14956-14957; Beatty, A.M.; Granger, K.E.; Simpson, A.E. *Chem. Eur. J.*, **2002**, 8, 3254-3259; Muthuraman, M.; Masse, R.; Nicoud, J.; Desiraju, G. *Chem. Mater.* **2001**, 13, 1473-1479; Desiraju, G. *Angew. Chem. Int. Ed.*, **2007**, 46, 8342-8356;

- Etter, M.C. *Acc. Chem. Res.*, **1990**, 120-126; Kahn, O. *Acc. Chem. Res.*, **2000**, 33, 647-657
- 37) Zhou, H.; Dang, H.; Yi, J.H.; Nanci, A.; Rochefort, A.; Wuest, J. *J. Am. Chem. Soc.* **2007**, 129, 13774-13775; Demers, E.; Maris, T.; Wuest, J.D. *Cryst. Growth Des.* **2005**, 5, 1227-1235
- 38) Alajarin, M.; Aliev, A.E.; Burrows, A.D.; Harris, K.D.M.; Pastor, A.; Steed, J.W.; Turner, D.R. *Supramolecular Assembly via Hydrogen Bonds I*. Mingos, D.M.P. Ed., Springer, **2004**
- 39) Bailey, M.; Brown, C.J. *Acta Crystallogr.* **1967**, 22, 387-391
- 40) Derissen, J.L. *Acta. Cryst.* **1974**, 30, 2764-2765
- 41) Duchamp, D.J.; Marsh, R.E. *Acta Crystallogr.* **1969**, B25, 5-19; Zaworotkko, M.J. *Chemical Communications* **2001**, 1-9
- 42a) Pivovar, A.M.; Holman, K.T.; Ward, M.D. *Chem. Mater.* **2001**, 13, 3018-3031
- 42b) Xiao, W.; Hu, C.; Ward, M.D. *J. Am. Chem. Soc.* **2014**, 136, 14200-14206
- 42c) Adachi, T.; Ward, M.D. *Acc. Chem. Res.* **2016**, 49, 2669-2679
- 42d) Soegiarto, A.C.; Ward, M.D. *Cryst. Growth Des.* **2009**, 9, 3803-3815
- 42e) Horner, M.J.; Holman, K.T.; Ward, M.D. *J. Am. Chem. Soc.* **2007**, 129, 14640-14660
- 42f) Swift, J.A.; Reynolds, A.M.; Ward, M.D. *Chem. Mater.* **1998**, 10, 4159-4168
- 42g) Soegiarto, A.C.; Comotti, A.; Ward, M.D. *J. Am. Chem. Soc.* **2010**, 132, 14603-14626
- 42h) Holman, K.T.; Pivovar, A.M.; Swift, J.A.; Ward, M.D. *Acc. Chem. Res.* **2001**, 34, 107-118

- 42i) Liu, Y.; Xiao, W.; Yi, J.J.; Hu, C.; Park, S.J.; Ward, M.D. *J. Am. Chem. Soc.* **2015**, *137*, 3386-3392
- 42j) Evans, C.C.; Sukato, L.; Ward, M.D. *J. Am. Chem. Soc.* **1999**, *121*, 320-325
- 42k) Custelcean, R.; Ward, M.D. *Cryst. Growth Des.* **2005**, *5*, 2277-2287
- 42l) Swift, J.A.; Pivovar, A.M.; Reynolds, A.M.; Ward, M.D. **1998**, *120*, 5887-5894
- 42m) Xiao, W.; Hu, C.; Ward, M.D. *Cryst. Growth, Des.* **2013**, *13*, 3197-3200
- 42n) Han, J.; Zhao, L.; Yau, C.W.; Mak, T.C.W. *Cryst. Growth Des.* **2009**, *9*, 308-319
- 42p) He, Y.; Xiang, S.; Chen, B. *J. Am. Chem. Soc.* **2011**, *133*, 14570-14573
- 43) M. Ward, R. Custelcean, *Crys, Growth Des.* **2005**, *5*, 6, 227
- 44a) Reddy, D.S.; Duncan, S.; Shimizu, G.K.H. *Angew. Chem. Int. Ed.* **2003**, *42*, 1360-1364; Dalrymple, S.A.; Shimizu, G.K. *J. Am. Chem. Soc.* **2007**, *129*, 12114-12116
- 44b) Beatty, A. M.; Helfrich, B. A.; Hogan, G. A.; Reed, B. A. *Cryst. Growth Des.* **2006**, *6*, 122-126; Chen, C.-L.; Beatty, A. M. *J. Am. Chem. Soc.* **2008**, *130*, 17222-17223; Aakeroy, C. B.; Beatty, A. M.; Leinen, D. S. *Angew. Chem., Int. Ed.* **1999**, *38*, 1815-1819
- 45) Braga, D.; Grepioni, F. *Acc. Chem. Res.* **2000**, *33*, 601-608
- 46) Reddy, D.S.; Duncan, S.; Shimizu, G.K.H. *Angew. Chem. Int. Ed.* **2003**, *42*, 1360-1364; Dalrymple, S.A.; Shimizu, G.K. *J. Am. Chem. Soc.* **2007**, *129*, 12114-12116
- 47) Yigit, M.V.; Biyiki, K.; Moulton, B.; MacDonald, J.C. *Cryst. Growth Des.* **2006**, *6*, 63-69

- 48) Prakash, M.J.; Sevov, S.C. *Inorg. Chem.* **2011**, *50*, 12739-12746; Wang, X.Y.; Justic, R.; Sevov, S.C. *Inorg. Chem.* **2007**, *46*, 4626-4631; Prakash, M.J.; Oliver, A.G.; Sevov, S.C. *Cryst. Growth Des.* **2012**, *12*, 2684-2690
- 49) Mugridge, J.S.; Bergman, R.G.; Raymond, K.N. *J. Am. Chem. Soc.* **2011**, *133*, 11205-11212; Li, K.; Zhang, L.; Yan, C.; Wei, S.; Pan, M.; Zhang, L.; Su, C. *J. Am. Chem. Soc.* **2014**, *136*, 4456-4459; Tiefenbacher, K.; Ajami, D.; Rebek, J. *Angewandte Chemie, Int. Ed.* **2011**, *50*, 12003-12007; Jiang, W.; Rebek, J. *J. Am. Chem. Soc.* **2012**, *134*, 17498-17501
- 50) Bajpai, A.; Natarajan, P.; Venugopalan, P.; Moorthy, J. *J. Org. Chem.* **2012**, *77*, 7858-7865
- 51) Umeyama, D.; Horike, S.; Inukai, M.; Kitagawa, S. *J. Am. Chem. Soc.* **2013**, *135*, 11345-11350; Hollingsworth, M.D.; Werner-Zwanziger, U.; Brown, M.E.; Chaney, J.D.; Huffman, J.C.; Harris, K.D.M.; Smart, S.P. *J. Am. Chem. Soc.* **1999**, *121*, 9732-9733
- 52) Fiedler, D.; Leung, D.H.; Bergman, R.G.; Raymond, K.N. *J. Am. Chem. Soc.* **2004**, *126*, 3674-3675
- 53) Haldar, R.; Inukai, M.; Horike, S.; Uemura, K.; Kitagawa, S.; Kumar, T. *Inorg. Chem.* **2016**, *55*, 4166-417223
- 54) Jeon, W.; Moon, J.; Park, S.H.; Chun, H.; Ko, Y.H.; Lee, J.; Lee, Eun S.; Samal, S.; Selvapalam, N.; Rekharsky, M.V.; Sindelar, V.; Sobransingh, D.; Inoue, Y.; Kaifer, A.E.; Kim, K. *J. Am. Chem. Soc.* **2005**, *127*, 12984-12989
- 55) Yang, J.; Dewal, M.B.; Profeta, S.; Smith, M.D.; Li, Y.; Shimizu, L.S. *J. Am. Chem. Soc.* **2008**, *130*, 612-621; Xiao, W.; Hu, C.; Ward, M.D. *J. Am. Chem. Soc.*

- 2014**, *136*, 14200-14206; Lusi, M.; Barbour, L.J. *Angew. Chem.*, **2012**, *124*, 3994-3997
- 56) Koito, Y.; Yamada, K.; Ando, S. *J. Incl. Phenom. Macrocycl. Chem.* **2013**, *76*, 143-150
- 57) Nassibeni, L.; Jacobs, A.; Nohako, K.; Su, H.; Taljaard, J. *Crys. Growth Des.*, **2008**, *8*, 1301-1305
- 58) Schatz, J.; Schildbach, F.; Lentz, A.; Rastatter, S. *J. Chem. Soc., Perkin Trans. 2*, **1998**, 75-77
- 59) Sawada, T.; Hisada, H.; Fujita, M. *J. Am. Chem. Soc.* **2014**, *136*, 4449-4451; Simard, M.; Su, D.; Wuest, J.D. *J. Am. Chem. Soc.* **1991**, *113*, 4696-4698; Choi, H.J.; Suh, M.P. *J. Am. Chem. Soc.* **1998**, *120*, 10622-10628
- 60) Swift, J.; Ward, M.D. *Chemistry of Materials*, **2000**, *12*, 1501-1504
- 61) Ajjaz, A.; Barea, E.; Bharadwaj, P.K. *Crystal Growth and Design*, **2009**, *9*, 4480-4486
- 62) Dewa, T.; Endo, K.; Aoyama, Y. *J. Am. Chem. Soc.* **1998**, *120*, 8933-8940
- 63) A. Beatty, N. Rath, G. Hogan, *Cryst. Growth Des.* **2011**, *11*, 2740; Fischer, M.; Beatty, A. *CrystEngComm*, **2014**, *16*, 7313-7319
- 64) Erra, Loredana; Tedesco, C.; Immediata, I; Gregoli, L.; Gaeta, C.; Merlini, M.; Meneghini, C.; Brunelli, M.; Fitch, A.N.; Neri, P. *Langmuir*, **2012**, *28*, 8511-8517
- 65) de Luis, R.F.; Urtiaga, M.K.; Mesa, J.L.; Larrea, E.S.; Iglesias, M.; Rojo, T.; Arriortua, M.I. *Inorganic Chemistry*, **2013**, *52*, 2615-2626
- 66) Matsuda, R.; Kitaura, R.; Kitagawa, S.; Kubota, Y.; Kobayashi, T.C.; Horike, S.; Takata, M. *J. Am. Chem. Soc.* **2004**, *126*, 14063-14070; Hollingsworth, M.D.;

- Brown, M.; Dudley, M.; Chung, H.; Peterson, M.; Hillier, A.C. *Angewandte Chemie, Int. Ed.* **2002**, *41*, 965-969
- 67) le Roex, T.; Nassimbeni, L.; Weber, E. *New Journal of Chemistry* **2008**, *32*, 856-863
- 68) Nassimbeni, L.; Su, H. *New J. Chem.* **2002**, *26*, 989-995
- 69) Warren, J.E.; Perkins, C.G.; Jelfs, K.E.; Boldrin, P.; Chater, P.A.; Miller, G.J.; Manning, T.D.; Briggs, M.E.; Stylianou, K.C.; Claridge, J.B.; Rosseinsky, M.J. *Angewandte Chemie*, **2014**, *53*, 4592-4596; Nassimbeni, L.; Weber, E.; Roex, T., *New J. Chem.* **2008**, *32*, 856-863; Nassimbeni, L.; Su, H. *New J. Chem.* **2002**, *26*, 989-995; K. Endo, T. Koike, T. Sawaki, O. Hayashida, H. Masuda, Y. Aoyama, *J. Am. Chem. Soc.* **1997**, *119*, 4117-4122
- 70) Pigge, F.C.; Ghasedi, F.; Zheng, Z.; Rath, N.; Nichols, G.; Chickos, J. *J. Chem. Soc., Perkin Trans. 2*, **2000**, 2458-2464
- 71) Gomes, R.; Parola, A.J.; Bastkowski, F.; Polkowska, Klarner *J. Am. Chem. Soc.* **2009**, *131*, 8922-8938
- 72) Yamamoto, A.; Hamada, T.; Hisaki, I.; Miyata, M.; Tohnai, N. *Angewandte Chemie, Int. Ed.* **2013**, *52*, 1709-1712
- 73) Klosterman, J.K.; Iwamura, M.; Tahara, T.; Fujita, M. *J. Am. Chem. Soc.* **2009**, *131*, 9478-9479
- 74) Khatua, S.; Goswami, S.; Biswas, S.; Tomar, K.; Jena, H.S.; Konar, S. *Chem. Mater.* **2015**, *27*, 5349-5360
- 75) Mugridge, J.S.; Szigethy, G.; Bergman, R.G.; Raymond, K.N. *J. Am. Chem. Soc.* **2010**, *132*, 16256-16264; Marquez, C.; Hudgins, R.R.; Nau, W.M. *J. Am. Chem.*

Soc. **2004**, *126*, 5806-5816; Scarso, A.; Onagi, H.; Rebek, J. *J. Am. Chem. Soc.* **2004**, *126*, 12728-12729; Leung, D.H.; Bergman, R.G.; Raymond, K.N. *J. Am. Chem. Soc.* **2006**, *128*, 9781-9797; Kirchoff, P.D.; Dutasta, J.P.; Collet, A.; McCammon, J.A. *J. Am. Chem. Soc.* **1997**, *119*, 8015-8022; Mugridge, J.S.; Zahl, A.; van Eldik, R.; Bergman, R.G.; Raymond, K.N. *J. Am. Chem. Soc.* **2013**, *135*, 4299-4306; Nuwaysir, L.M.; Castoro, J.A.; Yang, C.; Wilkins, C.L. *J. Am. Chem. Soc.* **1992**, *114*, 5748-5751; Jiang, W.; Rebek, J. *J. Am. Chem. Soc.* **2012**, *134*, 17498-17501; Liu, S.; Russell, D.H.; Zinne, N.F.; Gibb, B.C. *J. Am. Chem. Soc.* **2013**, *135*, 4314-4324; Bolliger, J.L.; Ronson, T.K.; Ogawa, M.; Nitschke, J.R. *J. Am. Chem. Soc.* **2014**, *136*, 14545-14553; Wagner, P.; Nakagawa, Y.; Lee, G.S.; Davis, M.E.; Elomari, S.; Medrud, R.C.; Zones, S.I. *J. Am. Chem. Soc.* **2000**, *122*, 263-273; Turega, S.; Cullen, W.; Whitehead, M.; Hunter, C.; Ward, M.D. *J. Am. Chem. Soc.* **2014**, *136*, 8475-8483; Bilbeisi, R.A.; Clegg, J.K.; Elgrishi, N.; Hatten, X.; Devillard, M.; Breiner, B.; Mal, P.; Nitschke, J.R. *J. Am. Chem. Soc.* **2012**, *134*, 5110-5119; Yaghi, O.M.; Davis, C.E.; Li, G.; Li, H. *J. Am. Chem. Soc.* **1997**, *119*, 2861-2868; Yang, J.; Dewal, M.B.; Profeta, S.; Smith, M.D.; Li, Y.; Shimizu, L.S. *J. Am. Chem. Soc.* **2008**, *130*, 612-621; Belanger, S.; Hupp, J.T.; Stern, C.L.; Slone, R.V.; Watson, D.F.; Carrell, T.G. *J. Am. Chem. Soc.* **1999**, *121*, 557-563; Halder, G.J.; Kepert, C. *J. Am. Chem. Soc.* **2005**, *127*, 7891-7900; Holman, K.T.; Martin, S.M.; Park, D.P.; Ward, M.D. *J. Am. Chem. Soc.* **2001**, *123*, 4421-4431

76) Webster, C.E.; Drago, R.S.; Zerner, M.C., *J. Am. Chem. Soc.*, **1998**, *120*, 5509-5516

- 77) Jae, J.; Tompsett, G.A.; Foster, A.J.; Hammond, K.D.; Auerbach, S.M.; Lobo, R.F.; Huber, G.W., *Journal of Catalysis*, **2011**, 279, 257-268
- 78) Choudhary, V.R.; Nayak, V.S.; Choudhary, T.V., *Ind. Eng. Chem. Res.*, **1997**, 36, 1812-1818
- 79) Pan, S.; Mandal, S.; Chattaraj, P.K. *J. Phys. Chem. B* **2015**, 119, 10962-10974
- 80) Branchi, B.; Balzani, V.; Ceroni, P.; Kuchenbrandt, M.C.; Klarner, F.G.; Blaser, D.; Boese, R. *J. Org. Chem.* **2008**, 73, 5839-5851
- 81) Shi, M.W.; Thomas, S.P.; Koutsantonis, G.A.; Spackman, M.A. *Crystal Growth and Design* **2015**, 15, 5892-5900
- 82) Meccozi, S.; West, A.P.; Dougherty, D.A. *Proc. Natl. Acad. Sci.* **1996**, 93, 10566-10571; Naray-Szabo, G.; Ferenczy, G.G. *Chem. Rev.* **1995**, 95, 829-847; Klarner, F.G.; Kahlert, B. *Acc. Chem. Res.* **2003**, 36, 919-932; Kamieth, M.; Klarner, F.G.; Diederich, F. *Angew. Chem. Int. Ed.* **1998**, 37, 3303-3306; Klarner, F.G.; Panitzky, J.; Preda, D.; Scott, L.T.; *J. Mol. Model.* **2000**, 6, 318-327; Branchi, B.; Balzani, V.; Ceroni, P.; Kuchenbrandt, M.C.; Klarner, F.G.; Blaser, D.; Boese, R. *J. Org. Chem.* **2008**, 73, 5839-585; Medhi, C.; Mitchell, J.B.O.; Price, S.L.; Tabor, A.B. *Biopolymers*, **1999**, 52, 84-93; Meyer, E.A.; Castellano, R.K.; Dierderich, F. *Angew. Chem. Int. Ed.* **2003**, 42, 1210-1250; Aakeroy, C.B.; Wijethunga, T.K.; Desper, J. *New J. Chem.* **2015**, 39, 822-828

Chapter 2

Solid Phase Microextraction (SPME) combined with TGA as a Technique for Guest Analysis in Crystal Engineering

2.1 Abstract

A method has been developed to extract evolved guest molecules from a TGA exhaust stream using solid phase microextraction fibers (SPME). The study was conducted using a known hydrogen bonded framework consisting of $\text{Zn}(\text{HPDCA})_2 \cdot (\text{H}_2\text{O})_2$ and *o*-tolidene which has been shown to contain guest molecules. These guests co-crystallize inside the 1-D channels formed during the self-assembly of the hydrogen bonded framework. Single guest, as well as mixed-guest-containing host frameworks, have been analyzed using this method. Guest molecules extracted in this fashion were successfully characterized using gas chromatography and mass spectrometry without the necessity of coupled TGA/GCMS.

2.2 Background

Examples of supramolecular frameworks held together through charge-assisted hydrogen bonding have been previously made in our laboratory using Cu(II), Co(II) and Ni(II) complexes that contain peripheral carboxylic acid functional groups.¹ The diamine frameworks are based on previous work in which mono-amine structures formed close-packed layered compounds.² Use of diamines affords very robust hydrogen-bonded frameworks having channels that are desirable for the study of host-guest chemistry.³ Studying frameworks of this nature is compelling as they have the potential to be used for gas storage, separations, or potential catalysts.^{4,5,6} It has been shown that networks can be formed that contain guest molecules by combining equimolar amounts of $\text{Zn}(\text{2,4-pyridinedicarboxylic acid})_2$ and 3,3'-dimethylbenzidine (*o*-tolidene) (Fig. 2.2.1).³

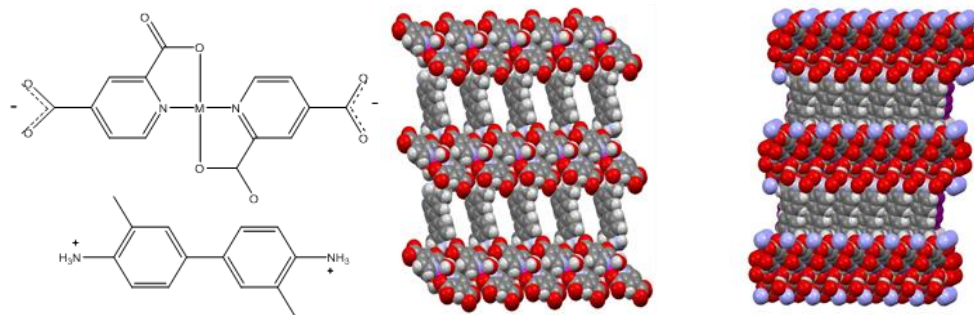


Figure 2.2.1 Representation of the zinc complex plus dimethylbenzidine which forms the layers and pillars of the framework, 1

These frameworks reproducibly form hydrogen-bonded lamellar networks similar to those reported for other charge-assisted hydrogen-bonded frameworks, such as guanidinium sulfonates or trimesic acid plus amines.^{7,8} Crystalline frameworks become host-guest materials when bridging hydrogen bonded components are used as pillars.^{5,9} In our case, the zinc(II) dicarboxylate combines with diammonium pillars, which are far enough apart to allow small molecule guests, such as toluene and hexanol, to be present in channels.³ The walls of the channels are close-packed so that molecular transport can occur only in one-dimensional (significant for transport across membranes, Fig. 2.2.2).



Figure 2.2.2 Diagram of one-directionality of the channels within the hydrogen bonded framework where the guest molecules reside.

We have shown the framework to be stable to guest removal and re-uptake, and are interested in guest selectivity when multiple guests are in competition with each other in solution. Therefore, a technique which not only shows the change in weight upon guest loss (TGA) but also the identity of the guest that evolves in specific temperature ranges is

ideal.¹⁰ However, for labs not equipped with tandem TGA/MS, this can be a challenge.^{11,12}

In the past, several techniques have been used to determine the identity of guest molecules in host-guest crystalline materials. If the crystals are soluble in a suitable solvent, the guests can be identified by proton NMR.¹³ The guest can also be analyzed from the prepared solution as well as the growth solution by gas chromatography.^{14,15} Previously our group has extracted the guest molecule from headspace using a gas tight syringe, and it was then analyzed using GCMS.⁶ Some have reported that a combination of TGA and DSC can be used to determine the host/guest ratio or the dominant guest from prepared competition reactions.¹⁶ It has been shown that the guest can be removed, and the crystal re-solvated with another guest or combination of guests by dipping the crystal and allow solvent guests to permeate the system.¹⁷ When the samples are not soluble in organic solvents, as in the case of MOFs, a variety of techniques can be used, but in fact the MOFs tend to lose guests without heating. In one case, a MOF was digested in basic methanol (NaOH), and UV-Vis absorption was used to determine the concentration of guest dyes in the resulting solution. In the same study, guest uptake into the MOF suspended in a mother liquor solution reduced the concentration of bromoarenes in the mother liquor. The reduced concentration was determined by gas chromatography.¹⁸

Our previous research on the $\text{Zn}(\text{HPDCA})_2 \cdot (\text{H}_2\text{O})_2 / o\text{-tolidine}$ framework, **1**, focused on the synthesis of the framework itself and characterization through methods such as TGA, single crystal X-ray diffraction, and powder X-ray diffraction. The guest was identified by heating the host/guest solid in a closed container fitted with a septum,

and by sampling the headspace with a syringe.^{19,20,21} Injecting the gas into a GC or GCMS allowed the characterization of the guest separate from the TGA analysis. An analyte extraction technique used by researchers in other disciplines, for example, water treatment facilities, forensic laboratories, and artificial flavoring developers is SPME. Using an approach outlined in the literature, we hypothesized that SPME could be used for guest detection by sampling off-gas from the TGA furnace exhaust port.^{22,23}

SPME was invented in 1989 by Janusz Pawliszyn.²⁴ Pawliszyn noted that a modified silica fiber using thermal desorption can eliminate the problems associated with solid phase extraction (SPE) while still retaining the advantages of SPE, which had proved to save lab and analysis time and eliminated the need for the use of solvents in the extraction process.²⁵ Prior to the introduction of SPME, SPE was the alternative to liquid-liquid extraction, because in SPE analytes are absorbed from the sample onto a modified solid support. However, in 1990 SPE required that expensive and time-consuming modifications be made to existing analytical instrumentation. Modifications would have to be made to the GC injector, or a desorption module would be needed.²⁶ SPE had other complications including large variations in the quality of SPE cartridges made by different manufacturers. SPE cartridges were made of plastic, which allowed it to absorb other analytes, giving greater opportunity for interference. SPME, on the other hand, can be seen as an extension of laser desorption from fused silica fibers, since they are made from fused silica fibers which have been coated with a specific thickness of polymer to extract analytes from headspace or aqueous solution.²⁷ The insertion needle is made of metal, so unlike the SPE cartridge, the entire coated section of SPME fiber is exposed to

the high temperatures of the injection port. Proper thermal desorption technique prevents carry over between samples.

SPME analysis has two fundamental steps to the technique. In the first step, the analytes are partitioned between both the sample matrix and the extraction phase. This is followed by desorption of those analytes into the analytical instrument, typically an injection port. It is currently and commonly used manually with GC, GCMS, HPLC and LCMS instruments with no additional changes made to the instrument other than a 23 or 24-gauge injection liner (GC applications, dependent on the needle size). If available, SPME can be used with a headspace autosampler.

Since SPME is mostly used as a headspace method, it is only able to analyze the molecules which are in equilibrium between the analyte in the sample, in the headspace above the sample and in the polymer coating on the fused silica fiber. While there is an equilibrium step, it need not be exhaustive. The rate determining step of SPME is either diffusion of the analyte from SPME polymer film surface into its inner layers or evaporation of the analyte from the condensed phase to the headspace of a sealed container.²⁸ Depending on the nature of the polymeric coating of the fiber, SPME can be used to detect hydrophobic or hydrophilic compounds and, in some cases, a modest mixture of the two. A recent review of SPME outlines how the technique has evolved in use and applications.²⁴

For liquid polymeric coatings, the level of analyte absorbed by the coating is directly related to the concentration of the analyte in the sample.²⁹

$$n = \frac{K_{fs}V_f C_0 V_s}{K_{fs}V_f + V_s}$$

where n = mass of the analyte

C_0 = Initial concentration of analyte in the sample

K_{fs} = partition coefficient for analyte between coating and sample matrix

V_f = volume of coating

V_s = volume of sample

More extensive work has been done however to explain the theory and practice of SPME.^{28,30,31} It has been demonstrated that an SPME fiber could be placed directly into the exhaust port of a TGA.^{22,23} The exhaust can contain volatile and semi-volatile molecules which have been released from the sample within the TGA furnace. These molecules are then absorbed by the SPME fiber, which is then placed into the injection port of a GCMS and desorbed for analysis. Using SPME in this fashion can have significant cost savings compared to the expense of coupling MS to a TGA.

As the guest molecules used in our host/guest framework have different characteristics (aromatic compounds, long chain alkyl alcohols, and others), it is important to use SPME fibers that absorb a wide range of molecules. In fact, SPME has a wide range of detection applications. SPME has been used to detect aroma compounds, halogenated volatiles in food, C2-C10 fatty acids in water, sulfur compounds, essential oils in hops, xylenes in palm oil, benzene and toluene in vegetable oil, stereoisomers in pulegone enantiomers, flavors in vodka, methylcyclopentadienyl manganese tricarbonyl in beverages, pesticides in wine, trichloroanisole in wine, organophosphorus pesticides,

selenium compounds, PCBs, methylmercury in fish, and insecticides and pheromones to name a few.^{32,33-46}

The coatings used in making the SPME fibers define which guests can be absorbed. The fibers have been modified through the use of metal fibers comprised of either platinum, stainless steel, or copper metal rather than fused silica due to the increased mechanical strength.⁴⁷ New coatings have been developed by building metal organic framework (MOF) coatings onto the metal wires. These new MOF coatings can be highly porous and thus increase sensitivity as well as selectivity compared to commercial coatings. These modified coatings have been used to detect benzene derivatives, organochlorine pesticides and other analytes of interest.^{48,49,50,51}

In crystal engineering, especially with host/guest systems, obtaining a good quality crystal can be a painstaking and lengthy process. Once a crystal has grown, decisions must be made on how to analyze it. The addition of SPME to the crystal engineer's toolkit allows for a non-destructive way to analyze small amounts of guest molecules as they evolve from a stable host framework. This allows the crystal to be further analyzed for any changes in internal arrangement and structure once the guest has been removed, rather than requiring the dismantling of the framework to analyze the guests. SPME used in conjunction with TGA allows the identification of guests that evolve over certain temperature ranges. Both are of interest when considering host-guest frameworks that are stable to hundreds of degrees Celsius.

2.3 Introduction

We have used a combination of thermogravimetric analysis (TGA) and solid phase microextraction fibers (SPME) to determine the identity of guest species that are freed from molecular framework hosts, as well as the temperature at which the guests evolve. While SPME has been used in other disciplines (such as for food and pesticide analysis), it has so far not been used by crystal engineers for identification of guest species. This method may be useful for those who do not have ready access to tandem TGA/GCMS for guest analysis.

2.4 Experimental

SPME fibers were purchased from Sigma Aldrich Chemical Company (Supelco). The 100 μm polydimethyl siloxane (PDMS) coated SPME fiber (Supelco, Cat# 57300-U), 7 μm PDMS coated SPME fiber (Supelco, Cat#57302) and the 85 μm polyacrylate (PA) coated SPME fiber (Supelco, Cat# 57305) were used. ZnCl_2 (>97%) was purchased Fisher Scientific. Toluene, m-xylene, and 1,3-diethylbenzene were reagent grade and purchased from Sigma Aldrich. O-Tolidine (>97%) was purchased from Sigma Aldrich Chemical Company. 2,4-pyridine-dicarboxylic acid (98%) was purchased from AK Scientific. Methanol was reagent grade from Sigma Aldrich Chemical Company. Dimethylformamide (anhydrous, 99.8%) was purchased from Fisher Scientific. TGA plots were collected using a Thermal Advantage TGA Q50 (TA Instruments), and TA Universal Analysis software was used to generate plots and analyze the output data. XRD patterns were collected on a Rigaku Ultima IV X-ray diffractometer containing a $\text{CuK}\alpha$ source ($\lambda = 1.54051 \text{ \AA}$) and viewed with MDI Jade 9 software. An HP gas chromatograph 5890 and HP gas chromatography-mass spectrometer 5988A were used to collect all chromatographic data. For GC/GCMS method development, the isolated

crystals were placed inside of a 20mL GC headspace vial (Xpertek, PJ. Cobert, Cat#954040) with a high temperature rated septa within the cap (Xpertek, PJ. Cobert, Cat#952237). All chemical reactions were carried out under ambient conditions.

2.4.1 Synthesis of **1**·guest

The Zn (II) metal complex was synthesized by combining ZnCl₂ (0.0146 moles, 2g) in 40mL of D.I. water and 2,4-pyridinedicarboxylic acid (0.0293 moles, 4.9g) in 400 mL of a 1:1 ratio of D.I. water and methanol. The resulting suspension was filtered through a Buchner filter funnel and paper filter. The white slurry was washed with D.I. water until the mother liquor tested pH neutral. The product was allowed to dry on the funnel and then air dried overnight. The resulting product was Zn(HPDCA)₂·(H₂O)₂. The Zn(HPDCA)₂·(H₂O)₂ (0.06 moles, 0.025g), and 3,3'-dimethylbenzidine (0.06mole, 0.012g) were separately dissolved in 2mL each of methanol. The two methanol solutions were then mixed together and stirred and a 1:1 mixture of water (1mL) and DMF (1mL) was then added. The guest molecule, in this case, toluene, was added in excess. In most instances, the guest molecule(s) was added to a 15mL glass vial and the methanol solution of components of the framework were added on top. Crystals of the neutral framework [1,(3,3'-dimethylbenzylidinium) (Zn(PDCA)₂·(H₂O)₂)] then grew from the resulting solution. The **1**·toluene crystals are brownish-red haystacks. Once crystal growth had ceased, the resultant crystals were washed in the glass vial with methanol (1x), then acetone (2x) and then dried under vacuum to remove any remaining surface residues which might bias the results. Samples were then analyzed using powder x-ray diffraction scanning from 2° to 40° in 2θ.²

2.4.2 Chromatographic Methods

In order to determine the GC/GCMS parameters, **1**·toluene (0.010g) crystals were heated to 200°C, which evolved all of the guest molecules being tested (temperature from TGA data). 200°C was also used as the upper limit because **1** decomposes at around 215°C. The 100 µm PDMS-coated SPME fiber was inserted and was allowed to absorb the guest molecules in the headspace for a period of two minutes. The SPME fiber was then placed into the injection port of a GCMS, and the mass data was collected for each of the eluted species. No traces of acetone or methanol were seen in the chromatography, though sometimes DMF would elute around 2.00 minutes. DMF seems to co-crystallize in small amounts. The standalone GC was only used for initial aspects of **1**·toluene analysis. The GC oven temperature was initially 30°C for 3.0 minutes, then ramped to 150°C at a rate of 20°C/min and held for 1.0 minute. The injection port temperature was 250°C. The total analysis time was 10.50 minutes. The retention times were slightly longer since the GC used an 15m SPB-1 column, 10µm film thickness, 0.2mm ID, bonded, 100% dimethyl siloxane stationary phase. GCMS guest determinations were performed using an 11m HP-1 Ultra column, with a 0.2mm I.D x 0.33µm film.

2.4.3 SPME Coupled TGA

For SPME/TGA analysis, the coated SPME fibers were used to identify toluene, m-xylene and 1,3-diethylbenzene guests. Using the SPME fibers, we were able to isolate each of the guests from the TGA exhaust port while **1**·guest was heated. The TGA provided insight into the temperatures at which the guest molecules were evolving out of **1** (Fig. 2.4.3.1). Using a similar method to that of Biswas *et al.*, an SPME fiber was used in conjunction with the TGA to discern the guest molecule being evolved from the framework.^{19,20} The TGA was programmed to jump to 40°C and perform an isotherm for

three minutes. Although no evidence of residual toluene had been found from room temperature head-space injections, this step was purposefully done to ensure that no residual solvent was left on the surface of the crystal. Once the isotherm was complete, the SPME fiber was placed in front of the TGA exhaust port. The plunger on the fiber holder was depressed so that the SPME fiber fully extended into the exhaust port, but did not touch the inside of the port walls. A heating ramp began, and the temperature was increased at a rate of 10°C/min. The fiber was allowed to absorb the off-gas from the TGA until 145°C, past the peak seen in the TGA graph expected to be toluene. The fiber was quickly transferred to the GC and inserted into the injection port where the SPME fiber was allowed to desorb and the guest molecule eluted through the SPB-1 column. **1** continued to ramp to a final temperature of 550°C.

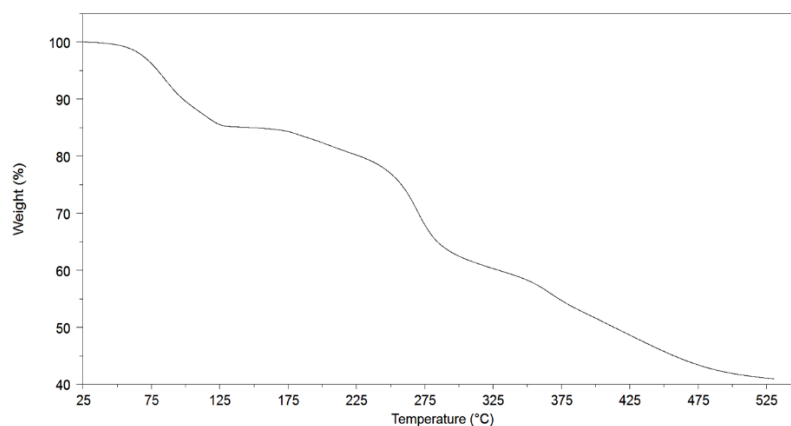


Figure 2.4.3.1 TGA plot of $\text{Zn(HPDCA)}_2 \cdot (\text{H}_2\text{O})_2$ plus o-tolidine framework containing toluene guest from 40°C to 550°C at a heating rate of 10°C/min

2.5 Results and Discussion

The crystals of **1**·toluene were analyzed using SPME fibers to absorb guest molecules from the TGA, with both GC alone and GCMS. In the GC analysis, the resultant chromatogram showed a sharp peak at 4m 27s (Peak Area = 555187). To ensure that the toluene was being detected, a stock solution of toluene in methanol was run to determine the retention time under the current GC conditions. Toluene eluted with a sharp peak at 4m 25s (Peak Area = 4518843). This confirmed that toluene was not only evolving from the framework, but being captured by the SPME fiber from the exhaust gas of the TGA.

In the GCMS analysis, the fiber was inserted into the GCMS and allowed to desorb. A peak was seen at 2m 61s (Peak Area = 1313133), and the corresponding fragmentation pattern was consistent with toluene (NIST database). The retention time changed due to the shorter column length. To our knowledge, this would be the first example of an SPME fiber extracting guest molecules from a hydrogen-bonded framework using TGA off-gas.

The TGA plot shows a very gradual onset for the weight change, so a different technique was used to determine a more definitive temperature range for guest evolution. In this case, the sample was placed in a vial equipped with a septum and heated to a precise temperature using a heating block. The vial was placed in a well of a heating block set to 40°C. The sample was allowed to heat for 10 minutes. During the last two minutes, the fiber was exposed to the headspace and then inserted into the GCMS and allowed to desorb at 250°C. There was no evidence found in the chromatogram, nor the

mass spectrum data of toluene evolving from the host. The temperature of the block was increased by 10°C until 120°C was reached (Table 2.5.1).

Table 2.5.1 Measured peak areas for 1-toluene detection during step-wise temperature gradient

Heating Block Temperature (°C)	Peak Area (Abundance)	Post Purging Peak Area (Abundance)
40	ND	
50	ND	
60	Detect	
70	Detect	
80	Detect	
90	Detect	
100	Detect	
110	Detect	Detect
120	Detect	ND

It can be seen that the onset temperature where toluene first becomes detectable is around 60°C. For each temperature set point tested, a clean, new vial was used, and a fresh crystal sample was tested. The average crystal weight was 20mg for each of the samples. The only guest peak that appeared throughout this temperature range was identified as toluene, whose retention time was based on standard injections. The peak area fluctuated as several 7µm PDMS fibers were used in this series. The 7µm fibers tended to be more fragile than the other fibers used in previous experiments. Other experiments have shown dimethylformamide present in the chromatography. It is not surprising since DMF is part of the crystal growth solution and some may become co-crystallized as well.

The temperature of the multi-well heating block was again set to 120°C and sampled using the same procedure as before. The SPME syringe was immediately inserted into the GCMS and allowed to desorb while the sample vial was cooled to room

temperature using a stream of compressed air. Once the sample was cool, the vial was purged with nitrogen for 1 minute. The cap was replaced, and the vial positioned back on the heating block at 120°C. The SPME fiber was then exposed to the headspace for 10 minutes. After 10 minutes, the fiber was removed and inserted into the GCMS. No guest was detected at 120°C after purging. The temperature was then reduced to 110°C and the heating, cooling, purging and injection cycle was repeated. The toluene guest was detected after the purge when the temperature of the block was 110°C (Table 2.5.1). The presence of the guest in the headspace post purging tells that at lower temperatures, not all of the guest is released. There is potential for partial release of the guest within a specific temperature range. The crystal could then be held for a period of time while part of the initial guest concentration is stored and released at a later date.

While the purge cycle sheds some light on the release of the guest from the framework, there is still a tail from the TGA plot around 130°C. The TGA/SPME method had to be revisited to be sure of the final temperature of guest release. An 85µm polyacrylate fiber (PA) was used for this test because it has lower detection limits for toluene than PDMS. The PA fiber has higher response factor than 7µm PDMS or even 100µm PDMS. Peaks will have a higher area count in the GC chromatograph. As can be seen in Table 2.5.2, the peak area does increase during exposure.

Table 2.5.2 Measured data for 1-toluene from the TGA and GCMS using 85 μ m PA SPME fiber.

Crystal Wt (mg)	Initial Temp of Fiber Exposure ($^{\circ}$ C)	Peak Area (Abundance)	Residence Time (Mins)	TGA, Wt Diff 40-145 $^{\circ}$ C (%)	TGA, Wt Diff (%) Extraction Temp to 145 $^{\circ}$ C
22.565	40	1313133	10.5	12.25	12.25
24.970	100	1004544	4.5	11.55	5.626
24.366	110	679366	3.5	11.83	4.030
21.337	120	389800	2.5	11.97	2.687
23.017	130	151190	1.5	11.65	1.494
22.577	140	173877	5	14.98	3.141

Does the amount of guest loss based on TGA weight change correspond to the peak area shown in the GCMS study? To answer this question, the weight difference from the TGA for the temperature range of 100-130 $^{\circ}$ C was plotted against the peak area. Here we see a linear response with an R^2 value of 0.9957 (Figure 2.5.1).

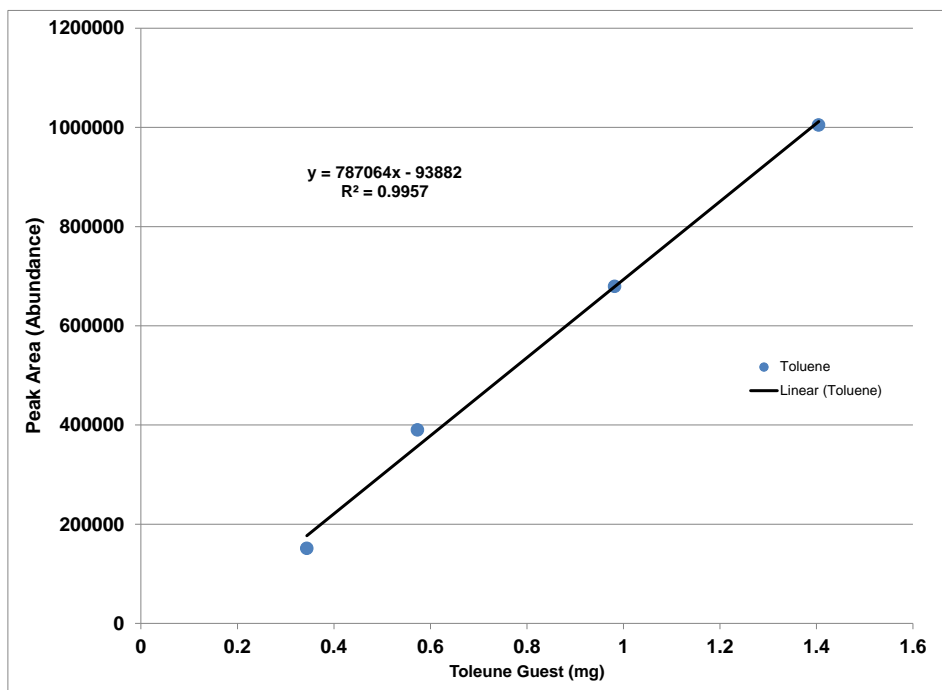


Figure 2.5.1 Plot of toluene guest TGA weight versus peak area

Considering how the guest was sampled, the linearity is impressive, demonstrating that the SPME technique is not only qualitative but also can determine relative quantities of guests. Having the ability to have the off-gas sampled from the TGA correlate with a change in concentration can have a significant impact on future studies. It would be interesting to detect the overall concentration of guest for each TGA event. While sampling, there was no disturbance of the TGA itself, thus yielding usable TGA data as well as GCMS data. An attempt was made to use an A-2 Luer gas-tight headspace syringe to sample the off-gas from the TGA and compare the results to the SPME fiber. Not only was there no evidence of the guest in the chromatogram, but a significant noise signal could be seen in the TGA when the gas sample was pulled. Using the headspace syringe contaminated the TGA data whereas the SPME fiber left no trace that any sampling had been performed.

1·m-xylene/1,3-diethylbenzene were tested in the same manner as **1**·toluene using the TGA/SPME method. The crystals used here were part of a series of competition reactions in which the guest molecules were added at different mole fractions over a series of 11 experiments. For this determination, the framework was assembled using the same previously mentioned synthetic pathway, however; mole fractions of m-xylene ($\chi_A = 0.4$) and 1,3-diethylbenzene ($\chi_B = 0.6$) were placed in the growth solution rather than a single potential guest molecule. As the crystal grows, the preferred guest will be the predominant species in the host cavities. Once the crystal was isolated from the growth solution, the crystals were washed, dried and then placed in the TGA for analysis. In the same manner, as the toluene experiment, the crystal was held isothermally for three minutes to ensure that no residual solvent was left of the surface of the crystal. Once the

isothermal period was complete, an SPME fiber with 85 μ m PA coating was placed in front of the exhaust port and the fiber exposed. A PA SPME fiber was chosen since its response factor is an order of magnitude larger than that of 100 μ m PDMS for xylenes. The same TGA program was run for all three samples. The fiber was quickly transported to and inserted into the GCMS rather than the stand-alone GC to differentiate between the guests.

Competition studies between *m*-xylene and 1,3-diethylbenzene can reveal what types of guest molecules will be dominant inside of the framework. Using crystals from an ongoing competition study between *m*-xylene and 1,3-diethylbenzene, it was determined whether the SPME fiber could absorb multiple guest molecules from the TGA off-gas. The same extraction conditions were set on the TGA as the toluene system using the 85 μ m PA coated fiber. The GCMS parameters were used to determine which of the two possible guests were absorbed by the fiber. Two distinct peaks appeared in the mass spec. The ratio of the areas of the peaks for the two guest molecules show 1,3-diethylbenzene as the dominant guest molecule. More work would have to be done to display the direct correlation between the TGA/SPME results and head-space analysis results.

2.6 Conclusions

We have demonstrated that SPME fibers can be a useful tool for analyzing guest molecules evolved from crystalline frameworks, either by headspace analysis or from TGA off-gas. The non-destructive nature of SPME headspace analysis allows for the framework to remain intact so that the crystal may be used for other studies. This is a great advantage over methods which dissolve the entire crystal. SPME requires little

sample volume for analysis, which is also useful in host/guest crystal systems that are hard to obtain. Using SPME in tandem with the TGA offers an effective option for analyzing guest molecules in conjunction with separate events observed by the TGA, but without the high coupling costs that tandem TGA/GCMS brings. SPME sampling does not contaminate the TGA plot data by creating noise which would make it difficult for accurate weight difference calculations. This method can also help identify guest molecules that might otherwise appear too disordered in XRD. We have shown that not only will SPME assist in the detection of a single guest but also multiple guests from TGA off-gas. It may be possible in the future to isolate separate TGA events to determine the guest from each event.

2.7 References

- 1) Beatty, A.; Chen, C.L. *J. Am. Chem. Soc.* **2008**, *130*, 17222
- 2) Beatty, A.; Helfrich, B.; Hogan, H.; Reed, A. *Cryst. Growth Des.* **2006**, *122*.
- 3) Beatty, A.; Rath, N.; Hogan, G. *Cryst. Growth Des.* **2011**, *11*, 2740
- 4) Yaghi, O. M.; Li, H.; Davis, C.; Richardson, D.; Groy, T. L. *Acc. Chem. Res.* **1998**, *31*, 474.
- 5) Pivovar, A.; Holman, K.; Ward, M. *Chem. Mater.* **2001**, *13*, 3018-3031.
- 6) Endo, K.; Koike, T.; Sawaki, T.; Hayashida, O.; Masuda, H.; Aoyama, Y. *J. Am. Chem. Soc.* **1997**, *119*, 4117-4122.
- 7) Ward, M.; Swift, J. *Chem. Mater.* **2000**, *12*, 6, 1501.
- 8) Zaworotko, M.; Biradha, K.; Dennis, D.; MacKinnon, V.; Sharma, K. *J. Am. Chem. Soc.*, **1998**, *120*, 11894.
- 9) Ward, M.; Custelcean, R.; *Crys, Growth Des.* **2005**, *5*, 6, 227.
- 10) Nassimbeni, L.; Su, H. *J. Chem. Soc. Perkin Trans. 2*, **2002**, 1246.
- 11) Koito, Y.; Yamada, K. *J Incl Phenom Macrocycl Chem* **2013**, *76*, 143-150.
- 12) Schatz, J.; Schildbach, F.; Lentz, A.; Rastatter, S. *J. Chem. Soc. Perkin Trans. 2*, **1998**, 75-77.
- 13) Bajpai, A.; Natarajan, P.; Venugopalan, P.; Moorthy, J. *J. Org. Chem.*, **2012**, *77*, 7858-7865.
- 14) Nassimbeni, L.; Weber, E.; Roex, T. *New J. Chem.* **2008**, *32*, 856;
Nassimbeni, L.; Su, H. *New J. Chem.* **2002**, *26*, 989-995.
- 15) Nassimbeni, L.; Jacobs, A.; Nohako, K.; Su, H. Taljaard, J. *Cryst. Growth Des.*, **2008**, *Vol 8 (4)*, 1301.

- 16) Jiang, J.; Pan, M.; Liu, J.; Wang, W.; Su, C. *Inorg. Chem.* **2010**, *49*, 10166-10173.
- 17) Chae, H.; Siberio-Perez, D.; Kim, J.; Go, Y.; Eddaoui, M.; Matzger, A.; O'Keiffe, M.; Yaghi, O. *Nature*, **2004**, *427*, 523.
- 18) Cadinael, P.; Peulon-Agasse, V.; Coquerel, G.; Combret, Y.; Combret, J. *J. Sep. Sci.* **2001**, *24*, 109-115.
- 19) Gorbachuk, V.; Tsifarkin, A.; Antipin, I.; Solomonov, B. Konovalov, A. *J. Inc. Phen. and Macro. Chem.* **1999**, *35*, 389-396.
- 20) Safina, G.; Ziganshin, M.; Gubaidullin, A.; Gorbachuk, V. *Org. Biomol. Chem.* **2013**, *11*, 1318.
- 21) Biswas, S.; Staff, C. *Journal of Cereal Science* **2001**, *33*, 223-229
- 22) Krohl, T.; Kastel, R.; Konig, W.; Ziegler, H.; Kohle, H.; Parg, A. *Pestic. Sci.*, **1998**, *53*, 300.
- 23) Pawliszyn, J.; Risticovic, S.; Niri, V.; Vuckovic, D. *Anal Bioanal Chem, B* **2009**, *393*, 781-795.
- 24) Pawliszyn, J.; Arthur, C. *Anal. Chem.* **1990**, *62*, 2145-2148.
- 25) Pankow, J.; Ligocki, M.; Rosen, M.; Isabelle, L.; Hart, K. *Anal. Chem.* **1988**, *60*, 40-47.
- 26) Pawliszyn, J.; Liu, S. *Anal. Chem.* **1987**, *59*, 1475-1478.
- 27) Ai, J. *Anal. Chem.* **1997**, *69*, 3260-3266.
- 28) Bulletin 923, Supelco T198923.
- 29) Ulrich, S. *J. Chromatography A*, **2000**, *902*, 167-194.

- 30) Servos, M.; Pawliszyn, J.; Metcalfe, C.; Wen, J.; Luong, D.; Oakes, K.; Zhang, X. *Anal. Chem.* **2010**, *82*, 9492-9499.
- 31) a) Kataoka, H.; Lord, H.; Pawliszyn, J. *Journal of Chromatography A*, **2000**, *880*, 35-62; (b) Barrio, R. J.; Goicolea, M. A.; Millan, S.; Rodriguez, E.; Sampedro, M. C.; Unceta, N. *Journal of Chromatography A*, **2003**, *995 (1-2)*, 135-142; Pan, C. L.; Adams, M.; Pawliszyn, J. *Anal. Chem* **1995**, *67(23)*, 4396-4403; (d) Murray, R. A. *Anal. Chem B*, **2001**, *73(7)*, 1646-1649; (e) Kovacevic, M.; Kac, M. *J. Chromatogr A*, **2001**, *918*, 159-167; (f) Asakawa, F.; Jitsunari, F.; Choi, J.; Suna, S.; Takeda, N.; Kitamado, T. *Bull. Environ. Contam. Toxicol* **1999**, *62(2)*, 109-116; (g) He, Y.; Wang, Y.; Lee, H. *J. Chromatogr. A*, **2000**, *874(1)*, 149-154; (h) Asafu-Adjaye, E.; Shiu, G. *J. Mass Spectrom.*, **1997**, *32(11)*, 1195-1204; (i) Ng, L.; Hupe, M.; Harnois, J.; Moccia, D. *J. Sci. Food Agric.* **1996**, *70*, 380-388; (j) Rodriguez-Bencomo, J.J.; Conde, J.E.; Rodriguez Delgado, M.A.; Garcia-Montelongo, F.; Perez-Trujillo, J.P. *J. Chromatogr. A*, **2002**, *963(1-2)*, 213-223; (k) Fisher, C.; Fischer, U. *J. Agric. Food Chem.* **1997**, *45*, 1995-1997; (l) Fernandez, M.; Padron, C. L.; Marconi, R.; Colombo, R.; Ghinie, Sabatini, S.; A.; Girotti, S. *J. Chromatogr. A*, **2001**, *922(1-2)*, 257-265; (m) Caruso, J. A.; Bryson, J. M.; Meija, J.; Montes-Bayon, M.; Vonderheide, A. P. *Journal of Agricultural and Food Chemistry*, **2003**, *51 (17)*, 5116-5122; (n) Yang, L.; Colombini, V.; Maxwell, P.; Mester, Z.; Sturgeon, R.E. *Journal of Chromatography, A*, **2003**, *1011 (1-2)*, 135-142; (o) Alix, A.; Collot, D. Nenon, D. J. Anger, J.

- Anal. Chem*, **2001**, 73(13), 3107-3111; (p) Rasmussen, L. E. L.; Lee, T. D.
Zhang, A.; Roelofs, W. L.; Daves Jr., G. D. *Chem. Senses*, **1997**, 22, 417-437.
- 32) Kataoka, H.; Lord, H.; Pawliszyn, J. *J. Chromatography A*, **2000**, 880, 35-62.
- 33) O'Reilly, J.; Wang, Q.; Setkova, L.; Hutchinson, J.; Chen, Y.; Lord, H.;
Linton, C.; Pawliszyn, J. *J. Sep. Sci.*, **2005**, 28, 2010-2022.
- 34) Ferreira, S. dos Santos, W.; Quintella, C.; Neto, B.; Bosque-Sendra, J. *Talanta*
2004, 63, 1061-1067.
- 35) Pawliszyn, J.; Zhang, Z. *Anal. Chem.* **1995**, 67, 34-43.
- 36) Pawliszyn, J.; Chen, Y. *Anal. Chem.* **2006**, 78, 5222-5226.
- 37) Pawliszyn, J.; Hosseinzadeh, S.; Ghiasvand, A. *J. Chromatography A*, **2006**,
1124, 35-42.
- 38) Ding, T.; Landrum, P.; You, J.; Harwood, A.; Lydy, M. *Envir. Toxic. Chem.*
2012, 31 (9), 2159-2167.
- 39) Pragst, F. *Anal Bioanal Chem* **2007**, 388, 1393-1414.
- 40) Pragst, F.; Spiegel, K.; Sporkert, F.; Bohnenkamp, M. *Forensic Science*
International, **2000**, 107, 201-223.
- 41) Pawliszyn, J.; Mousavi, F. *Analytica Chimica Acta*, **2013**, 803, 66-74.
- 42) Yang, Z.; Zeng, E.; Maruya, J.; Mai, B.; Ran, Y. *Chemosphere*, **2007**, 66,
1408-1414.
- 43) Francioso, O.; Rodriguez-Estradada, M.; Montecchio, D.; Salomoni, C.;
Caputo, A.; Palenzona, D. *J. Haz. Mat.*, **2010**, 175, 740-746.
- 44) Richardson, S. *Anal. Chem.*, **2003**, 75, 2831-2857.
- 45) Walker, V.; Mills, G. *J. Chromatography A* **2000**, 902, 267-287.

- 46) Jiang, S.; Liu, X.; Qiu, H.; Feng, J. *Trends in Anal. Chem.* **2013**, *46*, 44- 58.
- 47) Cui, X.; Gu, Z.; Jiang, D.; Li, Y.; Wang, H.; Yan, X. *Anal. Chem.* **2009**, *81*, 9771-9777.
- 48) Rahimi, A.; Hashemi, P.; Badiei, A.; Arab, P.; Ghiasvand, A. *Analytica Chimica Acta*, **2011**, *695*, 58-62.
- 49) Li, G.; Du, Z.; Zhang, S. *Talanta*, **2013**, *115*, 32-39.
- 50) Xu, J.; Zheng, J.; Tian, J. Zhu, F.; Zeng, F.; Su, C.; Ouyang, G. *Trends in Anal. Chem.* **2013**, *47*, 68-83.

Chapter 3

Guest Preference Studies to Determine Selectivity of a Hydrogen Bonded Host Framework: A Competition Between Guests of Different Size and Shape

3.1 Abstract

Our group has previously demonstrated that $\text{Zn(HPDCA)}_2 \cdot (\text{H}_2\text{O})_2$ and o-tolidene will assemble into a robust porous framework using charge-assisted hydrogen bonds. This host framework can co-crystallize pairs of guest molecules. Experimentation has shown that porous materials held together by hydrogen bonds will separate molecules. This framework's ability to separate guest molecule pairs has been explored to demonstrate its selectivity towards specific guest molecules. Using headspace gas chromatography to measure relative occupancy, we focused on how selectivity changes based on size and shape of the guest molecules. For size and shape comparison, we have narrowed our study to that of xylenes and diethylbenzenes. The effect on selectivity by the framework based on size was determined by comparing guests with methyl groups versus guests with ethyl groups. For the shape, we used guests whose substituents were in the *meta*-, *ortho*- and *para*- position. The preference of the host framework towards size and shape will be discussed.

3.2 Introduction

Charge assisted hydrogen bonds have been shown to form a flexible framework which also houses guest molecules. Michael Ward *et al.* have numerous publications outlining guanidinium sulfonate frameworks¹ As an example, a material forming a simple brick pattern that collapses upon guest removal is illustrated in Figure 3.2.1.

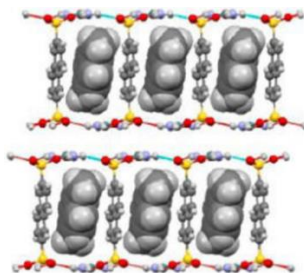


Figure 3.2.1 Guanidinium sulfonate charge-assisted hydrogen bonded frameworks where terminal sulfonates form pillars separating guanidinium layers, Ward *et al.*²

This type of material offers many different design strategies. The tecton units can be changed to make a channel longer or broader, thus adjusting the functionality. These materials capture the guest molecules through co-crystallization rather than adsorption.

A step closer to our framework is a charge-assisted hydrogen bonded material by George Shimizu *et al.* (Figure 3.2.2).³

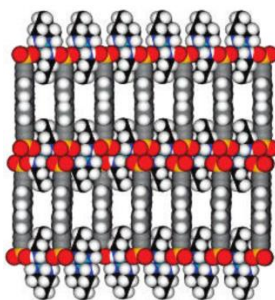


Figure 3.2.2 Permanently porous material, {[Ni(tame)₂]₁(PES)₂}.³ The red atoms are oxygen.

This framework was made from a combination of {[Ni(tame)₂]₁(PES)₂}. The tame is 1,1,1-tris(aminomethyl)ethane and PES is 2-phenylethynesulfonate. Similar charge-assisted hydrogen-bonded compounds were also made by Sevov *et al.* which had guests, but selectivity was not tested.⁴

3.2.1 Guest Molecule Separation Using Host Materials

Separation science is crucial to the field of chemistry whether for purification or as an analytical tool. According to Nassimbeni, host molecules can be broadly characterized as two main forms.⁵ The first would be those which form molecular complexes by fitting convex guests into the concave cavity.⁵ The form would include many of the carcerands,⁶ cyclodextrins,⁷ calixarenes,⁸ and cavitands⁹ just to name a few. Other organic molecules such as capsules,¹⁰ tweezers,¹¹ and pillarenes¹² have also played as hosts. The second would be hosts which form lattice inclusion compounds and allow for cavities,¹³ channels,¹⁴ and layers¹⁵ allowing for the inclusion of guests.⁵ Host can also form from metal-organic frameworks¹⁶ and porous coordination polymers.¹⁷

From 2006-2009, there have been 130 patents awarded for xylene isomer separation.¹⁸ Purification of the *p*-xylene molecule has been the focus of a significant amount of attention since it is the precursor to terephthalic acid. It is the monomer used to produce polyethylene terephthalate used for the manufacture of bottle, films, and fibers.^{19,20} Xylene and diethylbenzene isomers are coating precursors (xylenes isomers),²¹ heat transfer fluids²² or precursors to divinylbenzene which is used to produce crosslinked polystyrene (diethylbenzene isomers).²³ Xylene isomers and other aryl compounds have also been classified as pollutants by the EPA. These molecules are found in rainwater, soil samples, surface water, drinking water and aquatic organisms.²⁴ The separation and isolation of these types of molecules can have an industrial as well as environmental impact.

3.2.1.1 The Separation of Gaseous Species Using Host-Guest Materials

The adsorption or co-crystallization of a guest molecule inside of a host material can be a straightforward but also a selective process. Guest-containing materials can easily entrap some guests while others are entirely occluded.

Gas separations are important on the front and back end of many industrial chemical processes. Inclusion compounds, having a variety of cavity sizes, channels, and pores are capable of separating gases from solution. A calixarene was created which can store methane at temperatures well above its boiling point and at low pressures.²⁵ Cyclodextrins have been shown to bind with Cl₂, Kr, Xe, O₂, CO₂, C₂H₄, CH₄, C₂H₆, and C₄H₁₀ while in an aqueous environment.²⁶ Cryptophane-111 can be size and shape selective to simple gaseous hydrocarbons thus separating them.²⁷ O₂, N₂, CO₂, and Xe in organic solution have been encapsulated by hemicarcerands.²⁸ A self-assembled hydrogen bonded capsule demonstrated selectivity towards methane and nitrogen.²⁹

Metal-organic frameworks (MOFs) have performed gas separations. Kitagawa *et al.* have been able to develop a flexible MOF to selectively absorb CO₂ over acetylene, a difficult task due to the two gases similarities in molecular size, shapes, and sorption parameters.³⁰ Flexible MOFs have been shown to separate N₂/O₂ combinations.³¹ Flexible MOFs can effectively “breathe” or demonstrate structural deformations; this can lead to greater selectivity between gas molecules such as O₂ and N₂.³²

Hydrogen bonded materials are useful for gas separations as well. The flexibility of the material increases the selectivity of the hydrogen bonded framework. Flexible microporous hydrogen bonded organic framework will selectively absorb carbon dioxide over acetylene, methane and nitrogen.³³ Shimizu’s permanently porous framework, held

together by charge-assisted hydrogen bonds, demonstrated reversible CO₂ and N₂ absorption.³

3.2.1.2 Host-Guest Materials Capable of Small Molecule Separation

The separation and purification of small molecules is important for synthetic precursors as well as final products. Many manufactured products are reliant on high purity monomers as a starting material. Many of these are low molecular weight hydrocarbon and aromatic compounds. Inclusion compounds have been able to separate small aryl molecules through co-crystallization or as a stationary phase. The *para*-, *ortho*, and *meta*-xylene isomers have been separated by co-crystallization based on the size and shape of the molecule.³⁴ Selectivity studies demonstrate inclusion compounds capability of separating a mixture of xylenes through co-crystallization.³⁵ Crown ethers and cyclodextrins have been shown to separate hydrogen and deuterium homologs of small molecules when used in chromatographic columns.³⁶

Soft-materials such as porous coordination polymers have been explored for their small molecule selectivity. Kitagawa demonstrates how in the porous coordination polymer, $\{[\text{Co}(\text{NCS})_2(3\text{-pia})_2]\cdot 4\text{THF}\}_n$, THF molecules are held in the cavities through hydrogen bonding.³⁷ Metal-organic frameworks (MOFs), have also been shown to house and even separate small guest molecules. Their flexible nature and tunability allow for tailoring of the pores and channels which may allow for one guest but not another. Rosseinsky presents an example, $\text{Ni}_2(4,4'\text{-bipyridine})_3(\text{NO}_3)_4$, which readily uptakes toluene but will occlude 1,3,5-triethylbenzene.³⁸ A MOF constructed by Ghosh *et al.* has a flexible linker creates $\{[\text{ZnO}_4(\text{L})_3(\text{DMF})_2]\cdot x\text{G}\}_n$, where L is the flexible ligand and G

represents guest molecules.³⁹ This flexible framework undergoes a structural transformation which gives a nonporous phase (Figure 3.2.1.1).^{39,19}

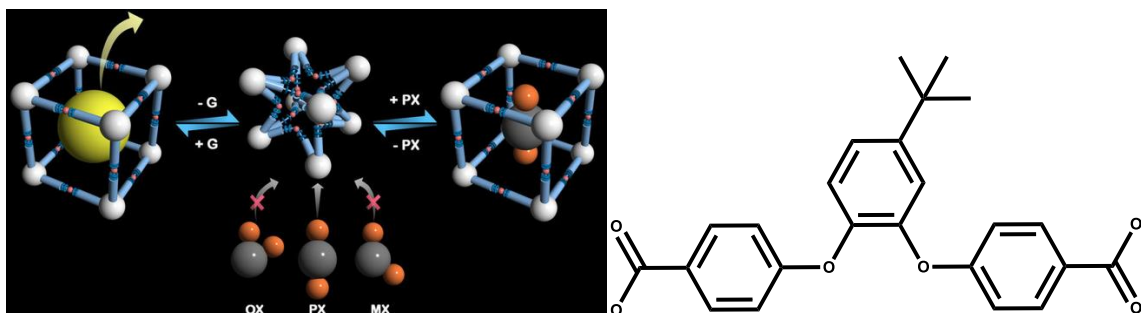


Figure 3.2.1.1 Representation with framework flexibility and selective guest accommodation (left). Strategically designed flexible ligand (right).¹⁹

When exposed to mixed xylene vapors, this new guest-free phase will selectively absorb *p*-xylene and occlude the *meta*- and *ortho*-xylene.¹⁹ It will also selectively absorb styrene over ethylbenzene.²⁰ Jeffrey Long's group has synthesized a microporous MOF capable of selective adsorption of xylenes.⁴⁰ The porous material selectively adsorbs *p*-xylene but occludes *o*-xylene and *m*-xylene (Figure 3.2.1.2).

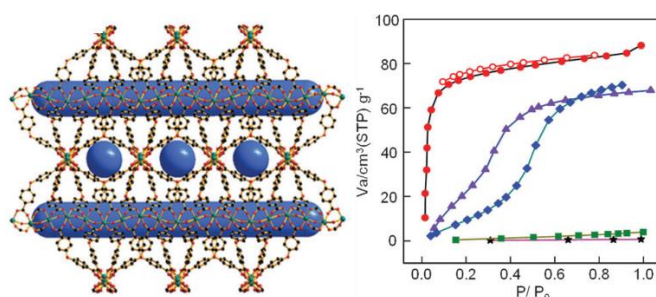


Figure 3.2.1.2 The MOF, ([In(OH)(OBA)]·DMF, H₂OBA = 4,4'-oxybis(benzoic acid), JUC-77. Vapor adsorption and desorption with benzene (red circles, adsorption, red open circles desorption), adsorption of toluene (purple triangles), adsorption of *p*-xylene (blue rhombus), adsorption of *o*-xylene (star), and adsorption of *m*-xylene (green rectangles).⁴⁰

3.2.1.3 Large Molecule Host-Guest Separation

In the same vein that gas and small molecule separation make up a fair amount of research and industrial processes, large molecule separation has been and will continue to be just as important. Large inclusion compounds can separate or be selective towards high molecular weight molecules species. Nau *et al* performed binding studies to selectively capture human steroids using cucurbit[n]urils.⁴¹ Nau argues that steroids cannot be bound by normal binding motifs such as hydrogen bonds or charge interactions and therefore focuses on recognition through size and shape (Figure 3.2.1.3).⁴¹

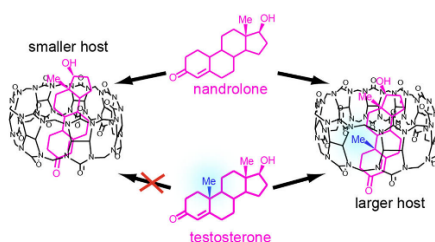


Figure 3.2.1.3 Selective binding of guest molecules in cucurbit[n]urils based on size.²⁷

The cucurbit[7]uril, with its smaller cavity, had high selectivity towards smaller steroids and cucurbit[8]uril would bind the larger and smaller steroids. This study was performed in solution. The expulsion of water from inside of the cucurbit[n]uril cavity would drive host-guest binding.⁴¹ A similar mechanism was observed for some of the guest inclusion work by Kenneth Raymond *et al.* found in the introduction (Chapter 1). Inclusion compounds such as urea and cyclodextrin have been shown to separate polyethylene glycol polymers with molecular weights ranging from 600 g·mol⁻¹ up to 20,000 g·mol⁻¹.⁴² Connected crown ethers, termed exTTF-(crown ether)₂, of different sizes have been made to act as receptors for fullerene, C₆₀, showing that the intensity of the molecular

interactions increases with the size of the ether.⁴³ A metallocsupramolecular tetrahedron with iron vertices can play host to C₆₀ in the pursuit of photo- and electrocatalytic processes.⁴⁴

When the void space is large enough and the structure robust enough for permanent porosity, MOFs are capable of absorbing and separating large molecular species. Zhao *et al* created a MOF with extended tricarboxylate ligands and Zn(II) ions giving it a larger pore which was shown to separate large organic dyes such as methyl yellow, methylene blue, and rhodamine 6g.⁴⁵ A Na(I) MOF, termed cage-in-cage framework structure, developed by Du *et al* shows selective absorption of large organic dyes and utility for the column-chromatographic separation of organic dyes.⁴⁶ The ability to absorb large molecules is an essential function for a MOF. Research by Jeffrey Long *et al.* uses MOFs as a drug delivery system for large molecule drugs like Olsalazine (3,3' - azobis (6-hydroxybenzoate)salicylic acid).⁴⁷

3.2.1.4 The Separation of Guest Molecules Based on Size and Shape

A primary method of separating a group of objects is based on their size. By varying the synthons used for construction, the pores of tubes built from macrocyclic rings can be tuned to separate a variety of aromatic compounds based on their size.⁴⁸ Ward *et al.* have generated cubic coordination cages to separate cyclic ketone guest molecules based on the number of carbon atoms in the guests.⁴⁹ Size-selective separation of large guest molecules, such as C₆₀ and C₇₀, has been performed through the synthesis of self-assembled metallarectangles.⁴⁸ Cucurbituril chemistry has been shown to have size selectivity towards steroids.⁴¹

Chemists have investigated host selectivity based on the size and shape of a guest molecule, exploiting both parameters can provide another mechanism for selective separation. Ward *et al.* explored changing the guanidinium sulfonate framework to be selective towards xylene isomers.⁵¹ Biradha *et al.* were able to use size and shape selectivity to separate 9-anthraldehyde from anthracene, and phenanthrene while also separating perylene from pyrene and phenanthrene.⁵² Competition studies have been performed where two potential hosts are vying for the same guest, though the size and shape of small hydrocarbons was still a factor.⁴⁵ Isostructural MOFs show shape and size selectivity by rejecting the small spherical argon atom and accepting the slightly larger and linear shaped nitrogen molecule.⁵⁴ By tailoring the host cavities with primary and secondary building units, one can be both size and shape selective.⁵⁵ By tuning the size of a cavity, researchers can see enzymatic like selectivity by the host based on size and shape of the guest.⁵⁶

3.3 Background Work

The concern of this work is to determine to what degree hydrogen bonded materials are suitable to host materials for the separation of small organic guest molecules. Beatty and others synthesize hydrogen bonded coordination compounds known to play host to small organic molecules.^{57,58,59} The host framework, **1**, developed previously in the Beatty lab, will be used to determine if small organic molecules can be separated based on size and shape.⁵⁷

The transition metal complex forms the layers of the supramolecular framework held together by charge-assisted hydrogen bonds.⁶⁰⁻⁶³ 3,3'-dimethylbenzidine pillars separate these layers. The Zn complex forms a close-packed lamellar sheet which bars

guest molecules from passing between layers. The pillars are oriented to provide approximately 20\AA of separation between the layers and form close-packed channels which also prohibit guest penetration. The distance from pillar centroid-to-pillar centroid across the channel is about 8.5\AA which is enough space for small guest molecules to co-crystallize inside the channels.⁵⁷ Again, the close-packed system prevents interpenetration and limits guest movement in all but one dimension. The result is a one-dimensional channel in which guest molecules can reside (Figure 3.3.1).

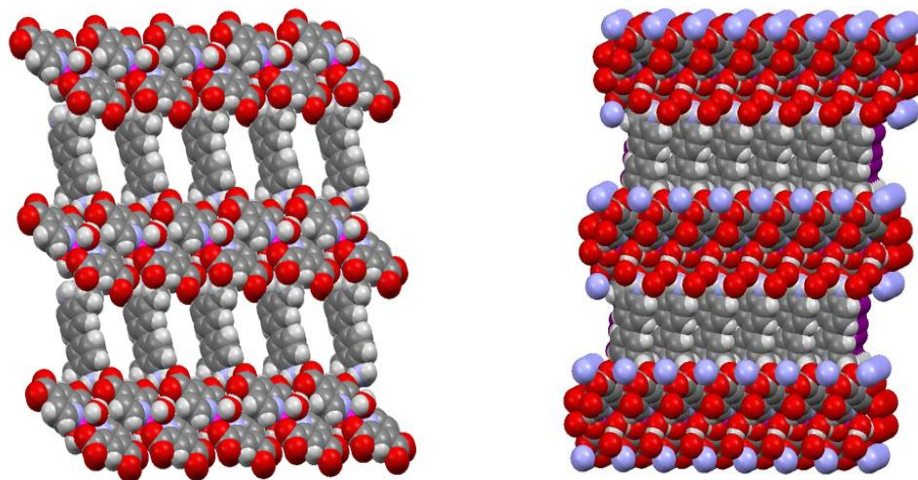


Figure 3.3.1 View of **1** (framework). One-Dimensional channels formed by layers of zinc (II) complex and di-ammonium pillars. The view from the side shows the channels being closed off.

The host framework is stable in air while containing a guest molecule and maintains integrity up to 180°C . The hydrogen bonds allow for flexibility to accommodate a variety of guests. Once a guest is removed, an entirely new guest can be inserted into the framework,^{57,58} signifying that the hydrogen-bonded host framework is robust enough to allow guests to be added and removed repeatedly. This is far different from inclusion compounds where the host no longer exists without the guest. The allows us to determine what other functions this framework can demonstrate. Since this is a

porous material, we investigated whether a combination of molecules could be separated by this framework via co-crystallization from solution.

The remaining questions we had about the framework were based on the following: we know this material is suitable for host/guest chemistry and we know that the guest can be removed through heating.²⁹ However, does this type of framework show a preference for very similar molecules? If so, how and why are specific molecules preferred? We aimed to demonstrate that these types of hydrogen-bonded frameworks are suitable for small molecule separations and if so, modifications to both the dicarboxylic acid and the diamine can be made when seeking specific types of molecular separations. Since this is a porous material, we wanted to investigate whether this framework could separate a mixture of different molecules.

3.4 Current Work

To determine if the host material will be selective towards size, and shape, a series of small organic compounds and xylene isomers were used to determine selectivity. Previous work has shown these molecules to be guests in the framework (Figure 3.4.1).⁵⁷

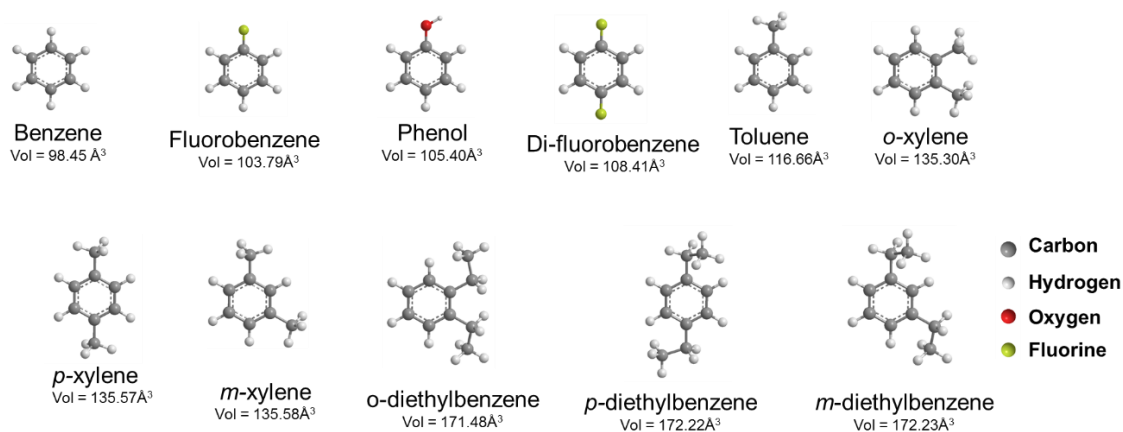


Figure 3.4.1 Summary of guest molecules used in the studies

3.5 Experimental

To determine the selectivity of our framework, our approach was to modify experimental methods which demonstrated host selectivity for guests.⁶⁴ This method would then be used for our porous material.²⁰ Eleven competition experiments were initiated to crystallize **1**. Each experiment used the same amount of starting materials to generate **1** and had a specific mole fraction (χ) of two potential guest molecules (Figure 3.5.1)

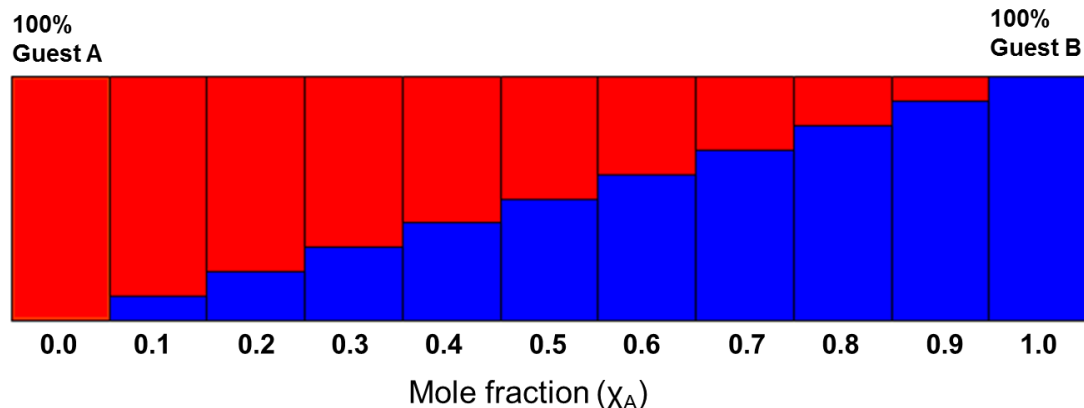


Figure 3.5.1. The mole fraction of guest molecules across each competition experiment

From Figure 3.5.1, the red bars show a decrease in guest A concentration while the blue bars show an increase in guest B concentration. The guest(s) are placed into the crystallization solution of self-assembling **1**. Guest molecule A and B are effectively in competition with each other to become guest molecules within the growing framework. Depending on the guest pair, one or both guests will co-crystallize. We determined how much of each guest resides in **1** compared to the initial mole fraction added.

Once each of the crystals of **1** formed in each of the eleven experiments, the guest ratio inside of **1** was determined. The data from these competition studies can be plotted to determine the selectivity of one guest (A) to another guest (B) (Figure 3.5.2).⁶⁴

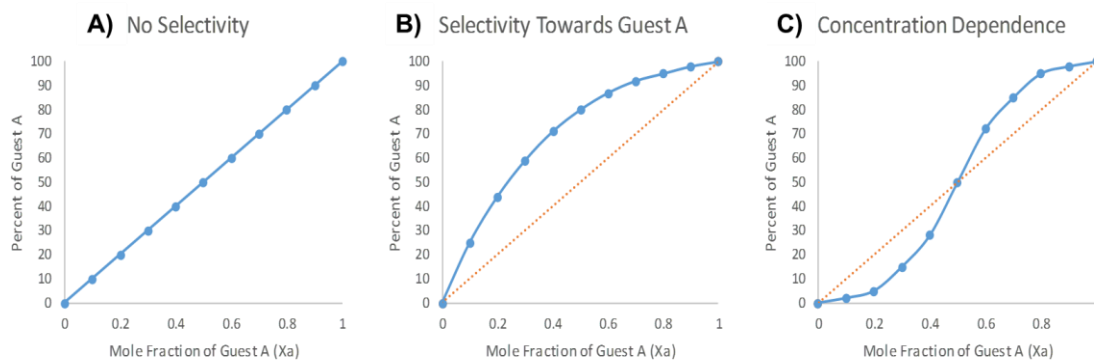


Figure 3.5.2 Selectivity profiles for a two-guest competition study. **A)** Represents no selectivity between guest A and B. **B)** Depicts a significant preference for guest A. **C)** Shows a selectivity which is concentration dependent as selectivity starts with guest B and moves to guest A.

3.5.1 Synthesis of 1•guest

The Zn (II) metal complex was synthesized by combining ZnCl₂ (0.0146 moles, 2g) in 40mL of D.I. water and 2,4-pyridinedicarboxylic acid (0.0293 moles, 4.9g) in 400mL of a 1:1 ratio of D.I. water and methanol. The solution was stirred for approximately 4 hours. The resulting suspension was filtered through a Buchner filter funnel and paper filter. The white slurry was washed with D.I. water until the mother liquor tested pH neutral. The product was dried on the funnel and then air dried overnight. The resulting product was Zn(HPDCA)₂•(H₂O)₂. The Zn(HPDCA)₂•(H₂O)₂ (0.06 moles, 0.025g), and 3,3'-dimethylbenzidine (0.06 moles, 0.012g) were separately dissolved in 2mL each of methanol. The two methanol solutions were then mixed, stirred, and a 1:1 mixture of water (1mL) and DMF (1mL) was then added. For two guest systems, both were added together using a positive displacement pipetter. In most instances, the guest molecule(s) was added to a 15mL glass vial, and the component solution of the framework was added on top. Crystals of the neutral framework, **1**, [(3,3'-dimethylbenzylidinium) (Zn(PDCA)₂•(H₂O)₂)] then grew from the resulting solution.

The crystals are usually brownish-red plates. Once crystal growth had ceased, the resultant crystals were washed in the glass vial with methanol (1x), then acetone (3x) and then dried by applying vacuum to remove any remaining surface residues which might bias the results. For competition studies, no vacuum was applied, but an extra acetone wash step was added. Samples were then analyzed using powder x-ray diffraction scanning from 2θ to 30θ to confirm structure.⁵⁷ Spartan Student V6 software was used for molecular model calculations at the B3LYP, 6-31G* level of theory.^{65,66}

3.6 Results

A new method was employed to determine the selectivity of **1** for guest molecules towards a pair of guest molecules. This method utilized headspace vials and a programmable heating block to precisely control the temperature at which the samples were heated. The reproducibility of our analyses was determined by running the same experiment multiple times. Crystals of **1**·guest_A + guest_B were grown in three separate vials using the same mole fraction ratio of each guest in each vial. For example, 1,4-difluorobenzene was used at 0.9X while *p*-diethylbenzene was used at 0.1X. Harvesting crystals from those three separate growth solutions, the ratio of guest A to guest B was tested using headspace vials and the heating block. Each crystal tested had a mass of 0.019 g. The results were then tabulated (Table 3.6.1)

Table 3.6.1 Reproducibility experiment where 1,4-difluorobenzene (0.9 χ) was in competition with *p*-diethylbenzene (0.1 χ)

Run #	1,4-difluorobenzene Peak Area	Run #	<i>p</i> -diethylbenzene Peak Area
1	6.40E+07	1	4.08E+07
2	6.10E+07	2	4.45E+07
3	6.78E+07	3	4.11E+07
<i>Avg</i>	6.43E+07	<i>Avg</i>	4.21E+07
<i>Std Dev</i>	3.39E+06	<i>Std Dev</i>	2.06E+06
<i>% RSD</i>	5.27	<i>% RSD</i>	4.90

As can be seen from Table 3.6.1, even though the crystals were grown in separate vials and tested independently of each other, the sample to sample reproducibility was excellent. Calculating the coefficient of variation, standard deviation divided by the average, and then multiplying by 100 gives the percent relative standard deviation (%RSD). The calculated %RSD was less than 6% for both guests across all three growing experiments. These results were considered very good and gave a high degree of confidence in our method.

3.6.1 Guest Preference: Size

To show that **1** is selective to guest molecules based on their size, a series of competition experiments were performed. Two molecules of different size were placed in competition with each other, benzene (98.5Å³) and phenol (106.7Å³). For each guest, the cubic volume was calculated using the Spartan software. A B3LYP, 6-31G* level of theory was used for the molecular model.⁶⁶ The two molecules are very close in size with phenol being only slightly larger by 8.2%. There is a red line which cuts the graph diagonally. If all the data points gathered fell onto the red line, this would be interpreted

as no selectivity for either guest. If all the data fell above the red line into the upper left half of the graph, this would indicate selectivity of **1** for benzene. If all the data points were present below the red line in the lower right half of the graph, **1** would be selective for phenol. (Figure 3.6.1).

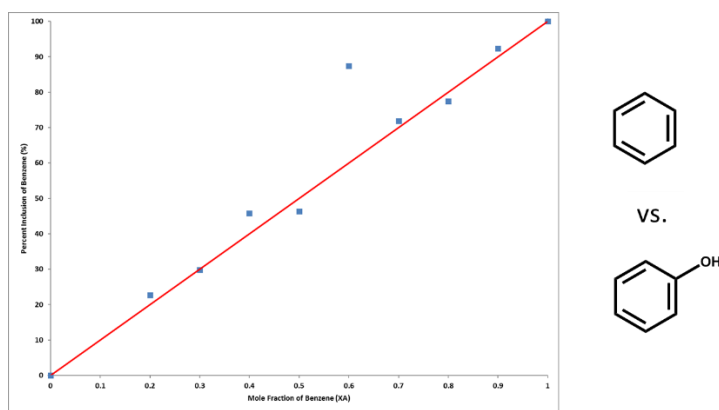


Figure 3.6.1.1 Competition study between benzene versus phenol; There was no selectivity between the two molecules.

For these two guests, **1** did not show much selectivity. Since each of the points fell on the line, the framework was not selective to one guest.

The size of the second guest was then increased, thus testing benzene (98.5\AA^3) and toluene (116.7\AA^3). These two molecules are similar as they are both small aromatic molecules, but with the methyl functional group, toluene is 15.6% larger (Figure 3.6.1.2).

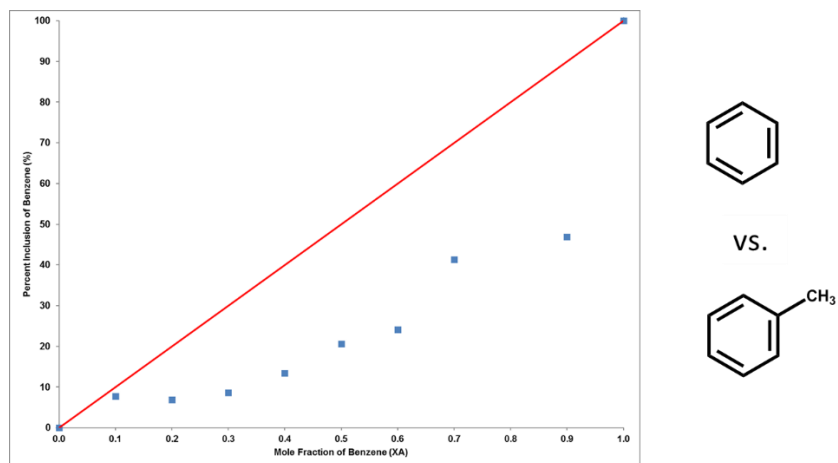


Figure 3.6.1.2 Competition between benzene versus toluene, toluene was shown to be preferred over benzene.

Based on the results of benzene versus toluene, 1 was selective towards toluene. The larger molecule was preferred over the smaller of the two. Going from almost equivalent size to a larger and a small molecule, we see that the smaller molecule lost.

The next competition reaction, placed a small molecule, fluorobenzene (102.9\AA^3), in competition with an even larger molecule than toluene, *p*-xylene (135.6\AA^3). With its two methyl groups, *p*-xylene is much larger than fluorobenzene (Figure 3.6.1.3).

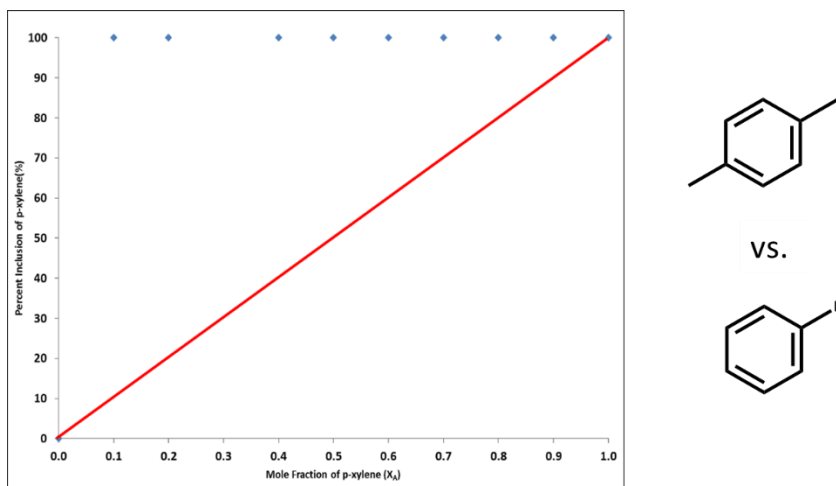


Figure 3.6.1.3 Competition between *p*-xylene versus fluorobenzene, *p*-xylene was shown to be preferred over fluorobenzene

The size difference between the two molecules for this series of experiments was 32.7%.

The size difference between the two guests was double from the previous experiment. In this case, *p*-xylene was completely preferred compared to fluorobenzene.

The next series of competition experiments pitted a single guest molecule against a series of guest molecules which steadily increased in size. 1,4-di-fluorobenzene (108.5\AA^3) was placed in competition with toluene (116.7\AA^3), *p*-xylene (135.6\AA^3), and finally with *p*-diethylbenzene (170.3\AA^3). This series had been tested previously,⁵⁸ but the results were to be verified using the new method of analysis.

1,4-di-fluorobenzene was tested against toluene. Toluene was calculated to be 7.0% larger. The two guests were placed in competition with each other (Figure 3.6.1.4).

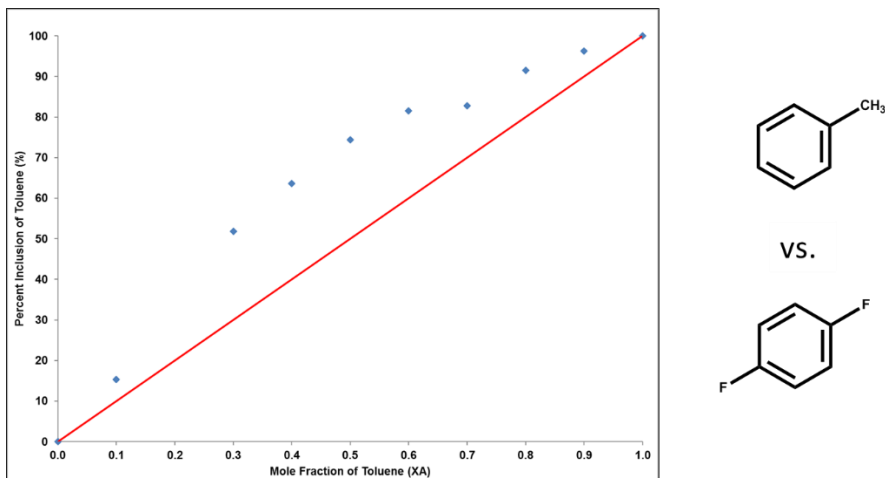


Figure 3.6.1.4 Competition between toluene versus 1,4-di-fluorobenzene, **1** was selective towards toluene.

The results of the competition experiments show that **1** was more selective towards toluene. These results matched what was previously seen using the prior method. The framework preferred toluene, but in few of the experiments such as 0.1X, it was not by much.

The next competition experiments would test 1,4-di-fluorobenzene versus *p*-xylene. The *p*-xylene guest was 20.0% larger than 1,4-di-fluorobenzene (Figure 3.6.1.5).

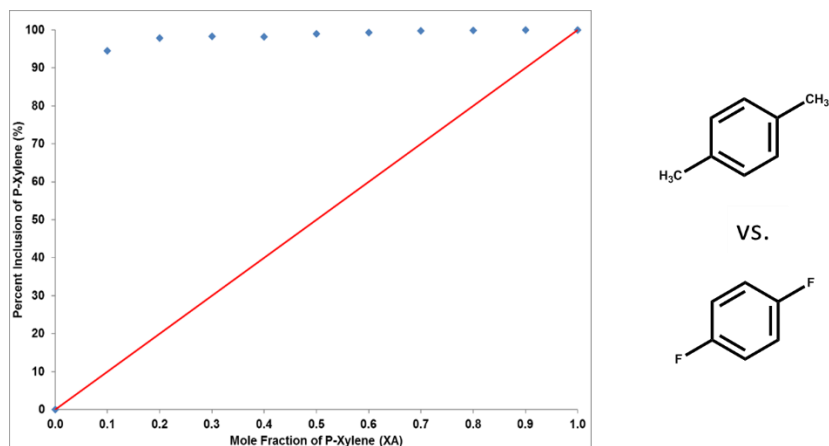
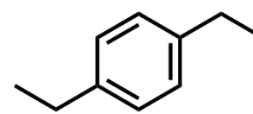
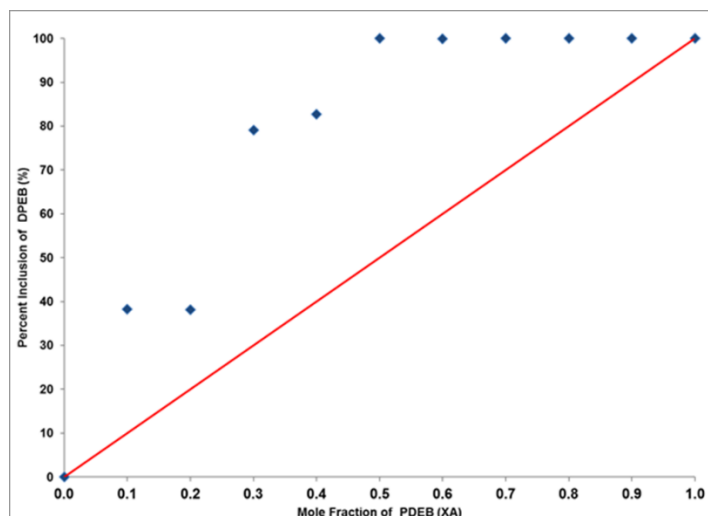


Figure 3.6.1.5 Competition between *p*-xylene versus 1,4-fluorobenzene, 1 was selective towards *p*-xylene

Increasing in the size of the second guest molecule, there was complete dominance by *p*-xylene in the framework. Compared to previous experiments, the framework completely avoided the other guest molecule. This data agreed with the previous investigation.

The 1,4-di-fluorobenzene was placed in competition with *p*-diethylbenzene. The *p*-diethylbenzene molecule is 36.3% larger than 1,4-di-fluorobenzene. The size difference should give the preference to *p*-diethylbenzene (Figure 3.6.1.6).



VS.

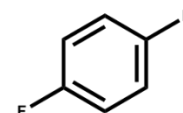


Figure 3.6.1.6 Competition between *p*-diethylbenzene versus 1,4-difluorobenzene, 1 had a concentration-dependent selectivity towards *p*-diethylbenzene.

In this competition experiment, we did see selectivity towards *p*-diethylbenzene, but it was not the usual curve seen in the previous experiment. The selectivity dipped at 0.2 and 0.4X. The data agreed with previous experiments; however, it also raises a question. The *p*-diethylbenzene molecule was the first to have this type of a selectivity profile. The *p*-diethylbenzene was the biggest molecule tested, but with its diethyl groups, the guest molecule had more shape to it than previous guests.

3.6.2 Guest Preference: Shape

The influence of guest shape was explored based on isomers of the previous competition studies. These experiments will provide evidence on how changing the shape of the guest can affect selectivity.

The first set of experiments revisited the competition between xylene and fluorobenzene. This time the shape of the xylene was changed. Instead of *p*-xylene being tested, *m*-xylene was placed in competition with fluorobenzene (Figure 3.6.2.1)

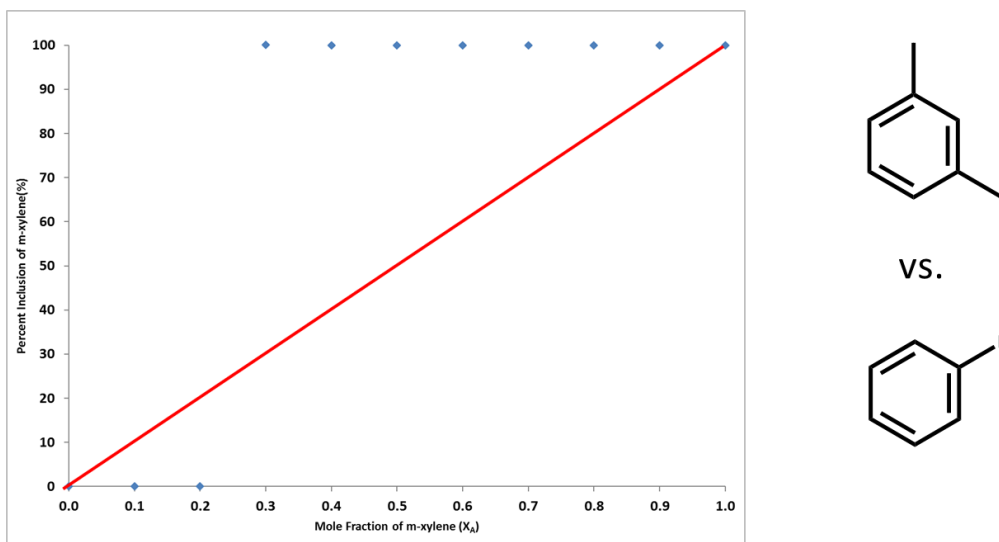


Figure 3.6.2.1 Competition between *m*-xylene versus fluorobenzene, **1** shows selectivity towards *m*-xylene.

1 has complete selectivity towards *m*-xylene over fluorobenzene. This was consistent with the experiment where *p*-xylene was placed in competition with fluorobenzene earlier. For this instance, changing the guest molecule's shape did not directly affect the selectivity of the guest. At 0.1 and 0.2X, crystals of **1**·guest could not be obtained for testing after multiple attempts.

The next competition series was to be between *o*-xylene and fluorobenzene. Much like the two the *m*-xylene experiments, the *o*-xylene/fluorobenzene experiments would not crystallize. The *o*-xylene/fluorobenzene series, although attempted numerous times, could not be isolated for testing.

The size experiments demonstrated preference of **1** for larger guest molecules. To confirm the results based on the size of the guest, a comparison was made where the size of each guest pair was held constant, for example, xylene vs. diethylbenzene. The difference will be that the shape of the guests will change from the *p*-position to the *m*- and *o*-position for each of the guest pairs. If only the size of the guest matters, then this

selectivity experiment would show a preference for the large molecule, *p*-diethylbenzene, every time as it did for the bigger molecules in the size section.

The first competition was between *p*-xylene and *p*-diethylbenzene. These two molecules were chosen because both molecules are aromatic, substituted in the para-position and *p*-diethylbenzene is larger than *p*-xylene. For each of guests, the cubic volume was calculated using the Spartan software. A B3LYP, 6-31G* level of theory was used for the molecular model.⁴⁶ The cubic volume of the diethyl benzene and xylene differs by 21%. The selectivity of **1** was tested (Figure 3.6.2.2).

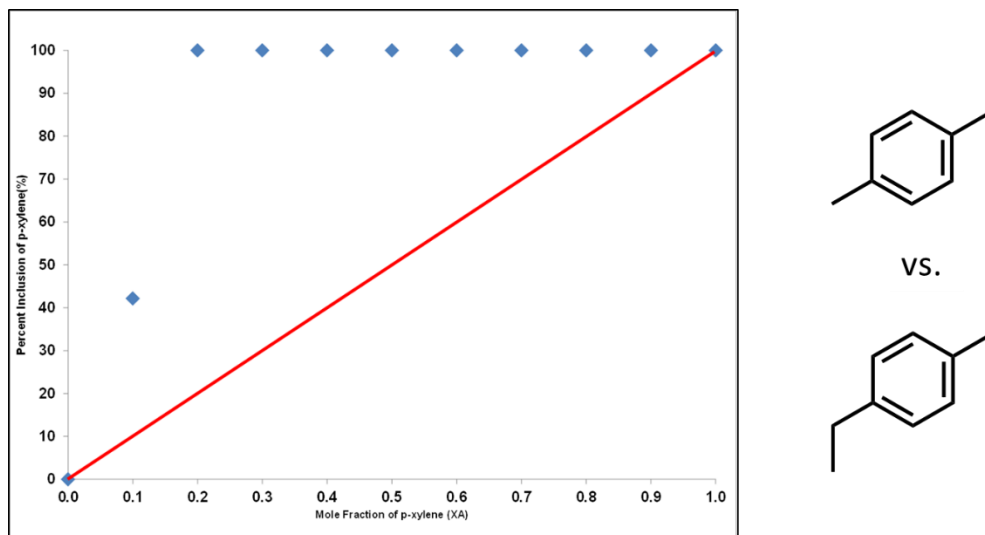


Figure 3.6.2.2 Competition study of *p*-xylene versus *p*-diethylbenzene, **1** was selective to *p*-xylene

In Figure 3.6.2.2, experimental results indicate that **1** was selective for *p*-xylene. This is already counter to what was seen based on size comparisons. Since the *p*-xylene only has methyl groups, its shape will not change. The *p*-diethylbenzene has ethyl groups which can rotate about their carbon-carbon bonds to different angles. This indicates that shape may be a limiting factor when two or more guest molecules are present in the crystal growth solution. At 0.1 χ of *p*-xylene, the percent inclusion is already 42% of the guest

ratio inside **1**. *p*-Xylene was added at 10% of the χ as this point while *p*-diethylbenzene was added at 90% χ . Moving to the right in Figure 3.6.1, at 0.2 χ *p*-xylene was at 100%. *p*-diethylbenzene was completely occluded by **1** in favor *p*-xylene. This pattern continues for the remainder of the χ until only *p*-xylene was added to the crystal growth solution where 100% inclusion of *p*-xylene would be expected. Figure 3.6.2.2 shows that **1** discriminates between the two guest molecules chosen for this series of experiments. Based on the differences between the guests and the data pattern shown, the selectivity of **1** can be affected by the shape of the guest molecule.

The shapes of the guest molecules were changed from the *para*- to the *meta*-isomers. The next competition series was between *m*-xylene and *m*-diethylbenzene. If only the size of the guest matters and the shape does not, then this selectivity experiment would show a preference for *m*-xylene in **1** just as it did for *p*-xylene (Figure 3.6.2.3).

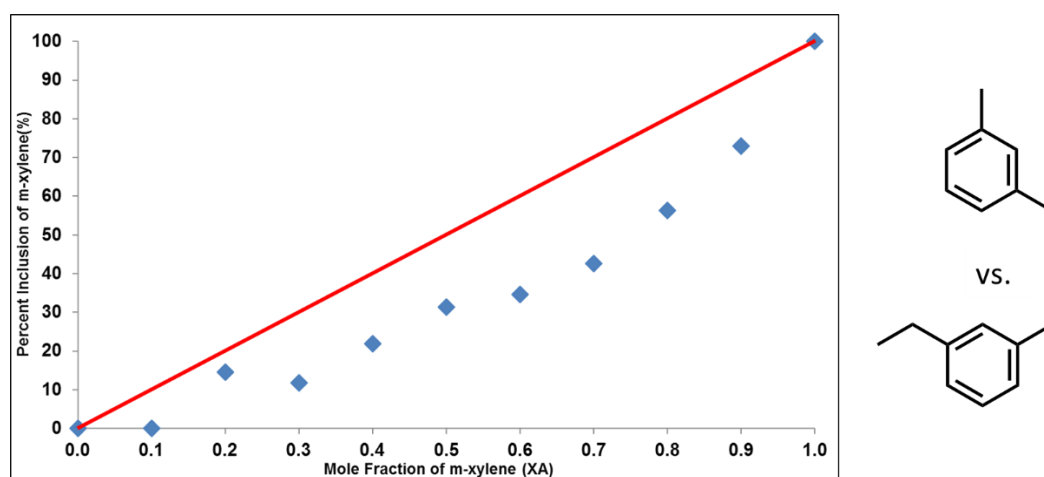


Figure 3.6.2.3 Competition study of *m*-xylene versus *m*-diethylbenzene, **1** is selective towards *m*-diethylbenzene.

When the series was tested, the selectivity profile was not the same for the *m*-position guests as it was for the *p*-position guests. It appears that changing the shape of the guest molecules has changed the selectivity of **1**.

To sum up, to this point, changing the shape of the guest has affected the selectivity of **1** while the size has been held constant. To determine whether the *p*-position or the *m*-position was the special case, *o*-xylene and *o*-diethylbenzene were tested for selectivity in **1**. (Figure 3.6.2.4).

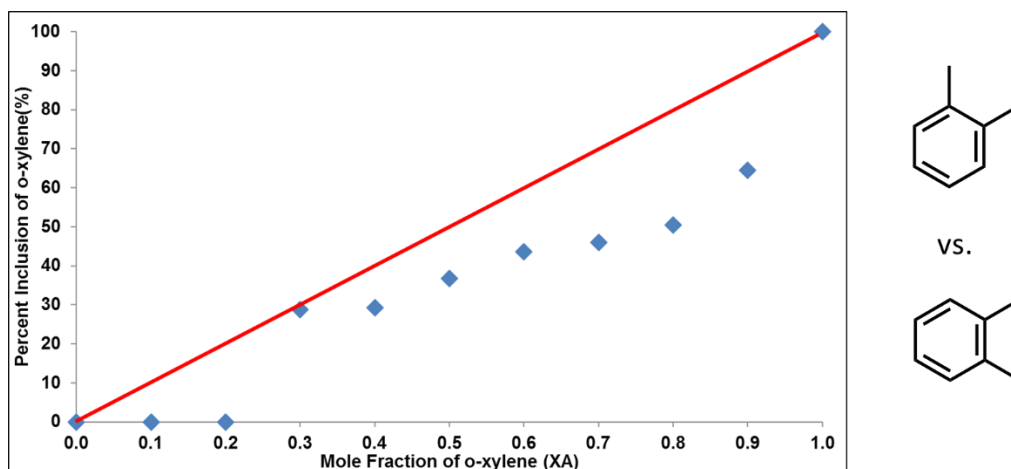


Figure 3.6.2.4 Competition study of *o*-xylene versus *o*-diethylbenzene, **1** was selective towards *o*-diethylbenzene

The results of the competition experiments show that **1** preferred *o*-diethylbenzene over *o*-xylene. The selectivity was not extreme as it was for *p*-xylene. There were a few points where there was no selectivity such as 0.3X. At 0.4X – 0.6X, the selectivity for *o*-diethylbenzene was marginal.

3.7 Discussion

The selectivity experiments have shown the effects of changing the size and shape of the guest molecules. As the size of the guest increased versus its competitive counterpart, the larger guest was the selected by **1**.

The initial experiment between benzene and phenol showed how the selectivity of **1** was affected by guests that are about the same size. Almost all the data points fell directly on the dividing line of the graph. This would indicate that for guests of the same size that **1** is not selective. The size difference between the two molecules based on cubic volume was 8.2%. When the percent size difference was almost doubled to 15.6% (benzene vs. toluene), selectivity towards the larger molecule was immediately seen. We then looked at a guest pair, *p*-xylene vs. fluorobenzene, where the percent size difference was 32.7%. At this point, the bigger guest molecule completely dominated inside the channels of **1**, as the framework demonstrated selectivity towards *p*-xylene over fluorobenzene.

For the next series of experiments, 1,4-difluorobenzene was held constant while different size guest molecules were separately placed in competition with it. Toluene and 1,4-difluorobenzene had the same size ratio as benzene to phenol. Here, we found that the slightly larger toluene guest was preferred by **1** to 1,4-difluorobenzene. The selectivity profile showed uptake of both guests, but there was a noticeable favoring towards toluene.

The size difference increased in the next experiment where *p*-xylene was placed in competition with 1,4-difluorobenzene. Both guests are di-substituted aromatics in the 1,4-position. The *p*-xylene molecule has a cubic volume which is 20% larger than 1,4-

difluorobenzene, but *p*-xylene ultimately takes over and is the only guest found in **1**. Only at low levels of *p*-xylene (0.1-0.2X) was 1,4-difluorobenzene found.

The competition between *p*-diethylbenzene and 1,4-difluorobenzene had the greatest difference in cubic volume, 36.3%. In this case, an observation occurs which had not been seen. The competition between the two molecules appears to be concentration dependent. It is true that all the data points fall into the upper left quadrant which dictates selectivity of **1** to *p*-diethylbenzene. However, this step-like data curve has characteristics of **c**) in Figure 3.5.2. At lower concentrations, 1,4-difluorobenzene is at ~60% of the total guest ratio until 0.3X. At 0.4X, *p*-diethylbenzene reaches a concentration where it begins to dominate the guest ratio even though it still is at the lower mole fraction in comparison to 1,4-difluorobenzene. After, 0.5X, the trend of the larger guest being completely preferred returns and the very large cubic volume *p*-diethylbenzene dominates the guest competition.

A clear trend begins to form for guest selectivity. If two guests, of nearly the same size, are placed in competition they will be nearly equivalent with regards to selectivity. The alternative is that the slightly larger guest will be selected, but it will not necessarily dominate the inside of the framework as seen when the size difference increases over 10% concerning cubic volume. When the guest becomes very large, such as *p*-diethylbenzene, the larger molecule was preferred, but in this case, there was concentration dependence.

Each of the previously tested guest molecules was structurally in the same position and the same shape. The *p*-diethylbenzene was the most different due to the

conformational mobility of the ethyl groups. When the shape of the guest molecule was changed to the *meta*- and *ortho*- positions, our previous hypothesis of preference for larger molecules was challenged.

As previously mentioned, one-dimensional channels are available to guest molecules within our framework. The data suggested that *p*-xylene can fill the one-dimensional channels with higher efficiency compared to the other potential guests. The *p*-xylene completely dominates **1**. Fluorobenzene had its highest concentration (Figure 3.6.1.5) at about 7% when it was at 0.9 χ when competing with *p*-xylene. **1**·*p*-xylene crystallizes quickly and contains a high concentration of *p*-xylene. Initial substitution of *p*-xylene for *m*-xylene vs fluorobenzene showed continued high selectivity for these larger molecules.

Compound **1**·*p*-diethylbenzene also crystallizes easy, but from competition studies, it was shown that **1** was still selective towards *p*-xylene. This is completely counter to the notion that larger guest molecules are always preferred. Due to the rotatable ethyl groups, *p*-diethylbenzene requires extra steps to correctly orient itself before taking up space within the one-dimensional channel. The ease with which *p*-xylene co-crystallizes with **1** gives it an advantage. This comes through in the competition studies.

It was believed that the *meta*- and *ortho*- do not pack as efficiently when co-crystallizing inside the one-dimensional channel. The *m*- and *o*-ethyl groups must rotate themselves correctly to pack inside of the one-dimensional channel, but the *m*- and *o*-

xylene molecules must also orient themselves to fit within the existing channel space properly.

The selectivity for *m*-diethylbenzene was not as extreme as *p*-xylene, but *m*-diethylbenzene was preferred over *m*-xylene (Figure 3.6.2.3). This ratio was more in-line with what was observed for the first series of size competition studies. At 0.1 χ , there was 100% inclusion *m*-diethylbenzene. As the mole fraction (χ) of *m*-xylene increased in the crystal growth solution, *m*-diethylbenzene continued as the preferred guest in **1**. When there was a 1:1 mole fraction of each guest molecule in the growth solution, *m*-diethylbenzene was recovered from **1** at 68.6% compared to *m*-xylene at 31.4%. The percent inclusion for *m*-xylene does not reach 50% until 0.8 χ . At 0.8 χ , **1** is still selective towards *m*-diethylbenzene over *m*-xylene.

For 0.1 and 0.2 χ , **1** had 100% selectivity towards *o*-diethylbenzene (Figure 3.6.2.4). For the *m*-position guests, at 0.3 χ *m*-diethylbenzene was at 88% of the recovered guest from **1** (Figure 3.6.2.3). Now at 0.3 χ , there was no selectivity between the two guests as the data point fell directly on the dividing line (Figure 3.6.2.4). The *o*-xylene doesn't hit 40% inclusion until 0.6 χ whereas for *m*-xylene (Figure 3.6.2.3) it was 42.8% at 0.7 χ . At 0.8 χ , **1** contained *o*-diethylbenzene at 49.5% of the guest ratio vs. *m*-diethylbenzene at 0.8 χ was at 43.6%. At 0.9 χ , *m*-diethylbenzene (Figure 3.6.2.3) was 27.1% of the guest ratio. Comparatively, *o*-diethylbenzene increased to 35.5% (Figure 3.6.2.4). While changing the shape of the molecules shifted the selectivity of **1** back towards the larger molecule, none of the new guests demonstrated the same selectivity as *p*-xylene. Why were the other two positions not at high concentrations like the *p*-xylene?

There was a shared factor for both *meta*- and *ortho*- position guests. This was low concentration inside **1**. TGA experiments were previously performed on **1**•single guest isomers for xylene and diethylbenzene.⁵⁷ With only one possible guest, theoretically, the guest can occupy 100% of the one-dimensional channel. It was found that *meta*- and *ortho*- guests occupy less than 20% of the channel. The fact that both were present in low concentration indicates that neither was a good fit, and there is virtually no preference for one ill-fitting molecule over the other (Table 3.7.1).⁵⁷

Table 3.7.1 TGA analysis of co-crystallized single guests in **1**⁵⁷

Guest Molecule	% Occupied (TGA)
<i>p</i> -xylene	78.73
<i>m</i> -xylene	14.52
<i>o</i> -xylene	13.81
<i>p</i> -diethylbenzene	32.67
<i>m</i> -diethylbenzene	16.74
<i>o</i> -diethylbenzene	11.16

This means that for non-*p*-xylene guests it is already difficult to fill the host. Placing it in competition with another guest that has low occupancy explains why for *ortho*- and *meta* positions there was only a small deviation from no selectivity. It also demonstrates why *para*-diethylbenzene cannot compete with *para*-xylene. The *p*-diethylbenzene intercalates at 32.67% inside **1** without competition from other guests. This is 58.5% lower than *p*-xylene. It is likely that that **1** continues to form while a lower percentage of *p*-diethylbenzene is in the correct conformation to co-crystallize. Single crystal x-ray diffraction was performed for **1**•*m*-xylene and **1**•*m*-diethylbenzene. The framework of **1** was well defined, however; neither *m*-xylene nor *m*-diethylbenzene could be resolved to

determine orientation inside of the framework. Powder x-ray diffraction data showed correct d-spacing for guest intercalation, so there was confidence of a guest being present within **1**, but neither of the *m*- isomers was found in high quantities.

3.8 Conclusions

We have further demonstrated that **1** is suitable for host/guest chemistry. Not only does the framework have the capability of co-crystallizing aryl guest molecules, which are also removable; it can effectively be used to separate guest molecules in solution. This type of framework has been shown to have a particular preference for one of two competing guest molecules.

Size

It has been shown that the size of a guest molecule can be a contributing factor to what type of guest molecule will co-crystallize inside of **1**. Experiments based on size demonstrate that guests of near equal size will have no selectivity or only a minor selectivity as observed with benzene vs. phenol and toluene vs. fluorobenzene. As one guest molecule was held constant, 1,4-difluorobenzene, it was observed that the larger guests are consistently preferred to this smaller guest. As the guest becomes very large, such as *p*-diethylbenzene, there was still selectivity towards the larger guest, but it becomes concentration dependent. This would indicate that there is a maximum size where guest becomes too large.

When *p*-xylene competed with a larger molecule such as *p*-diethylbenzene, the smaller guest was found at a higher guest ratio, a shift from the norm. It is believed that *p*-xylene was the dominant guest due to ease of co-crystallization. It was more facile for *p*-xylene with its' methyl groups to co-crystallize within **1** than *p*-diethylbenzene. The *p*-

diethylbenzene had to orient itself in the proper conformation to fit within the one-dimensional channel. The *p*-diethylbenzene having concentration-dependent selectivity against 1,4-difluorobenzene would undoubtedly come in second to a molecule like *p*-xylene. The was the same 1,4-difluorobenzene guest where *p*-xylene was so strongly preferred by **1**. This selectivity for *p*-xylene was also supported through prior TGA analysis of **1** where only a single guest was added. Here, *p*-xylene occupied approximately 78% of the available space within the one-dimensional channel when it had no competition. By comparison, *p*-diethylbenzene only occupied about 33% and without any other aromatic guest molecules in solution. A ratio of both guests was not seen when *p*-xylene and *p*-diethylbenzene were placed in competition for space within the framework. The only exception being the lowest concentration of *p*-xylene, the framework was selective towards *p*-xylene.

Shape

Changing to different positional isomers significantly impacted the dominant molecule inside of the framework. When *p*- and *m*- were tested against fluorobenzene, it appeared that the larger guest molecule was always selected. This changed when xylenes were compared to diethylbenzenes. In the *o*-position, selectivity was in favor of *o*-diethylbenzene over *o*-xylene, although the preference was not swayed significantly. The preference for *o*-diethylbenzene was not far from no selectivity between the two guest molecules. Looking back to the TGA data, the *ortho*- guests did not intercalate to a very high percentage. This was also true of the *meta*-position guests. Each of them intercalated at less than 20% of the available space within **1**. Since both the *ortho*- and *meta*- position

guests were of such low concentration, it is unlikely that there would be enough of each guest within the crystal to show a distinct preference for one guest over another.

We have demonstrated that our hydrogen-bonded framework is suitable for small molecule separations. In future studies, it is possible to make modifications to both the dicarboxylic acid and the diamine when seeking specific types of molecule separation. We may also separate guest molecules based on their electronic nature and their interaction with the one-dimensional channel of the framework.

3.9 References

- 1) Pivovar, A.M.; Holman, K.T.; Ward, M.D. *Chem. Mater.* **2001**, *13*, 3018-3031;
Xiao, W.; Hu, C.; Ward, M.D. *J. Am. Chem. Soc.* **2014**, *136*, 14200-14206;
Soegiarto, A.C.; Ward, M.D. *Cryst. Growth Des.* **2009**, *9*, 3803-3815; Horner,
M.J.; Holman, K.T.; Ward, M.D. *J. Am. Chem. Soc.* **2007**, *129*, 14640-14660;
Swift, J.A.; Reynolds, A.M.; Ward, M.D. *Chem. Mater.* **1998**, *10*, 4159-4168;
Soegiarto, A.C.; Comotti, A.; Ward, M.D. *J. Am. Chem. Soc.* **2010**, *132*, 14603-
14626; Holman, K.T.; Pivovar, A.M.; Swift, J.A.; Ward, M.D. *Acc. Chem. Res.*
2001, *34*, 107-118; Liu, Y.; Xiao, W.; Yi, J.J.; Hu, C.; Park, S.J.; Ward, M.D. *J.*
Am. Chem. Soc. **2015**, *137*, 3386-3392; Evans, C.C.; Sukato, L.; Ward, M.D. *J.*
Am. Chem. Soc. **1999**, *121*, 320-325; Custelcean, R.; Ward, M.D. *Cryst. Growth*
Des. **2005**, *5*, 2277-2287; Swift, J.A.; Pivovar, A.M.; Reynolds, A.M.; Ward,
M.D. **1998**, *120*, 5887-5894; Xiao, W.; Hu, C.; Ward, M.D. *Cryst. Growth, Des.*
2013, *13*, 3197-3200; Han, J.; Zhao, L.; Yau, C.W.; Mak, T.C.W. *Cryst. Growth*
Des. **2009**, *9*, 308-319; M. Ward, R. Custelcean, *Crys, Growth Des.* **2005**, *5*, 6,
227
- 2) Adachi, T.; Ward, M.D. *Acc. Chem. Res.* **2016**, *49*, 2669-2679
- 3) Dalrymple, S.; Shimizu, G. *J. Am. Chem. Soc.* **2007**, *129*, 12114-12116
- 4) Prakash, M.J.; Oliver, A.G.; Sevov, S. *Cryst. Growth Des.* **2012**, *12*, 2684-2690;
Wang, Y.X.; Sevov, S. *Cryst. Growth & Des.* **2008**, *8*, 1265-1270
- 5) Nassimbeni, L.R. *Acc. Chem. Res.* **2003**, *36*, 631-637; Cram, D.J.; Cram, J.M.
Container Molecules and Their Guests; Royal Society of Chemistry; Cambridge,
1994

- 6) Cram, D.J.; Tanner, M.E.; Thomas, R. *Angew. Chem., Int. Ed.* **1991**, *30*, 1024-1027; Jankowska, K.I.; Pagba, C.V.; Piatnitski Chekler, E.L.; Deshayes, K.; Piotrowiak, P. *J. Am. Chem. Soc.* **2010**, *132*, 16423-16431
- 7) Auletta, T.; De Jong, M.R.; Mulder, A.; Van Veggel, F.C.J.M.; Huskens, J.; Reinhoudt, D.N.; Zou, S.; Zapotoczny, S.; Schoenherr, H.; Vancso, G.J.; Kuipers, L. *J. Am. Chem. Soc.* **2004**, *126*, 1577-1584; Zhou, H.; Yamada, T.; Kimizuka, N. *J. Am. Chem. Soc.* **2016**, *138*, 10502-10507; Wenz, G. *Angewandte Chemie Int. Ed.*, **1994**, *33*, 803-822; Li, H.; Li, F.; Zhang, B.; Zhou, X.; Yu, F.; Sun, L. *J. Am. Chem. Soc.* **2015**, *137*, 4332-4335
- 8) Sawada, T.; Hisada, H.; Fujita, M. *J. Am. Chem. Soc.* **2014**, *136*, 4449-4451
- 9) Schramm, M.P.; Hooley, R.J.; Rebek, J. *J. Am. Chem. Soc.* **2007**, *129*, 9773-9779; Zhang, K.; Ajami, D.; Gavette, J.V.; Rebek, J. *J. Am. Chem. Soc.* **2014**, *136*, 5264-5266; Butterfield, S.M.; Rebek, J. *J. Am. Chem. Soc.* **2006**, *128*, 15366-15367; Kobayashi, K.; Ishii, K.; Sakamoto, S.; Shirasaka, T.; Yamaguchi, K. *J. Am. Chem. Soc.* **2003**, *125*, 10615-10625
- 10) Tiefenbacher, K.; Ajami, D.; Rebek, J. *Angew. Chem., Int. Ed.*, **2011**, *50*, 12003-12007; Shivanyuk, A.; Rebek, J. *Angew. Chem., Int. Ed.* **2003**, *42*, 684-686
- 11) Brown, S.P.; Schaller, T.; Seelbach, U.P.; Koziol, F.; Ochsenfeld, C.; Klarner, F.; Spiess, H.W. *Angew. Chem., Int. Ed.* **2001**, *40*, 717-720
- 12) Dvornikovs, V.; House, B.E.; Kaetzel, M.; Dedman, J.R.; Smithrud, D.B. *J. Am. Chem. Soc.* **2003**, *125*, 8290-8301; Wang, X.; Bao, X.; McFarland-Mancini, M.; Isaacsohn, I.; Drew, A.F.; Smithrud, D.B. *J. Am. Chem. Soc.* **2007**, *129*, 7284-7293

- 13) Rychlewska, U.; Warzajtis, B. *Journal of Molecular Structure* **2003**, *647*, 141-150; Bock, H.; Nagel, N.; Nather, C. *Chem. Eur. J.* **1999**, *5*, 2233-2236; Bishop, R.; Craig, D.; Maroungkas, A.; Scudder, M.L. *Tetrahedron* **1994**, *50*, 8749-8756
- 14) Sada, K.; Kondo, T.; Miyata, M.; Tamada, T.; Miki, K. *Journal of the Chemical Society, Chemical Communications* **1993**, 753-755
- 15) Han, J.; Yau, C.W.; Chan, C.W.; Mak, T.C.W. *Cryst. Growth and Des.* **2012**, *12*, 4457-4465; Li, Q.; Hu, H.Y.; Lam, C.K.; Mak, T.C.W. *Journal of Supramolecular Chemistry* **2002**, *2*, 473-478
- 16) Li, H.; Eddaoudi, M.; Groy, T.L.; Yaghi, O.M. *J. Am. Chem. Soc.* **1998**, *120*, 8571-8572; Li, H.; Eddaoudi, M.; O’Keeffe, M.; Yaghi, O.M. *Nature* **1999**, *402*, 276-279; Suzuki, T.; Kotani, R.; Kondo, A.; Maeda, K. *J. Phys. Chem. C*, **2016**, *120*, 21571-21579; Peterson, V.K.; Southon, P.D.; Halder, G.J.; Price, D.J.; Bevitt, J.J.; Kepert, C.J. *Chem. Mater.*, **2014**, *26*, 4712-4723; Li, J.; Fu, H.; Zhang, J.; Zheng, L.; Tao, J. *Inorg. Chem.*, **2015**, *54*, 3093-3095; Millange, F.; Guillou, N.; Medina, M. E.; Ferey, G.; Carlin-Sinclair, A.; Golden, K. M.; Walton, R. I. *Chem. Mater.*, **2010**, *22*, 4237-4245; Ling, S.; Walton, R. I.; Slater, B. *Molecular Simulation*, **2015**, *41*, 1348-1356; El Osta, R.; Carlin-Sinclair, A.; Guillou, N.; Walton, R. I.; Vermoortele, F.; Maes, M.; de Vos, D.; Millange, F. *Chem. Mater.*, **2012**, *24*, 2781-2791; Sumida, K.; Foo, M.L.; Horike, S.; Long, J.R. *Eur. J. Inorg. Chem.* **2010**, 3739-3744; Geier, S.J.; Mason, J.A.; Bloch, E.D.; Queen, W.L.; Hudson, M.R.; Brown, C.M.; Long, J.R. *Chem. Sci.* **2013**, *4*, 2054-2061; Krishna, R.; Long, J.R. *J. Phys. Chem. C*, **2011**, *115*, 12941-12950; Levine, D.J.; Runcevski, T.; Kapelewski, M.T.; Keitz, B.K.; Oktawiec, J.; Reed, D.A.;

- Mason, J.A.; Jiang, H.Z.H.; Colwell, K.A.; Legendre, C.M.; FitzGerald, S.A.; Long, J.R. *J. Am. Chem. Soc.*, **2016**, *138*, 10143-10150; Herm, Z.R.; Bloch, E.D.; Long, J.R. *Chem. Mater.*, **2014**, *26*, 323-338; Bloch, E.D.; Queen, W.L.; Krishna, R.; Zadrozny, J.M.; Brown, C.M.; Long, J.R. *Science*, **2012**, *335*, 1606-1610; Li, J.; Sculley, J.; Zhou, H. *Chem. Rev.*, **2012**, *112*, 869-932; Li, B.; Ma, D.; Li, Y.; Zhang, Y.; Li, G.; Shi, Z.; Feng, S.; Zaworotko, M.J. *Chem. Mater.*, **2016**, *28*, 4781-4786
- 17) Batten, S.R.; Turner, D.R.; Neville, S.M. *Coordination Polymers: Design, Analysis and Application*. The Royal Society of Chemistry, Thomas Graham House Cambridge, Cambridge CB4 0WF, UK 2009; Desiraju, G.R.; Vittal, J.J.; Ramanan, A. *Crystal Engineering, A Textbook*. World Scientific Publishing Company. Pte. Ltd., **2011**; Duan, J.; Higuchi, M.; Krishna, R.; Kiyonaga, T.; Tsutsumi, Y.; Sato, Y.; Kubota, Y.; Takata, M.; Kitagawa, S. *Chemical Science* **2014**, *5*, 660-666; Roy, S.; Chakraborty, A.; Tapas, K. *Coordination Chemistry Reviews* **2014**, *273-274*, 139-164; Sato, H.; Kosaka, W.; Matsuda, R.; Hori, A.; Hijikata, Y.; Belosludov, R. V.; Sakaki, S.; Takata, M.; Kitagawa, S. *Science* **2014**, *343*, 167-170
- 18) Jae, J.; Tompsett, G.A.; Foster, A.J.; Hammond, K.D.; Auerbach, S.M.; Lobo, R.F.; Huber, G.W., *Journal of Catalysis*, **2011**, *279*, 257-268
- 19) Mukherjee, S.; Joarder, B.; Manna, B.; Desai, A. V.; Chaudhari, A.K.; Ghosh, S. *K. Sci. Rep.* **2015**, *4*, 5761, 1-7
- 20) Mukherjee, A.M.; Joarder, B.; Desai, A.V.; Manna, B.; Krishna, R.; Ghosh, S.K. *Inorganic Chemistry*, **2015**, *54*, 4403-4408

- 21) Yoo, J. S.; Donohue, J. A.; Kleefisch, M. S.; Lin, P. S.; Elfline, S. D. *Applied Catalysis A.: General* **1993**, *105*, 83-105
- 22) Buske, G. R.; Wenger, T. L.; Beyrau, J. A. Heat Transfer Fluid, US Patent 4622160 A, November 11th, 1986
- 23) Chen, S.; Sun, A.; Qin, Z.; Wang, J. *Catalysis Communications* **2003**, *4*, 441-447
- 24) Agency for Toxic Substances and Disease Registry (ATSDR). 2007. Toxicological profile for Xylenes. Atlanta, GA: U.S. Department of Health and Human Services, Public Health Service
- 25) Atwood, J.L.; Barbour, L.J.; Jerga, A. *Science*, **2002**, *296*, 2367-2369
- 26) Fenyvesi, E.; Szente, L.; Russel, N.R.; McNamara, M. *Compr. Supramol. Chem.* **1996**, *3*, 305
- 27) Chaffee, K.E.; Fogarty, H.A.; Brotin, T.; Goodson, B.M.; Dutasta, J.P. *J. Phys. Chem. A*, **2009**, *113*, 13675-13684
- 28) Cram, D.J.; Tanner, M.E.; Knobler, C.B. *J. Am. Chem. Soc.* **1991**, *113*, 7717-7727
- 29) Scarso, A.; Pellizzaro, L.; De Lucchi, O.; Linden, A.; Fabris, F. *Angew. Chem. Int. Ed.* **2007**, *46*, 4972-4975
- 30) Foo, M.L.; Matsuda, R.; Hijkata, Y.; Krishna, R.; Sato, H.; Horike, S.; Hori, A.; Duan, J.; Sato, Y.; Kubota, Y.; Takata, M.; Kitagawa, S. *J. Am. Chem. Soc.* **2016**, *138*, 3022-3030
- 31) Demessence, A.; Long, J.R. *Chem. Eur. J.* **2010**, *16*, 5902-5908
- 32) Wang, H.; Li, B.; Wu, H.; Hu, T.L.; Yao, Z.; Zhou, W.; Xiang, S.; Chen, B. *J. Am. Chem. Soc.* **2015**, *137*, 9963-9970
- 33) Pivovar, A.M.; Holman, K.T.; Ward, M. *Chem. Mater.* **2001**, *13*, 3018-3031

- 34) Jacobs, A.; Nassimbeni, L.R.; Nahako, K.L.; Su, H.; Taljaard, J.H. *Cryst. Growth and Des.* **2008**, *8*, 1301-1305
- 35) Zlatkis, A.; Wu, Z.; Andrews, A.R.J. *Chromatographia* **1992**, *34*, 457-460
- 36) Uemura, K.; Kitagawa, S.; Kondo, M.; Fukui, K.; Kitaura, R.; Chang, H.C.; Mizutani, T. *Chem. Eur. J.* **2002**, *8*, 3586-3600
- 37) Cussen, E.J.; Claridge, J.B.; Rosseinsky, M.; Kepert, C.J. *J. Am. Chem. Soc.* **2002**, *124*, 9574-9581
- 38) Karmaker, A.; Samanta, P.; Desai, A.V.; Ghosh, S.K. *Acc. Chem. Res.* **2017**, [Online early access]. DOI:10.1021/acs.accounts.7b00151. Published Online: September 5, 2017. <http://pubs.acs.org/doi/abs/10.1021/acs.accounts.7b00151>
- 39) Jin, Z.; Zhao, H.Y.; Zhao, X.J.; Fang, Q.R.; Long, J.R.; Zhu, G.S. *Chem. Commun.* **2010**, *46*, 8612-8614
- 40) Lazar, A.I.; Biedermann, F.; Mustafina, K.R.; Assaf, K.I.; Henning, A.; Nau, W.M. *J. Am. Chem. Soc.* **2016**, *138*, 13022-13029
- 41) Rusa, C.; Tonelli, A.E. *Macromolecules*, **2000**, *33*, 1813-1818
- 42) Moreira, L.; Calbo, J.; Krick Calderon, R.M.; Santos, J.; Illescas, B.M.; Arago, J.; Nierengarten, J.F.; Guldi, D.M.; Orti, E.; Martin, N. *Chem. Sci.* **2015**, *6*, 4426-4432
- 43) Mahata, K.; Frischmann, P.D.; Wurthner, F. *J. Am. Chem. Soc.* **2013**, *135*, 15656-15661
- 44) Li, P.Z.; Su, J.; Liang, J.; Liu, J.; Zhang, Y.; Chen, H.; Zhao, Y. *Chem. Commun.* **2017**, *53*, 3434-3437

- 45) Chen, D.M.; Tian, J.Y.; Wang, Z.W.; Liu, C.S.; Chen, M.; Du, M. *Chem. Comm.* **2017**, *53*, 10668-10671
- 46) Levine, D.J.; Runcevski, T.; Kapelewski, M.T.; Keitz, B.K.; Oktawiec, J.; Reed, D.A.; Mason, J.A.; Jiang, H.Z.H.; Colwell, K.A.; Legendre, C.M.; Fitzgerald, S.A.; Long, J.R. *J. Am. Chem. Soc.* **2016**, *138*, 10143-10150
- 47) Xiao, D.; Zhang, D.; Chen, B.; Xie, D.; Xiang, Y.; Li, X.; Jin, M. *Langmuir* **2015**, *31*, 10649-10655
- 48) Ward, M.D.; Hunter, C.A.; Williams, N.H. *Chem. Lett.* **2017**, *46*, 2-9
- 49) Mishra, A.; Jung, H.; Lee, M.H.; Lah, M.S.; Chi, K.W. *Inorganic Chemistry* **2013**, *52*, 8573-8578
- 50) Kim, J.; Lee, S.O.; Yi, J.; Kim, W.S.; Ward, M.D. *Separation and Purification Technology*, **2008**, *62*, 517-522
- 51) Dey, A.; Bera, S.; Biradha, K. *Crystal Growth and Design* **2015**, *15*, 318-325
- 52) Chaffee, K.E.; Fogarty, H.A.; Brotin, T.; Goodson, B.M.; Dutasta, J.P. *J. Phys. Chem. A.* **2009**, *113*, 13675-13684
- 53) Liu, X.; Oh, M.; Lah, M.S. *Inorganic Chemistry* **2011**, *50*, 5044-5053
- 54) Moon, D.; Lah, M.S. *Inorganic Chemistry* **2005**, *44*, 1934-1940
- 55) Merlau, M.L.; del Pilar Mejia, M.; Nguyen, S.T.; Hupp, J.T. *Angew. Chem. Int. Ed.* **2001**, *40*, 4239-4242; Pluth, M.D.; Bergman, R.G.; Raymond, K.N. *Acc. Chem. Res.* **2009**, *42*, 1650-1659
- 56) Beatty, A.; Rath, N.; Hogan, G. *Cryst. Growth Des.* **2011**, *11*, 2740; Fischer, M.; Beatty, A. *CrystEngComm*, **2014**, *16*, 7313-7319

- 57) Hogan, G., The Molecular Transport and Intercalation of Guest Molecules into Hydrogen-Bonded Metal-Organic Frameworks (HMOFs), PhD Dissertation, University of Missouri – St. Louis, St. Louis, Missouri, August 2010
- 58) Friscic, T.; Mestrovic, E.; Samec, D.S.; Kaitner, B.; Fabian, L. *Chem. Eur. J.* 2009, *15*, 12644-12652; Soldatov, D.V.; Ukraintseva, E.A.; Logvinenko, V.A. *Journal of Structural Chemistry* 2007, *48*, 938-948; Soldatov, D.V.; Sokolov, I.E.; Suwin'ska, K. *Journal of Structural Chemistry* **2005**, *46*, S158-S164; Aakeroy, C.B.; Beatty, A.M.; Leinen, D.S.; *Angew. Chem. Int. Ed.* **1999**, *38*, 1815-1819; Beatty, A.M. *Coordination Chemistry Reviews* **2003**, *246*, 131-143; Sekiya, R.; Nishikiori, S. *Chem. Comm.* **2001**, 2612-2613; Kabir, M.K.; Miyazki, N.; Kawata, S.; Adachi, K.; Kumagai, H.; Inoue, K.; Kitagawa, S.; Iijima, K.; Katada, M. *Coordination Chemistry Reviews*, **2000**, *198*, 157-169
- 59) Beatty, A.; Chen, C.L *J. Am. Chem. Soc.* **2008**, *130*, 17222
- 60) Beatty, A.; Helfrich, B.; Hogan, G.; Reed, A. *Cryst. Growth Des.* **2006**, *6*, 122
- 61) O. M. Yaghi, H. Li, C. Davis, D. Richardson, T. L. Groy, *Acc. Chem. Res.* **1998**, *31*, 474; A. Pivovar, K. Holman, M. Ward, *Chem. Mater.* **2001**, *13*, 3018-3031; K. Endo, T. Koike, T. Sawaki, O. Hayashida, H. Masuda, Y. Aoyama, *J. Am. Chem. Soc.* **1997**, *119*, 4117
- 62) M. Ward, J. Swift, *Chem. Mater.* **2000**, *12*, 6, 1501; M. Zaworotko, K. Biradha, D. Dennis, V. MacKinnon, K. Sharma, *J. Am. Chem. Soc.*, **1998**, *120*, 11894
- 63) Ward, M. *Chem. Mater.* **2001**, *13*, 3018-3031; Nassimbeni, L. *Crystal Growth & Design* **2008**, *8*, 1301-1305; Nassimbeni, L. *J. Chem. Soc. Perkin Trans 2*, **2002**, 1246-1250; Nassimbeni, L. *Acta Cryst.* **2001**, *B57*, 394-398; Nassimbeni, L. J.

- Chem.Soc.Perkin Trans 2*, **2001**, 2119-2124; Kim, W. *Separation and Purification Technology* **2009**, 66, 57-64; Nassimbeni, L. *Eur. J.Org.Chem.* **2001**, 1887-1892
- 64) Wheeler, S.E.; Houk, K.N., *J. Chem. Theory Comput.* **2009**, 5, 2301-2312
- 65) Meccozi, S.; West, A.P.; Dougherty, D.A. *Proc. Natl. Acad. Sci.* **1996**, 93, 10566-10571; Naray-Szabo, G.; Ferenczy, G.G. *Chem. Rev.* **1995**, 95, 829-847; Klarner, F.G.; Kahlert, B. *Acc. Chem. Res.* **2003**, 36, 919-932; Kamieth, M.; Klarner, F.G.; Diederich, F. *Angew.Chem. Int. Ed.* **1998**, 37, 3303-3306; Klarner, F.G.; Panitzky, J.; Preda, D.; Scott, L.T; *J. Mol. Model.* **2000**, 6, 318-327; Branchi, B.; Balzani, V.; Ceroni, P.; Kuchenbrandt, M.C.; Klarner, F.G.; Blaser, D.; Boese, R. *J. Org. Chem.* **2008**, 73, 5839-585; Medhi, C.; Mitchell, J.B.O.; Price, S.L.; Tabor, A.B. *Biopolymers*, **1999**, 52, 84-93; Meyer, E.A.; Castellano, R.K.; Dierderich, F. *Angew. Chem. Int. Ed.* **2003**, 42, 1210-1250; Aakeroy, C.B.; Wijethunga, T.K.; Desper, J. *New J. Chem.* **2015**, 39, 822-828

Chapter 4

Probing the Selectivity of the Hydrogen Bonded Framework by Focusing on the Electronic Differences of the Guest Molecules When Placed in Competition

4.1.1 Abstract

We have previously demonstrated that the charge-assisted hydrogen bonded framework consisting of $\text{Zn}(\text{HPDCA})_2 \cdot (\text{H}_2\text{O})_2$ and *o*-tolidene will separate guest molecules based on size and shape. This separation occurs through the selective co-crystallization of the guest molecules. We asked the question, will this framework separate based on another property such as the electronics of the molecule? The framework's ability to separate guest molecule pairs based on the electronic configuration of those molecules has been explored to show that it can selectively co-crystallize one guest versus another. Using headspace gas chromatography, we focused on how selectivity of the framework changes based on the electronic nature of the guest molecule. To do this, we examined a series of mono-substituted benzene molecules placed in competition with each other. The guest molecules Hammett σ_p -values ordered the guest's substituents from electron donating to electron withdrawing functional groups. Electrostatic potential maps were then calculated to demonstrate how electron density changed for each guest molecule. This was then used to show favorable electrostatic interactions between preferred guests and the framework. The selectivity of the host framework towards guests based on their electronic configuration is the focus of the following discussion.

4.1.2 Background

The separation of two or more molecular species can be one of the most significant challenges facing researchers as they strive to discover critical reagents which have significant biological and economic impact in the world at large. Of particular interest to this research has been the ability to exploit the separating power of the host-guest interaction. Researchers, as well as ourselves, have observed that host materials

have the capability to separate guest molecules based on their size and shape.¹ There are molecular properties which can also be used to isolate a molecule of interest selectively.

Another means of host-guest interaction is through the electrostatic interactions between the guest molecule and its host. If the electronic nature of a host molecule and its guest are complementary, then the two should come together with relative ease.² The question to be answered would be how much of a role do electronics play when separating molecular species? There are numerous examples where researchers have found examples where electronics play a large factor in host selectivity. Ward *et al.* found that electron rich areas of the guest molecule will converge with electron deficient areas of the host, providing evidence for how a guest might bind.³ Yaghi *et al.* found that to be competitive for space in a specific host, a guest would require a hydroxyl groups.⁴ These findings demonstrated a selectivity mechanism which was based than size and shape of the guest. Selectivity based on the electronic character of the guest molecule would have to be complementary to the channel within which that guest resides.⁴ Ward, Hunter, and Williams described a coordination cage where tris-chelate metal centers at the corners of the cage created hydrogen donor pockets for electron-rich guest molecules.⁵ Guest uptake can be pH dependent as the host, and the guest can switch between being cationic, neutral or anionic thus affecting the electrostatic interactions responsible for uptake and release.⁶ The concept covers selective guest uptake from a mixture of multiple guest.⁷ Calculating the electrostatic potential surface of the inside of the host; Ward *et al.* were able to discern where guests with favorable electrostatic interactions would bind.⁸ Fujita *et al.* were able to selectively bind tripeptide sequences when electrostatically and sterically different sequences were tested against each other.⁹

Hammett constants for functional groups provide a pathway for systematically changing the electronics of a guest molecule without dramatically changing the size and overall shape of the guest molecule.¹⁰ Known Hammett constant values can numerically order the electron withdrawing or electron donating capabilities of a functional group.¹⁰ There is a linear correlation between σ_m -value and the calculated electrostatic potential of the centroid for aromatic molecules (Figure 4.1.2.1).¹¹

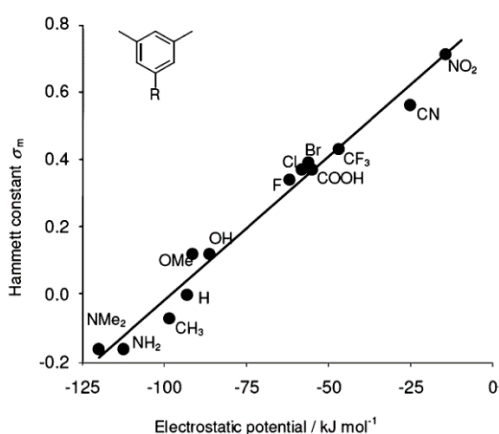


Figure 4.1.2.1 B3LYP/6-31G* electrostatic potentials (ESPs) at the ring centers of *para*-substituted *meta*-xylenes correlate well with Hammett *meta*-substituent constants that have previously been used in structure-activity relationships describing aromatic stacking interactions.¹¹

These types of relationships are of great interest here since the electrostatic interaction of a guest molecule with its host could dictate whether that interaction is favorable or not. Gokel *et al.* found a linear correlation between the relative rate for sodium ion transport and the Hammett σ of *p*-methoxybenzyl substituent to *p*-nitrobenzyl attached to a synthetic ion channel for sodium ion transport.¹² Hunter *et al.* looked at the effect substituents had an electron donating group to face interactions.¹³ His group found that “electronic polarization of π systems can have a dramatic effect on the magnitude of the non-covalent interaction between two simple aromatics.”¹³ Their results showed

correlation to Hammett substituent constants, and this indicated that differences in interactions energies were electrostatic in origin.¹³ Hunter points out that electrostatic potentials on the surfaces of aromatic rings are sensitive to the nature of the attached substituents. While the values measured for their system may not transfer to other systems, the trends observed may have broader applications.¹⁴ Hunter and Sanders proposed guidelines for the interactions between aromatic molecules. Two negatively charged electron clouds sandwiched a positively charged σ -framework.¹⁵ The orientation of two aromatic systems will determine whether there is an attraction between the σ -framework or π -electron repulsion. However, Hunter elaborates by showing that electron withdrawing or donating substituents can change the stacking interaction as they affect the π -electrons (Figure 4.1.2.2).¹⁶

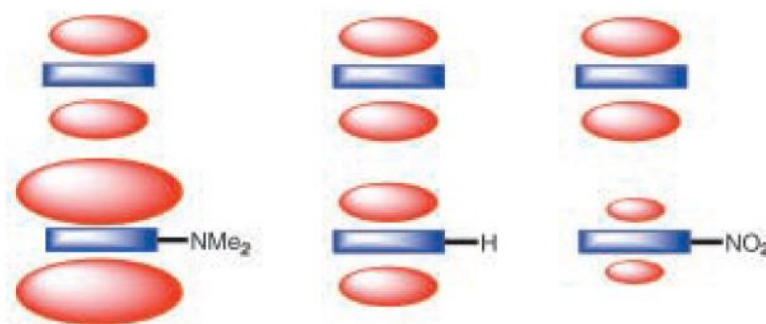


Figure 4.1.2.2 Schematic representation of the effect of substituents on stacking interactions.¹⁶

We want to understand what drives selectivity for this material. Knowing what drives selectivity can help distinguish use or application. To that end, we studied the relationship between guest electron density and selectivity of our framework with the following guest molecules: *p*-xylene, *p*-dichlorobenzene, *p*-chlorotoluene, N,N-

dimethylaniline, ethylbenzene, toluene, benzene, fluorobenzene, chlorobenzene, bromobenzene, iodobenzene, and nitrobenzene.

4.2.1 Experimental Procedures

ZnCl₂ (>97%) was purchased Fisher Scientific. *O*-Tolidine (>97%) was purchased from Sigma Aldrich Chemical Company. 2,4-pyridine-dicarboxylic acid (98%) was purchased from AK Scientific. *p*-xylene, *p*-dichlorobenzene, *p*-chlorotoluene, N,N-dimethylaniline, ethylbenzene, toluene, benzene, fluorobenzene, chlorobenzene, bromobenzene, iodobenzene, and nitrobenzene were all reagent grade and purchased from Sigma Aldrich. Methanol was reagent grade from Sigma Aldrich Chemical Company. Dimethylformamide (anhydrous, 99.8%) was purchased from Fisher Scientific. PXRD patterns were collected on a Rigaku Ultima IV X-ray diffractometer containing a CuK α source ($\lambda = 1.54051 \text{ \AA}$) and viewed with MDI Jade 9 software.

In section 4.3.2 and 4.3.3, eleven experiments were performed for each guest pair tested. We used the same method as Chapter 3. The mole fraction of each guest was adjusted moving from one experiment to the next. As guest A would increase by 0.1 χ , guest B would decrease by 0.1 χ . Crystals were isolated, ground and then tested for the ratio of each guest molecule using gas chromatography.

For section 4.3.4, each guest pair added to the crystal growth solution was at equal molar concentrations. Due to a large number of guests, performing eleven experiments for each combination would add a significant number of experiments as well as another variable since selectivity can be concentration dependent. Therefore, in each guest pair, only a 0.5 mole fraction of each guest was added to the growth solution. Performing the experiments in this manner, allowing for the guests to be on equal footing

regarding concentration. Each experiment would allow for focus on the significance of the electronic differences between the molecules.

4.2.2 Synthesis of 1•guest

The synthesis of guest containing framework can be found within the experimental section in Chapter 3.

4.2.3 Chromatographic Methods

An HP gas chromatography-mass spectrometer (model 5988A) was used to collect all chromatographic data. For GC/GCMS, the isolated crystals were placed inside of a 20mL GC headspace vial (Xpertek, PJ. Cobert, Cat#954040) and sealed with a magnetic cap containing a high temperature rated septum (Xpertek, PJ. Cobert, Cat#952237). A 1mL, A-2 Luer gas-tight syringe was used for headspace analysis. All chemical reactions were carried out under ambient conditions. For the GC/GCMS experiment, lightly crushed 1•guest (0.010g) crystals and heated them to 200°C using a multi-welled hotplate. The guests evolved into the headspace and sampled for GC injection. The temperature used was based on thermogravimetric analysis (TGA) data. 200°C was also used as the upper limit because **1** decomposes at around 215°C based on melt point studies. No traces of acetone or methanol were seen in the MS data. The column used was a Supelco SLB – 5MS 30M x 0.25mm x 0.5µm film thickness. The GC oven was initially 50°C for 2 minutes, then ramped to 180°C at a rate of 20°C/min and held for 1 minute. The total run time was 12 minutes.

4.3 Results and Discussion

4.3.1 Calculation of Electrostatic Potential for Guest Molecules

We understand that the size and shape of a guest molecule can influence their co-crystallization within the framework. Our attention turns toward guests who are approximately the same size, the same shape but differ markedly in electronic configuration. By calculating the electrostatic potential maps of each guest and the framework, we can visually compare these guests and explain why the selectivity of the framework is affected by the electron density changes between the guests. We compared the following molecules: *p*-xylene, *p*-chlorotoluene, and *p*-dichlorobenzene first. The *p*-xylene was preferred compared to the guests with electron withdrawing substituents. The guests with electron donating substituents, such as methyl groups, were preferred to electron withdrawing groups, such as chlorine. In a separate set of experiments, we further compared N,N-dimethylaniline, ethylbenzene, toluene, benzene, fluorobenzene, chlorobenzene, bromobenzene, iodobenzene, and nitrobenzene against each other. Guests with electron withdrawing substituents were not preferred, but there were exceptions such as iodobenzene. Based on the results of our findings, we formed the hypothesis that the interaction between the guest and framework was driving selectivity.

Electrostatic potential maps were calculated to highlight the differences in electron density for each guest molecule discussed herein. The electrostatic potential map is determined by having a unit of positive charge at each point on the surface of the molecule and measuring the interaction energy of this charge with the nuclei and electrons in the molecule.¹⁷ The surface is then painted a specific color depending on the magnitude of this interaction. For areas of high electron density, the surface is colored

red-orange and areas of lower electron density are colored blue-green. The electrostatic potential was calculated using Spartan Student V6 software. The calculations performed were equilibrium geometry, B3LYP, and 6-31G* level of theory. Further calculations were energy (single point energy) using the same level of theory (Figure 4.3.1.1).

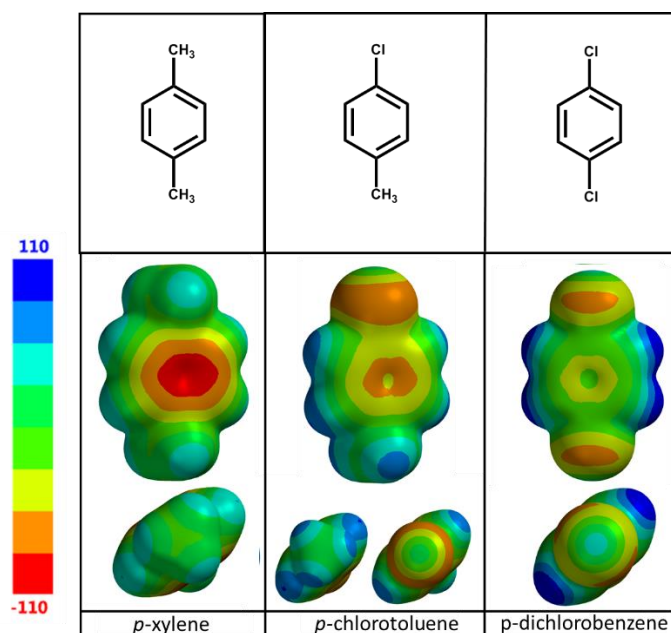


Figure 4.3.1.1 Electrostatic potential maps of *p*-dichlorobenzene, *p*-chlorotoluene, and *p*-xylene, legend units are in $\text{kJ}\cdot\text{mol}^{-1}$

Figure 4.3.1.1 shows that each of these guest molecules has a very different electrostatic potential topography. The legend on the side of Figure 4.3.1.1 shows the color-scheme for the maps in $\text{kJ}\cdot\text{mol}^{-1}$. Areas of high electron density are in red while areas of low electron density are blue. Beginning with *para*-xylene on the left (Figure 4.3.1.1), electron density at the centroid of the aromatic ring is high and shows as a deep red color on the model. The *p*-xylene has light blue colors for the methyl hydrogens which have low electron density. For *p*-chlorotoluene (middle of Figure 4.3.1.1), one electron donating methyl group is replaced by an electron withdrawing chlorine atom. The light blue color on the lone methyl group hydrogens is now a dark blue color showing a

decrease in electron density. Electron density has decreased inside the centroid of the aromatic ring (orange color). The σ -hole, spot of low electron density (light green color), can be seen at the tip of each chlorine atom on *p*-chlorotoluene as well as in *p*-dichlorobenzene. A significant amount of orange envelopes the torus of the chlorine atom indicating a high degree of electron density. In *p*-dichlorobenzene, the hydrogen atoms on the aromatic ring have low electron density (blue colored overlay). The central core of the aromatic ring shows medium electron density (green to yellow). High levels of electron density (orange color) concentrate around the sides of the chlorine atoms. Since there are two chlorine atoms on *p*-dichlorobenzene, these electronegative atoms pull electron density away from the centroid of the aromatic ring. While the size and shape of these potential guests do not differ significantly, Figure 4.3.1.1 highlights the differences in electron density distribution for these molecules.

The electrostatic potential maps were calculated for N,N-dimethylaniline, ethylbenzene, toluene, benzene, fluorobenzene, chlorobenzene, bromobenzene, iodobenzene, and nitrobenzene using the same level of theory as before (Figure 4.3.1.2).

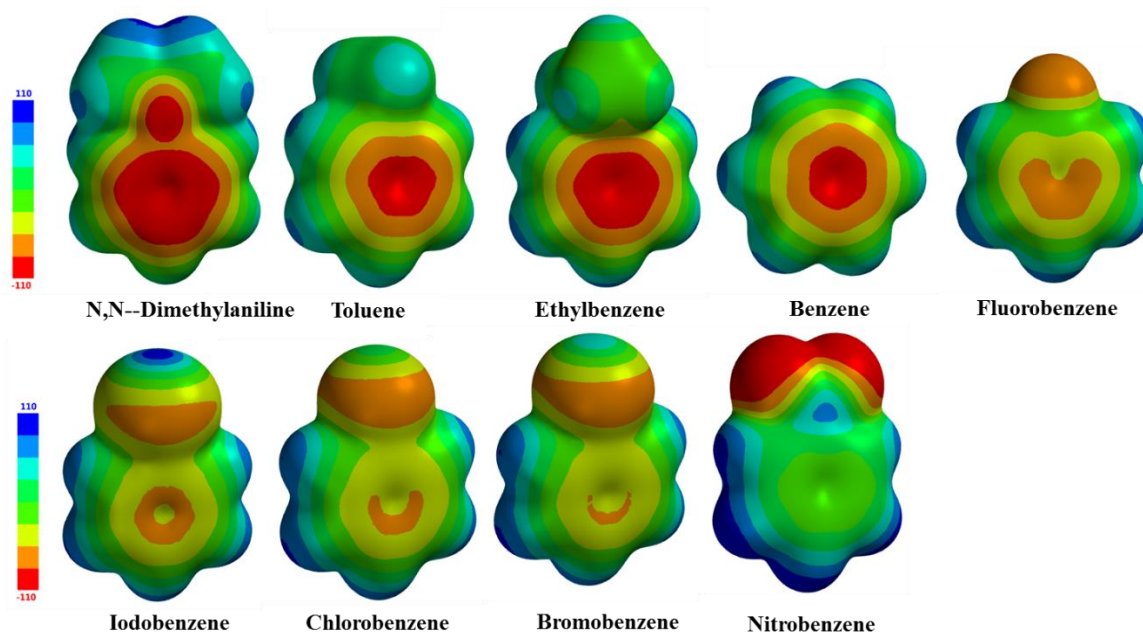


Figure 4.3.1.2 Calculated guest electrostatic potential maps; guests with electron donating substituents were preferred with a few outliers such as iodobenzene and bromobenzene

Figure 4.3.1.2 shows the molecules ordered according to their Hammett σ_p -values (Figure 4.3.1.2). Starting with N,N-dimethylaniline, the $-\text{N}(\text{CH}_3)_2$ is the most electron donating substituent and this can be seen by the significant amount of red or a high degree of electron density at the center of the aromatic ring. In Figure 4.3.1.2, moving to the right along the first row, the electron density begins to decrease at the centroid from toluene down to benzene. After benzene, the fluorine substituent causes electron density to pull away from the center of the aromatic ring (orange color). The electron withdrawing nature of fluorine has now changed the topography of the molecule. The pattern continues from left to right in the second row of Figure 4.3.1.2. The center of the ring continues to lose electron density as the functional group changes. With nitrobenzene, the electron density at the center of the ring is entirely different from N,N-dimethylaniline. For nitrobenzene, the functional group has a high concentration of electron density (red color) around the oxygens. By comparison, N,N-dimethylaniline is blue at the methyl

hydrogen atoms in the functional group. This gradient of electron density on the guest molecules provides a step-wise change in guest electronics.

The electrostatic potential maps of the guests are an excellent start, but to create a full picture, we move on to the framework itself. The electrostatic potential map of pieces of the framework was calculated to understand the host-guest interaction better. Due to limited computational capacity, only fragments of the framework were able to be modeled using Spartan '14 modeling software. To perform the calculations, the level of theory used was equilibrium geometry, semi-empirical, Austin Model 1 (AM1). Followed by energy (single point energy) calculation using the same level of theory. The electrostatic potential surfaces were calculated separately, after the initial calculations. For this calculation, the dihedral angle between the two aromatic rings of *o*-tolidine was locked at zero to mimic conditions of the 1-D channel within the framework. The *o*-tolidine pillar, walls of the 1-D channel, was combined with an isonicotinate salt at each of the ammonium groups (Figure 4.3.1.3).

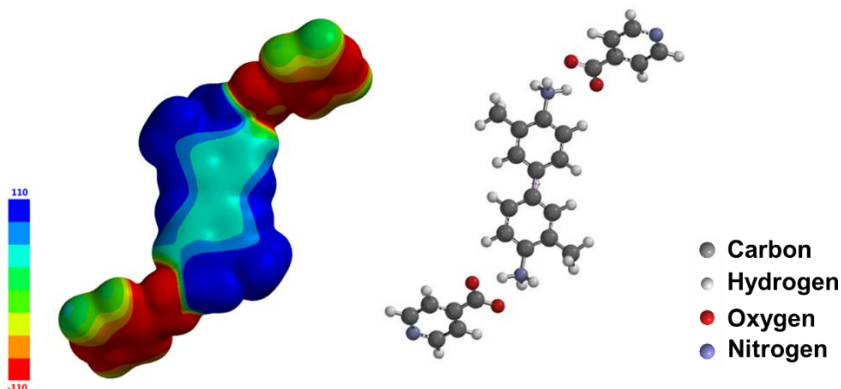


Figure 4.3.1.3 Calculated ESP map of the *o*-tolidine pillar, salted with isonicotinate

From the electrostatic potential map, the walls of the pillar are partially positive. In the full framework, the blue area near the $R-NH_3^+$ would be covered by oxygen in the carboxylate groups in the layer. The methyl groups on the pillar are a deep blue color which insinuates a low level of electron density. Each pillar of the framework wall overlaps in a louver fashion. In that case, most of what the guest will see of the walls would have low electron density (blue color). The oxygen atoms on the isonicotinate remain exposed to the potential guest molecules and are rich in electron density. These aspects of the 1-D channels may give insight into why guests are preferred based on the pattern seen in Figure 4.3.1.2. The ESP map was also calculated for the zinc complex as well (Figure 4.3.1.4).

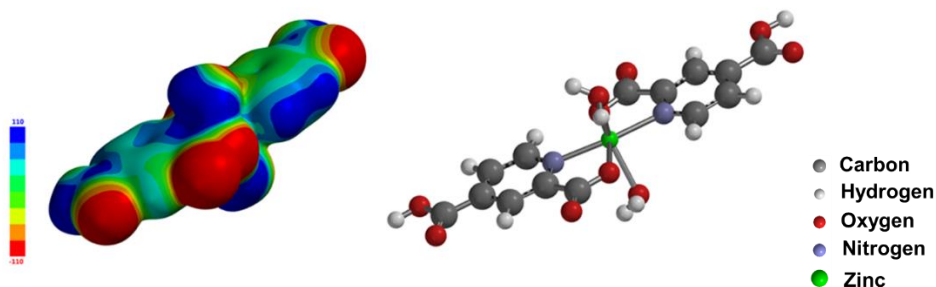


Figure 4.3.1.4 Zn (II) coordination complex, forms the layers of 1

The oxygens from two of the carboxylic acids on Zn complex point down towards the 1-D channel. The guests will have to interact with an electron-rich surface. If there is a high degree of electron density on the functional group of the guest molecule, the layer and the guest may repel each other. Consequently, functional groups with low electron density would have less repulsion and would comfortably fit into the channel. Guests with electron donating functional groups also have an electron-rich aromatic ring. The

electron-rich ring would have a positive interaction with electron deficient walls of the framework. Since opposite charges attract, we can use these electrostatic potential maps to theorize which guests will have the best interaction with the framework.

Using the electrostatic potential maps as a reference, we can begin to understand the results of the competition studies and observe how changes in electron density between the guests can affect selectivity within the framework.

4.3.2 Electron withdrawing versus donating in para-substituted aromatics

The *p*-xylene and *p*-dichlorobenzene guests were placed in competition. The guests have the same shape and size but are very different electronically (Figure 4.3.1.1). The *p*-xylene has two electron donating groups which push electron density to the center of the aromatic ring. The *p*-dichlorobenzene's electron withdrawing chloro- groups pull electron density away from the center of the molecule and concentrate it around the halides (Figure 4.3.1.1). To represent the results of the competition between *p*-xylene and *p*-dichlorobenzene, a plot was made for percent inclusion of *p*-xylene found in the framework vs. the mole fraction of *p*-xylene used in the competition study. Selectivity is represented by which side of the red line the data points fall. In Figure 4.3.2.1, all the data points are above the red line; this indicated a preference for *p*-xylene.

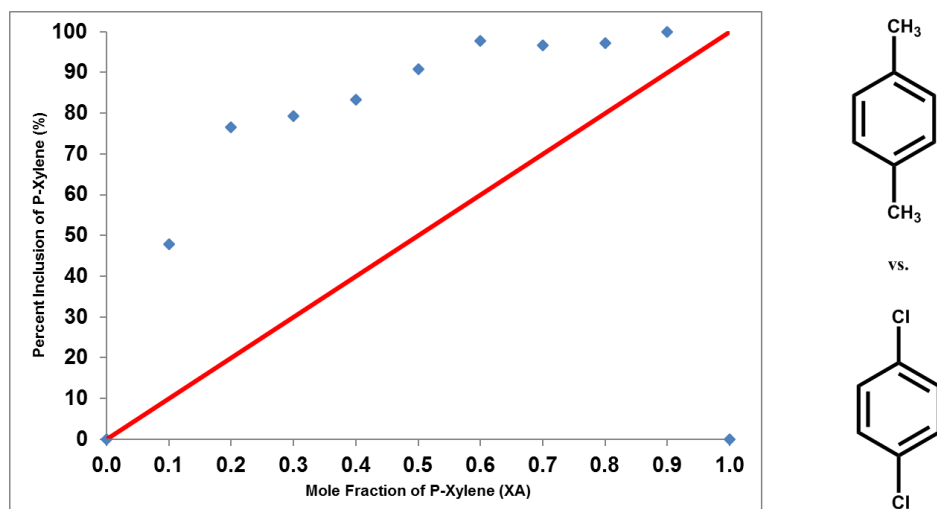


Figure 4.3.2.1 Competition study of *p*-xylene versus *p*-dichlorobenzene, 1 was selective for *p*-xylene

Looking at the results of the competition study, the electronic difference between the molecules was substantial, and there was a strong preference for *p*-xylene. The results of this competition study demonstrate an evident selectivity towards *p*-xylene compared to *p*-dichlorobenzene.

4.3.3 *p*-xylene vs. *p*-chlorotoluene

The next series of experiments placed *p*-xylene in competition with *p*-chlorotoluene to determine the preferred guest within the framework. By introducing a methyl group, we expect the electronic differences between the guest molecules to be more subtle. The question will be how sensitive the framework is when there are only minor changes in the guest electronics (Figure 4.3.3.1).

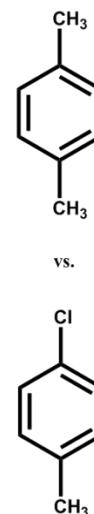
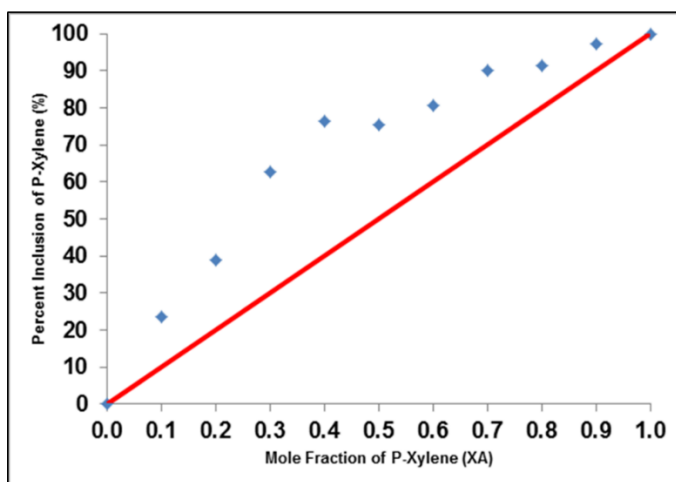


Figure 4.3.3.1 Competition study of *p*-xylene versus *p*-chlorotoluene, **1** was selective for *p*-xylene.

We can see in Figure 4.3.3.1, that the data points fall to the left of the red line. The *p*-xylene is incorporated preferentially into the framework. At 0.1 χ , *p*-xylene was 23.7% of the guest ratio. *p*-xylene's inclusion in **1** climbed steeply over the next few mole fractions. It practically doubled from 0.1 to 0.2 χ and was 62.5% by 0.3 χ . At less than 50% of the added guest ratio in the crystal growth solution, *p*-xylene was 76.3% (at 0.4 χ) of the recovered guests from **1**. The added methyl group influenced the selectivity of **1**. The size and shape of the guests are the same, but it becomes apparent that selectivity is sensitive to subtle changes in the guest electronics.

With all this in mind, switching to a guest with a more electron withdrawing group increases selectivity towards *p*-xylene. We can form a hypothesis about the selectivity of the framework when size and shape of the guests are held constant. As the number of electron withdrawing substituents increases, the selectivity of **1** increases for the guest with more alkyl/electron donating substituents on a benzene ring.

To determine the soundness of this theory, we move to the larger group of guest molecules for the test.

4.3.4 Varying Guest Electronics to Probe Sensitivity of Framework Selectivity

To determine the universality of our observation regarding electron withdrawing/donating substituents, a series of nine guest molecules were placed in competition with each other. The guests are of similar size and shape but have different electronic configurations. These guests were chosen to probe how electrostatic interactions between the guest and the framework would influence the results. In this case, we selected one concentration per competition. Each guest molecule was at the same mole fraction as its competitor, thereby significantly decreasing the number of experiments required.

All the molecules chosen were mono-substituted derivatives of benzene. Their Hammett σ_p -values ordered the guest molecules. Negative Hammett values indicate electron donating, while positive values are electron withdrawing. Nine guests were tested in the competition which led to 36 experiments. Only mono-substituted benzenes were used to limit size differences as much as possible (Table 4.3.4.1).

Table 4.3.4.1 Guest molecules to be tested in competition series, in the order of most electron donating to electron withdrawing

Guest Molecule	Size (Å³)	σ-para value
<i>N,N-Dimethylaniline</i>	147.1	-0.83
<i>Toluene</i>	116.7	-0.17
<i>Ethylbenzene</i>	135	-0.15
<i>Benzene</i>	98.45	0.0
<i>Fluorobenzene</i>	102.9	0.06
<i>Iodobenzene</i>	123.5	0.18
<i>Chlorobenzene</i>	112.1	0.23
<i>Bromobenzene</i>	116.6	0.23
<i>Nitrobenzene</i>	119.4	0.78

We observed the following trends from the experiments: electron withdrawing substituents were not preferred by the framework while electron donating groups were. The exception to this trend was iodobenzene, and bromobenzene. Iodobenzene was the most preferred of the guests overall. Bromobenzene was more preferred than toluene, even though the methyl group is more electron donating and usually preferred by the framework. Looking back to Section 4.3.1, iodobenzene and bromobenzene have partial positive sigma holes at the tip of the halide. This partial positive area would have to be attracted rather than repelled by the partial negative region of the framework layers.

In each graphical representation, the result for a single guest versus the guests in the series was plotted. Each point in the graph represents a separate comparison. The results were reported as a percentage of total peak area as retrieved from the GC (gas chromatography) chromatogram for each guest pair experiment.

Since there are no substituents on the molecule, benzene is considered the baseline. Benzene was not preferred by the framework when compared to any of the other guest molecules (Figure 4.3.4.1).

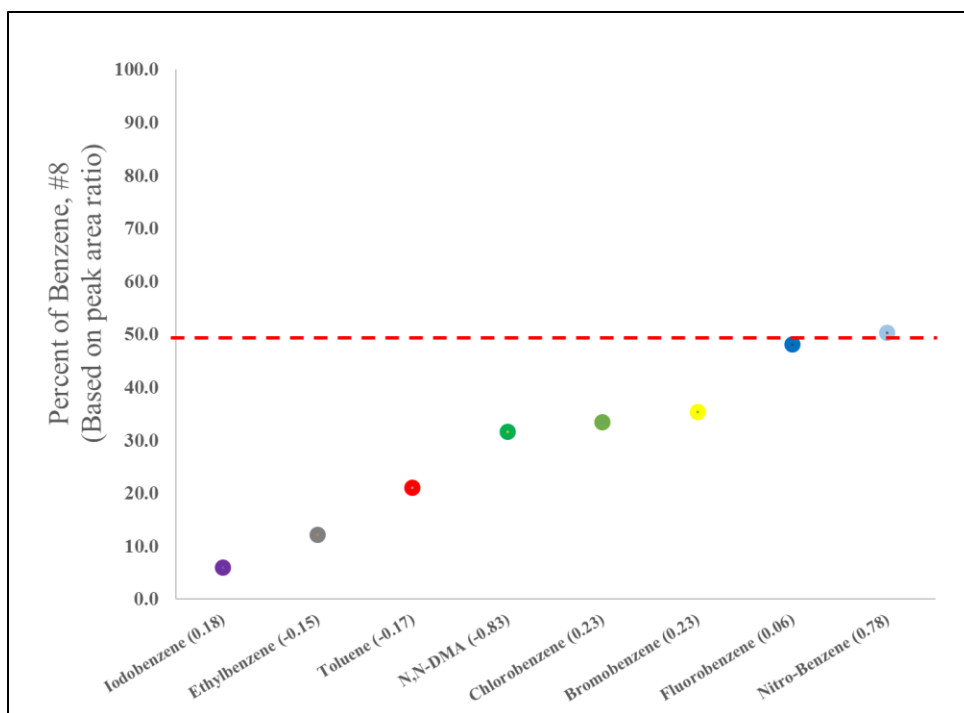


Figure 4.3.4.1 Guest competition study with benzene used as the control; all guests were preferred over benzene.

Benzene was on par with fluorobenzene and nitrobenzene. Benzene and fluorobenzene had some of the lowest concentrations from mono-guest filled framework quantitation (Ch 5). These molecules also have the smallest cubic volumes. Benzene has 95% of the volume of fluorobenzene, but that difference only increases in comparison with other guest molecules. Iodobenzene performed the best against benzene, but the next three guest molecules all have electron donating substituents attached. All electron withdrawing substituents follow these. Already, there is an indication that iodobenzene interacts differently with the framework compared to other electron withdrawing substituents. Since benzene does not have any functional groups, it should be easier to incorporate into the framework because there is no proper orientation during co-crystallization. Benzene has a low boiling point and high vapor pressure. These properties could have been a factor and been the cause of guest loss during sample prep as well.

Fluorobenzene was dominated by all the guest molecules in the series just like benzene (Figure 4.3.4.2).

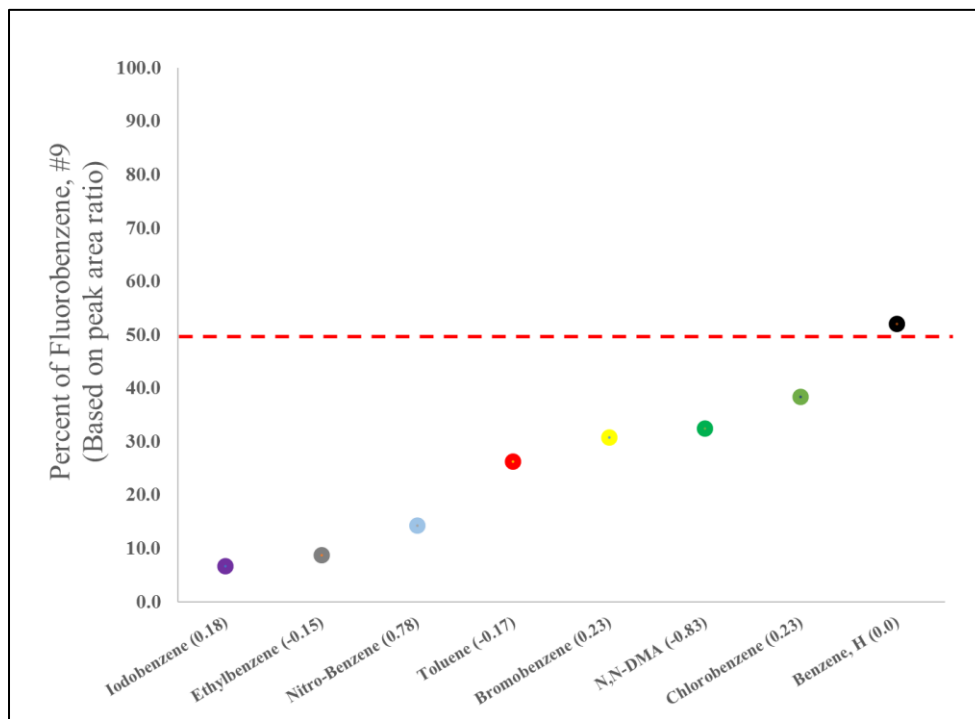


Figure 4.3.4.2 Guest competition study with fluorobenzene used as the control; all guests, except benzene, were preferred over fluorobenzene.

Fluorobenzene once again shows that low molecular weight does not imply dominance against the other guests. From the electrostatic potential maps, fluorobenzene has a high concentration of electron density at the fluorine, and this would repel it from the framework layer. When quantified, fluorobenzene had the lowest guest concentration within the framework based on GC data of 0.6% versus 12.7% theoretical (Ch. 5). It made sense that fluorobenzene would be of low concentration against other guests.

Nitrobenzene begins to show dominance against the other molecules; specifically benzene and fluorobenzene. This guest had the highest σ_p -value (0.78) of the series. It was not, however, the most or least dominant guest (Figure 4.3.4.3).

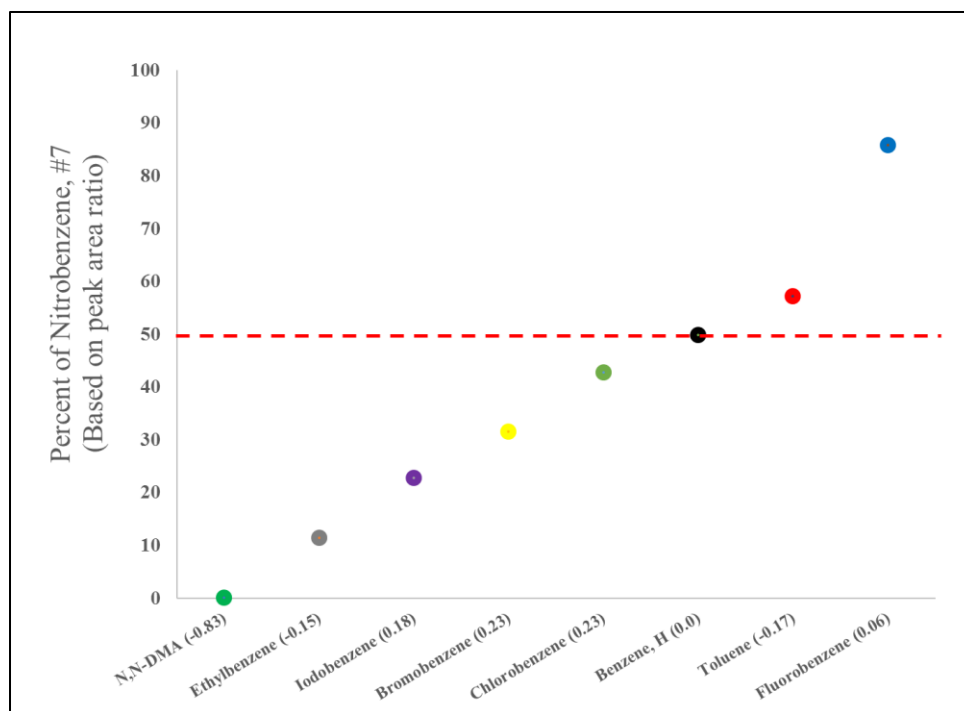


Figure 4.3.4.3 Guest competition study with nitrobenzene used as the control; N,N-DMA, ethylbenzene, benzene, iodobenzene, chlorobenzene, and bromobenzene were preferred over nitrobenzene.

Nitrobenzene was more dominant than fluorobenzene and on par with benzene.

Nitrobenzene has a cubic volume larger than bromobenzene, chlorobenzene and fluorobenzene, but is smaller than iodobenzene. N,N-DMA was apparently the dominant guest species. N,N-dimethylaniline and nitrobenzene have entirely opposite σ_p -values.

Ethylbenzene was preferred. Iodobenzene was preferred, but not to the same extent as has been seen in previous competitions. Iodobenzene also does not hold the number one spot for the first time.

Chlorobenzene was dominant for 38% of the experiments when in competition with the other guests (Figure 4.3.4.4).

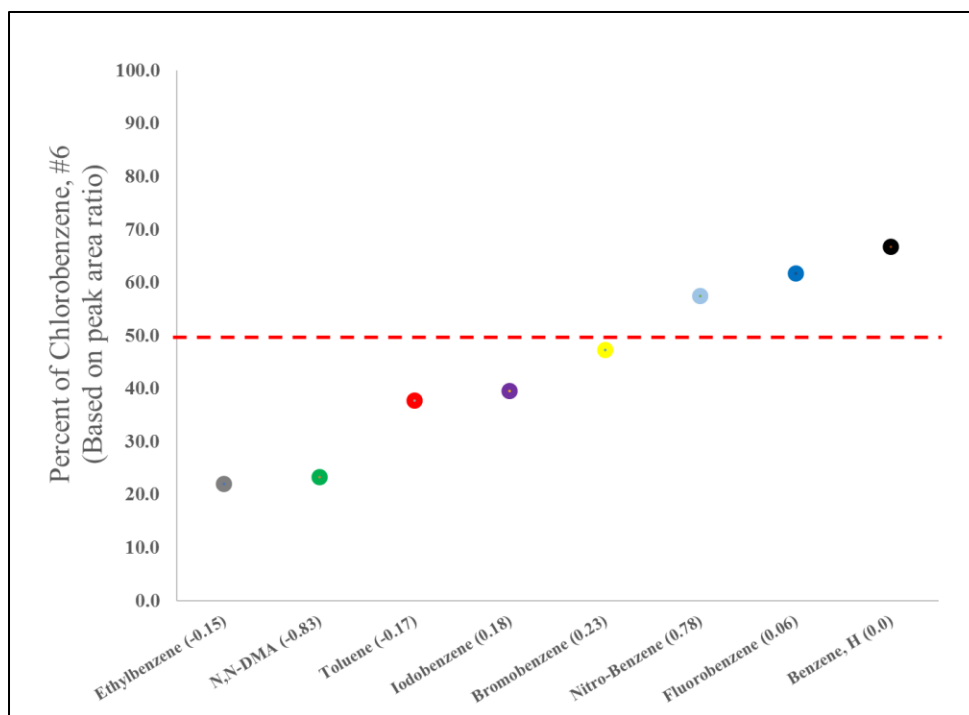


Figure 4.3.4.4 Guest competition study with chlorobenzene used as the control; N,N-DMA, toluene, ethylbenzene, iodobenzene, and bromobenzene were preferred over chlorobenzene.

Chlorobenzene was preferred to benzene, fluorobenzene, nitrobenzene and was almost equal with bromobenzene. The σ_p -values for chlorobenzene and bromobenzene are the same at 0.23. Bromobenzene only held a narrow advantage over chlorobenzene.

Bromobenzene's cubic volume is 4% larger than chlorobenzene. One would expect bromo- and chloro- to be in an even ratio inside **1**. For guests with electron donating groups, all were more preferred, but there was not necessarily a trend between them.

Toluene had the next highest degree of preference after chlorobenzene (Figure 4.3.4.5).

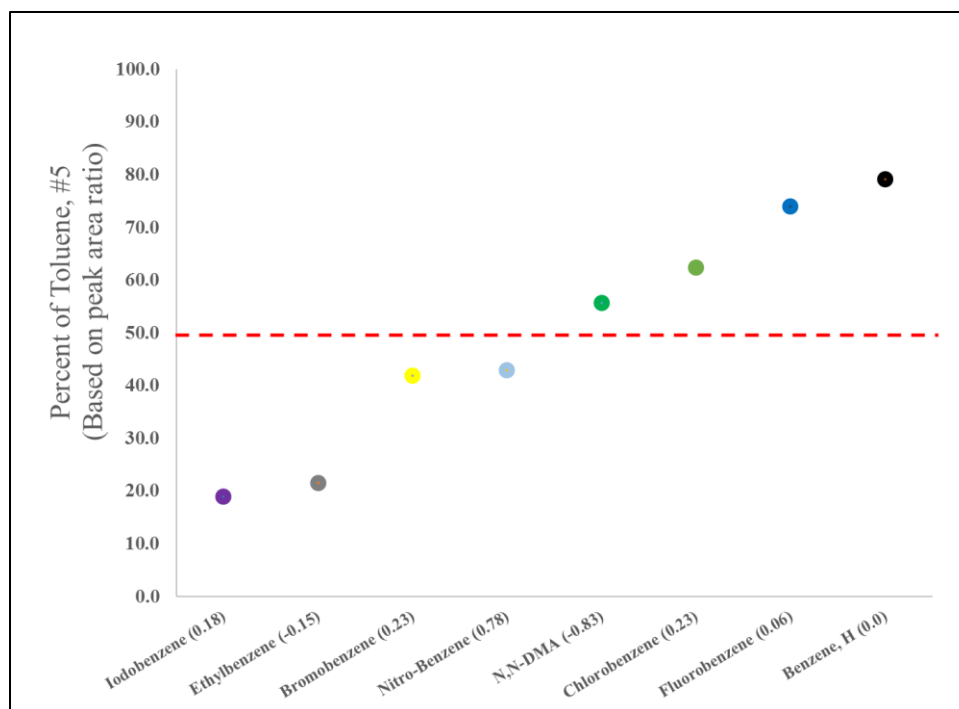


Figure 4.3.4.5 Guest competition study with toluene used as the control; ethylbenzene, iodobenzene, bromobenzene, and nitrobenzene were preferred over toluene.

Toluene is preferred over benzene, fluorobenzene, chlorobenzene, and N,N-dimethylaniline. Toluene was outperforming 50% of the guests. Iodobenzene continues to be preferred over toluene. Ethylbenzene was highly preferred to toluene. Ethylbenzene has about 16% greater cubic volume than toluene, and yet it was still found at higher concentrations. From Chapter 3, toluene is smaller and has methyl group just like *p*-xylene while ethylbenzene contains an ethyl group and has a larger cubic volume. The size difference did not help toluene vs. ethylbenzene.

Bromobenzene was preferred over a significant number of guest molecules though, for N,N-dimethylaniline, and chlorobenzene, it was very close (Figure 4.3.4.6).

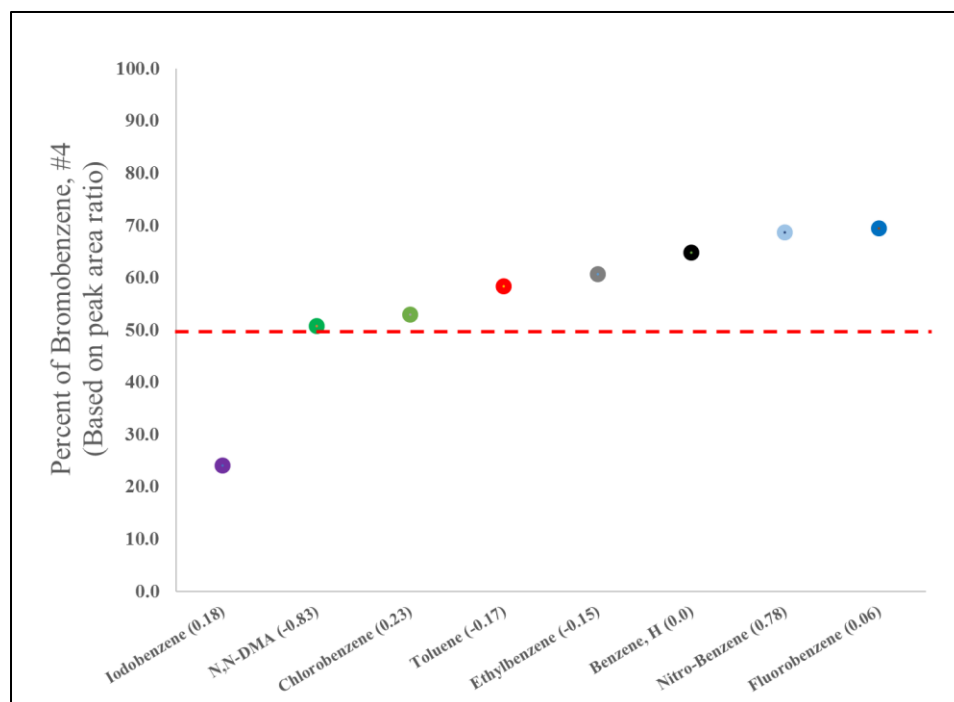


Figure 4.3.4.6 Guest competition study with bromobenzene used as the control; iodobenzene was preferred over bromobenzene.

Bromobenzene creates a stark contrast to chlorobenzene. Chlorobenzene beat out about 50% of the other guests while bromobenzene was only beaten significantly by iodobenzene. There was not a clear trend of electron donating to electron withdrawing groups. The preference alternated back and forth between the two types of substituents. Bromobenzene was the most preferred against benzene, nitrobenzene, and fluorobenzene. Based on the electrostatic potential maps, bromobenzene is the closest to iodobenzene. Both molecules have a measurable sigma hole which presents an area of low electron density compared to molecules like nitrobenzene and fluorobenzene.

The guest with the highest electron donating Hammett value, N,N-dimethylaniline (N,N-DMA), demonstrated a significant preference versus the guests in the series (Figure 4.3.4.7).

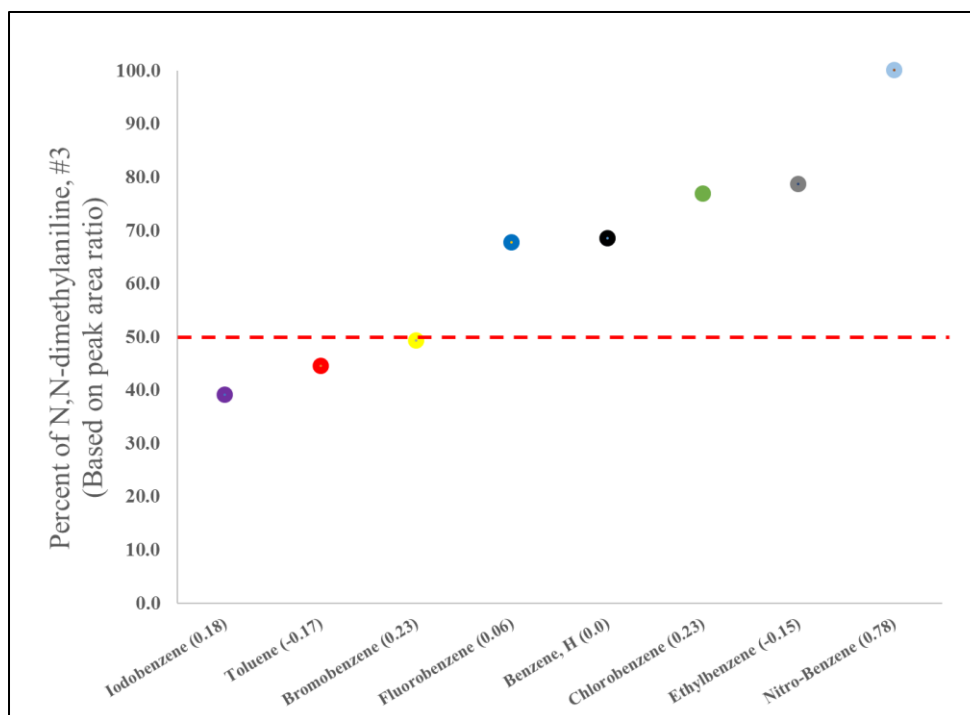


Figure 4.3.4.7. Guest competition study with N,N-DMA used as the control; only toluene, iodobenzene, and bromobenzene were preferred over N,N-DMA.

N,N-DMA had a high degree of preference except for toluene, bromobenzene, and iodobenzene. There is a clear preference for N,N-DMA over 60% of the guests in the study. Toluene was just ahead of N,N-DMA, and iodobenzene was first overall. Bromobenzene, while more electron withdrawing than iodobenzene and certainly toluene, was significantly ahead of chlorobenzene when in competition with N,N-dimethylaniline.

The ethylbenzene results were impressive in that as a guest, it did not have the highest volume and did not have the highest σ_p -value. Ethylbenzene demonstrated a high degree of selectivity within the framework (Figure 4.3.4.8).

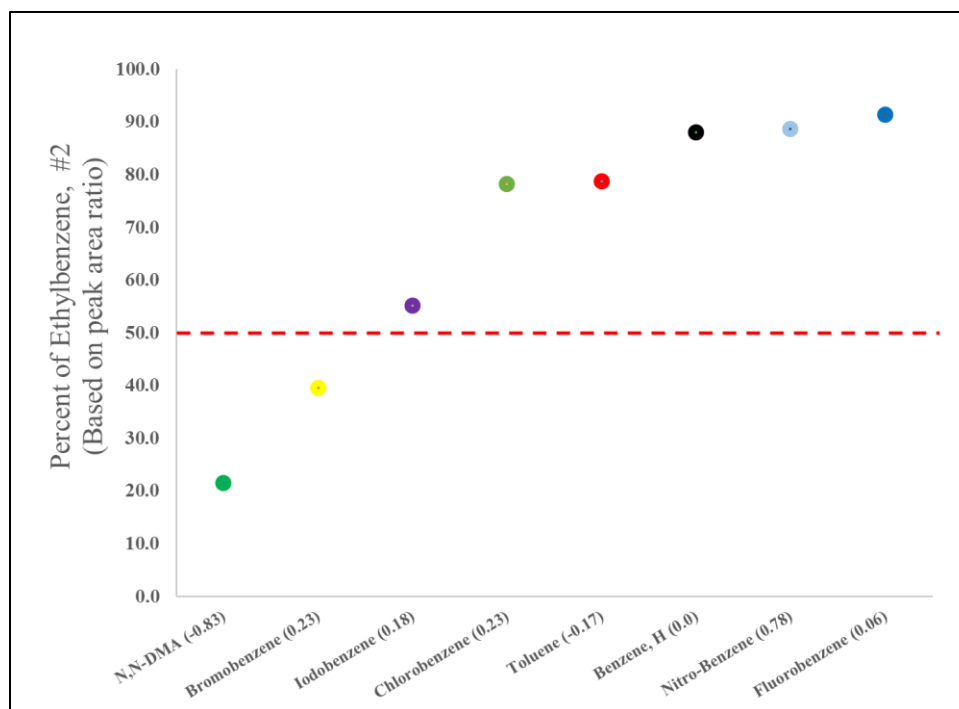


Figure 4.3.4.8 Guest competition study with ethylbenzene used as the control; N,N-DMA, and bromobenzene were preferred over ethylbenzene.

Except for bromobenzene and dimethylaniline, ethylbenzene was a distant first amongst its competition. From single guest level quantitation (Chapter 5), ethylbenzene did have one of the highest concentrations of single guest occupancy vs. the other guests.

Ethylbenzene is only about 9% larger in volume than iodobenzene but is 15% larger than bromobenzene. Size may have some influence in this case. It was not the controlling factor, and something about bromobenzene and iodobenzene was assisting in their co-crystallization considering that both have electron withdrawing groups.

Iodobenzene was the most dominant guest molecule; second only to ethylbenzene (Figure 4.3.4.9).

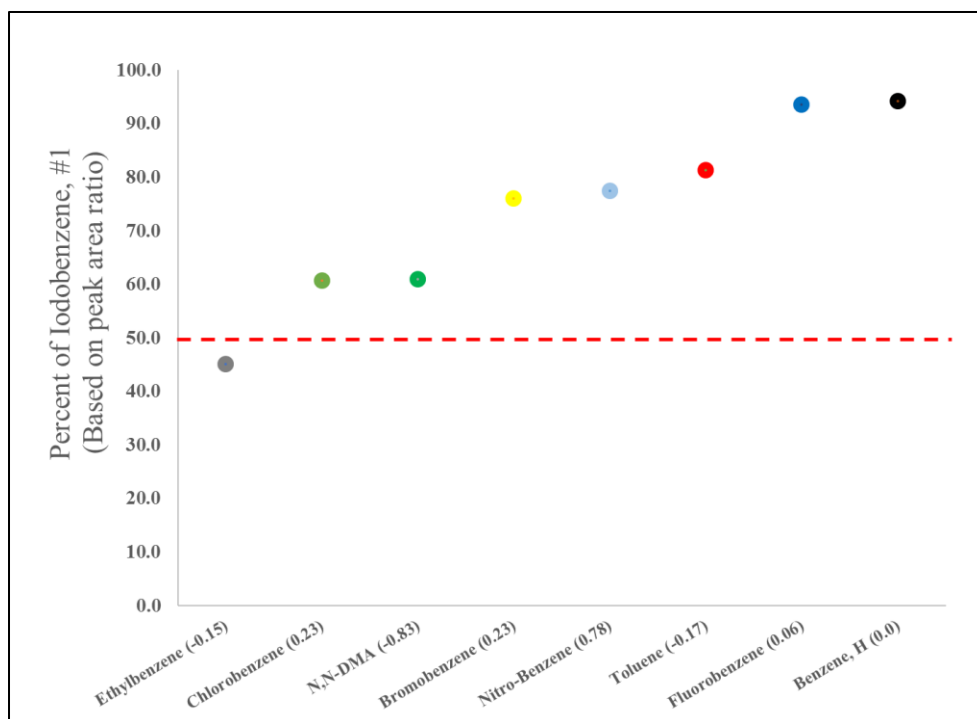


Figure 4.3.4.9 Guest competition study with iodobenzene used as the control; ethylbenzene was preferred over iodobenzene.

Iodobenzene was the third largest guest behind N,N-DMA, and ethylbenzene. It was close to the middle of the series concerning σ -value. Iodobenzene was only slightly larger than nitrobenzene but was a distinct preference over nitrobenzene. N,N-DMA has such a high preference compared to the other guests in the series, but still loses to iodobenzene and toluene. With N,N-DMA (-0.83) and nitrobenzene (0.78) on either end of the spectrum, if preference within the framework had nothing to do with electron withdrawing or electron donating capability of the functional group, then it would have been expected that benzene would have a higher level of dominance.

The result of this work demonstrated that while electronics appeared to be a factor, there was not a direct linear correlation between the Hammett value of each functional group and selectivity. Iodobenzene was the most preferred guest molecule based on the data, but it did not have the most electron withdrawing sigma value. Nitro-

benzene had the most electron withdrawing sigma value, and it was in seventh place with regards to selectivity. Ethylbenzene was second for selectivity, but it does not contain the most electron donating group either. We will focus now on some of the properties of these guest molecules. They may shed more light on how one guest is chosen over another.

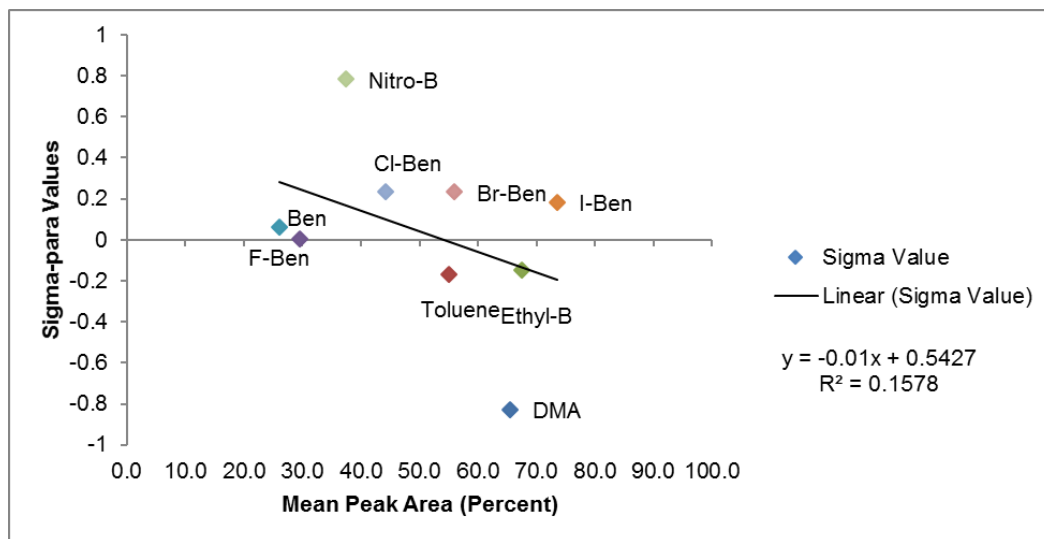
4.3.5 Using the Properties of the Guest Molecules to Understand the Order of Selectivity

An attempt was made to look at the data more holistically to extrapolate any non-obvious trends. For each comparison in the previous graphs (Figure 4.3.4.1 - 4.3.4.9), the guest ratio was compared by plotting the peak area percent between two guests. For example, N,N-dimethylaniline versus ethylbenzene the peak area percent ratio (Figure 1) was 78.6% (N,N-DMA) and 21.4% (ethylbenzene) where $78.6\% + 21.4\%$ add up to 100% of the peak area between the two guests based on the chromatography. Nine plots were made for each of the guest comparisons; this gives nine peak area percent values for each guest. For each guest, we calculated the average peak area percent across each of the nine plots. These were then ranked to determine which guest had the overall highest peak area percent across the studies and which guest had the lowest.¹⁸ The over-all order was then compared (Table 4.3.5.1).

Table 4.3.5.1 Ranked Guest Peak Area Percent Average

Guest Molecule	Avg. Peak Area %	Rank
Iodobenzene	73.6	1
Ethylbenzene	67.5	2
N,N-DMA	60.6	3
Bromobenzene	56.1	4
Toluene	55.1	5
Chlorobenzene	44.4	6
Nitrobenzene	43	7
Benzene	29.6	8
Fluorobenzene	26.1	9

The guest ranked number 9 had the lowest average peak area percent, while the guest ranked number 1 had the highest. By ranking the guests, comparisons can then be made of the chemical and physical properties of each guest to determine any trends that may exist. The first comparison was made using the σ_p -values for each functional group attached to the benzene ring (from Table 4.3.4.1). As a reminder, the more negative the Hammett value, the more electron donating the substituent. The more positive σ_p -value, the more electron withdrawing. The σ_p -value vs. mean peak area was plotted (Figure 4.3.5.1).

**Figure 4.3.5.1** Comparison plot of guest mean peak area versus σ -para value

As can be seen the graph (Figure 4.3.5.1), there doesn't appear to be a trend using σ_p -value. Even when nitrobenzene and dimethylaniline (N,N-DMA) were dropped from the plot, the R^2 -value for the linear regression does not show improvement; in fact, the R^2 -value decreases further.

The next comparison was made using the density of each guest molecule (Figure 4.3.5.2) The idea being that less dense guests would be more volatile reducing their likelihood of co-crystallizing.

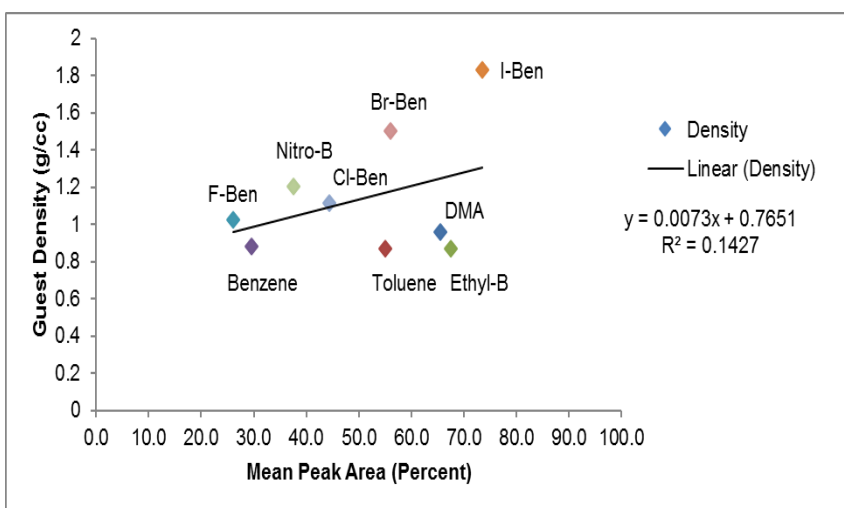


Figure 4.3.5.2 Comparison plot of mean peak area vs. guest density (g/cc)

There appears to be the beginning of what could be a trend, but the linear correlation is weak at $R^2 = 0.1427$. To have an established trend there needs to be a stronger correlation. The same comparison was then made using only the electron withdrawing substituents whose σ_p -values were > 0 . Benzene was removed. (Figure 4.3.5.3).

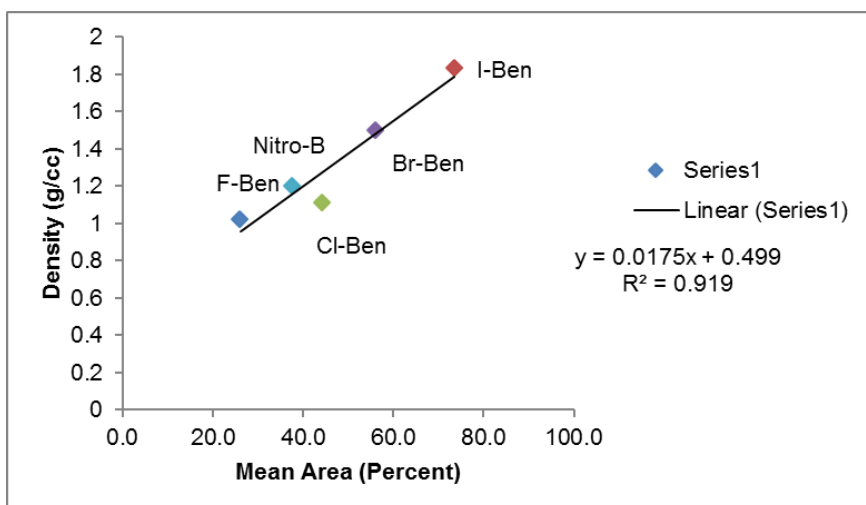


Figure 4.3.5.3 Comparison of mean peak area versus density (g/cc), electron withdrawing only

By only comparing the guests with electron withdrawing substituents, there appears to be a very high correlation with density of the guest and rank. The R^2 -value has increased to 91.9%. The shift is dramatic from the previous plot which included all the guests.

As discussed in the previous chapter, size can play an essential factor for guest co-crystallization. Each of the guest's cubic volume was calculated using Spartan Student V6 software using equilibrium geometry, B3LYP, 6-31G* level of theory. The calculation was followed by single point energy calculation with the same basis sets. These values we then compared against the percent peak area of the guests from the competition study (Figure 4.3.5.4).

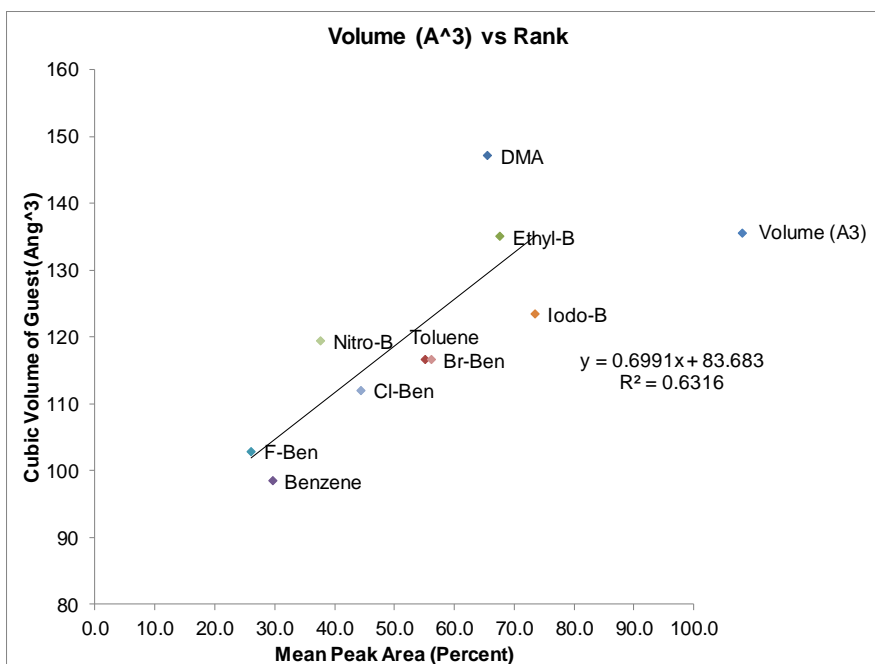


Figure 4.3.5.4 Comparison of mean peak area vs. guest volume (Å³)

There was a weak correlation with an $R^2 = 0.63$. If nitrobenzene and N,N-DMA are removed from the list, $R^2 = 0.82$. Looking at the trend-line from Figure 4.3.5.4, N,N-DMA could be an outlier, but nitrobenzene falls within another cluster of guest molecules in the graph, and it does not make sense to remove it. These two guests have disubstituted functional groups, NO₂ and NMe₂. There was, however, a cluster of guests within this plot. Fluorobenzene (102.91 Å³) and benzene (98.45 Å³) were calculated to be within 4% of each other's size. Fluorobenzene is 9% smaller than chlorobenzene (112.06 Å³). Chlorobenzene (112.06 Å³), bromobenzene (116.57 Å³), toluene (116.66 Å³) and nitrobenzene (119.42 Å³) were within 4% or less of each other's size. The most considerable discrepancy was between chlorobenzene and nitrobenzene at 6.5% which was still less than fluorobenzene vs. chlorobenzene. N,N-DMA (147.1 Å³), ethylbenzene (135.01 Å³) and iodobenzene (123.47 Å³) were the largest. Iodobenzene is within 3% of nitrobenzene, however, and nitrobenzene is ranked 7th while iodo was on the top.

Removing N,N-DMA from the plot gives an $R^2 = 0.69$. The improvement was not considerable.

The guests were compared against each other's boiling point (Figure 4.3.5.5).

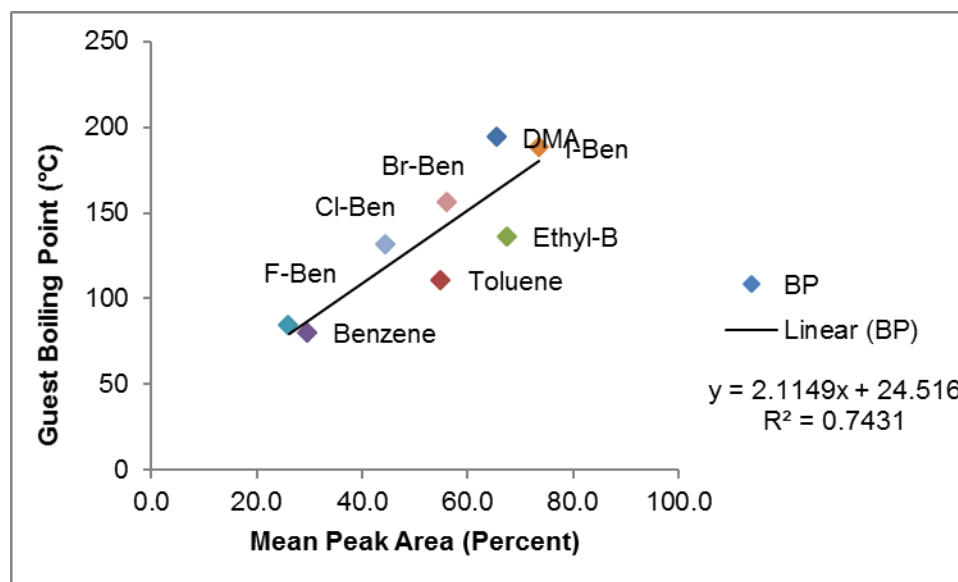


Figure 4.3.5.5 Comparison of mean peak area versus boiling point (°C)

Nitrobenzene was removed from the plot. Nitrobenzene has a boiling point of 210.9°C.

The data point for nitrobenzene was far off on the left side of the trendline. Removing nitrobenzene and fitting a linear trendline to the remaining guests generated an $R^2 = 0.74$.

The boiling point of the guests has some effect on which guest preference within the framework. The crystallization experiments took place under closed conditions at 25°C.

There was confidence that the guest ratios were not biased by reagents evaporating out of the growth solution, and artificially unbalancing guest ratios within the solutions. Also, if guest evaporation were the case, then nitrobenzene would have been the dominant guest, not seventh.

The electrostatic potential of each molecule was the last characteristic to be compared. Here, our discussion has come full circle. We started with the idea of a

correlation based on electronics. We now offer another comparison of electronics but based on measured values from parts of the molecule, not the Hammett values. Figure 4.3.1.2 gives a clear depiction of where electron density lies within each guest. If the guests orient themselves so that the substituent interacts with the layer, then the electrostatic potential at the end of the molecule may hold some answers. Spartan was used to measure ESP values (kJ/mol) from hydrogens on methyl groups (toluene) or σ -hole values from iodobenzene. A plot was made using the electrostatic potential at the tip of the guest (Figure 4.3.5.6).

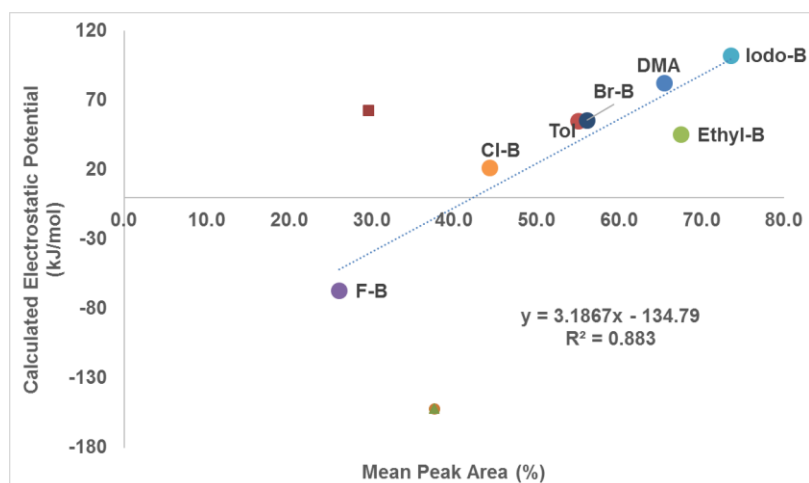


Figure 4.3.5.6 Comparison of mean peak area versus functional group σ -hole/tip ESP value.

There was a very high correlation between the electrostatic potential on the tip of the functional group for each of the guest molecules when compared to the mean peak area ($R^2 = 0.883$). Benzene was omitted from the trendline calculation since it does not contain functional groups in the same manner as the other guests. Nitrobenzene was omitted from the plot since it appeared very far down and to the right of fluorobenzene. Nitrobenzene and benzene apparently follow a different mechanism compared to the rest of the guests tested. For the rest of guests, the trend appears to fit.

4.4 Conclusions

We have measured the selectivity of **1** towards a series of guest molecules which differ based on their electronic properties to determine any trends which dictate preference. We used this series to help refine the conclusions outlined in the previous chapter showing that the size and shape of the guest can make a difference for the selectivity of **1**.

The initial studies are built on the previous work based comparing size and shape. The size and the shape of the guest molecule were held constant during the first set of selectivity experiments. The goal was to determine the effect of removing electron donating substituents, such as the methyl groups, from *p*-xylene, and replacing them with electron withdrawing substituents, such as chlorine atoms. A comparison between *p*-xylene and *p*-dichlorobenzene revealed a significant preference for alkyl electron donating groups on the guest molecule. The amount selectivity, in the guest ratio between *p*-xylene and *p*-dichlorobenzene, was overwhelmingly in favor of *p*-xylene. By holding the size and shape of the guest molecules constant, it was shown that the electronics of the guest molecule would have an impact on the selectivity of **1**. We then compared the selectivity of **1** for *p*-xylene and *p*-chlorotoluene. We found that the framework still contained a higher guest ratio of *p*-xylene than *p*-chlorotoluene. By only having one functional group different, the preference for *p*-xylene was not as extreme as before. The experiments showed that selectivity is affected by subtle changes in the guest molecules. Overall, this series of experiments showed a preference for the guest with more electron donating alkyl groups when size and shape were held constant.

We delved deeper into the interaction between the framework and the guest molecules by measuring selectivity using an experimental design containing a wide range of guest molecules. By selecting only small aromatic guest molecules which were mono-substituted and ordering these substituents from electron withdrawing to electron donating based on their Hammett constants, specifically the σ_p -values, a comparison could be made. Here we did not find selectivity of **1** to lie at one extreme or the other. There was not a clear trend showing complete selectivity for the guest which had the most electron withdrawing or the most electron donating functional group on the aromatic ring. The most electron donating group, $-\text{N}(\text{Me}_3)_2$, was not the most preferred, it was third, behind ethylbenzene and iodobenzene.

The guest molecules were ordered based on selectivity and plotted against chemical and physical properties of the guest. We found correlations between the selectivity of **1** and these properties. The guest size was an important parameter as it has been shown in previous work that the framework was selective towards larger guest molecules. Indeed, as the guest volume increased, so did the selectivity. When all the data was plotted against cubic guest volume, the $R^2 = 0.63$. The strength of the correlation improved when the nitrobenzene and N,N-dimethylaniline were removed from the dataset. These two guests have a slight shape difference compared to the rest of the guest molecules. After this change, the fit had an $R^2 = 0.82$.

A strong correlation was found between the electron withdrawing guest molecules and their respective densities. When fitted with a linear correlation, the data had a fit of $R^2 = 0.92$. Such a high degree of correlation would indicate that denser molecules would fair better in a competition reaction. The denser guest molecules would have less

interaction with the air/solvent interface and likely have a higher concentration in growth solution. This same level of correlation was not seen for the electron donating guests, indicating other mechanisms are also at play.

Pressing further into the guest properties, there was a correlation between the boiling point of the guest molecules and their selectivity. Unlike with density, a linear correlation was observed for the boiling point with almost all the guest molecules. The fit has an $R^2 = 0.74$, but there was a definite trend for increased guest selectivity and a higher boiling point. The one guest that did not follow this trend was nitrobenzene, indicating some other interaction between it and **1**. Combining this information and the density, we see that denser molecules with high boiling points have a high selectivity within **1**.

Finally, we calculated the electrostatic potential map for a section of the framework and each of the guest molecules. The explanation of what caused the guest selectivity order pertains to the lack of electron density at the terminal end of the functional group on the aromatic ring. In the case of halogens, the area of low electron density would be at the σ -hole. A correlation was found between the positive value for this area of low electron density for halogens, methyl hydrogens for alkyl groups, and the level of guest inclusion. As the tip of the guest has lower electron density, the more dominant the guest was shown to be. The low electron density area works as an anchor within the framework making the guest more dominant. The layers of the framework were calculated to be areas of high electron density. Guests with low electron density at the terminus of their functional group would have a favorable interaction. Guests with

areas of high electron density would have more repulsion from the framework layer and therefore would have an unfavorable interaction.

We have shown that guest electronics plays an important role when it comes to guest selectivity. Comparing the electronic nature of two guest molecules provides a preview as to which guest the framework will have a propensity to select. As has been seen in previous studies, selectivity can prefer one guest over another; however, that selectivity does not dictate a high concentration in **1**. Our next goal will be to look at the trends observed and correlate them to how the individual guests fill the framework.

4.5 References

- 1) Jae, J.; Tompsett, G.A.; Foster, A.J.; Hammond, K.D.; Auerbach, S.M.; Lobo, R.F.; Huber, G.W., *Journal of Catalysis*, **2011**, *279*, 257-268; Mukherjee, S.; Joarder, B.; Manna, B.; Desai, A. V.; Chaudhari, A.K.; Ghosh, S. K. *Sci. Rep.* **2015**, *4*, 5761, 1-7; Mukherjee, A.M.; Joarder, B.; Desai, A.V.; Manna, B.; Krishna, R.; Ghosh, S.K. *Inorganic Chemistry*, **2015**, *54*, 4403-4408; Yoo, J. S.; Donohue, J. A.; Kleefisch, M. S.; Lin, P. S.; Elfline, S. D. *Applied Catalysis A: General* **1993**, *105*, 83-105; Buske, G. R.; Wenger, T. L.; Beyrau, J. A. Heat Transfer Fluid, US Patent 4622160 A, November 11th, 1986; Chen, S.; Sun, A.; Qin, Z.; Wang, J. *Catalysis Communications* **2003**, *4*, 441-447; Atwood, J.L.; Barbour, L.J.; Jerga, A. *Science*, **2002**, *296*, 2367-2369; Fenyvesi, E.; Szenté, L.; Russel, N.R.; McNamara, M. *Compr. Supramol. Chem.* **1996**, *3*, 305; Chaffee, K.E.; Fogarty, H.A.; Brotin, T.; Goodson, B.M.; Dutasta, J.P. *J. Phys. Chem. A*, **2009**, *113*, 13675-13684; Cram, D.J.; Tanner, M.E.; Knobler, C.B. *J. Am. Chem. Soc.* **1991**, *113*, 7717-7727; Scarso, A.; Pellizzaro, L.; De Lucchi, O.; Linden, A.; Fabris, F. *Angew. Chem. Int. Ed.* **2007**, *46*, 4972-4975; Foo, M.L.; Matsuda, R.; Hijikata, Y.; Krishna, R.; Sato, H.; Horike, S.; Hori, A.; Duan, J.; Sato, Y.; Kubota, Y.; Takata, M.; Kitagawa, S. *J. Am. Chem. Soc.* **2016**, *138*, 3022-3030; Demessence, A.; Long, J.R. *Chem. Eur. J.* **2010**, *16*, 5902-5908; Wang, H.; Li, B.; Wu, H.; Hu, T.L.; Yao, Z.; Zhou, W.; Xiang, S.; Chen, B. *J. Am. Chem. Soc.* **2015**, *137*, 9963-9970; Pivovar, A.M.; Holman, K.T.; Ward, M. *Chem. Mater.* **2001**, *13*, 3018-3031; Jacobs, A.; Nassimbeni, L.R.; Nahako, K.L.; Su, H.; Taljaard, J.H. *Cryst. Growth and Des.* **2008**, *8*, 1301-1305; Zlatkis, A.; Wu, Z.; Andrews, A.R.J. *Chromatographia* **1992**, *34*, 457-460; Uemura, K.; Kitagawa, S.;

Kondo, M.; Fukui, K.; Kitaura, R.; Chang, H.C.; Mizutani, T. *Chem. Eur. J.* **2002**, *8*, 3586-3600; Cussen, E.J.; Claridge, J.B.; Rosseinsky, M.; Kepert, C.J. *J. Am. Chem. Soc.* **2002**, *124*, 9574-9581; Karmaker, A.; Samanta, P.; Desai, A.V.; Ghosh, S.K. *Acc. Chem. Res.* **2017**, [Online early access].
DOI:10.1021/acs.accounts.7b00151. Published Online: September 5, 2017.
<http://pubs.acs.org/doi/abs/10.1021/acs.accounts.7b00151>; Jin, Z.; Zhao, H.Y.; Zhao, X.J.; Fang, Q.R.; Long, J.R.; Zhu, G.S. *Chem. Commun.* **2010**, *46*, 8612-8614; Lazar, A.I.; Biedermann, F.; Mustafina, K.R.; Assaf, K.I.; Henning, A.; Nau, W.M. *J. Am. Chem. Soc.* **2016**, *138*, 13022-13029; Rusa, C.; Tonelli, A.E. *Macromolecules*, **2000**, *33*, 1813-1818; Moreira, L.; Calbo, J.; Krick Calderon, R.M.; Santos, J.; Illescas, B.M.; Arago, J.; Nierengarten, J.F.; Guldi, D.M.; Orti, E.; Martin, N. *Chem. Sci.* **2015**, *6*, 4426-4432; Mahata, K.; Frischmann, P.D.; Wurthner, F. *J. Am. Chem. Soc.* **2013**, *135*, 15656-15661; Li, P.Z.; Su, J.; Liang, J.; Liu, J.; Zhang, Y.; Chen, H.; Zhao, Y. *Chem. Commun.* **2017**, *53*, 3434-3437; Chen, D.M.; Tian, J.Y.; Wang, Z.W.; Liu, C.S.; Chen, M.; Du, M. *Chem. Comm.* **2017**, *53*, 10668-10671; Levine, D.J.; Runcevski, T.; Kapelewski, M.T.; Keitz, B.K.; Oktawiec, J.; Reed, D.A.; Mason, J.A.; Jiang, H.Z.H.; Colwell, K.A.; Legendre, C.M.; Fitzgerald, S.A.; Long, J.R. *J. Am. Chem. Soc.* **2016**, *138*, 10143-10150; Xiao, D.; Zhang, D.; Chen, B.; Xie, D.; Xiang, Y.; Li, X.; Jin, M. *Langmuir* **2015**, *31*, 10649-10655; Ward, M.D.; Hunter, C.A.; Williams, N.H. *Chem. Lett.* **2017**, *46*, 2-9; Mishra, A.; Jung, H.; Lee, M.H.; Lah, M.S.; Chi, K.W. *Inorganic Chemistry* **2013**, *52*, 8573-8578; Kim, J.; Lee, S.O.; Yi, J.; Kim, W.S.; Ward, M.D. *Separation and Purification Technology*, **2008**, *62*, 517-522; Dey, A.;

- Bera, S.; Biradha, K. *Crystal Growth and Design* **2015**, *15*, 318-325; Chaffee, K.E.; Fogarty, H.A.; Brotin, T.; Goodson, B.M.; Dutasta, J.P. *J. Phys. Chem. A* **2009**, *113*, 13675-13684; Liu, X.; Oh, M.; Lah, M.S. *Inorganic Chemistry* **2011**, *50*, 5044-5053; Moon, D.; Lah, M.S. *Inorganic Chemistry* **2005**, *44*, 1934-1940; Merlau, M.L.; del Pilar Mejia, M.; Nguyen, S.T.; Hupp, J.T. *Angew. Chem. Int. Ed.* **2001**, *40*, 4239-4242; Pluth, M.D.; Bergman, R.G.; Raymond, K.N. *Acc. Chem. Res.* **2009**, *42*, 1650-1659; Rebek Jr, J. *Acc. Chem. Res.* **2009**, *42*, 1660-1668
- 2) Shi, M.W.; Thomas, S.P.; Koutsantonis, G.A.; Spackman, M.A. *Crystal Growth and Design* **2015**, *15*, 5892-5900
 - 3) Taylor, C.G.; Cullen, W.; Collier, O.M.; Ward, M.D. *Chem. Eur. J.* **2017**, *23*, 206-213
 - 4) Yaghi, O.M.; Davis, C.E.; Li, G.; Li, H. *J. Am. Chem. Soc.* **1997**, *119*, 2861-2868
 - 5) Ward, M.D.; Hunter, C.A.; Williams, N.H. *Chem. Lett.* **2017**, *46*, 2-9
 - 6) Cullen, W.; Turega, S.; Hunter, C.; Ward, M.D. *Chem. Sci.* **2015**, *6*, 625-631
 - 7) Cullen, W.; Thomas, K.W.; Hunter, C.A.; Ward, M.D. *Chem. Sci.* **2015**, *6*, 4025-4028
 - 8) Turega, S.; Whitehead, M.; Hall, B.R.; Meijer, A.J.H.M.; Hunter, C.A.; Ward, M.D. *Inorg. Chem.* **2013**, *52*, 1122-1132
 - 9) Tashiro, S.; Tominaga, M.; Kawano, M.; Therrin, B.; Ozeki, T.; Fujita, M. *J. Am. Chem. Soc.* **2005**, *127*, 4546-4547

- 10) Hammett, L.P. *Chem. Rev.* **1935**, *17*, 125-136; Taft, R. W.; Hansch, C.; Leo, A. *Chem. Rev.* **1991**, *91*, 165-195; Hansch, C.; Leo, A.; Taft, R.W. *Chem. Rev.* **1991**, *91*, 165-195
- 11) Hunter, C.; Cockroft, S.L.; Perkins, J.; Zonta, C.; Adams, H.; Spey, S.; Low, C.; Vinter, J.; Lawson, K.; Urch, C. *Organic and Biomolecular Chemistry*, **2007**, *5*, 1062-1080
- 12) Murillo, O.; Suzuki, I.; Abel, E.; Gokel, G. *J. Am. Chem. Soc.* **1996**, *118*, 7628-7629
- 13) Hunter, C.; Carver, F.; Livingstone, D.; McCabe, J.; Seward, E. *Chem. Eur. J.* **2002**, *8*, 2848-2859
- 14) Hunter, C.; Cockroft, S.; Lawson, K.; Perkins, J.; Urch, C. *J. Am. Chem. Soc.* **2005**, *127*, 8594-8595
- 15) Hunter, C.; Sanders, J. *J. Am. Chem. Soc.* **1990**, *112*, 5525 – 5534
- 16) Hunter, C.; Lawson, K.; Perkins, J.; Urch, C. *J. Chem. Soc., Perkin Trans. 2*, **2001**, 651-669
- 17) Wavefunction, Inc. *Spartan '14 for Windows, Macintosh and Linux: Tutorial and User's Guide*. Irvine, CA, 10 January 2014. Electronic .pdf document
- 18) Aakeroy, C.B.; Baldrighi, M.; Desper, J.; Metrangolo, P.; Resnati, G. *Chem. Eur. J.* **2013**, *19*, 16240-16247

Chapter 5

Understanding Guest Selectivity by Probing Single Guest

Systems with Multiple Analysis Techniques

5.1 Abstract

We observed several trends competition reactions, and it was necessary to understand how a series of guests individually interact with our hydrogen bonded framework. We look to gain further insight about which properties of the guest molecules contribute to their selectivity. Nine aromatic guest molecules were co-crystallized individually into the framework consisting of $\text{Zn}(\text{HPDCA})_2 \cdot (\text{H}_2\text{O})_2$ and o-tolidene. We probed each host-guest combination using thermogravimetric analysis, head-space gas chromatography and powder x-ray diffraction. Multiple techniques were used to determine if there was a special relationship between the host and any of these guests. We found that some of the preferred molecules from previous studies do not fully occupy the framework, e.g., iodobenzene via thermogravimetric analysis and gas chromatography testing. Guest recoveries were typically higher for thermogravimetric analysis than gas chromatography when compared to theoretical occupancy. Tracking guest evolution over a wide temperature range by powder x-ray diffraction revealed that the framework would empty at temperatures significantly below the boiling point of the guest. Finally, thermogravimetric analysis approximated the activation energy for guest evolution. It was found to be a single step process for each of the guest molecules. After compilation of the results, a comparison between from each guest molecules for all of the tests performed. Guests that have high occupancy and showed retention at higher temperatures in the framework correlated well to preferences observed earlier, though others had been preferred but demonstrated low occupancy and retention.

5.2 Background

Characterizing a host-guest system can require using a multitude of analytical techniques to characterize the host-guest relationship. Ando *et al.* used ^{13}C NMR, ^{19}F MAS NMR, wide-angle x-ray diffraction, thermogravimetric analysis (TGA) and thermogravimetric mass spectrometry to understand the structural changes from ambient to elevated temperatures that occur in an inclusion compound between hydrofluoroether and β -cyclodextrin.¹ To measure molecular recognition of *tert*-butylcalix[6]arene for previously bound guests, Gorbachuk simultaneously used TGA, differential scanning calorimetry (DSC) all combined with gas analysis by mass spectrometry.² Utilizing this multi-instrument setup, he could measure mass loss, enthalpy and temperatures at which guests were leaving.² Ward *et al.* used a series of gas chromatography experiments to determine selectivity of the guanidinium organodisulfonates, as well as ^1H NMR, single crystal X-ray analysis, and TGA.³ Differences in reactivity of [2+2] cycloaddition of α/β -unsaturated ketones reactions, which take place inside self-assembled bis-urea macrocycles, are monitored using TGA, ^1H NMR, powder X-ray diffraction and molecular modeling.⁴

Static headspace analysis is a relatively simple technique that suits our needs as it has low detection limits. Static headspace has been used to determine the concentration of guest molecules such as methylcyclohexane, pentane, cyclohexane, hexane, pinene while deriving the overall host-guest ratios.⁵ Static headspace analysis provided a pathway for investigation of the potential for β -cyclodextrin-thioethers to solubilize volatile organic compounds such as benzene, toluene, ethylbenzene, isopropylbenzene, *tert*-butylbenzene and cyclohexane derivatives.⁶ A mixture of cyclodextrin and β -cyclodextrin created controlled release materials which dispersed linalool and camphor

was studied using static headspace and multiple headspace extraction (MHE) techniques to monitor guest evolution.⁷ MHE takes successive aliquots from the headspace in a step-wise fashion.⁷

Variable temperature powder x-ray diffraction (VT-PXRD) can provide thermal stability data over a broad range of temperatures by tracking any changes in the structure. Using VT-PXRD, Lah *et al.* performed thermal stability tests of a Cu based MOF to determine its degradation temperature at 325°C.⁸ Kitagawa *et al.* was able to track the dehydration of a porous coordination polymer which was reversible through rehydration under humid conditions.⁹ Being able to monitor structural changes in a framework can be especially important when observing guest loss and insertion.¹⁰ Upon heating a MOF containing gates, the original structure pattern is lost until the MOF is rehydrated returning it to its original structure.¹¹

As with any reaction mechanism, a certain amount of energy is required to remove a guest from the host molecule. Typically, that energy comes in the form of heat as applied from an instrument or other apparatus. Luigi Nassembeni's group performed a significant amount of work determining activation energies for guest desolvation from inclusion compounds.¹² Nassimbeni's group utilized a method developed by Flynn and Wall to approximate activation energy of desolvation of inclusion compounds using TGA.¹³ This method has been performed by other groups as well.¹⁶ The samples are heated at several heating rates, usually from 2°K/min to 50°K/min depending on the research.

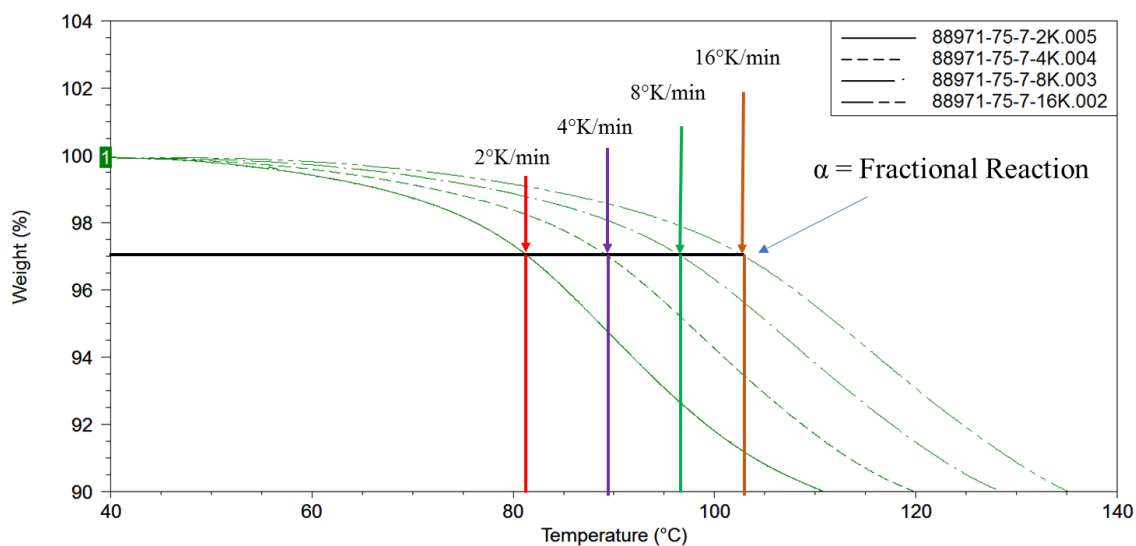


Figure 5.2.1 Example TGA plot using multiple heating ramp rates to study the guest evolution of N,N-dimethylaniline from 1; the calculated α -level is at a point of 3% mass loss.

Using the natural log of the heating rate vs. $1/\text{temperature}$, a plot is generated and the activation energy calculated using the Arrhenius equation.¹³ Luigi Nassimbeni's group determined an activation energy window for inclusion compounds.^{12,13} Nassimbeni *et al.* found that the T_{on} (onset temperature) was a function of both the host-guest non-bonding interactions and the physical properties of the guest itself.¹⁴ Using the boiling point of the guest itself, and calculating $T_{\text{on}}-T_{\text{b}}$, the calculation could measure the relative stabilities of inclusion compounds.¹⁵ If the calculated $T_{\text{on}}-T_{\text{b}}$ has a negative value, E_{a} is much lower than if $T_{\text{on}}-T_{\text{b}}$ is a positive value.^{12,15} $T_{\text{on}}-T_{\text{b}}$ indicates whether an inclusion compound could be considered stable or not.¹⁵ When the mode of action is the same, a high E_{a} indicates a stable compound, while a low E_{a} , this indicates a less stable compound.¹⁵ The activation energy is typically higher when the inclusion compound has a cavity compared

to a channel.¹² In a cavity, the guest is critical to the structure and when the guest is released, the empty cavity collapses the framework.¹⁸ Nessembe *et al.* compared the kinetics of desolvation with a similar, although different, host, but used the same guest molecule. The research found that activation energy was strongly dependent on the mode of inclusion, whether channel or cavity. The activation energy was lower for acetone leaving a channel and higher for acetone leaving a cavity.¹⁸ While a straightforward method for measurement of host-guest materials, Nassembeni warns against bad interpretations.¹⁴ They recommend looking at guests that are geometric isomers and compounds which have the same host-guest ratio.¹⁴ Test data is plotted at different levels of α to determine the activation energy. The alpha levels are the fractional reactions, segments of the guest loss as viewed from the TGA mass loss step (Figure 5.2.1).¹³ The α -value is directly proportional to the extent of the reaction/desolvation.^{13,17} This is defined as the change in the mass of the sample. The Flynn and Wall method desolvates using a range of heating rates, typically from 2°K/min to 32°K/min. The shape of all the mass loss curves should be the same if the mechanism is the same.¹⁴

For each fractional reaction, percent of the mass loss step, a plot made from the log (or natural log) of the heating rate vs. 1/T in kelvin provides a slope equation to calculate activation energy.¹³ Typically, the test uses a minimum of three different alpha ranges.¹⁷ If the slopes of the lines are parallel on the plots, it indicates a single step decomposition for the desolvation reaction.¹⁴ The slope of the line is directly related to activation energy, E_a , of the desorption reaction.¹⁷

We performed several analytical techniques to further understand the interaction between the individual guests and the host framework. We aim to use this information

and further decipher the interaction between host and guest for our framework. The work presented here provides measured the interaction between the framework, N,N-dimethylaniline, ethylbenzene, toluene, benzene, fluorobenzene, chlorobenzene, bromobenzene, iodobenzene, and nitrobenzene.

5.3.1 Experimental

ZnCl₂ (>97%) was purchased Fisher Scientific. N,N-dimethylaniline, toluene, ethylbenzene, benzene, fluorobenzene, iodobenzene, chlorobenzene, bromobenzene, and nitrobenzene were reagent grade and purchased from Sigma Aldrich. O-Tolidine (>97%) was purchased from Sigma Aldrich Chemical Company. 2,4-pyridine-dicarboxylic acid (98%) was purchased from AK Scientific. Methanol was reagent grade from Sigma Aldrich Chemical Company. Dimethylformamide (anhydrous, 99.8%) was purchased from Fisher Scientific.

5.3.2 Synthesis of 1•guest

The Zn (II) metal complex was synthesized by combining ZnCl₂ (0.0146 moles, 2g) in 40mL of D.I. water and 2,4-pyridinedicarboxylic acid (0.0293 moles, 4.9g) in 400mL of a 1:1 ratio of D.I. water and methanol. This was allowed to stir for approximately 4 hours. The resulting suspension was filtered through a Buchner filter funnel and paper filter. The white slurry was washed with D.I. water until the mother liquor tested pH neutral. The product was allowed to dry on the funnel and then air dried overnight. The resulting product was Zn(HPDCA)₂•(H₂O)₂. The Zn(HPDCA)₂•(H₂O)₂ (0.06 moles, 0.025g), and 3,3'-dimethylbenzidine (0.06mole, 0.012g) were separately dissolved in 2mL each of methanol. The two methanol solutions were then mixed together, stirred and a 1:1 mixture of water (1mL) and DMF (1mL) was then added. The

single guest molecule was added to a 15mL glass vial and the component solution of the framework was added on top.

5.3.3 Thermogravimetric Analysis Studies

TGA was run for each of the guest/framework systems. Each sample was held isothermally for three minutes at 40°C, then a ramp rate of 2°C/min was run until a temperature of 550°C (Figure 5.3.3.1).

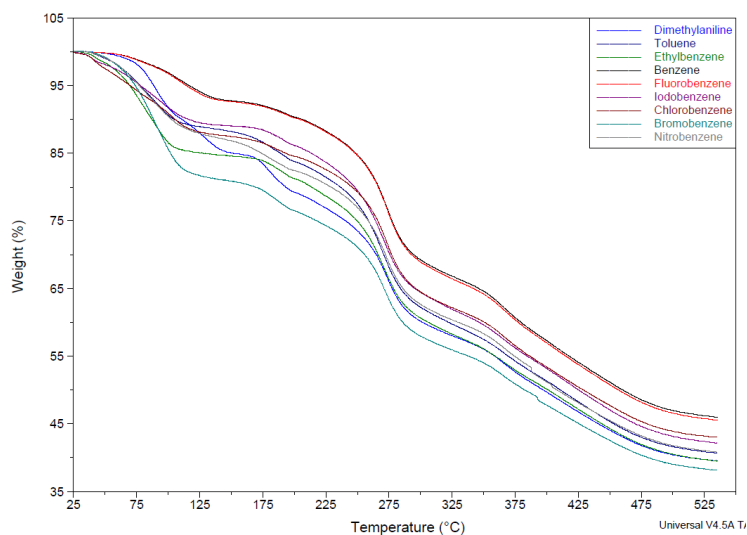


Figure. 5.3.3.1. TGA plot of each 1• guest sample. The guests used were N,N-dimethylaniline, ethylbenzene, toluene, benzene, fluorobenzene, chlorobenzene, bromobenzene, iodobenzene and nitrobenzene

The initial mass loss for each TGA plot is indicative of the guest evolving from the sample (Figure 5.3.3.2).

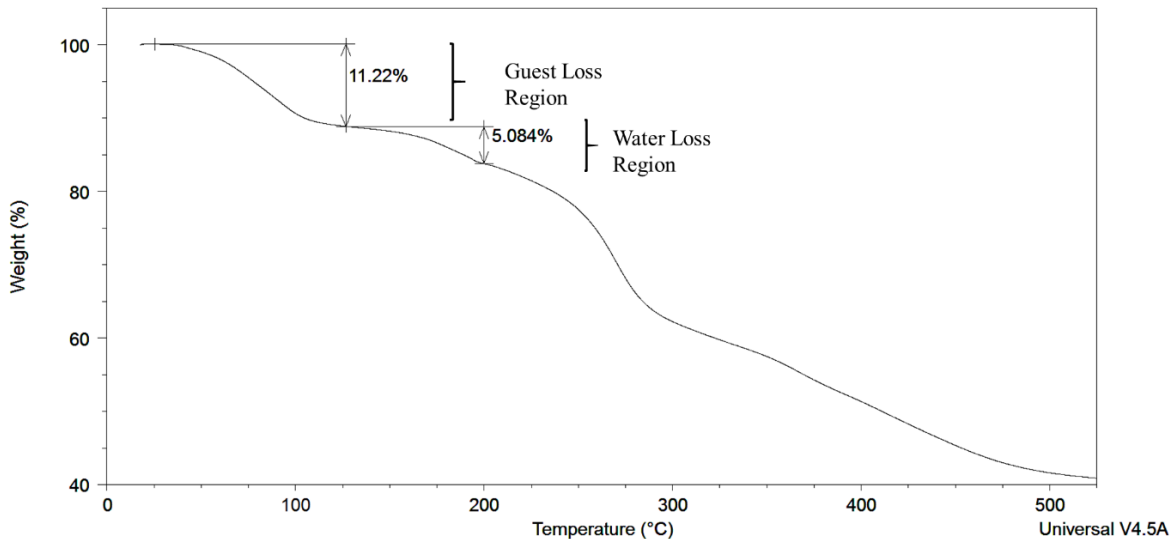


Figure. 5.3.3.2. TGA plot of toluene guest within 1•framework

For Figure 5.3.3.2, a total mass loss was observed between 25°C and 125°C of 11.22%.

From this data, the amount of toluene guest is calculated. The theoretical amount of toluene within the framework would be approximately 12.2%. If 15.11% is attributed to toluene only, then the framework was approximately 91.5% occupied. The theoretical mass loss of two axial waters from the Zn metal centers within the channel would be approximately 4.8%. The mass loss observed was 5.1% which was ~106% of theoretical.

5.3.4 Chromatographic Methods

An HP gas chromatography mass spectrometer (model 5988A) was used to collect all chromatographic data. For GCMS method development, the isolated crystals were placed inside of a 20mL GC headspace vial (Xpertek, PJ. Cobert, Cat#954040) and sealed with a magnetic cap containing a high temperature rated septa (Xpertek, PJ. Cobert, Cat#952237). A 1mL, A-2 Luer gas-tight syringe was also used headspace analysis. All chemical reactions were carried out under ambient conditions. To determine the GC/GCMS parameters, lightly crushed 1•framework (0.010g) crystals were heated to 200°C. This evolved all the guest molecules being tested. The temperature used was

based on thermogravimetric analysis (TGA) data. 200°C was also used as the upper limit because the framework decomposes at around 215°C based on melt point studies. No traces of acetone or methanol were seen in the MS data, though sometimes DMF would elute in the chromatogram. DMF seems to co-crystallize in small amounts. The column used was a Supelco SLB – 5MS 30M x 0.25mm x 0.5µm film thickness. The GC oven was initially 50°C for 2 minutes, then ramped to 180°C at a rate of 20°C/min and held for 1 minute. The total run time was 12 minutes.

5.3.5. Gas Chromatography Studies

A sample of the guest containing framework was ground and placed into a 20mL headspace vial with magnetic cap. A special cap was engineered where a GC septum was affixed to the top of it with high-temperature silicon. This was done purposefully because GC septa allow for pressure within the injection port of a GC to be maintained after a needle has punctured it. In this same manner, the headspace vial could be sampled multiple times without losing much of the generated headspace volume other than what was extracted. To test this, a temperature probe was set in an empty vial and maintained an internal temperature within 1°C of the set-point temperature from 40°C-230°C. This was to ensure proper heating of the sample over the temperature range. The sample containing vial was heated from 40°C to 230°C using a ramp rate of 2°C per minute. This was the same ramp rate which was used for the TGA plot from Figure 5.3.3.1. 100µL headspace samples were taken once every 10°C step. Using Figure 5.3.3.1 as a guide for guest evolution, the range between 40°C to 150°C can be focused on. GC headspace was sampled every 10°C, and the peak area plotted versus temperature. The peak areas were

normalized to the highest value peak area within the 40°C-150°C temperature range. This was subtracted from 100% to create a descending plot like that of the TGA plot in Figure 5.3.3.2. The two plots were then overlaid and plotted on the separate y-axis. GC parameters in 5.3.4 were used.

5.3.6. Powder x-ray diffraction

Powder X-ray diffractions patterns were collected on a Rigaku Ultima IV X-ray diffractometer containing a CuK α source ($\lambda = 1.54051 \text{ \AA}$) and viewed with MDI Jade 9 software Samples were ground then analyzed using powder x-ray diffraction scanning from 2θ to 30θ .

5.3.7. Temperature-dependent powder x-ray diffraction

A temperature dependent powder x-ray diffraction study was performed where a powder pattern was taken of the guest containing material at increasing temperatures. A powdered sample of **1**-guest was initially scanned at 25°C using the parameters in 5.3.6. the sample was removed and heated to 40°C for 10 minutes, then scanned again. This cycle was repeated for the remain temperatures. The temperature was increased until the framework was empty or the framework degraded.

5.3.8. Approximating Energy of Activation for Guest Loss

The determination of the activation energy of xylene isomer guest desorption from isoquinoline-based Werner clathrates¹³ used a non-isothermal technique devised by Flynn and Wall¹³ was recently published. This method was used to approximate the energy of activation (E_a) for the desorption of guests listed in Table 5.4.1.1.¹³ E_a was approximated using multiple heating ramp rates on a TGA within the guest loss step of a TGA curve (Figure 5.3.3.2). The heating rates used were termed β . The fixed heating rates were 2, 4, 8, 16 and 32K min⁻¹. For the guest loss step, the activation energy was

calculated over α ranges for each of the different guests (Equation 1). The definition for α was as follows:

$$\text{Eq. 1:} \quad \alpha = (m_t - m_0)/(m_\infty - m_0)$$

For calculated α , m_0 = initial mass, m_t = mass at time t and m_∞ = final mass. Using the Arrhenius equation (Equation 2), it was then possible to calculate activation energy for loss of each guest from Table 1.

$$\text{Eq. 2:} \quad k = Ae^{-E_a/(RT)}$$

For Equation 2, k is defined as the rate constant; A is the frequency factor, E_a is the activation energy, R is the gas constant (8.3145 J/mol•K), and T is the temperature in Kelvin. Taking the natural log (ln) of Equation 2 gives Equation 3:

$$\text{Eq. 3:} \quad \ln(k) = -\left(\frac{E_a}{R}\right)\left(\frac{1}{T}\right) + \ln(A)$$

Equation 3 now shows the same form as $y = mx + b$ which using the heating ramps rates ($\log \beta$) allows for plotting $\log \beta$ vs. $1/T$ (Flynn and Wall notation). A linear regression trend line can be fit to the data. Using the slope of this line, the activation energy for guest loss can be approximated by the different values of α .

5.4 Results and Discussion

We have gone to great lengths to use competition studies to determine the selectivity of our framework. From Chapter 3, it was observed that the size and shape of a molecule could be an important factor for the selectivity of the framework. It was also observed that neither small or big molecules are automatically the preferred species. We

also found that changing the shapes of the molecule, in the case of the *m*- and *p*-substituted aromatics, reduced incorporation of the guest molecule into the framework. This means certain shape guests have a better fit. In Chapter 4, the focus changed to guests of similar size and shape, *p*-xylene vs. *p*-dichlorobenzene. It was found that the electronic nature of the guest molecule had a significant impact on the selectivity of the framework. The framework was sensitive enough to the change of guest electronics that comparing *p*-xylene vs. *p*-chlorotoluene shifted the selectivity profile. Nine guest molecules were placed in competition with each other to determine preference. While these guests were originally chosen by their size, the degree of substitution, and Hammett σ_p -value, their incorporation into the framework appeared more reliant on the interaction between the guest and the framework. Each of the highly preferred guests had a way of interacting or anchoring themselves into the framework which made them win a competition reaction. This interaction was based on electrostatic interactions between the guest and the framework. We believe this to be why guests such as iodobenzene performed so well. The partial positive tip of the iodine atom was attracted to the negative oxygen atoms in the layer. From these competition experiments, we find that electrostatic interactions between the guest and the framework play a significant role in the host-guest interaction.

This still leaves the question of why specific molecules perform better than others? If guest A is preferred over guest B, then it would stand to reason that guest A, when co-crystallized by itself, has a high degree of occupancy within the host. This was not always the case. Guests with alkyl substituents, such as ethylbenzene, had a high degree of occupancy when co-crystallized on its own. Ethylbenzene was preferred over

may of the guests when in competition. Iodobenzene was preferred over many other guests as well but had a significantly lower occupancy when co-crystallized on its own. It was necessary to explore how each of the nine guest molecules tested in Chapter 4 co-crystallized by themselves with the host framework. It will be shown that while guests may be preferred, they do not always have a high concentration in the framework.

5.5 Thermogravimetric Analysis of Single Guest

To determine the single co-crystallized guest concentration in the framework, we started with the TGA. This was performed on samples where only one guest was co-crystallized within the framework. No competition was involved with another guest for these experiments (Table 5.5.1).

Table 5.5.1 Thermogravimetric analysis of co-crystallized single guests within the host framework.

Guest	% Guest TGA	% Guest, Theoretical	% Occupied
Iodobenzene	10.9	23.6	46.0
Ethylbenzene	14.9	13.8	107.3
N,N-Dimethylaniline	15.1	15.5	97.5
Bromobenzene	18.3	19.2	95.2
Toluene	11.2	12.2	91.5
Chlorobenzene	12.2	14.6	83.8
Nitrobenzene	12.1	15.7	77.3
Benzene	7.2	10.6	68.4
Fluorobenzene	7.3	12.7	57.2

The guests in Table 5.5.1 are ordered by preference as determined in Chapter 4.

Iodobenzene was ranked first since it was preferred over the rest of the guests with fluorobenzene coming in last. Iodobenzene had the lowest occupancy. This was very interesting considering how well it outperformed the other guest molecules. With

ethylbenzene and N,N-dimethylaniline, the framework was nearly full of guest. N,N-dimethylaniline will not crystallize in the framework without a secondary guest.

Numerous crystallization experiments were performed and yet a crystal would not form without a catalytic amount of ethylbenzene. The recovery of N,N-dimethylaniline is very good with TGA, but we know from gas chromatography quantitation that ethylbenzene contaminates the crystal. Bromobenzene was one of the few guests with an electron withdrawing functional group that still had better than 95% occupancy. After toluene, the level of occupancy begins to decrease significantly down to fluorobenzene.

Fluorobenzene had a higher occupancy than iodobenzene, and the two were on opposite ends of the preference spectrum. TGA reports a mass loss over temperature ranges. The method itself, while very useful, is not specific unless linked to a real gas analyzer gas chromatography mass spectrometer. It only shows a mass loss. What if we were to check recovery another way?

5.6 Guest Quantitation by Gas Chromatography

We wanted to use a more specific method of determining how many guests were co-crystallized in the host. Gas chromatography (GC) was used to determine percent recovery of each guest molecule. Calibration curves were made to back-calculate guest concentration in the framework. We compared this to the TGA data and found the values to be different (Table 5.6.1).

Table 5.6.1 Comparison of TGA recovery vs. GC recovery results for co-crystallized single guest molecules, in many cases the GC values were lower

Guest	Boiling Point (°C)	% Guest, Theoretical	% Guest, TGA	TGA Occupancy (%)	% Guest, GC	GC Occupancy (%)	% Diff. in Occ. (TGA-GC)
Iodobenzene	188.0	23.6	10.9	46.0	4.7	19.9	56.7
Ethylbenzene	136.0	13.8	14.9	107.3	19.4	140.6	31.0
N,N-Dimethylaniline	194.0	15.5	15.1	97.5	12.6	81.3	16.6
Bromobenzene	156.0	19.2	18.3	95.2	6.9	35.9	62.3
Toluene	110.6	12.2	11.2	91.5	6.2	50.8	44.5
Chlorobenzene	131.0	14.6	12.2	83.8	9.8	67.1	19.9
Nitrobenzene	210.9	15.7	12.1	77.3	4.5	28.7	62.9
Benzene	80.1	10.6	7.2	68.4	1.6	15.1	77.9
Fluorobenzene	85.0	12.7	7.3	57.2	0.6	4.7	91.7

Comparing the TGA and GC data, we see the GC recovery was typically lower than the TGA. In the GC recovery, we are detecting the guest. In TGA, we are observing a mass loss. For many of the guests, such as iodobenzene, benzene, fluorobenzene, bromobenzene, nitrobenzene, and toluene, the overall recovery was lower by GC than TGA. N,N-dimethylaniline, and chlorobenzene had the closest agreement to the TGA % occupancy. These guests still had a percent difference of 16 – 20% from the TGA occupancy. N,N-dimethylaniline chromatogram showed a contaminate of ethylbenzene. The peak area ratio of the two guests was 73% N,N-dimethylaniline to 27% ethylbenzene.

Some of the guests, such as fluorobenzene and benzene, have recovered values less than 2% by GC analysis. Comparing the GC data to the fluorobenzene and benzene TGA values where the guest was less than 8%, the competition data from Chapter 4 begins to make sense. There are guests which do not fill much of the channel in the framework. We have two methods now which show that benzene and fluorobenzene do not fill the framework. Fluorobenzene and benzene were the least preferred from the competition studies of Chapter 4. Table 5.6.1 also lists the boiling points for all the

molecules tested. These two guests have the lowest boiling points (and highest vapor pressures) and therefore are more likely to evolve while preparing samples or once the crystals have been isolated. Iodobenzene has a boiling point well above room temperature. There is no explanation why it should have such a low recovery for both methods just based on boiling point. Also, from the competition studies, iodobenzene was preferred to most other guests. While iodobenzene may be able to beat other guest molecules in competition, it does not appear to co-crystallize to a high degree in the framework.

5.7 Comparison of Guest Loss by Gas Chromatography and Thermogravimetric Analysis

When the guests are evolved from the TGA, we observe a mass loss. From the TGA plot, an onset temperature can be determined for each guest molecule. Using the GC, a similar plot can be generated, and the chromatography will show if the guest is evolving from the framework. This evolution data can then be plotted to show the temperature profile over which the guest evolves. We wanted to compare the onset temperature from the TGA with the onset temperature from the GC to see if they were the same. In many of the cases, the GC evolution profile matched or was very close to the TGA mass loss profile. The TGA and GC used the same ramp rate of 2°C/min. Plotting the TGA data and the GC data together, we can see how well the two methods overlap (Figure 5.7.1)

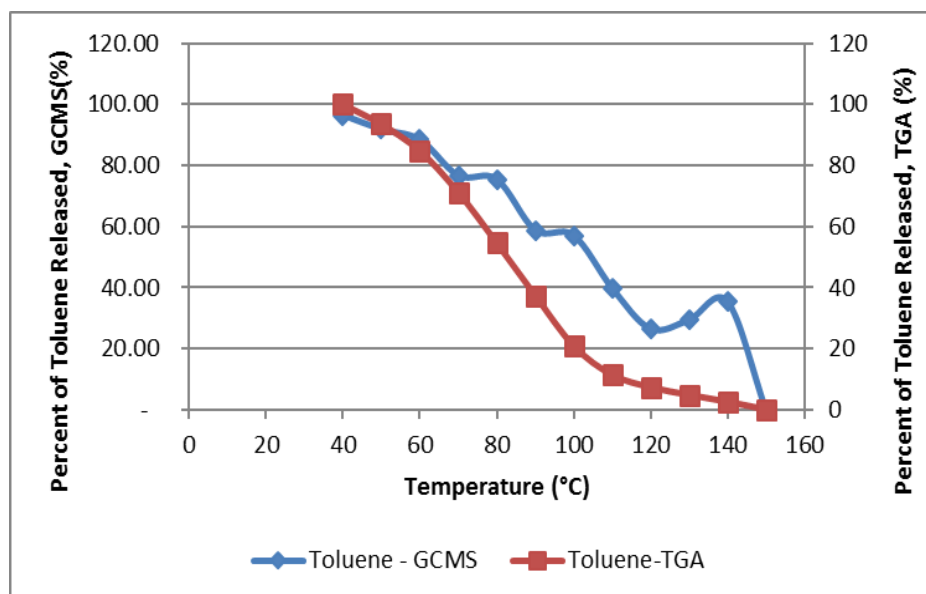


Figure. 5.7.1 Comparison plot of the guest, toluene evolving from the host framework, the TGA and GC evolution data are overlaid to show a similar profile

In Figure 5.7.1, there was good agreement between the TGA and the GC until 80°C. The guest evolves in the same manner between the two methods. Moreover, the GC confirms that the mass loss observed in the TGA is toluene. From the TGA plot, the onset point is the temperature at which the slope of the curve in the TGA plot begins to change. This was determined by drawing two tangential lines on the curve. The temperature where the two tangential lines intersect is where the slope begins to change. The onset point temperatures for all nine guests were determined from their TGA plots. For the GC data, it was more simple. We consider the onset temperature the temperature at which the guest was first detected in the chromatography. In many cases, the guest was detected earlier than the TGA onset temperature (Table 5.7.1).

Table 5.7.1 Onset temperatures for guest evolution, the comparison between onset temperature from TGA and first detection temperature in the GC

Rate = 2°C/min for TGA and GC	Boiling Point (°C)	TGA (°C)	GC (°C)
Iodobenzene	188.0	50.1	50
Ethylbenzene	136.0	54.0	40
N,N-DMA	194.0	73.5	60
Bromobenzene	156.0	62.8	70
Toluene	110.6	52.2	40
Chlorobenzene	131.0	49.7	40
Nitrobenzene	210.9	52.4	70
Fluorobenzene	80.1	77.9	40
Benzene	85.0	77.4	40

From Table 5.4.1.3, many of the guests were detected by GC at 40°C. Ethylbenzene, toluene, chlorobenzene, fluorobenzene, and benzene were all detected at 40°C.

Fluorobenzene and benzene have the lowest boiling points, and it is expected that they would be detected early on by GC. What's attractive to us was that GC detected high boiling point guests such as N,N-dimethylaniline, iodobenzene and to some extent nitrobenzene at low temperatures. It questions how strongly these guests are held within the framework. In the case of bromobenzene, the TGA onset temperature was lower than the GC detection temperature. This was because headspace samples were pulled every 10°C for the GC experiment rather than continuous mass loss via TGA. At 60°C, bromobenzene was not found in the chromatography, but by 70°C, it was. This highlights the need for multiple methods to characterize these host-guest systems fully. The results of this comparative study also show that the temperature windows in the TGA plots do correlate with guest loss. As shown in Figure 5.7.1, the evolution profile between the two

methods can be very similar, though this was not the case for all the guest molecules. An example would be ethylbenzene (Figure 5.7.2).

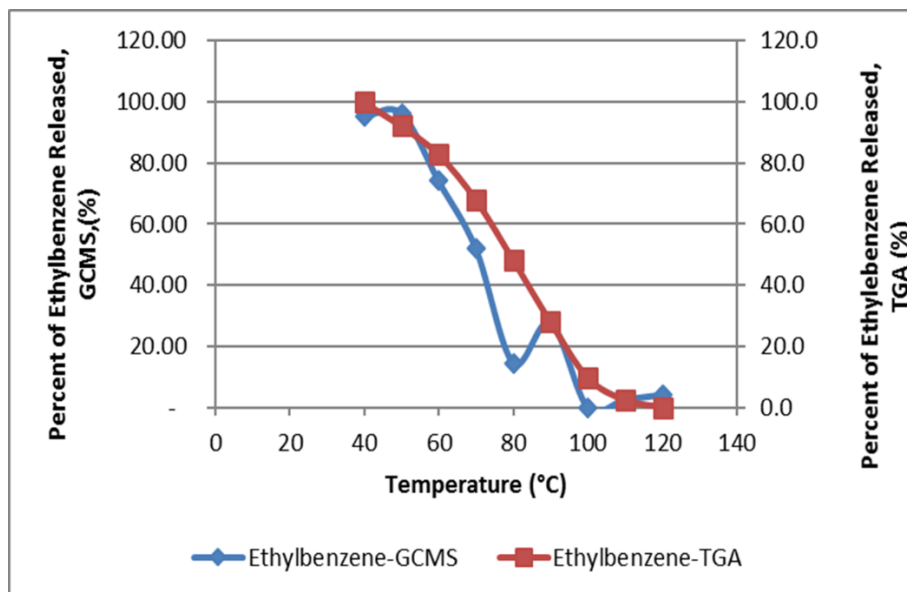


Figure 5.7.2 Comparison plot of the guest, ethylbenzene, evolving from the host framework, the TGA and GC evolution data are overlaid to show a similar profile

Ethylbenzene was detected at 40°C by GC, but the onset temperature was calculated as 54°C by TGA. What was the takeaway message from all of this? It was not surprising that the GC can detect guest evolution early on. Sometimes earlier than the TGA. Each method was within a close temperature range of the other. The most significant disparity between TGA and GC evolution data occurred between fluorobenzene, benzene, and nitrobenzene. Which method would be considered correct? In short, they both are. Each method tells about what is going between the guest and the framework. It tells how much of each there are, and how the guest comes out of the framework. How do we know that guest evolution was from within the framework? The TGA shows that the guest was lost due to a mass loss observation. The GC measured that the same guest is being evolved from the sample. The data generated does not say conclusively that mass loss or presence

in the chromatograph is the final say. There is one more tool in our array of methods to determine how the guest is evolving from the framework.

5.8 Tracking Guest Evolution by Powder X-ray Diffraction

The framework changes shape as the co-crystallized guest molecule is lost. There is a contraction along the c-axis which reduces the distance between the layers. This contraction can be observed using powder x-ray diffraction since there is a change in the d-spacing. This can be used to track whether a guest remains in the framework as the surrounding environment changes. More specifically, just like with the other tests performed thus far, we can monitor the change in the structure of the framework as we raise the temperature. This way, when we observe a mass loss or a peak in the chromatography, it can be determined whether the guest resides in the framework or is evolving off the sample. To do this, the framework would be ground up, and an initial powder x-ray diffraction scan taken at room temperature (25°C). The powdered sample was then heated for 10 minutes at 40°C. Another scan was then taken. This process was repeated until the framework was emptied of its guest molecule. Toluene is shown as an example (Figure 5.8.1).

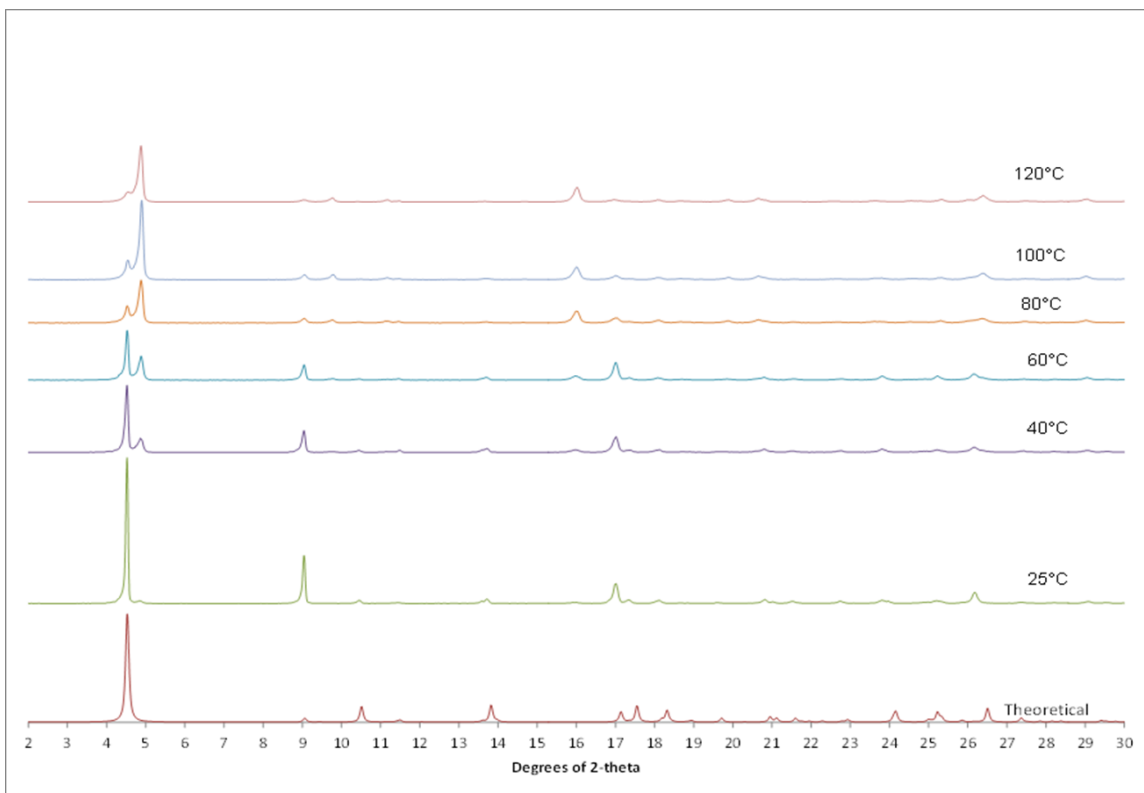


Figure 5.8.1. Temperature-dependent powder x-ray diffraction, toluene has filled the framework as can be seen at 25°C, by 40°C the framework is beginning to evolve guest molecule.

Toluene fills the framework at room temperature. The intensity at 4.5° of 2-theta indicates this. We then raised the temperature of sample 20°C and performed another scan. At 40°C, we see an intensity beginning to show itself at 4.85° of 2-theta. When this appears, it means the framework has begun to empty. This would be considered an onset temperature, just like in the TGA plot and the GC chromatograph. By 60°C, the emptied framework was coming on strong. At 80°C, the framework had a small amount of guest remaining. At 120°C, the framework was empty. Here we only see the intensity at 4.85° of 2-theta. These plots were made with the other eight guests from the Chapter 4 competition study. The onset temperature values of guest loss from the powder X-ray diffraction tests were compiled and compared against the previous methods used to

determine the temperature of guest evolution from the framework using this method (Table 5.8.1).

Table 5.8.1. Onset temperatures for guest evolution, the comparison between onset temperature from TGA, first detection temperature in the GC, and powder x-ray diffraction

Rate = 2°C/min for TGA and GC	Boiling Point (°C)	TGA (°C)	GC (°C)	PWXRD (°C)
Iodobenzene	188.0	50.1	50	40
Ethylbenzene	136.0	54.0	40	40
N,N-DMA	194.0	73.5	60	60
Bromobenzene	156.0	62.8	70	25
Toluene	110.6	52.2	40	40
Chlorobenzene	131.0	49.7	40	25
Nitrobenzene	210.9	52.4	70	25
Fluorobenzene	80.1	77.9	40	25
Benzene	85.0	77.4	40	25

The most striking point was that from chlorobenzene to benzene. The electron withdrawing guests had partially full frameworks at room temperature (25°C). Bromobenzene did as well, but the onset temperature for GC and TGA guest loss was closer to 70°C. Looking back to Table 5.4.1.2, chlorobenzene to benzene showed an unfilled framework from the TGA data. It remains that the powder x-ray diffraction confirms that not all the guests fill the framework. The powder x-ray for fluorobenzene shows empty framework. Even though iodobenzene had a weak recovery from the TGA and the GC, at 25°C it only shows the full framework, though it readily begins to empty at 40°C. All of this gives further evidence that while the guest co-crystallizes into the framework, they are easily removed. A new question arises. If the onset temperatures of guest loss are typically much lower than the boiling points than each these molecules, can we ascertain how firmly they are bound inside the framework?

5.9 Approximation of Activation Energy

In other systems, such as clathrates and polymers, a method for determining the amount of energy required to remove the guest from its host has been developed. This method was first developed back in 1966 by Flynn and Wall to use a non-isothermal TGA method to determine the activation energy (E_a) required to lose a guest molecule. It was used many times by Nassembeni *et al.* to determine the activation energy of guests evolving from clathrates.

We estimated the stability of **1**·guest for each of the nine by using the simple calculation of $T_{on}-T_{bp}$.^{12,15} Nassembeni *et al.* determined that a positive value for this calculation would indicate a stable host-guest while a negative value would indicate an unstable host-guest.^{12,15} The relationship carried over to activation energy, since positive $T_{on}-T_{bp}$ values would give higher activation energies.^{12,15} Negative values would give lower activation energies (Table 5.9.1).

Table 5.9.1 Calculation of $T_{on}-T_b$ to estimate the stability of the **1**·guest for each of the single co-crystallized guest molecules. TGA onset temperatures were used.

Guest	BP	Ton	Ton-Tbp
Fluorobenzene	80.1	77.9	-2.2
Benzene	85	77.4	-7.6
Toluene	110.6	52.2	-58.4
Chlorobenzene	131	49.7	-81.3
Ethylbenzene	136	54	-82
Bromobenzene	156	62.8	-93.2
Iodobenzene	188	50.1	-137.9
N,N-DMA	194	73.5	-120.5
Nitrobenzene	210.9	52.4	-158.5

Table 5.9.1 creates a very telling story based on a simple calculation. As the boiling point of the guest increases, the host-guest material should be considered less stable.

We approximated the activation energy for each of the nine guest molecules. An Arrhenius plot was made for each of the guests using the previous mentioned methods. From this plot, an equation was generated which allowed us to solve for the activation energy (E_a). The plot for ethylbenzene was used as an example (Figure 5.9.1).

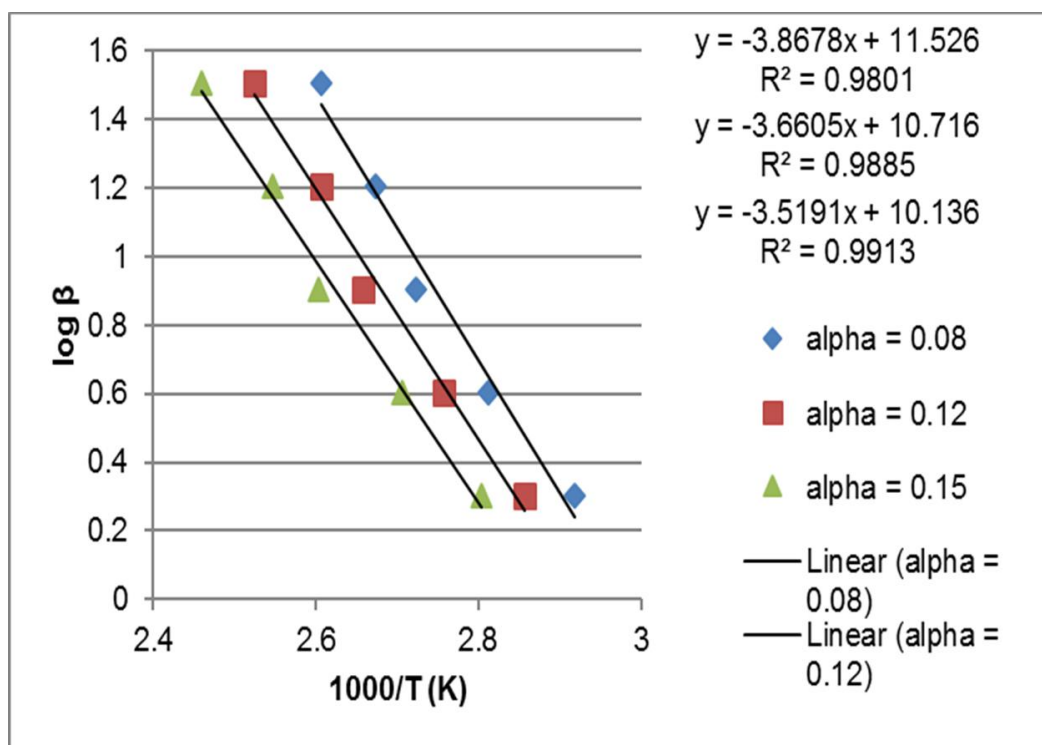


Figure 5.9.1. Arrhenius plot used to approximate the activation energy (E_a) required to evolve ethylbenzene from the framework.

Section 5.3.8 explains how to calculate the values of alpha, but what is this calculating?

When mass loss begins in a TGA plot, the total percent mass loss can be calculated for each step. We are interested in the guest loss steps and the energy associated with guest loss. The alpha values are just fractions of the guest loss step from the TGA plot. For

example, when $\alpha = 0.08$, 5% of the mass has been lost from the sample. At $\alpha = 0.12$, 7% of the mass in the sample has been lost. For $\alpha = 0.15$, 9% of the mass from sample has been lost. Using these three mass loss ranges termed α ; we plotted the log of the heating ramp rate versus $1/T$ ($^{\circ}\text{K}$)*1000. The temperature used (in $^{\circ}\text{K}$) was the same temperature for m_t or mass at time = t , for that α range at that ramp rate. For example, in Figure 5.9.1, the farthest blue diamond on the bottom right of the graph. At 5% mass loss, the log of $2^{\circ}\text{K}/\text{min}$ would equal 0.301, and this would be the y-value on the scatter plot. The temperature where the 5% mass loss occurs was 69.5°C or 342.6°K . This calculates as $1/(342.6^{\circ}\text{K})$ and then multiplied by 1000 was equal to 2.92, which was the x-value. The rest of the y-values, for $\alpha = 0.08$ are the log of the ramp rates from 2 through $32^{\circ}\text{K}/\text{min}$. The temperature, m_t , changes as the ramp rate increases. This temperature change provides the rest of the x-values. Plotting out these values provides a slope which can then be used to calculate the activation energy, E_a , based on the Arrhenius equation.

The plot in Figure 5.9.1 was made for all the guest molecules, and from the equations, their activation energies were approximated. Each plot had parallel straight lines which based on literature would indicate a single-step reaction.¹⁴ We compared these activation energies against the other data we have generated thus far for these guest molecules (Table 5.9.1).

Table 5.9.1. Onset temperatures for guest evolution, the comparison between onset temperature from TGA, first detection temperature in the GC, onset temperatures from powder x-ray diffraction, and approximated activation energy, E_a , for guest loss

Rate = 2°C/min for TGA and GC	Boiling Point (°C)	TGA (°C)	GC (°C)	PWXR D (°C)	E_a (kJ/mol)
Iodobenzene	188.0	50.1	50	40	53.5
Ethylbenzene	136.0	54.0	40	40	67.0
N,N-DMA	194.0	73.5	60	60	109.3
Bromobenzene	156.0	62.8	70	25	78.9
Toluene	110.6	52.2	40	40	64.2
Chlorobenzene	131.0	49.7	40	25	75.8
Nitrobenzene	210.9	52.4	70	25	75.2
Fluorobenzene	80.1	77.9	40	25	147.0
Benzene	85.0	77.4	40	25	148.0

Referencing the activation energies in the Table 5.9.1, we see that the two guest molecules which have had the hardest time in the competition studies have the highest calculated activation energy approximation. Typical values for other small, aromatic molecules evolving from an inclusion compound ranges from 34 – 150 kJ/mol while cavity containing inclusion compounds ranged from 100 kJ/mol – 300 kJ/mol.¹² Nitrobenzene in channeled inclusion compound had an $E_a = 151$ kJ/mol, about double ours.¹² Our calculated activation energy for benzene is about double for a channeled inclusion compound.¹³ Looking at the low temperatures that most of the guest begin to evolve out of the framework, having activation energy lower than clathrate systems makes sense. This is because the framework has a 1-D channel and has shown to lose the guests readily, especially when the heat was applied. Clathrates tend to trap the guest molecules making it more difficult for them to be released. The fact that the two guests, benzene, and fluorobenzene had some of the highest energy values, but some of the lowest concentrations/occupancies mean that this method may not work as well for materials which readily lose their guests at room temperature. We were looking to see

energies for iodobenzene being the highest. If this were the case, iodobenzene might not fill up the framework, but at least it was held tightly. The guest with a higher energy value that makes sense would be N,N-dimethylaniline. Its large functional group would be difficult to wiggle out of the 1-D channel and therefore require more energy. Overall, no clear trend was observed for the approximated activation energies. Given the structure of the framework, where we have an open channel for the guests to exit from, low activation energies would be expected as there were low temperatures required to evolve the guests as well.

5.10. Conclusions

The goal of this chapter was to have a deeper understanding of the results of the competition study in Chapter 4. We have previously shown how calculated electrostatic potential maps could explain the selectivity order of our framework. We wanted to show further evidence of the guest interacting with the framework in ways that might explain competition order.

We began by determining the occupancy of each of the nine guest molecules using the TGA. Even though the framework highly preferred iodobenzene, it had a low occupancy of 46% by TGA. Ethylbenzene, and N,N-dimethylaniline, each containing an electron donating substituents, had nearly 100% occupancy. This would be expected of a guest molecule that beats out other guest molecules in a competition. Bromobenzene, with its partial positive σ -hole, also ranks highly at 95.2% by TGA. From toluene on down, the percent occupancy also drops. These guests were not as competitive and tended to be outperformed by the other guests in the series. Overall, the TGA data was in-line with the competition data, except for iodobenzene. We believe that iodobenzene was

a particular case due to its structure. The large σ -hole at the tip of the iodine atom can anchor the guest molecule inside the framework and doesn't allow for other guests to compete as crystallization occurs.

The second method of recovery was performed using GC. The GC recovery was lower than the TGA analysis. For example, the iodobenzene concentration dropped in half compared to the TGA results. Some of the other guests who were highly preferred tended to have high recovery from the GC method, including ethylbenzene, and N,N-dimethylaniline. In many of the cases, there was a 50% difference between the TGA results and the GC. A calibration curve was generated for each of the guest molecules, but there are more steps to prepare a sample for GC testing compared to TGA. Once the sample is crushed, there is always potential to lose analyte. In each of the samples, the guest of choice was recovered. This experiment confirmed that the mass loss observed in the TGA was the guests we put into the growth solution.

A comparison was made between the guest evolution via TGA to guest evolution by GC. For most of the guests, the evolution profile of the guest matched between the TGA and GC experiments. We confirmed that the mass loss in the TGA was the guest in question. Guests with electron withdrawing groups had the most significant deviations in the guest evolution profile. Bromobenzene showed a slower mass loss in the GC as compared to the TGA. The detection temperature for bromobenzene matched with the TGA onset temperature. Nitrobenzene was the only guest where the GC detection temperature was about 20 degrees higher than the TGA temperature. This study provides confidence that we are evolving the guest molecules over the temperature ranges we see in the TGA.

Powder x-ray diffraction was used to confirm structural changes in the framework at different temperatures to confirm when the guests were leaving the framework. We found excellent agreement between the TGA, GC and powder x-ray data for the onset temperature of guests leaving such as iodobenzene, ethylbenzene, N,N-dimethylaniline, and toluene. For the remaining guests, we knew there was a tendency not to have a high occupancy value. If the framework were half-full, to begin with, the onset temperature for guest loss from the powder pattern would appear low. Iodobenzene and bromobenzene were a bit surprising. Iodobenzene appeared full in the powder pattern, but we know it did not appear full based on the TGA and the GC recovery values. Bromobenzene had a high TGA occupancy, was preferred in the competition study but had a low GC recovery and had some empty framework at room temperature. Guests who were preferred in the competition study tended to have higher onset temperature values from the powder x-ray data. Since sample prep for this method has a grinding step, there is some expected guest loss. Heat generated in the sample from grinding could prematurely evolve the guest.

Finally, we approximated the activation energy, E_a , for each of the guest molecules. Using the TGA, we did this to show that the guest order from the competition study may be tied back to the amount of energy needed to release a guest molecule. If a guest is highly preferred, we would expect it to be harder to remove from the framework and therefore have higher activation energy. Ultimately, this was not the case. The activation energies for each guest appeared to go up and down. Comparing to other co-crystallized guest systems, our lower activation energies for a majority of our guest molecule make sense considering the 1-D channel of the framework.

We have shown multiple methods of analysis, such as GC, TGA, and powder x-ray to analyzed **1**·single guest under a multitude of conditions to help explain the order discovered in the previous chapters competition study. We feel that in addition to the electrostatic potential interactions, having a guest that can fill the framework on its own will increase its likely-hood of beating out other guest molecules. While nothing beats a head to head competition to determine selectivity, it can be said that molecules which are more stable guests within the framework have a higher probability of winning that competition.

5.5 References

- 1) Koito, Y.; Yamada, K.; Ando, S. *J. Incl. Phenom. Macrocycl. Chem.* **2013**, *76*, 143-150
- 2) Safina, G.D.; Ziganshin, M.A. Gubaidullin, A.T.; Gorbachuk, V.V. *Org. Biomol. Chem.*, **2013**, *11*, 1318.
- 3) Pivovar, A.M.; Holman, K.T.; Ward, M.D. *Chem. Mater.* **2001**, *13*, 3018-3031
- 4) Yang, J.; Dewal, M. B.; Profeta, S.; Smith, M.D.; Li, Y.; Shimizu, S. *J. Am. Chem. Soc.* **2008**, *130*, 612-621
- 5) Cardinael, P.; Peulon-Agasse, V.; Coquerel, G.; Combert, Y.; Combret, J.C. *J. Sep. Sci.* **2001**, *24*, 109-115
- 6) Fourmentin, S.; Ciobanu, A.; Landy, D.; Wenz, G. *Beilstein Journal of Organic Chemistry*, **2013**, *9*, 1185-1191
- 7) Ciobanu, A.; Mallard, I.; Landy, D.; Brabie, G.; Nistor, D.; Fourmentin, S. *Carbohydr. Polym.* **2012**, *87*, 1963-1970
- 8) Liu, X.; Oh, M.; Lah, M.S. *Inorg. Chem.* **2011**, *50*, 5044-5053
- 9) Umeyama, D.; Horike, S.; Inukai, M.; Kitagawa, S. *J. Am. Chem. Soc.* **2013**, *135*, 11345-11350
- 10) Hu, S.; Zhang, J.P.; Li, H.X.; Tong, M.L.; Chen, X.M.; Kitagawa, S. *Cryst. Growth Des.* **2007**, *11*, 2286-2289
- 11) Seo, J.; Matsuda, R.; Sakamoto, H.; Bonneau, C.; Kitagawa, S. *J. Am. Chem. Soc.* **2009**, *131*, 12792-12800
- 12) Gifford Nash, K.L. Inclusion Compounds of Multipedal Hosts. PhD Dissertation, University of Cape Town. Rondebosch, South Africa, September 1997; Barbour, L.J.; Caira, M.R.; Coetzee, A.; Nassimbeni, L. *J. Chem. Soc. Perkins Trans 2*,

- 1995**, 1345-1349; Caira, M. Coetzee, A.; Nassimbeni, L.; Weber, E.; Wierreg, A.; *J. Chem. Soc., Perkin Trans. 2*, **1997**, 237-242; Su, H.; Nassimbeni, L. *New J. Chem.* **2002**, 26, 989-995; Nassimbeni, L.; Su, H. *J. Chem. Soc. Perkin Trans. 2* **2002**, 1246-1250; Jacobs, A.; Nassimbeni, L.; Nokaho, K.L.; Su, H.; Taljaard, J.H. *Cryst. Growth and Des.* **2008**, 8, 1301-1305; Nassimbeni, L.; Su, H. *Acta Cryst. Section B* **2001**, B57, 394-398; Coetzee, A.; Nassimbeni, L.; Su, H.; *J. Chem. Res.* **1999**, 436-437; Nassimbeni, L.; Su, H. *J. Phys. Org. Chem.* **2000**, 13, 368-371; Vries, E.; Nassimbeni, L.; Su, H. *Eur. J. Org. Chem.* **2001**, 1887-1892; Bourne, S.; Oom, B.M.; Toda, F. *J. Chem. Soc.; Perkin Trans. 2*, **1997**, 585-587;
- 13) Flynn, J.H.; Wall, L.A. *Polymer Letters* **1966**, 4, 323-328; Ozawa, T. *Bulletin of the Chemical Society of Japan*, **1966**, 39, 2071-2085; Wicht, M.M.; Bathori, N.B.; Nassimbeni, L. *Dalton Transactions* **2015**, 44, 6863-6870
- 14) Bourne, S.A.; Nassimbeni, L. *J. Org. Chem.* **1992**, 57, 2438-2442
- 15) Johnson, L.; Nassimbeni, L.; Toda, F. *Acta Cryst.* **1992**, B48, 827-832; Caira, M.R.; Nassimbeni, L.R.; Winder, N.; Weber, E.; Wierreg, A. *Supramolecular Chemistry*, **1994**, 4, 135-138
- 16) Uemura, K.; Kitagawa, S.; Fukui, K.; Saito, K. *J. Am. Chem. Soc.* **2004**, 126, 3817-3828; Soldatov, D. *Journal of Chemical Crystallography*, **2006**, 36, 747-768; Herman, M.A.; Hofmans, H.; Desseyn, H.O. *Thermochimica Acta.* **1985**, 85, 63-66
- 17) Brown, Michael E. *Introduction to Thermal Analysis: Techniques and Applications*. Springer Netherlands, 2004.

18) Caira, M. Coetzee, A.; Nassimbeni, L.; Weber, E.; Wierreg, A.; *J. Chem. Soc., Perkin Trans. 2*, **1997**, 237-242

Chapter 6

Conclusions

6.1 Final Conclusions

We have shown that the sum of many small forces working in concert can lead to a robust and stable material capable of selective molecule separation. Supramolecular chemists have worked tirelessly for many decades proving the simple fact that with careful planning, new materials are possible even when held together by weak forces. The sheer volume of knowledge, structures, and applications that have come out of this field of research is indeed awe-inspiring. We have explored the interactions of a variety of guest molecules with our charge-assisted hydrogen bonded framework consisting of $\text{Zn}(\text{HPDA})_2 \cdot (\text{H}_2\text{O})_2$ and *o*-tolidene. We have used a multitude of analytical techniques to detect the guest molecules as well as changes in the framework itself. Ultimately, this framework has demonstrated that molecules can be separated by the selective co-crystallization of one guest vs. another. We have tested the capability of the framework to separate guest pairs based on relative size, by shape, and by electronic nature of the guest molecule. The observed selectivity led to further questions about why a particular guest was preferred. What was it about a guest that caused it to co-crystallize over another?

In the first study, we devised a new method of analysis using solid phase microextraction. This method can test for co-crystallized guest molecules as they evolve from the 1-dimensional channels but it does not destroy the framework. Previously, GC methods heated the sample to a point where the framework degraded. In this method, the hydrogen bonded framework releases the guest molecules, and they are adsorbed onto a solid-phase microextraction fiber. This fiber is inserted into GC, and the guest is then detected. Three advantages come from this method of analysis. The framework is retained during the analysis leaving it available for further testing. The test allows for TGA analysis coupled to a GC or GCMS at a low cost to entry. The SPME fibers have

low detection limits. The sample size can be small as well, which when dealing with crystals is an advantage. After the guest has been detected, the sample can still be used to look at changes in the host utilizing other analytical methods. If two guest molecules have a similar response factor with the polymer coating on the SPME fiber, both guests can be detected qualitatively from the TGA exhaust gas using this method.

In the second study, the selectivity of the framework towards guest size and shape was evaluated. A series of guest molecules of varying size and shape were placed in competition reactions and allowed to co-crystallize inside of the framework. Several different selectivity profiles were observed. The competition between benzene and phenol showed almost no selectivity. Another experiment showed that toluene was preferred to benzene. When one particular size molecule, *p*-difluorobenzene, was held constant, it appeared that the larger guest was preferred. Then diethylbenzene showed concentration-dependent selectivity when compared against *p*-fluorobenzene. It was thought that guest preference moved from smaller to larger, but there appears to be a maximum size for a guest molecule. The smaller guest can take its place. That is until a particular concentration. Latter, the guest size was held constant, but the shape was changed. We focused on smaller molecules, such as *p*-xylene vs. *p*-diethylbenzene, and then compared the geometric isomers in the *m*- and *o*- position as well. The geometric isomers of xylene and diethylbenzene had different selectivity profiles compared to the *para*-position. The selectivity was not specific or slightly in favored one molecule. Based on TGA results, the shape does play a significant factor selectivity and uptake. The *meta*- and *ortho*- position isomers had low inclusion rates compared to the *para*- molecules. The lack of selectivity between molecules was due to a lack of guests co-crystallizing.

The data does show a sweet spot for the guest molecules, not too big or too small. The issues with selectivity arrive when the guests struggle to co-crystallize.

The third study delved deeper into a new set of properties held by the selected guest molecules. During the size and shape testing, it was observed that fluorinated guests did not perform well against xylenes or another guest with electron donating groups. The trend provided the next question that needed to an answer. What if two guest molecules, with entirely different electronics but the same size and shape, are placed in competition? Would the trend continue? Two very similar molecules were selected, *p*-xylene and *p*-dichlorobenzene. The electrostatic potential maps were calculated for each to show just how different they were. The same trend was observed in the previous study, the guest with the electron donating substituent was preferred. The preference was not extreme, so two guests of even closer similarity were chosen, *p*-xylene and *p*-chlorotoluene were introduced. The selectivity towards *p*-xylene had decreased. The frameworks selectivity is sensitive to subtle changes in the guest type. Nine mono-substituted benzene molecules were chosen for competition to explore this idea further. The electronic nature of the guest molecule did make a difference in selectivity. Guests with alkyl donating groups were preferred but with some exceptions. Iodobenzene and bromobenzene performed very well during the study. Electrostatic potential maps of the guests and pieces of the framework were calculated. Based on the areas of electron density, it appeared that iodobenzene and bromobenzene had perfect anchor points at the terminal end of the halogen, σ -hole, and in the centroid of the aromatic ring to have a non-repulsive interaction with the framework. These features of the molecules are why both faired much better in the competition reaction than initially expected. Plotting values

pulled from the ESP maps against the guest order from the competition reactions gave a linear correlation. Comparing other physical properties of the molecules against selectivity order provided other insights. There was a linear correlation observed between guests with electron withdrawing groups and density of the molecule. The boiling point also showed a linear correlation but the fit applied to the data was weaker than density. The guests did not show a linear correlation between selectivity and Hammett constant.

In the fourth study, we wanted to improve our understanding of the interaction between the guest and the framework. What drove selectivity for one guest versus another? If we could find evidence of strong interactions between the guest and framework, it might shed more light on the selectivity trend observed in the third study. Several analytical instruments were used to perform this series of test. By coming at the problem from many angles, one may provide the answers needed. The TGA results measured high inclusions of electron donating guests and low inclusions of electron withdrawing guest. The percent recovery from TGA did not follow a specific trend. Consequently, iodobenzene had meager recovery though it faired well in the competition. The GC recovery study found even lower values of the guests compared to the TGA results but confirmed that presence of each guest molecule. A different approach was taken to compare the GC and TGA. The guests were evolved using the heating ramp as the TGA, and the release profiles were compared. In most cases, the profiles between the GC and TGA data had a high degree of overlap. The data from these two methods showed the guest evolving within the temperature range expected for guest release while confirming the guest presence throughout the range. Temperature-dependent powder x-ray diffraction monitored the presence of the guest and at what temperature the

framework began to empty. We found excellent agreement between the TGA, GC and powder x-ray data for the onset temperature of guests leaving such as iodobenzene, ethylbenzene, N,N-dimethylaniline, and toluene. For the remaining guest molecules, the framework was partially empty at room temperature. The TGA was also used to approximate the activation energy for the desorption of the guest molecule from the 1-dimensional channel. A simple calculation of $T_{\text{on}} - T_{\text{b}}$ gave negative values for all nine of the guest molecules. From the literature, a negative value for this calculation indicates that the system is not stable and the guest is likely to leave. The approximate activation energies for each of the guest were within the same window value as inclusion compounds that contain channels. The trend for highest to lower activation energy did not correlate back to what was observed in the competition study. A few of the energy values were surprising such as benzene and fluorobenzene considering how poorly these two molecules co-crystallized.

The goal of this body of work was to establish a set of rules for the type of molecules which would be selectively co-crystallized by our hydrogen bonded framework. Each of the studies provided new insights expanding our understanding of the framework's capabilities. Therefore, we offer the following rules of attraction based on our research:

- 1) The framework can co-crystallize molecules with a variety of sizes, but when in competition, the guest cannot be too large or too small. Guest molecules such as *p*-xylene have the best fit.
- 2) If a potential guest is a geometric isomer of a high inclusion guest, it does not dictate that the same results will follow.

- 3) Guest electronics can order selectivity. The framework is sensitive to subtle electronic changes in the guest molecules when size and shape are constant.
- 4) Aromatic guests with electron donating groups are preferred to electron withdrawing groups but with exceptions. If the electron withdrawing group provides an anchor point between the molecule and the framework, selectivity will increase for that guest.
- 5) For aromatic guest with electron withdrawing functional groups, the density of the guest can affect selectivity where more dense molecules were favored.

Future studies for this work would utilize this research to determine what characteristics of a guest would increase the stability of the host-guest relationships. The objective would be to have a host-guest system with a $T_{on} - T_b > 0$ so that the applications for the framework can be developed. A stronger binding of the guest to the host would also be possible through modification of the pillars which separate the layers. The tools used in this research, such as electrostatic potential mapping, could paint a picture of what the internal framework environment should look like for targeted guest selectivity.

Appendix I – Powder Pattern Data

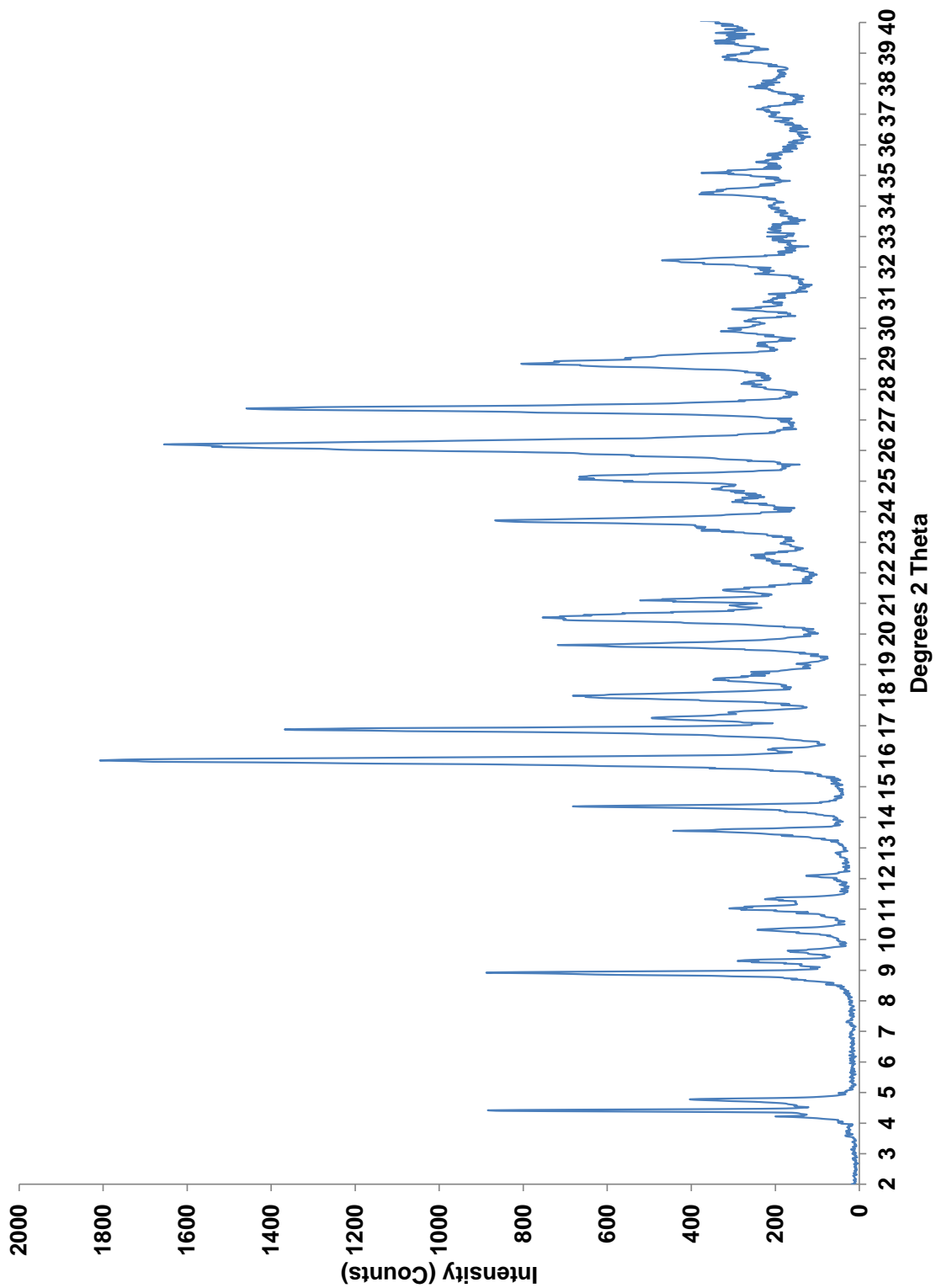


Figure I.1. – Powder XRD of **1**•toluene guest filled framework

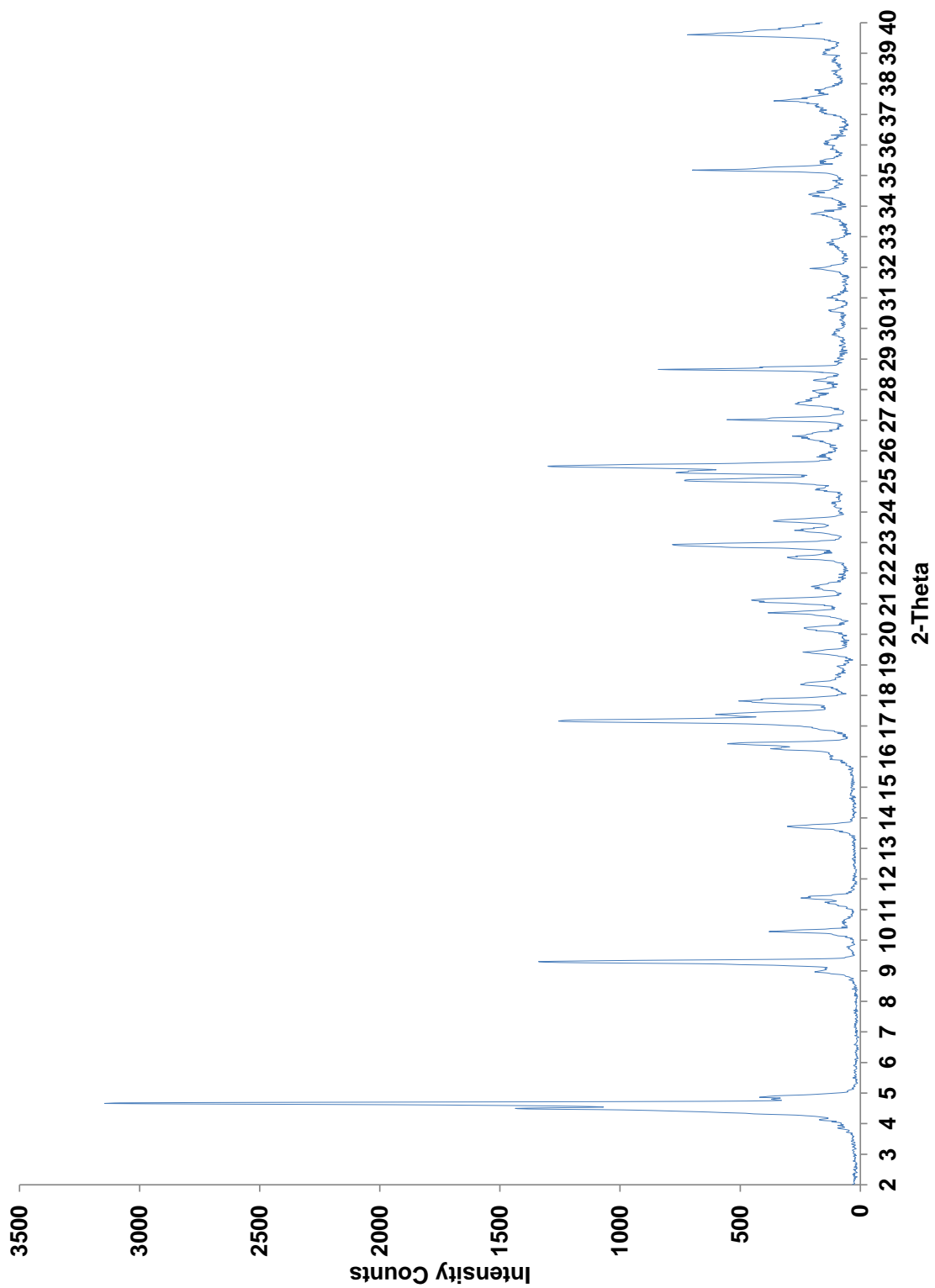


Figure I.2 – Powder XRD of **1**-m-xylene and 1,3-diethylbenzene guest filled framework

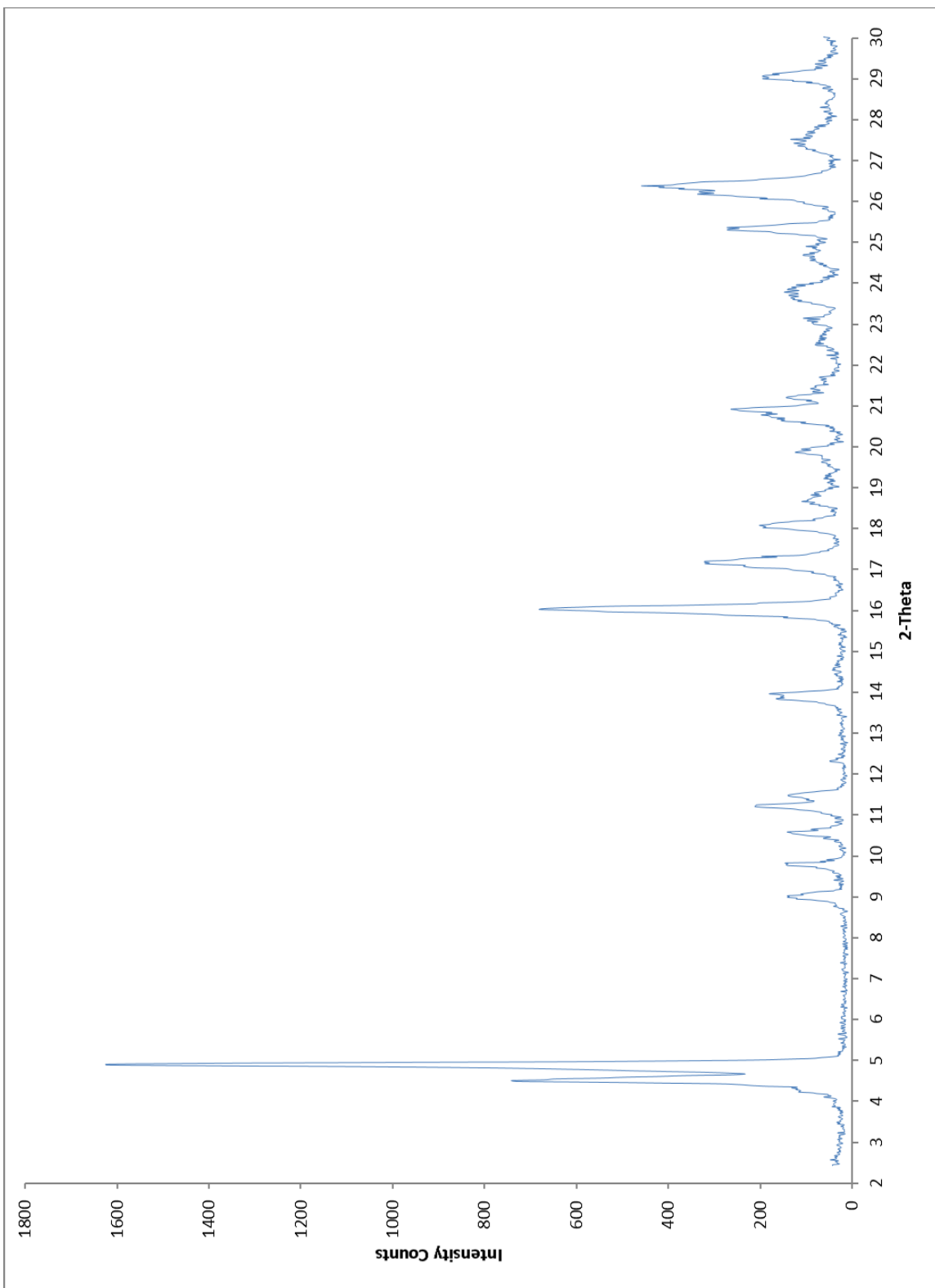


Figure I.3 – Powder XRD of **1•benzene** and phenol guest filled framework

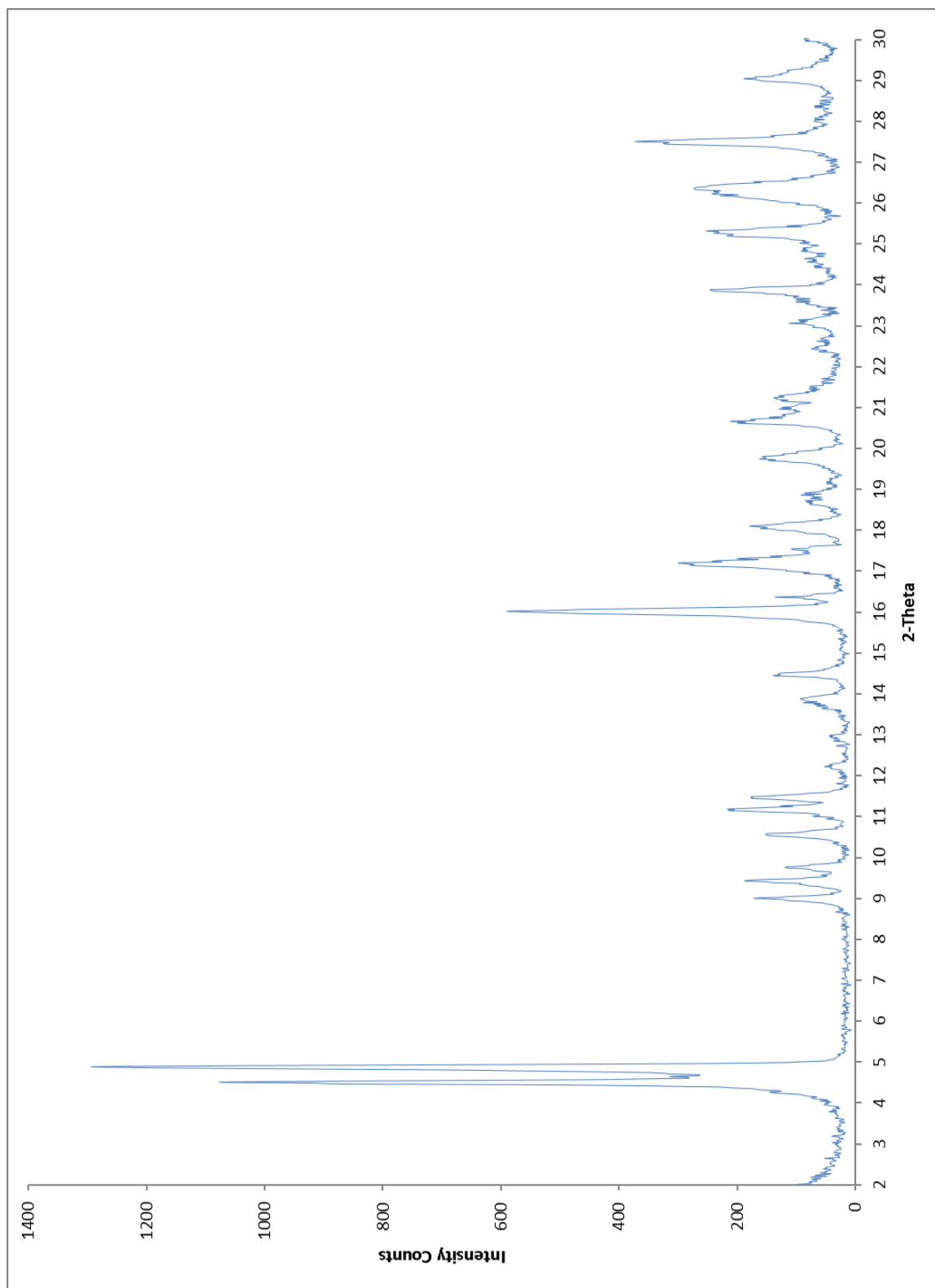


Figure I.4 – Powder XRD of **1•benzene** and toluene guest filled framework

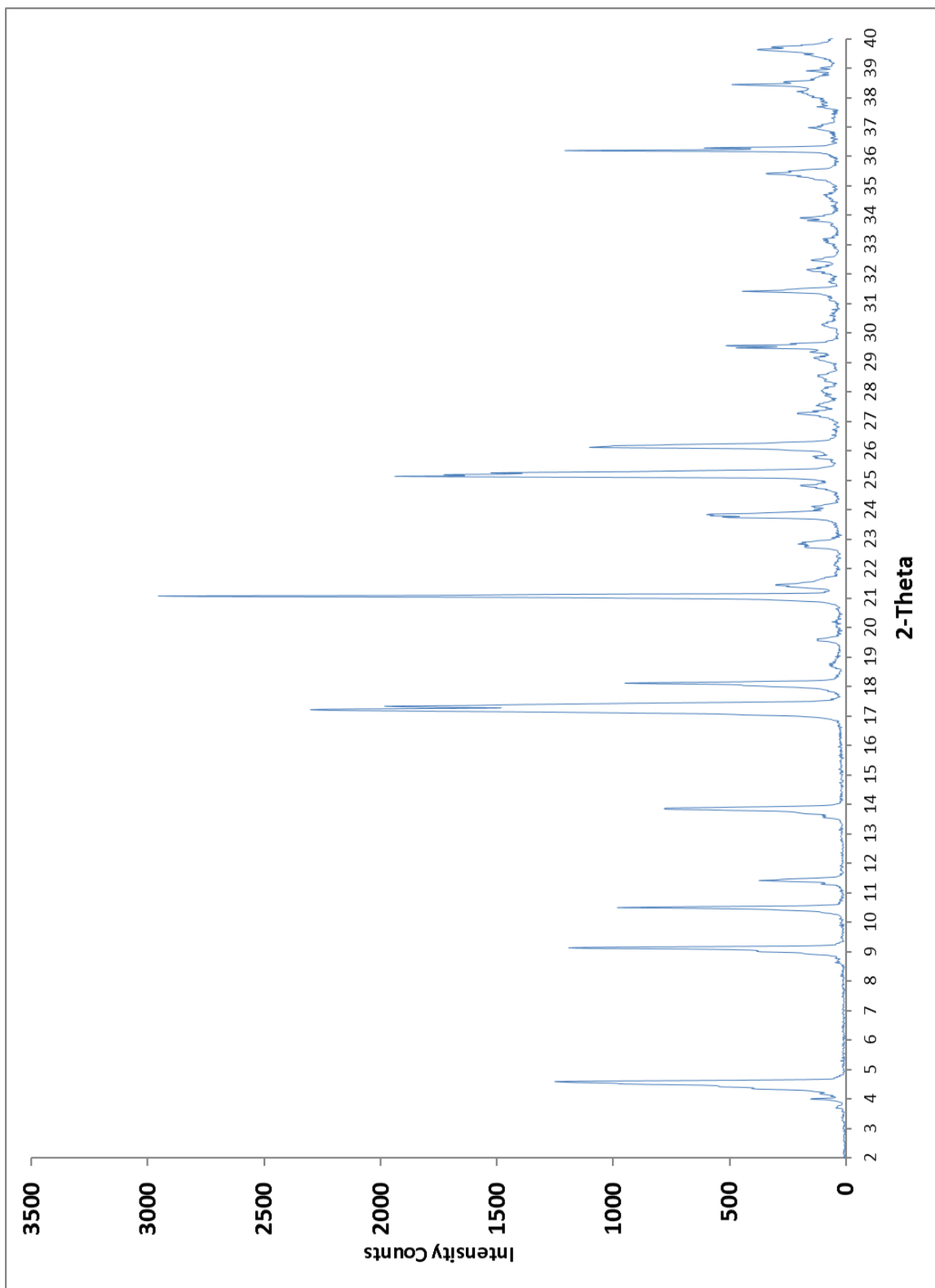


Figure I.6 – Powder XRD of 1•*p*-xylene and *m*-xylene guest filled framework

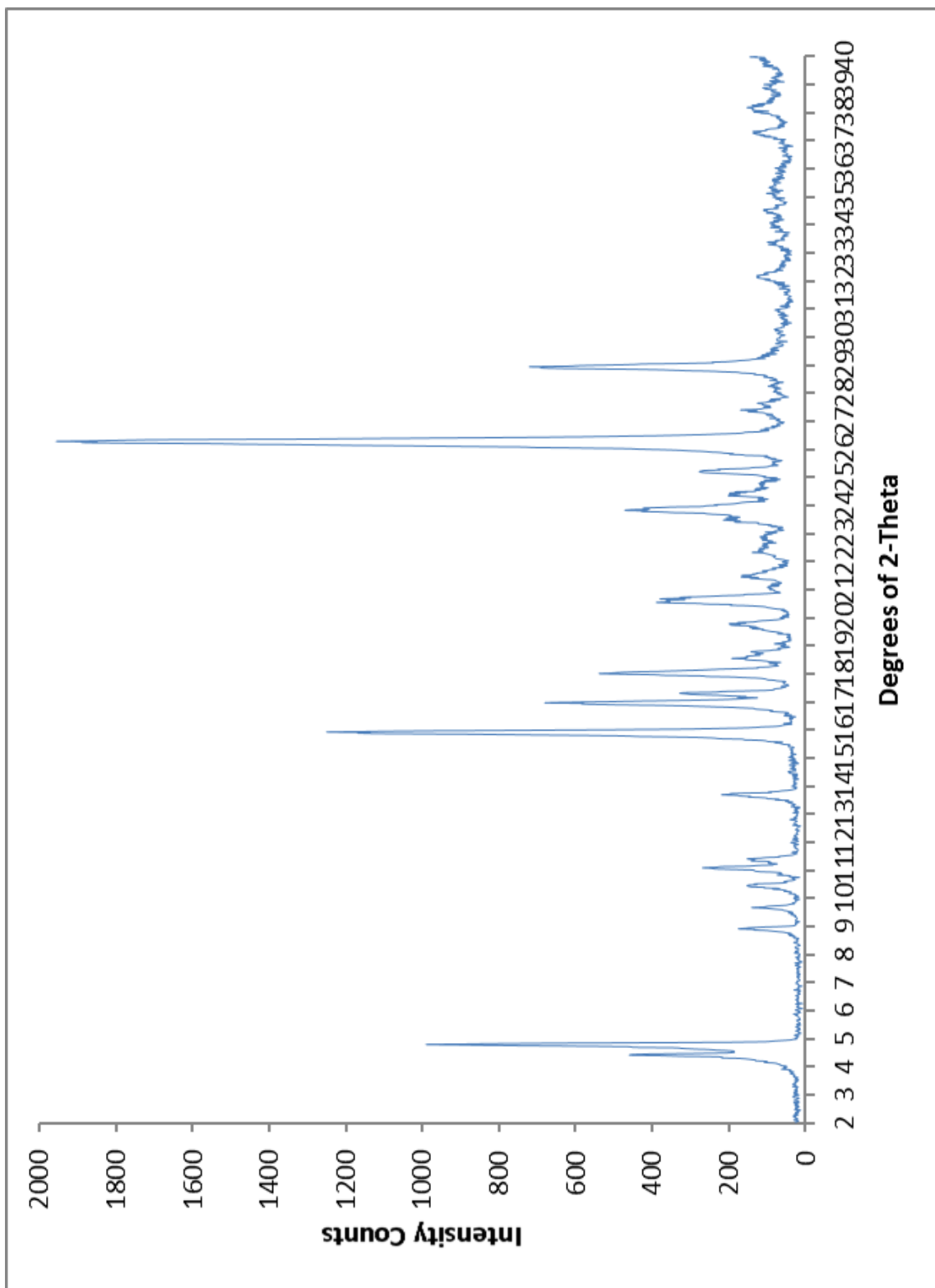


Figure I.6 – Powder XRD of **1**•toluene and di-fluorobenzene guest filled framework

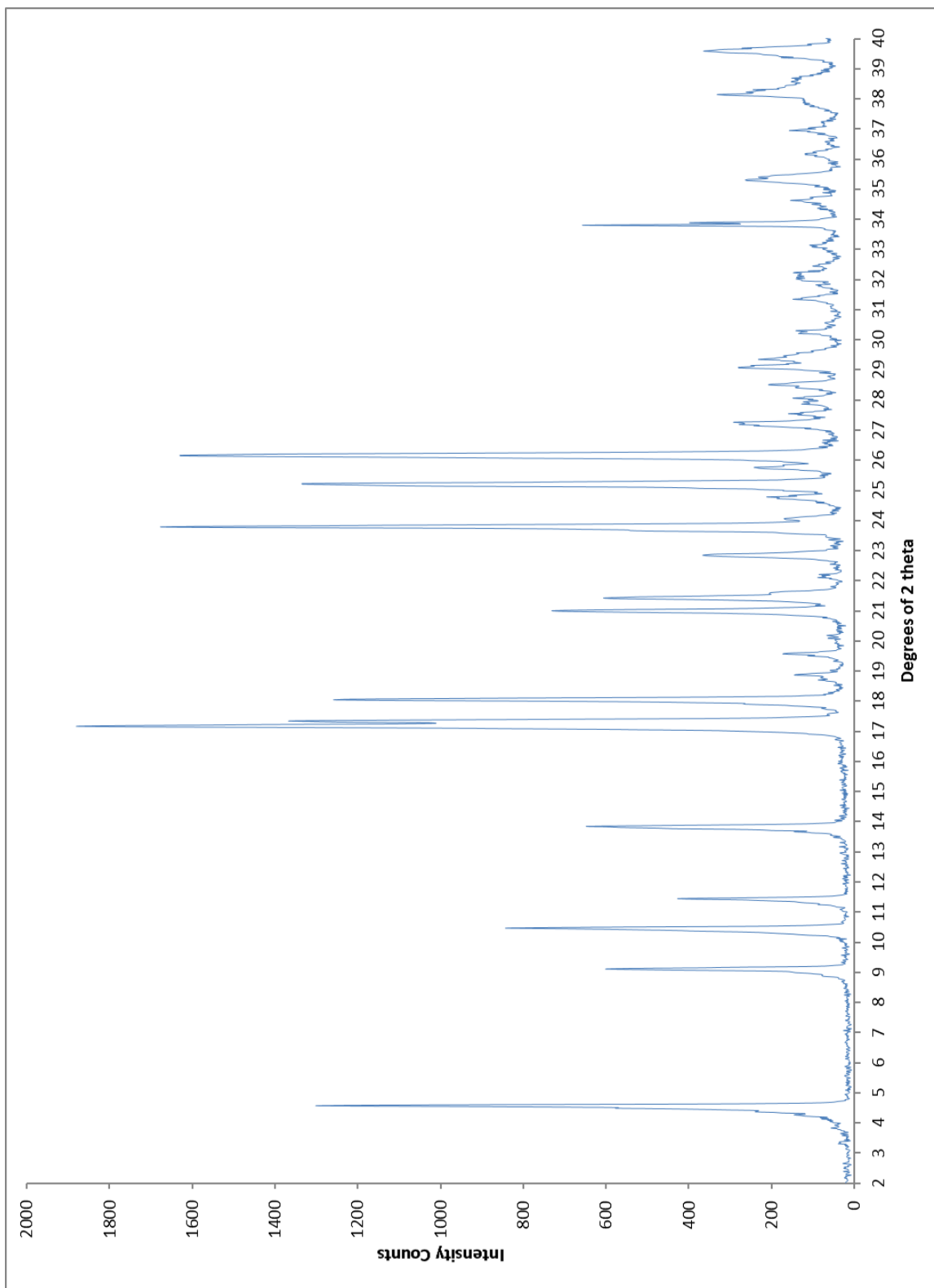


Figure I.5 – Powder XRD of **1**•*p*-xylene and *p*-di-fluorobenzene guest filled framework

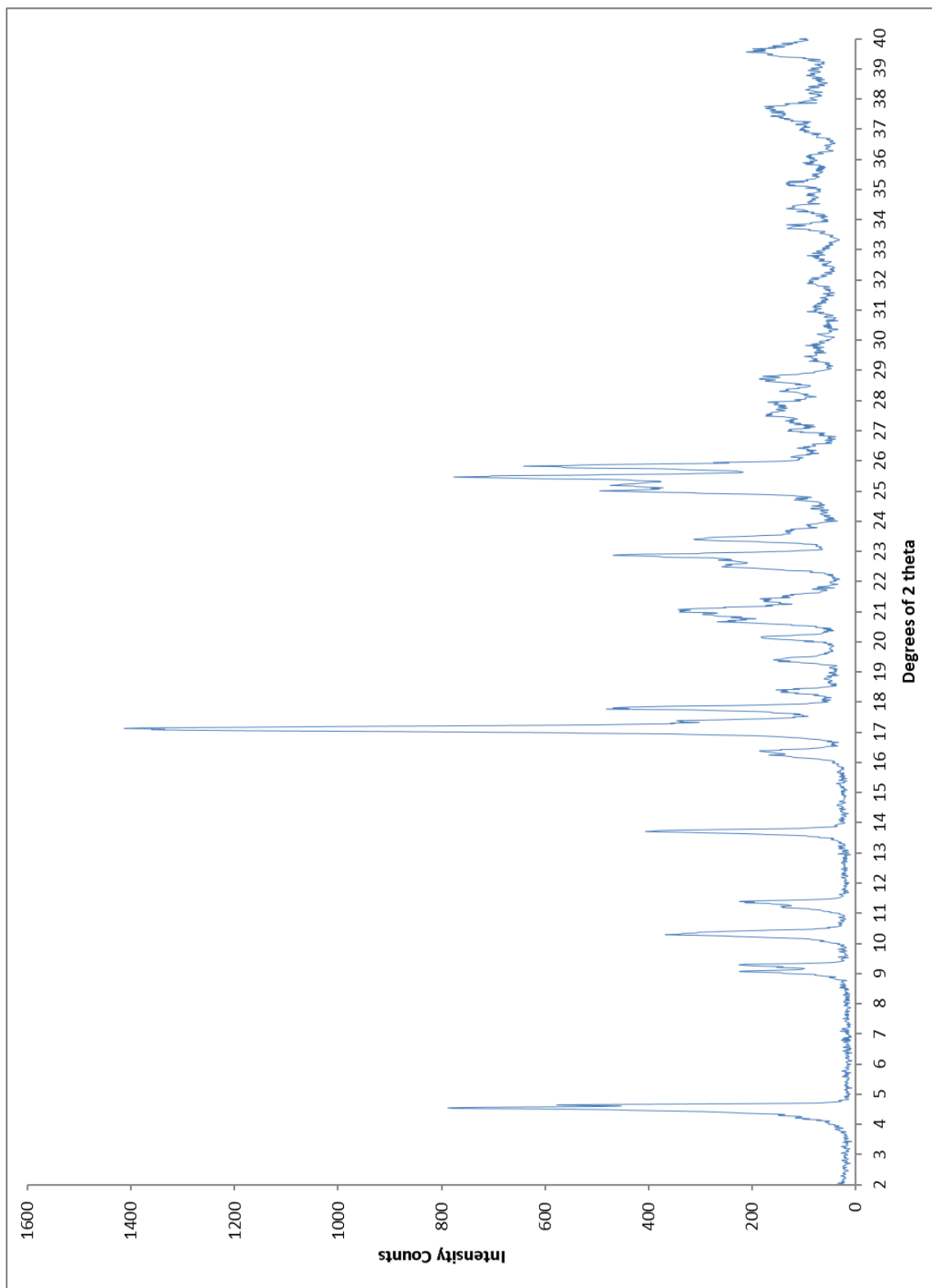


Figure I.6 – Powder XRD of **1**•*p*-diethylbenzene and *p*-di-fluorobenzene guest filled framework

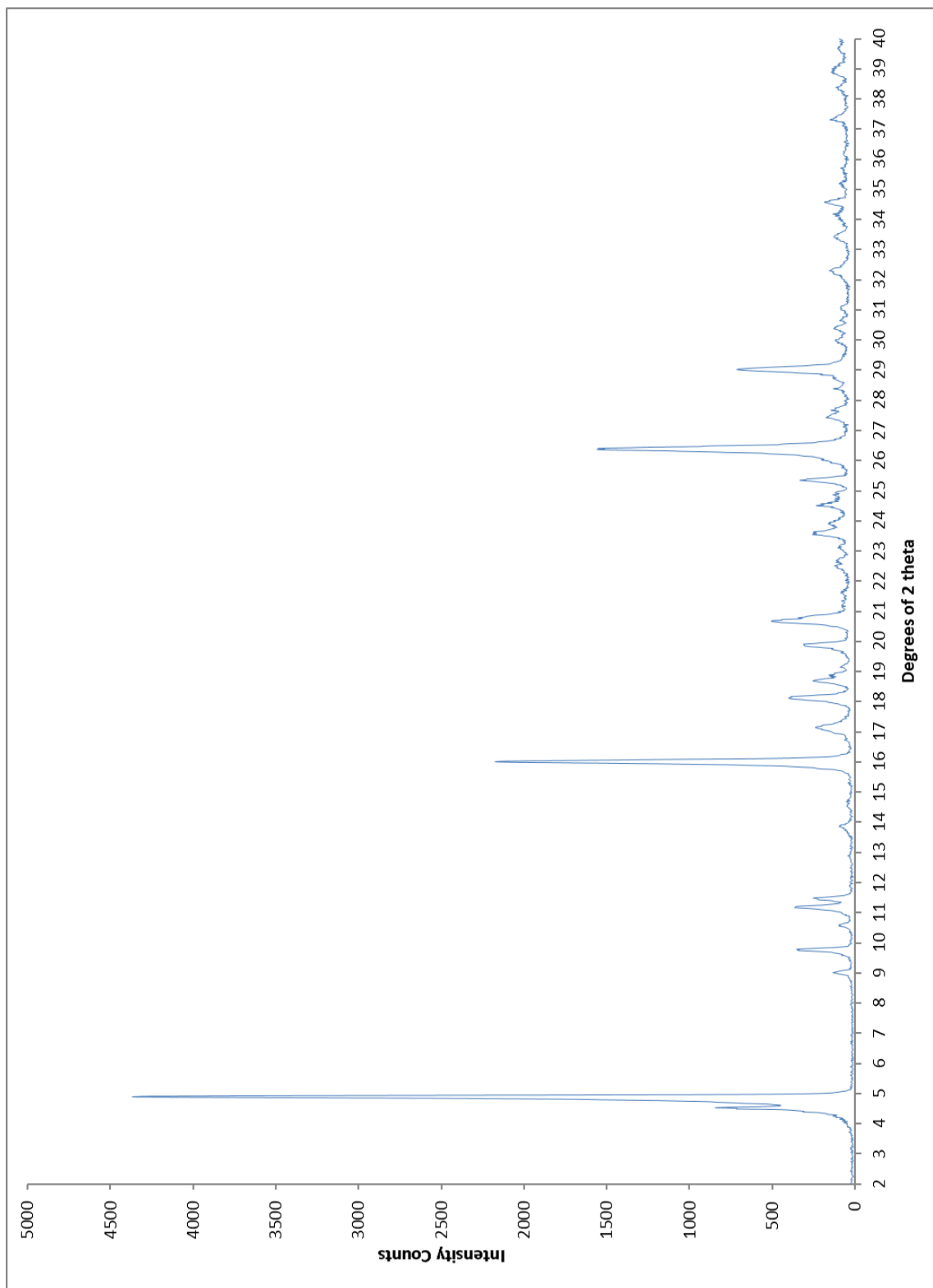


Figure I.7 – Powder XRD of **1**•*p*-di-fluorobenzene empty framework

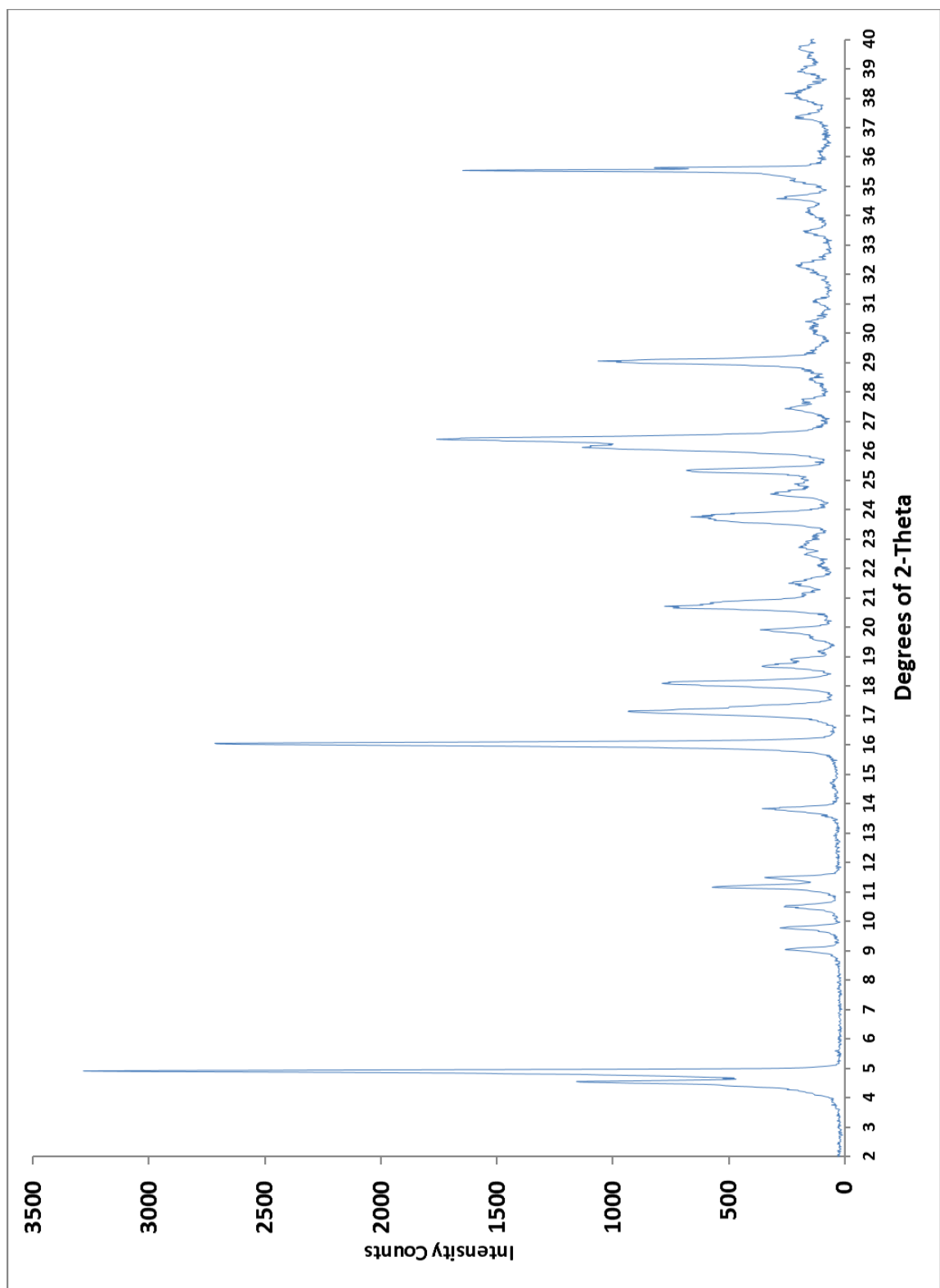


Figure I.8 – Powder XRD of **1**•*m*-xylene and fluorobenzene guest filled framework

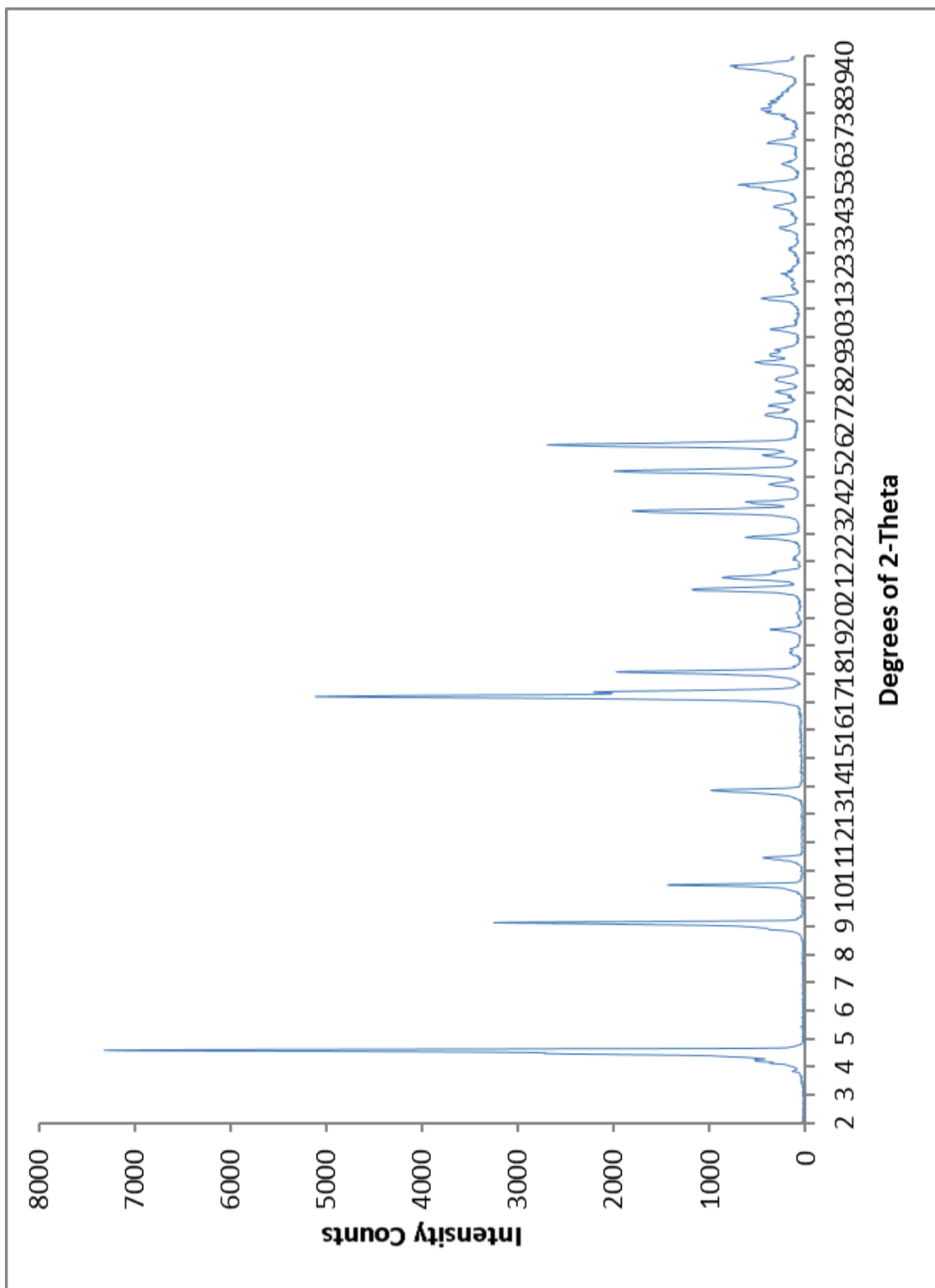


Figure I.9 – Powder XRD of **1**•*p*-xylene and *p*-diethylbenzene guest filled framework

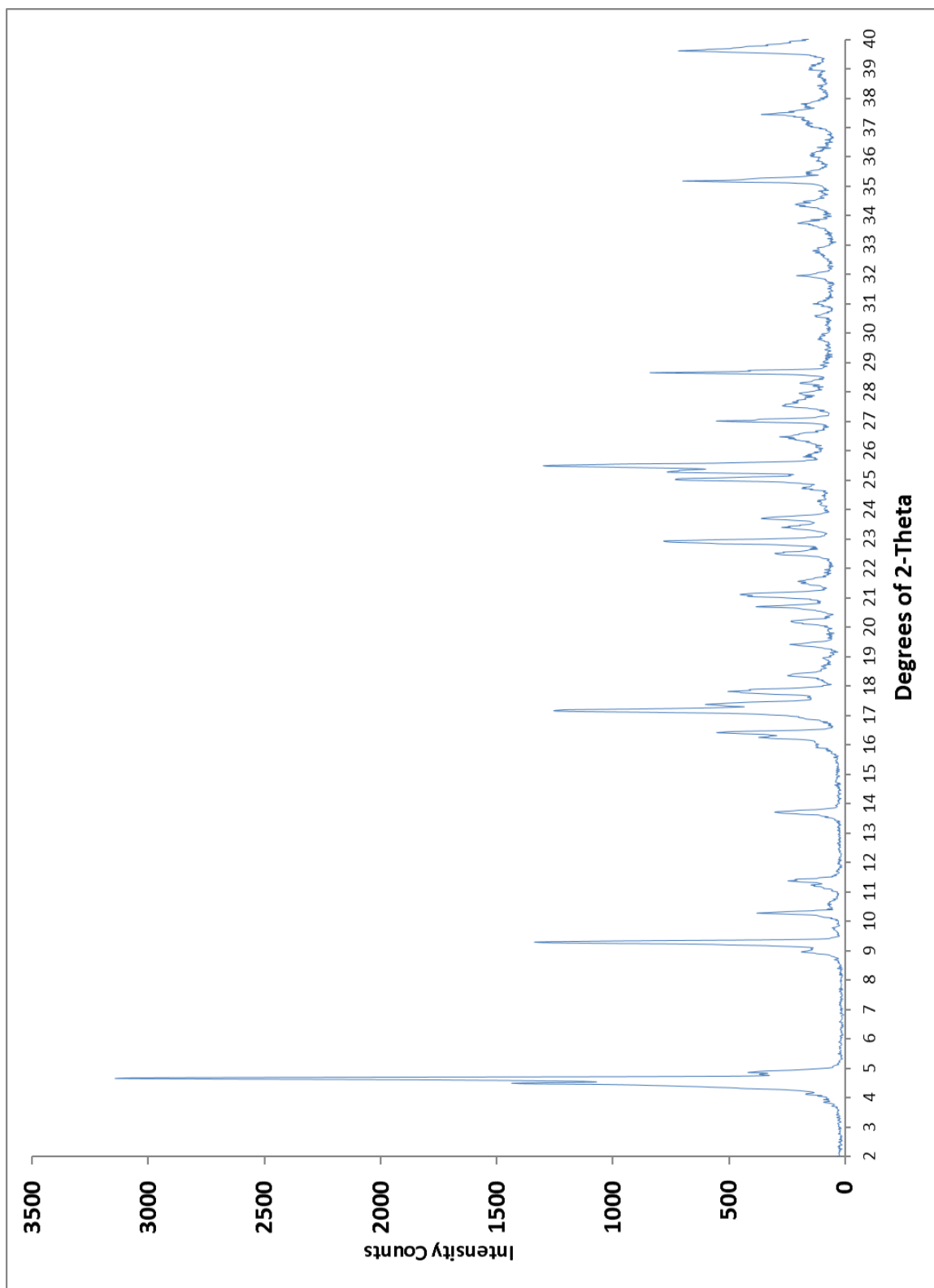


Figure I.10 – Powder XRD of **1•*m*-xylene** and *m*-diethylbenzene guest filled framework

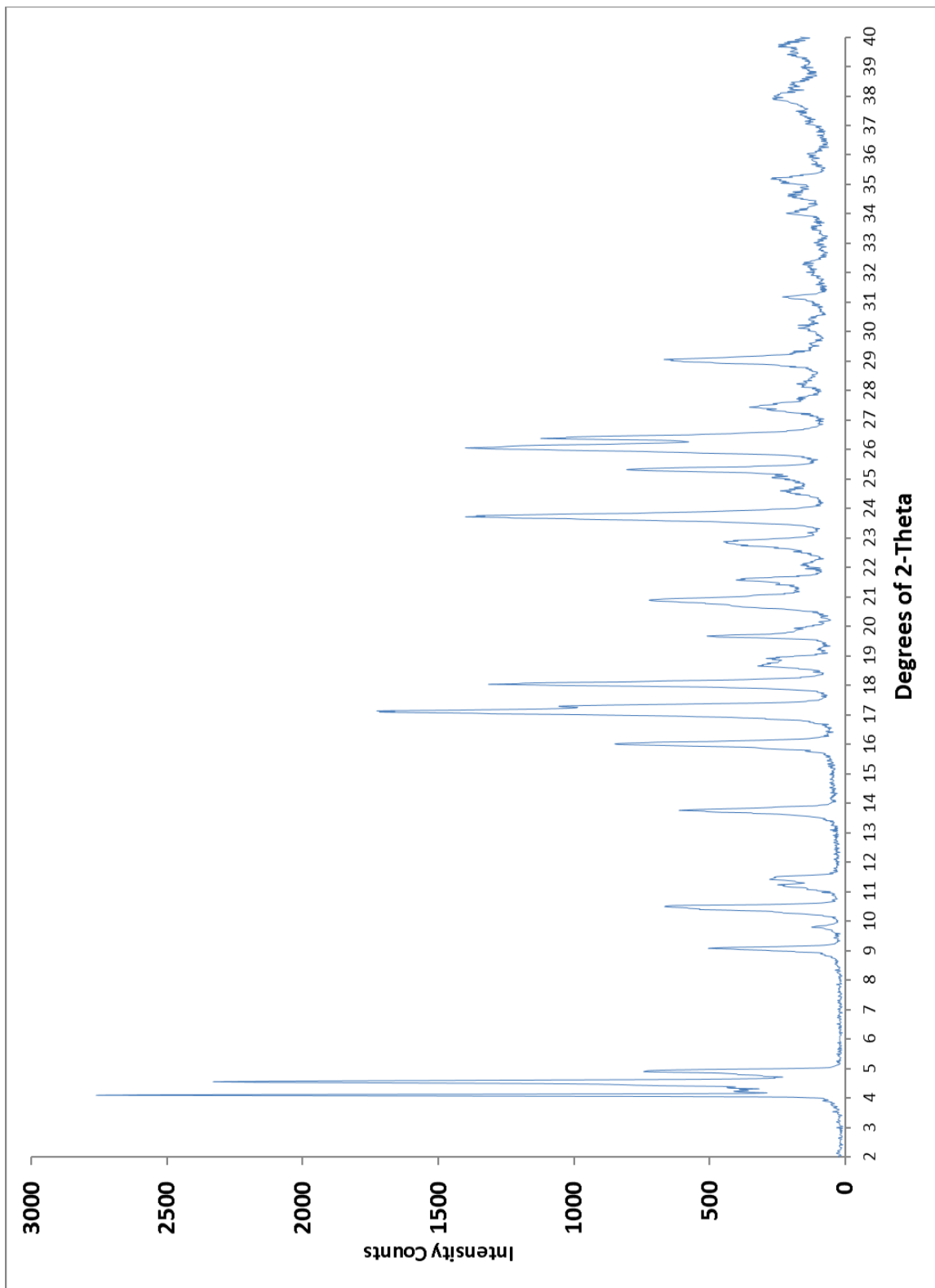


Figure I.10 – Powder XRD of 1•*o*-xylene and *o*-diethylbenzene guest filled framework

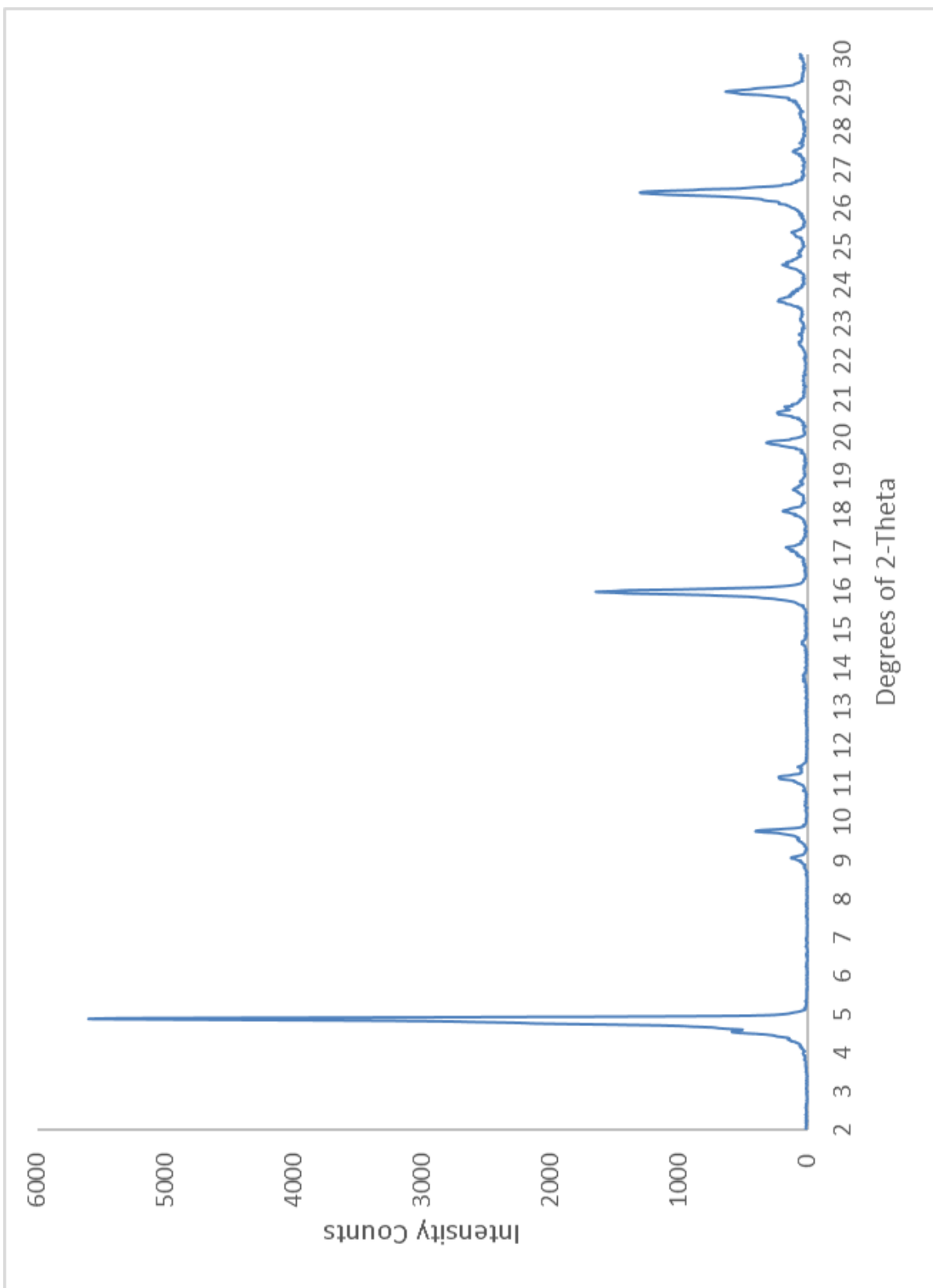


Figure I.11 – Powder XRD of **1•*p*-chlorotoluene**, empty framework

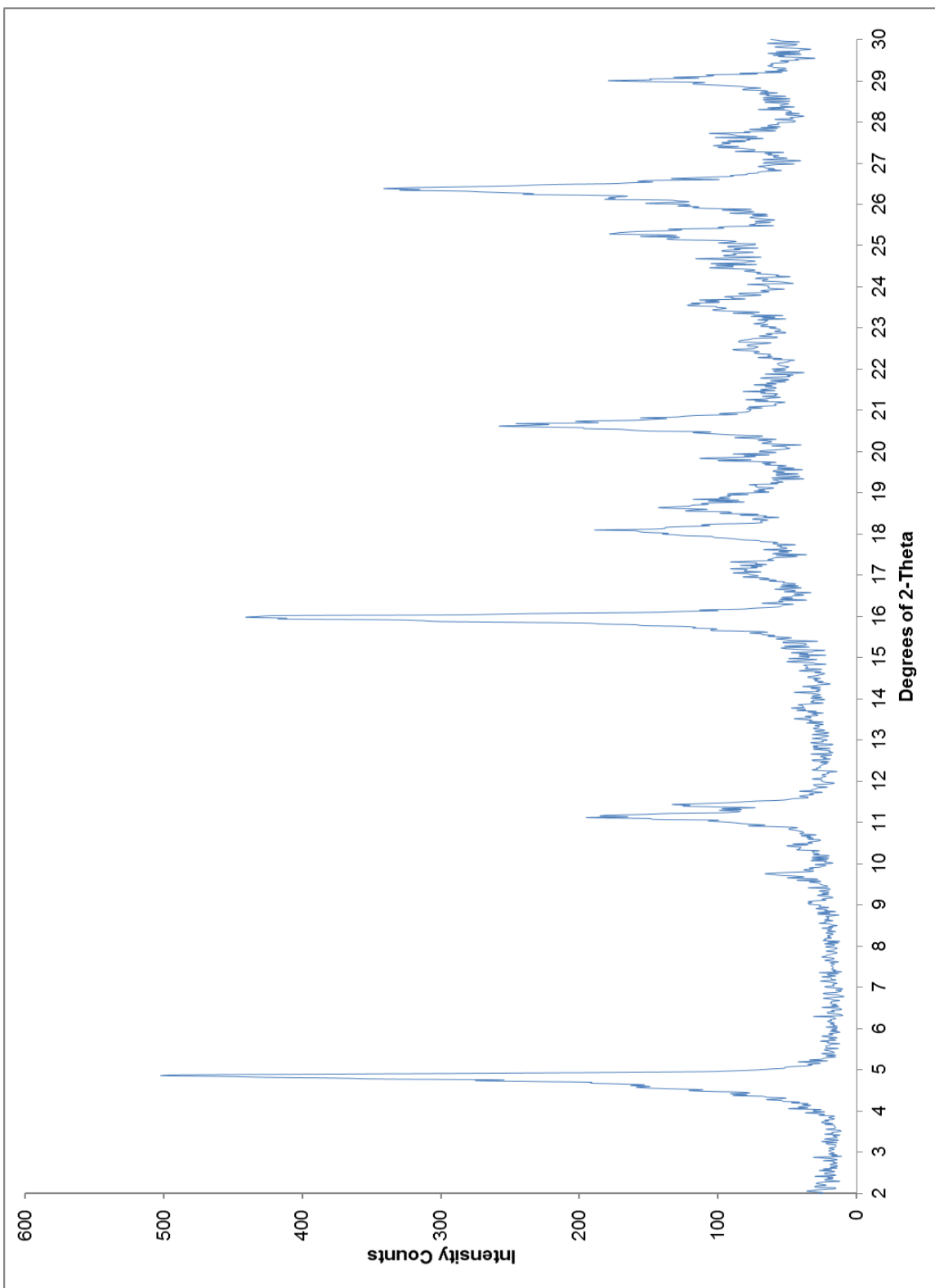


Figure I.12 – Powder XRD of **1•d**-dichlorobenzene, empty framework

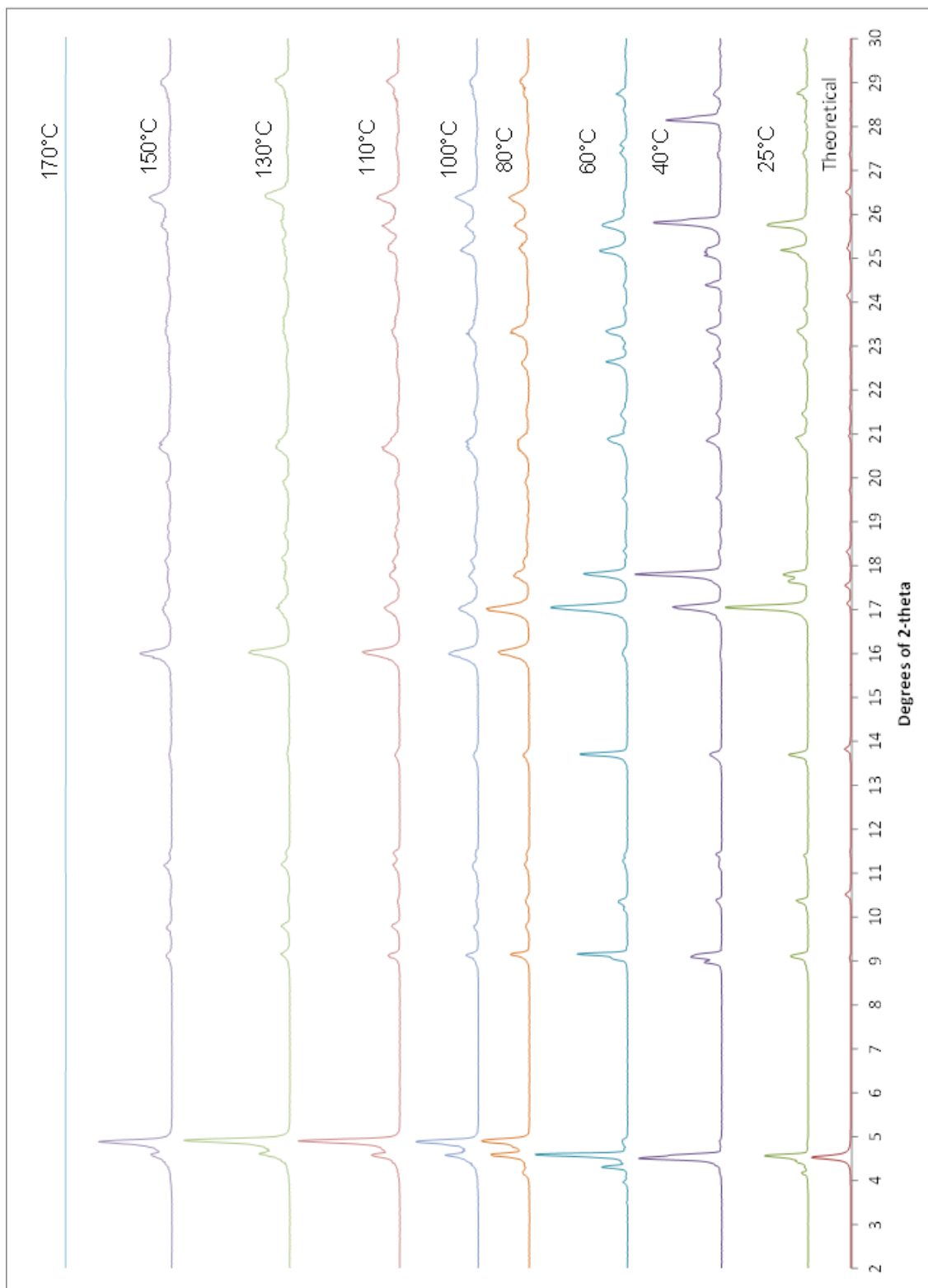


Figure I.13. Temperature dependent powder x-ray diffraction, the N,N-dimethylaniline guest molecules appear to be evolving at 80°C, initiating the emptying of 1.

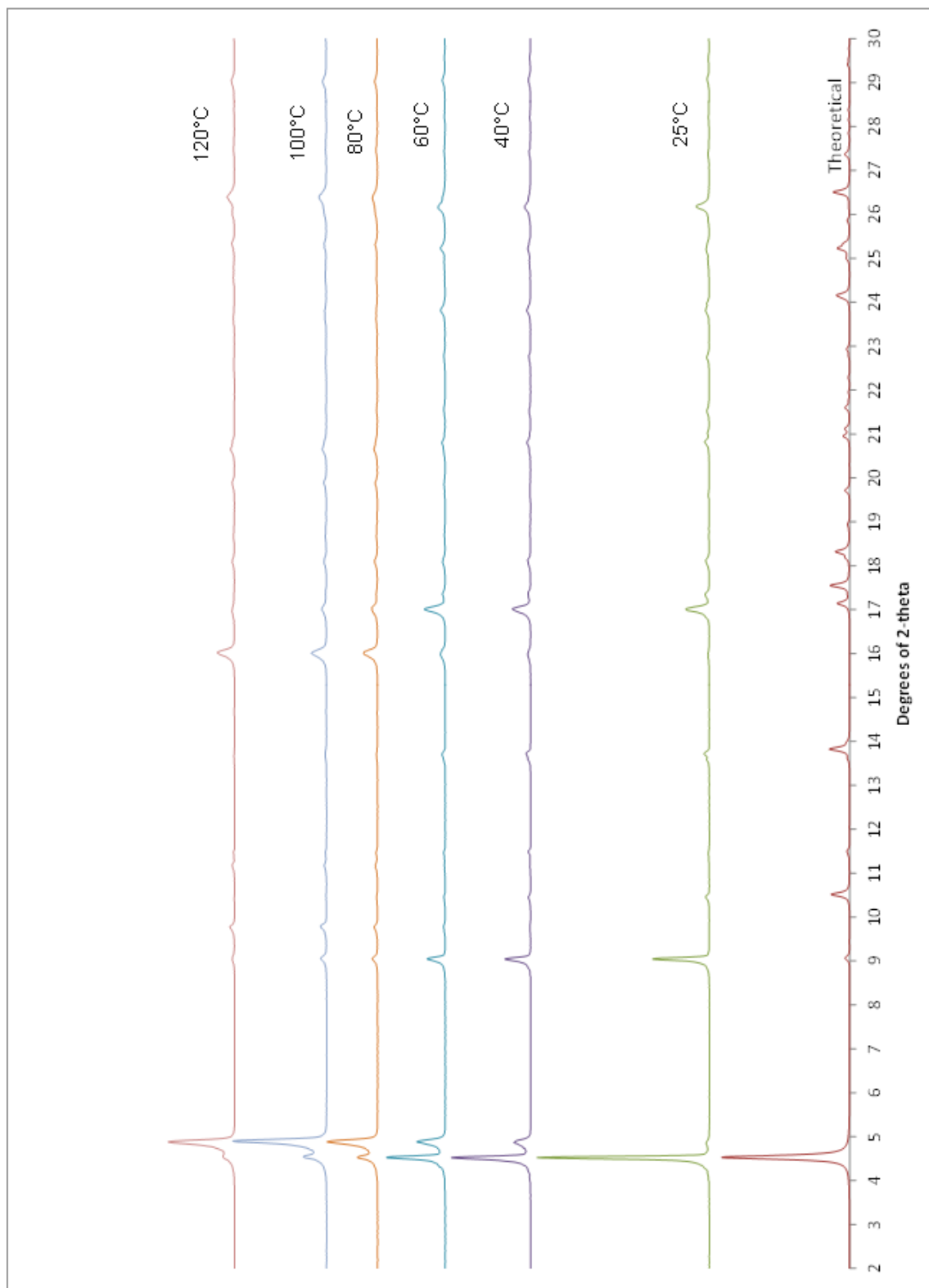


Figure I.14 Temperature dependent powder x-ray diffraction, the toluene guest molecules appear to be evolving at 40°C, initiating the emptying of 1.

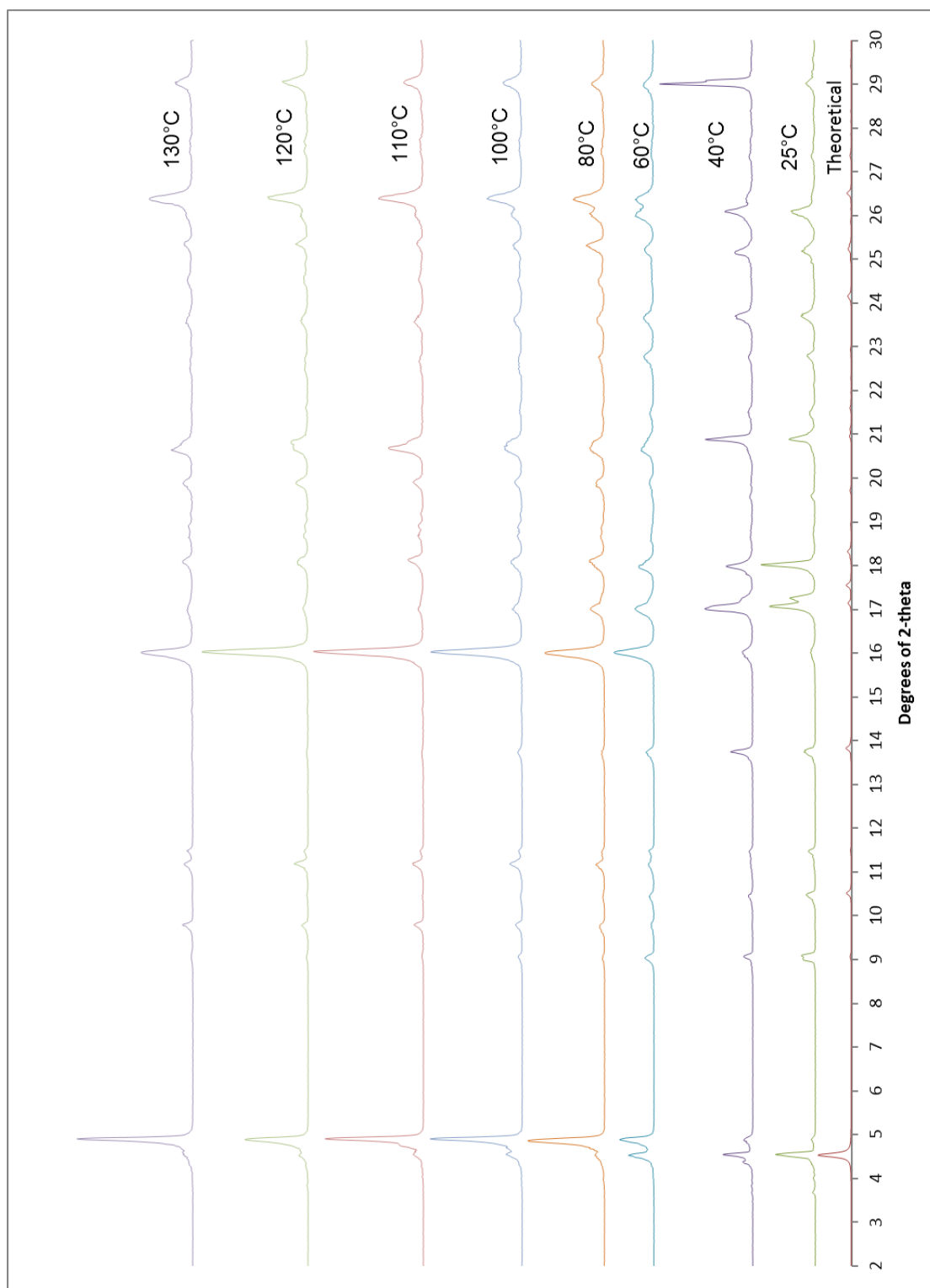


Figure I.15 Temperature dependent powder x-ray diffraction, the ethylbenzene guest molecules appear to be evolving at 40°C, initiating the emptying of 1

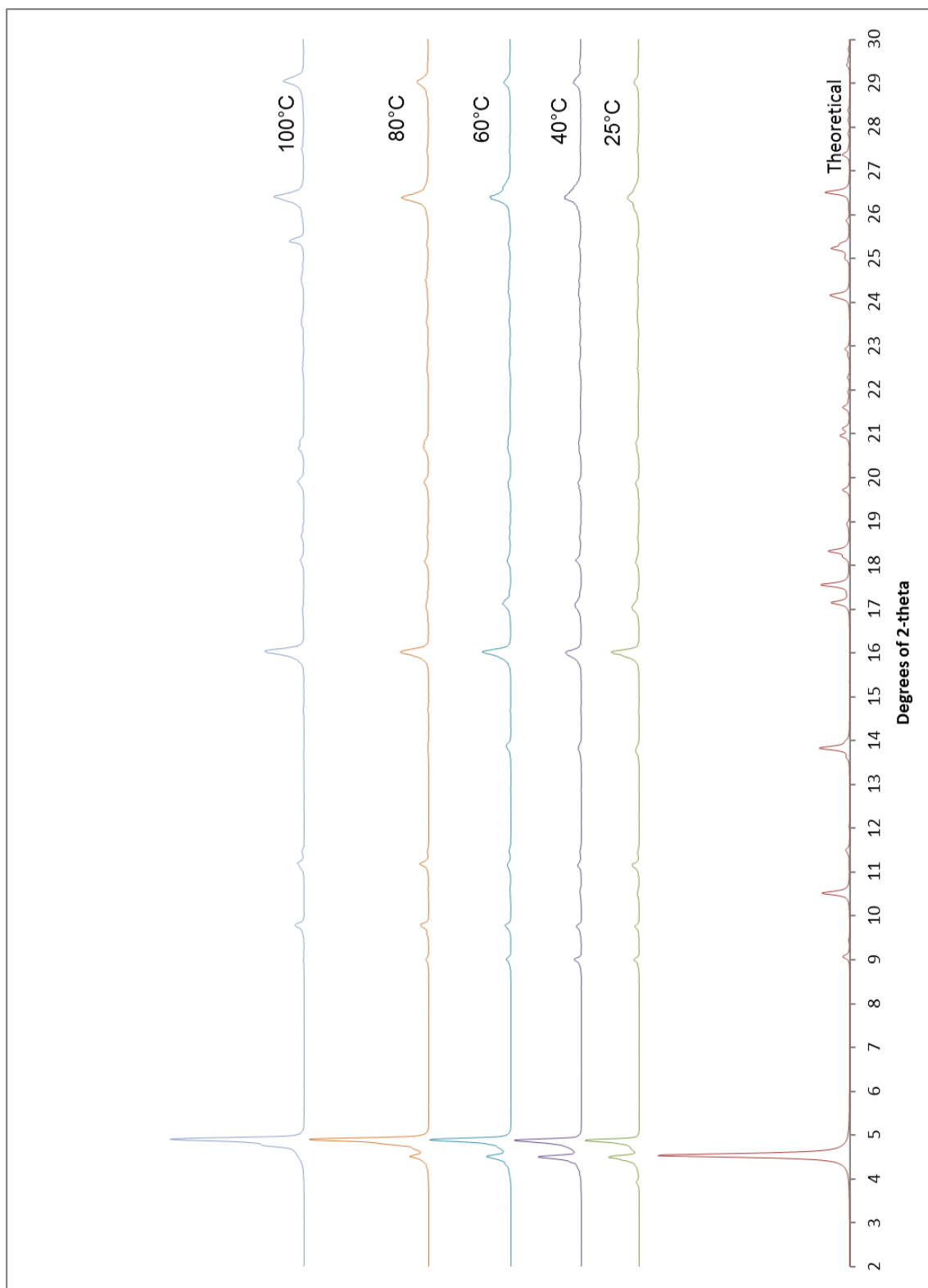


Figure I.16 Temperature dependent powder x-ray diffraction, the benzene guest molecules appear to be evolving at 25°C, initiating the emptying of 1.

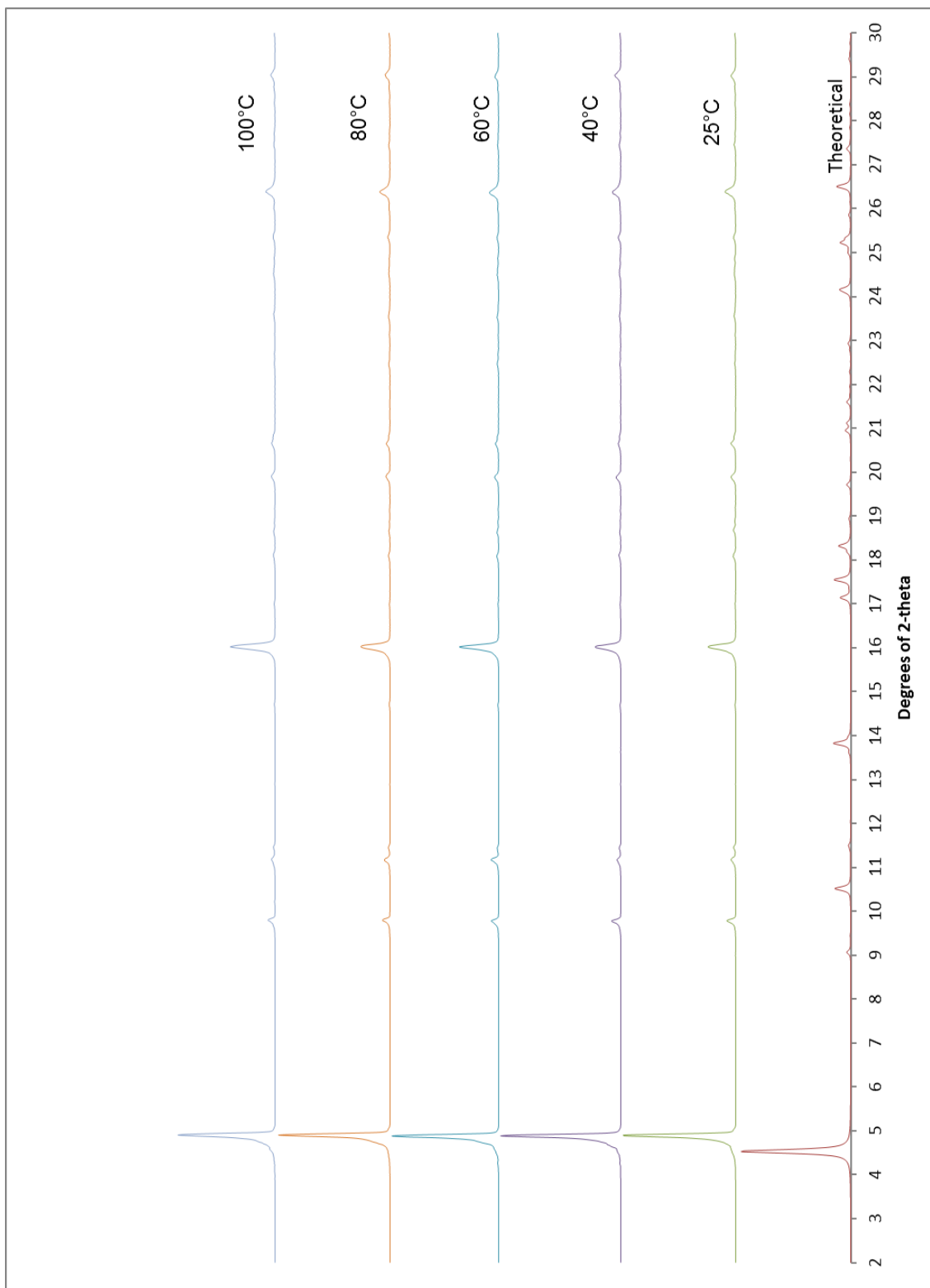


Figure I.19. Temperature dependent powder x-ray diffraction, the fluorobenzene guest molecules appear to be absent at 25°C, giving an empty 1.

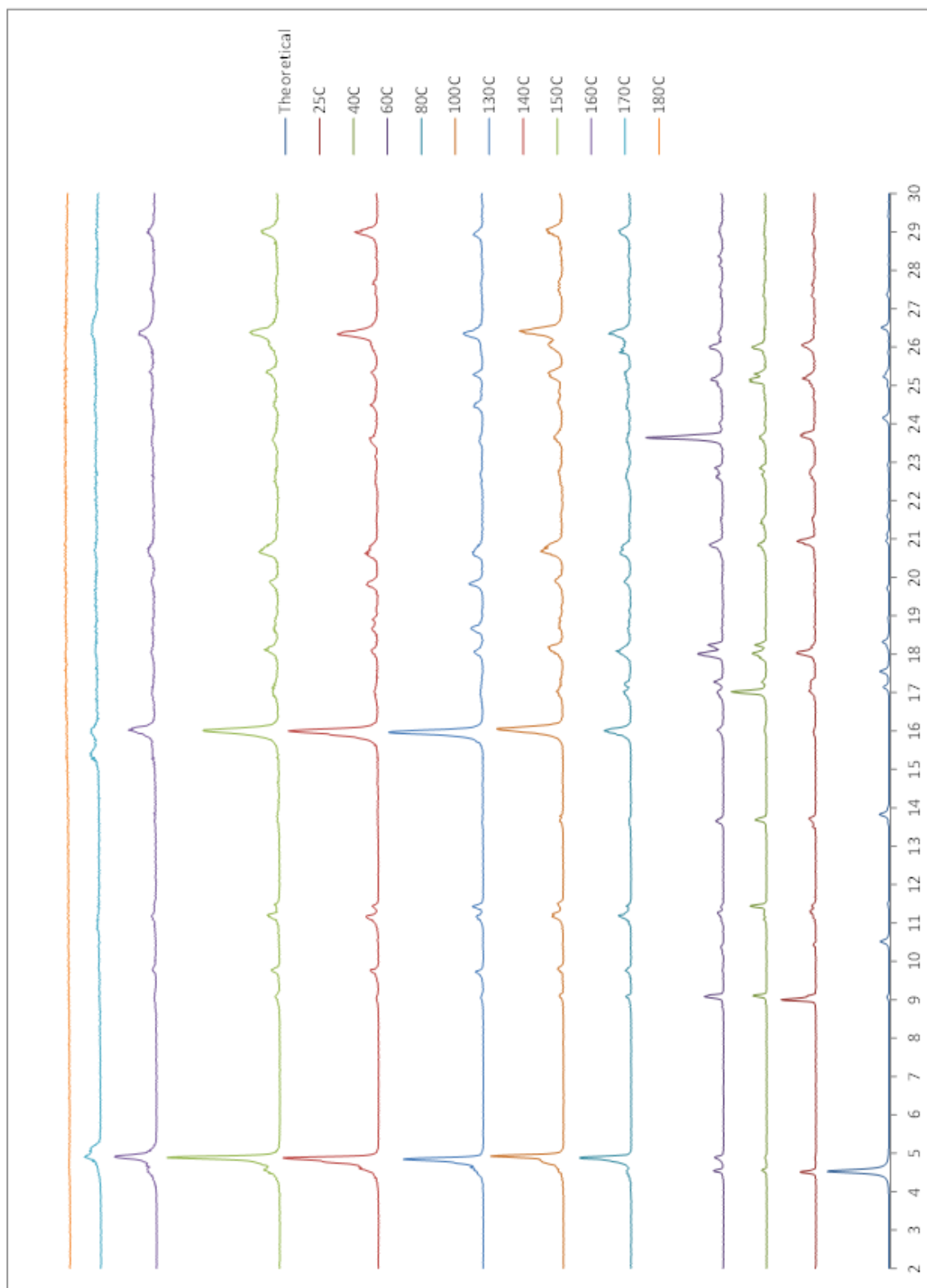


Figure 1.20 Temperature dependent powder x-ray diffraction, the iodobenzene guest molecules appear to be evolving at 40°C, initiating the emptying of 1.

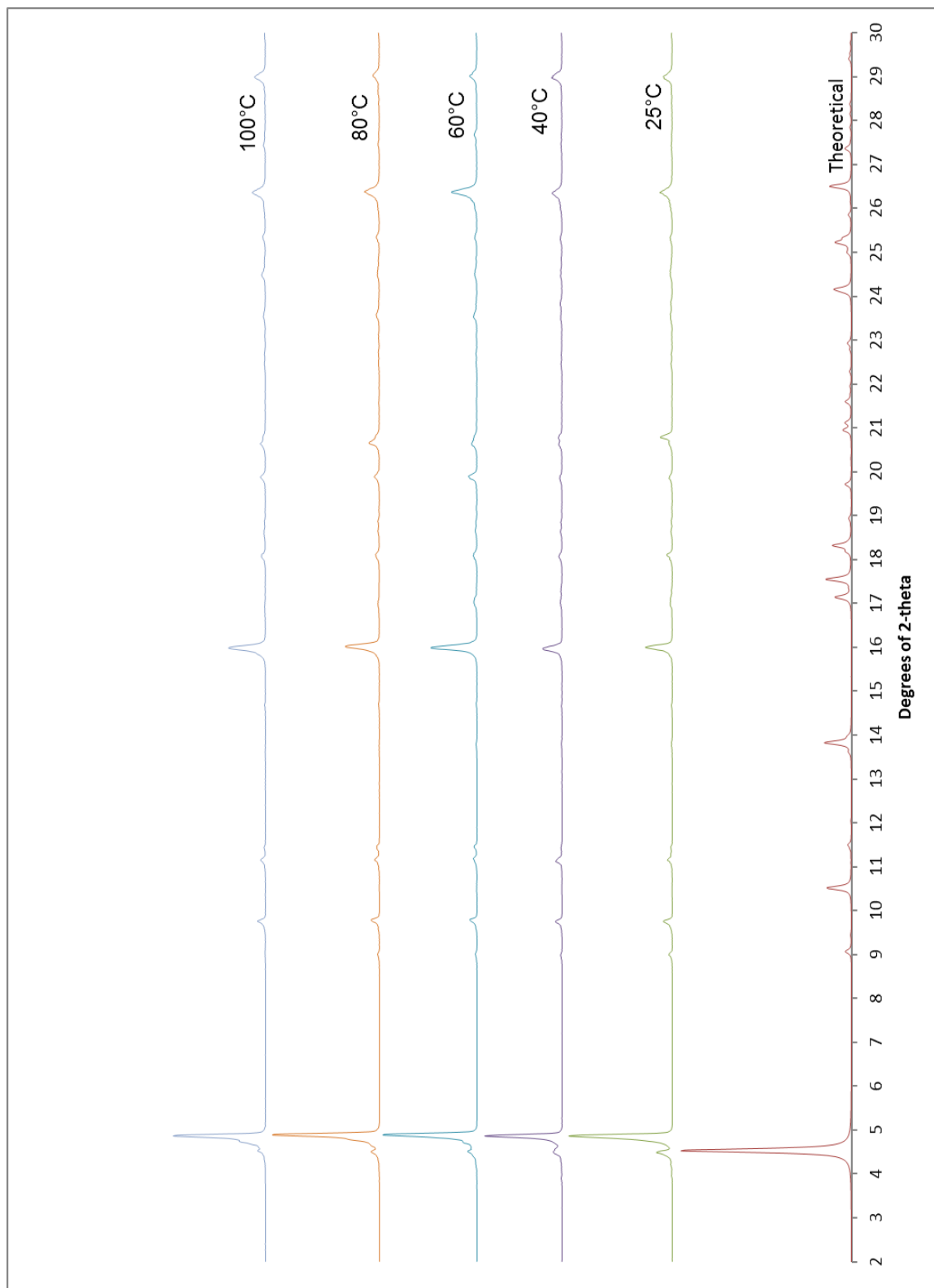


Figure I.21. Temperature dependent powder x-ray diffraction, the chlorobenzene guest molecules appear to be evolving at 25°C, initiating the emptying of 1.

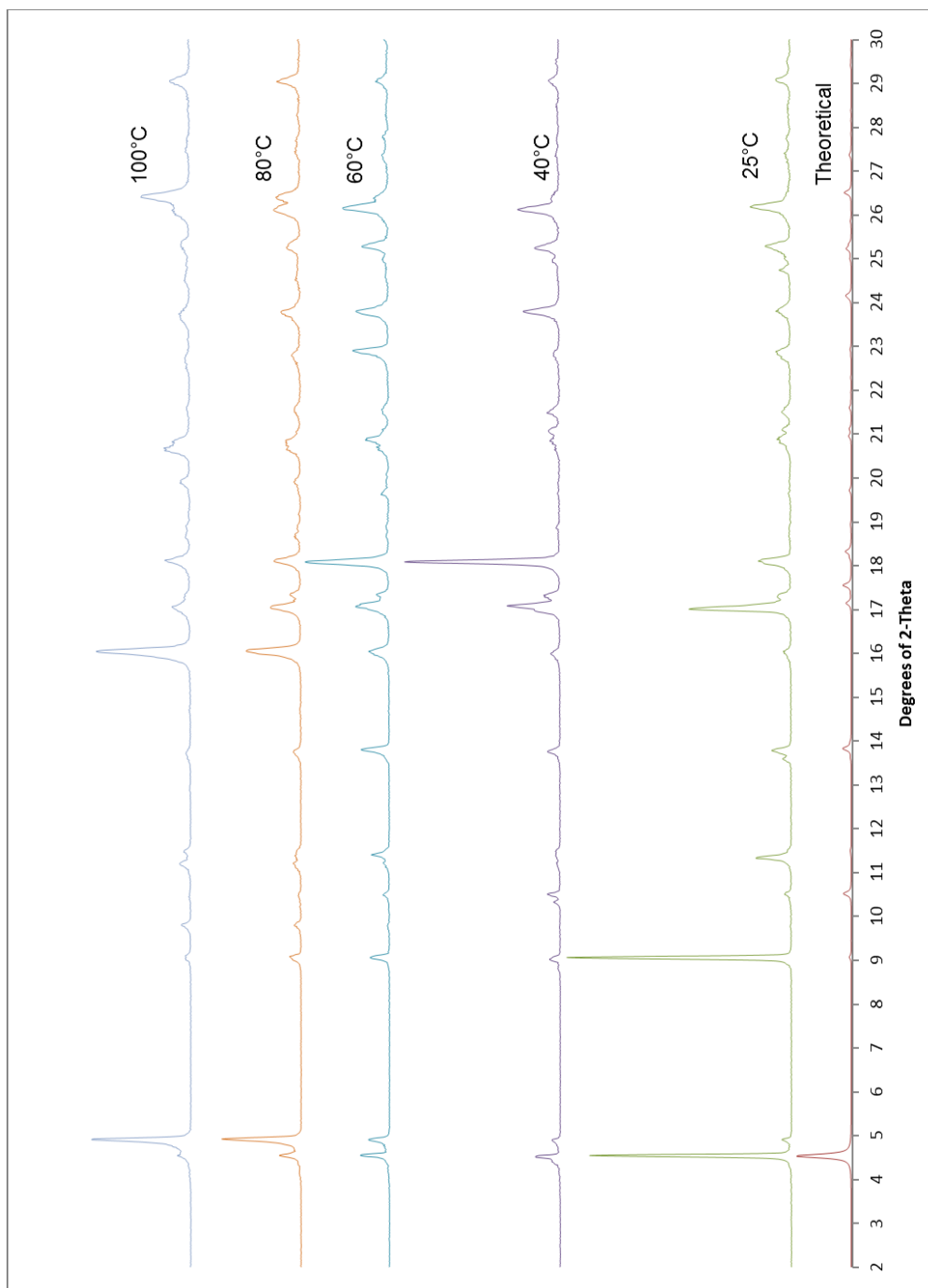


Figure I.22 Temperature dependent powder x-ray diffraction, the bromobenzene guest molecules appear to be evolving at 25°C, initiating the emptying of 1.

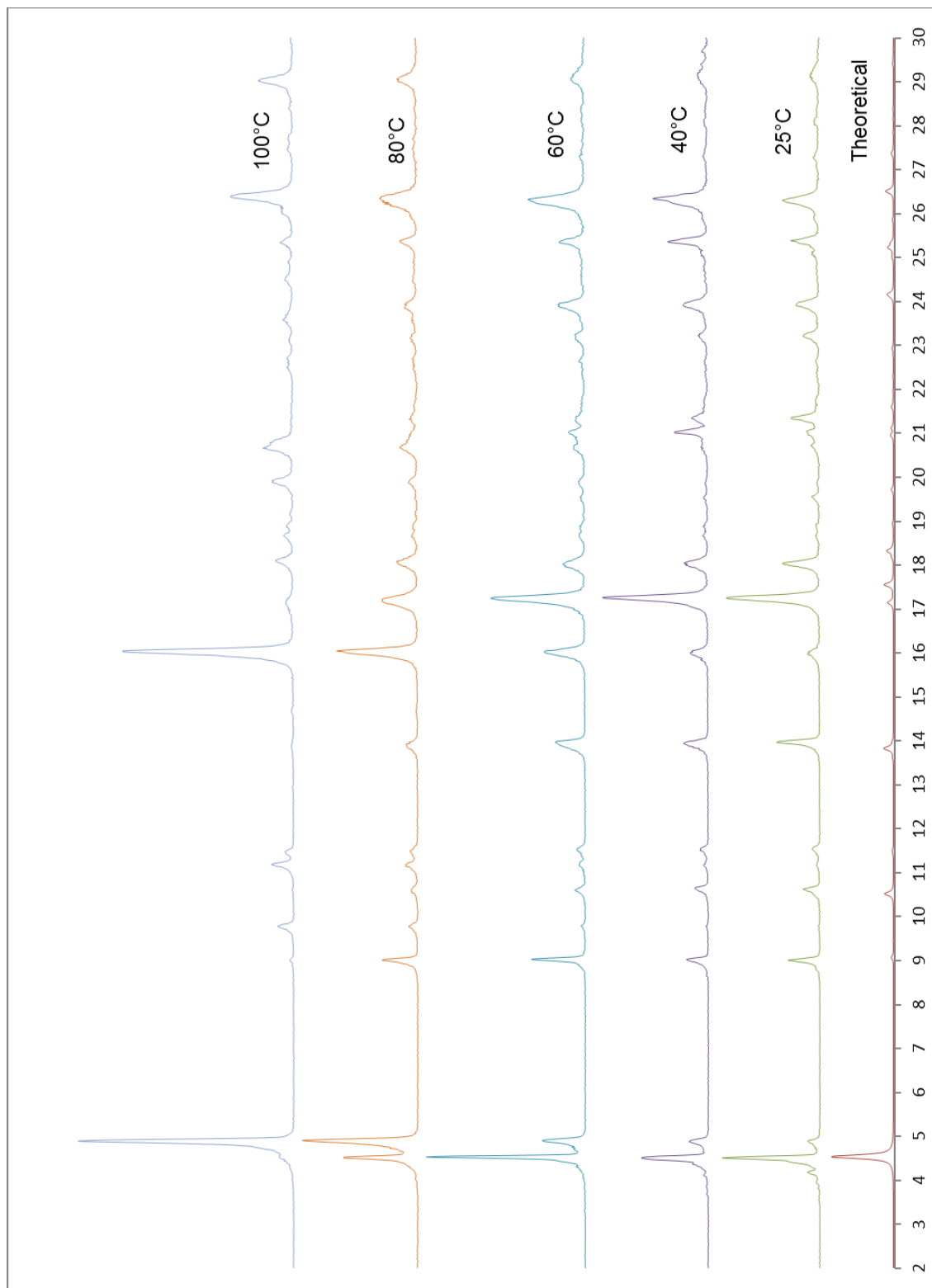


Figure I.23 Temperature dependent powder x-ray diffraction, the nitrobenzene guest molecules appear to be evolving at 25°C, initiating the emptying of 1.

Appendix II – Thermogravimetric Analysis Data

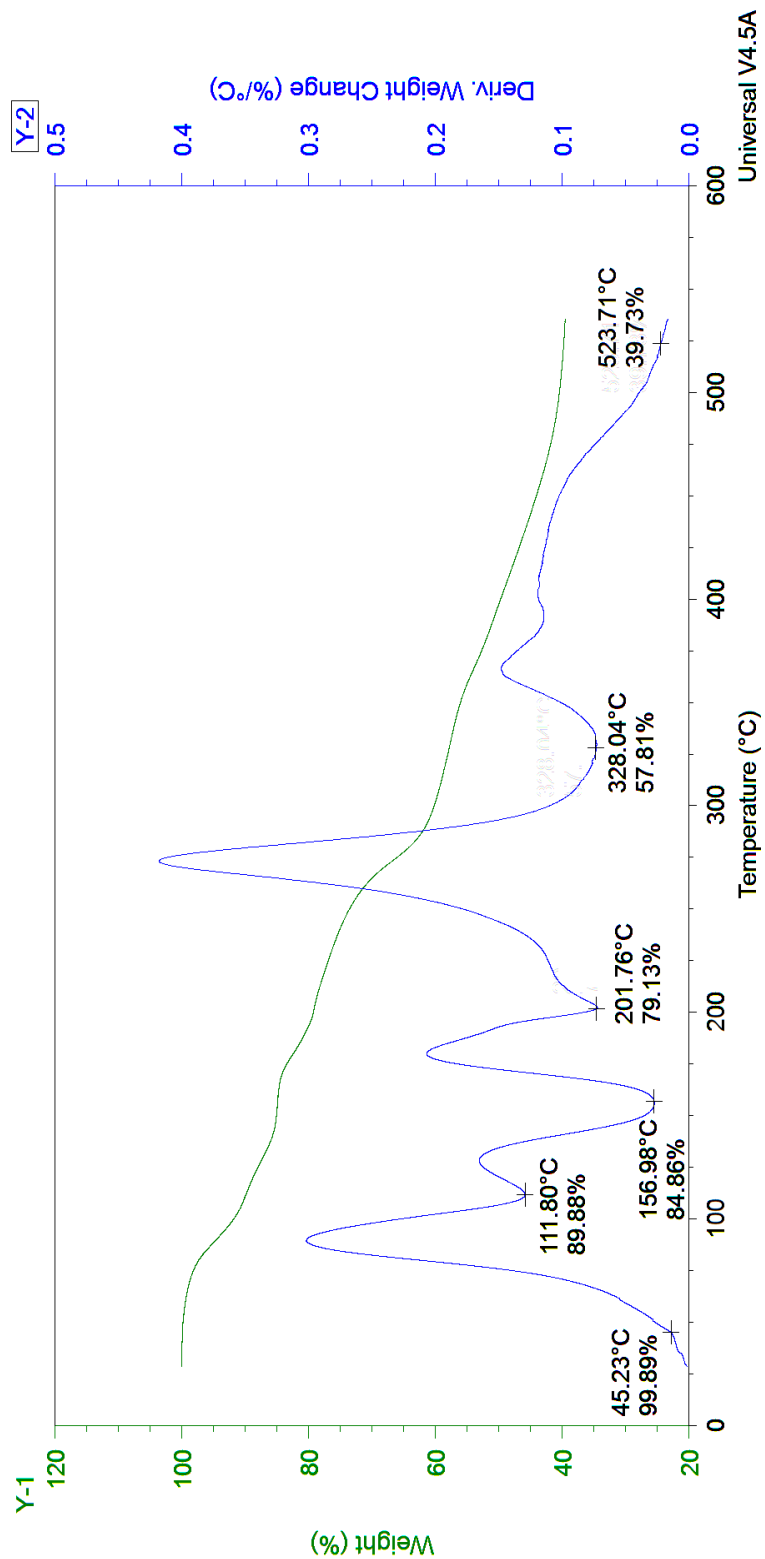


Figure II.1 Thermogravimetric analysis of N,N-methylaniline, heating rate of 2°C/min

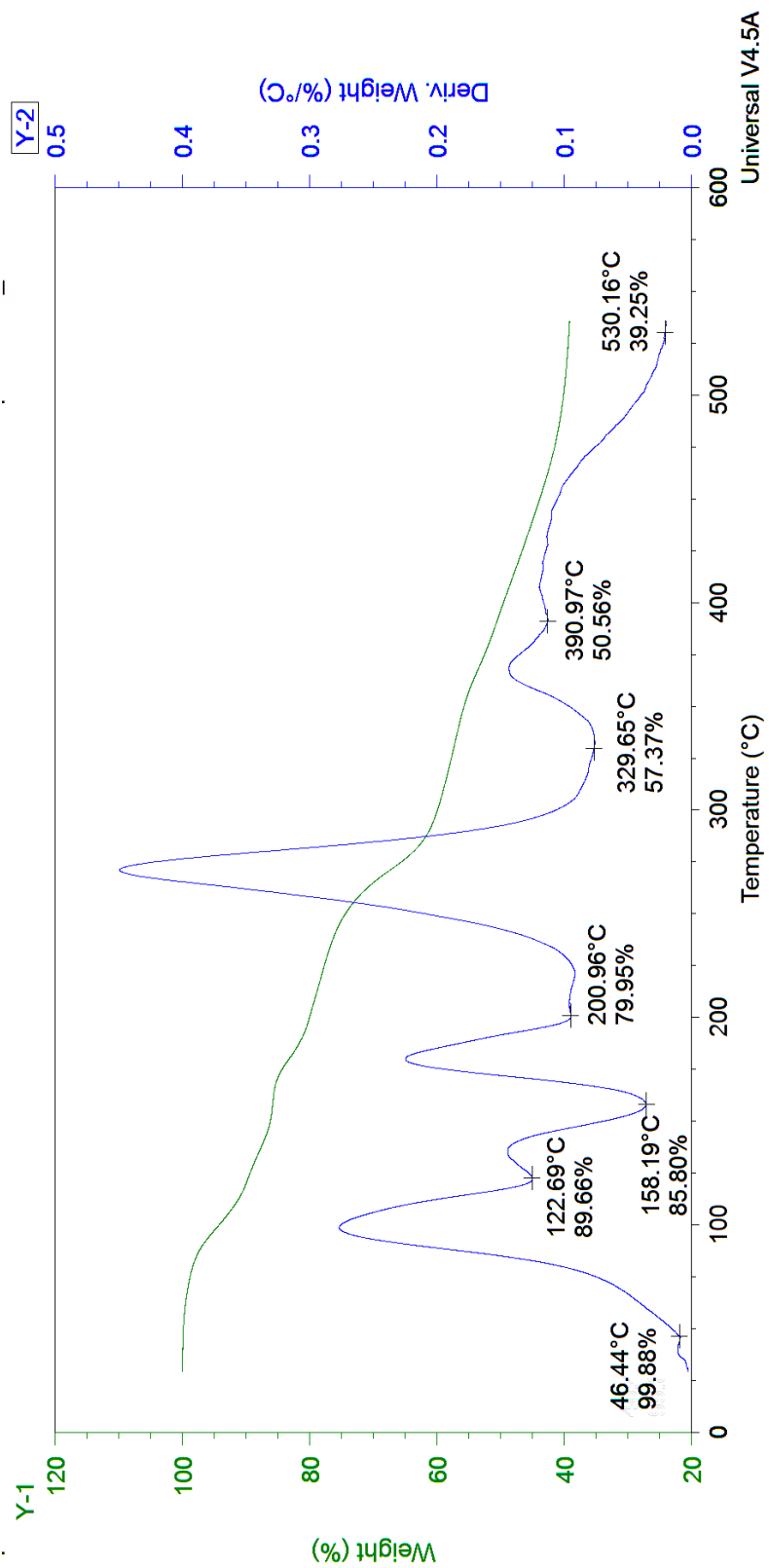


Figure II.2 Thermogravimetric analysis of N,N-methylaniline, heating rate of 4°C/min

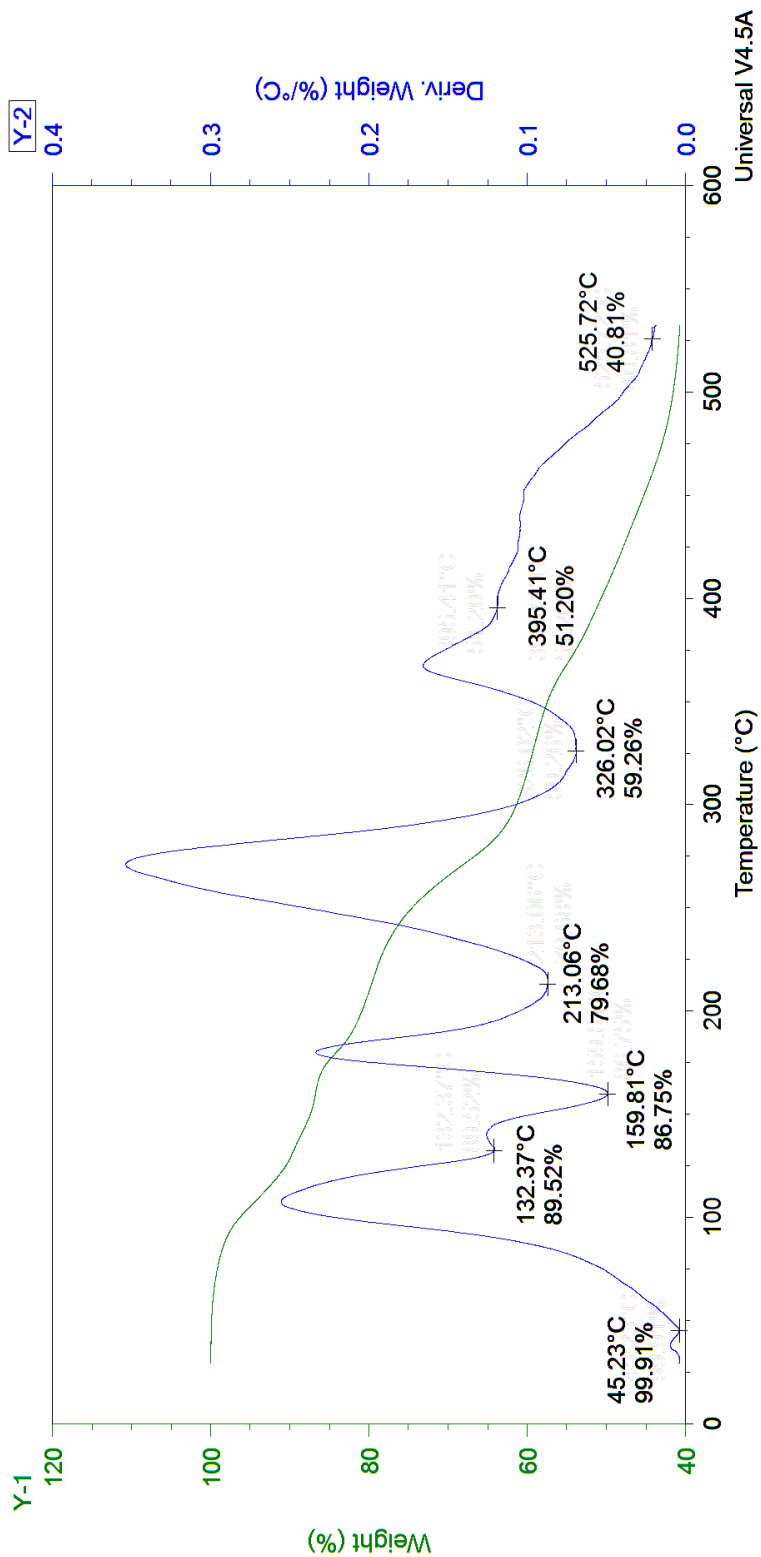


Figure II.3 Thermogravimetric analysis of N,N-methylaniline, heating rate of 8°C/min

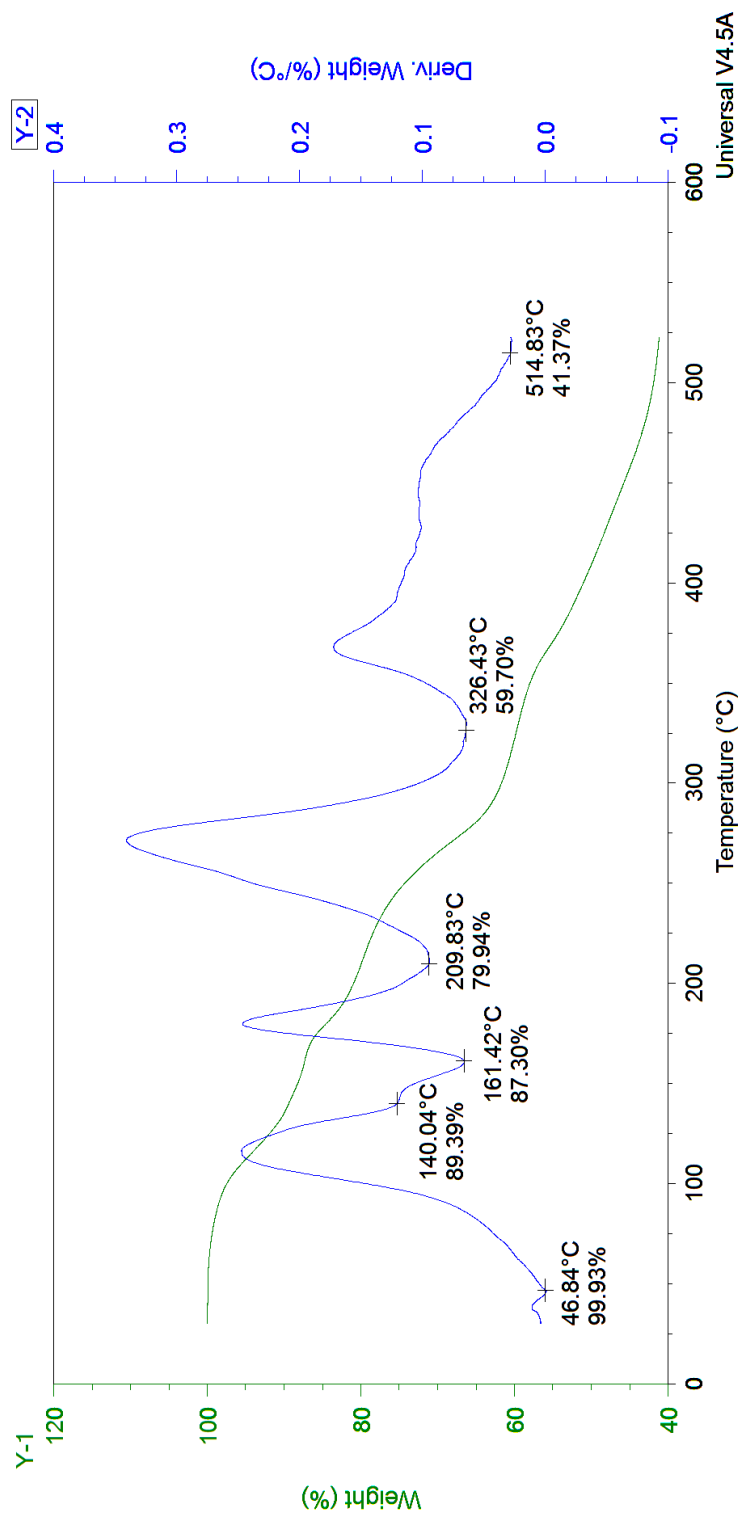


Figure II.4 Thermogravimetric analysis of N,N-methylaniline, heating rate of 16°C/min

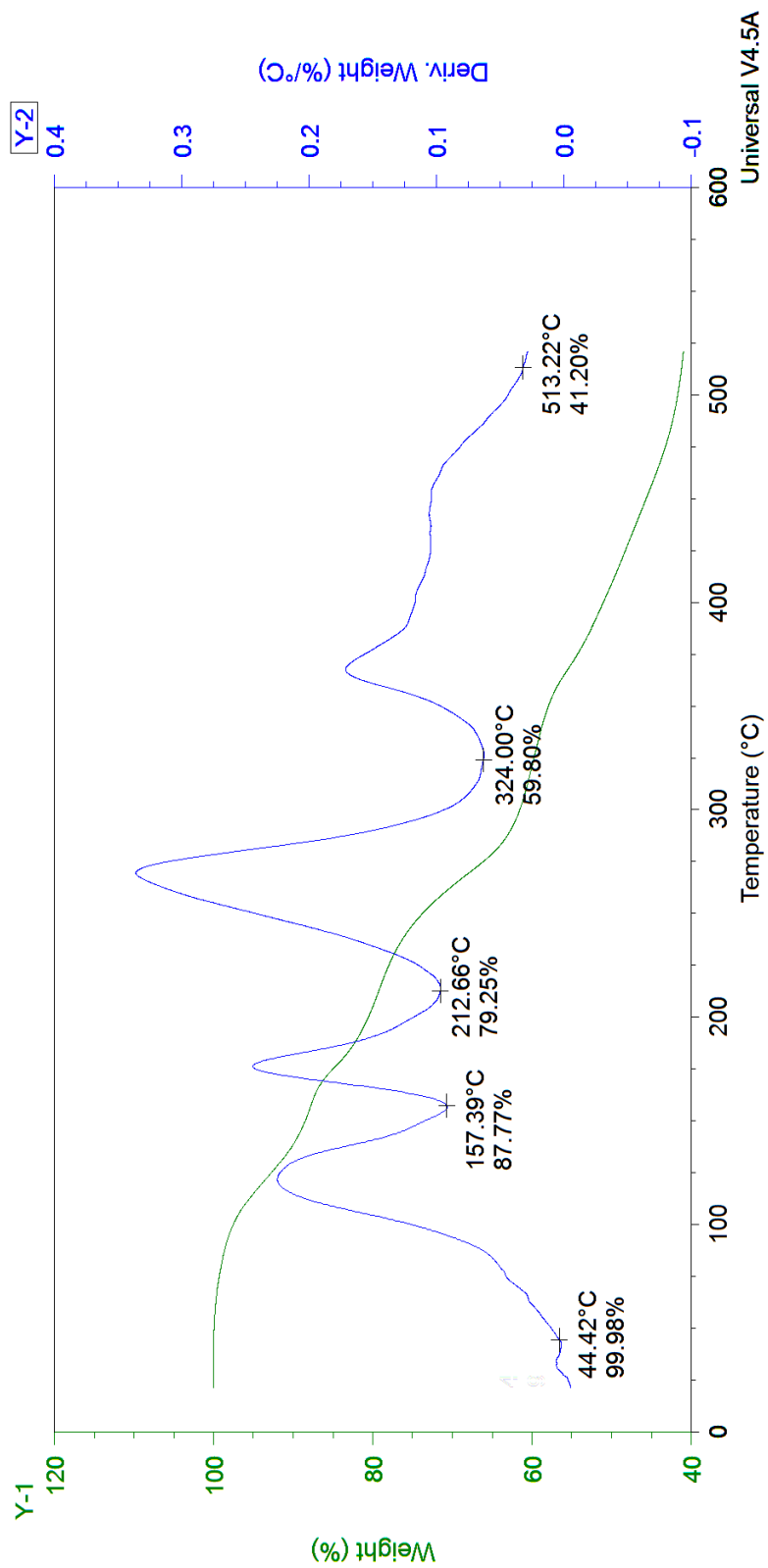


Figure II.5 Thermogravimetric analysis of N,N-methylaniline, heating rate of 32°C/min

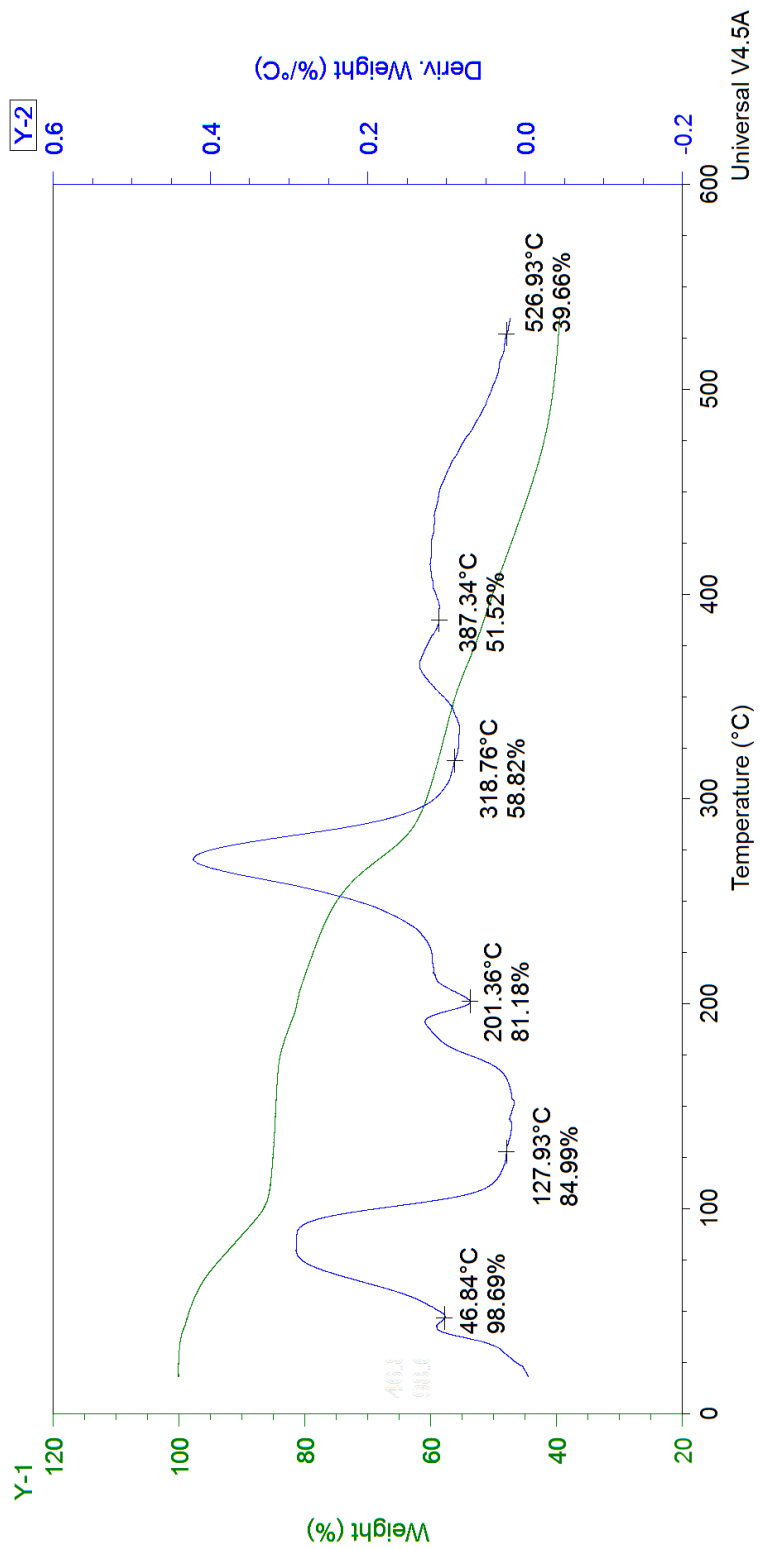


Figure II.6 Thermogravimetric analysis of ethylbenzene, heating rate of 2°C/min

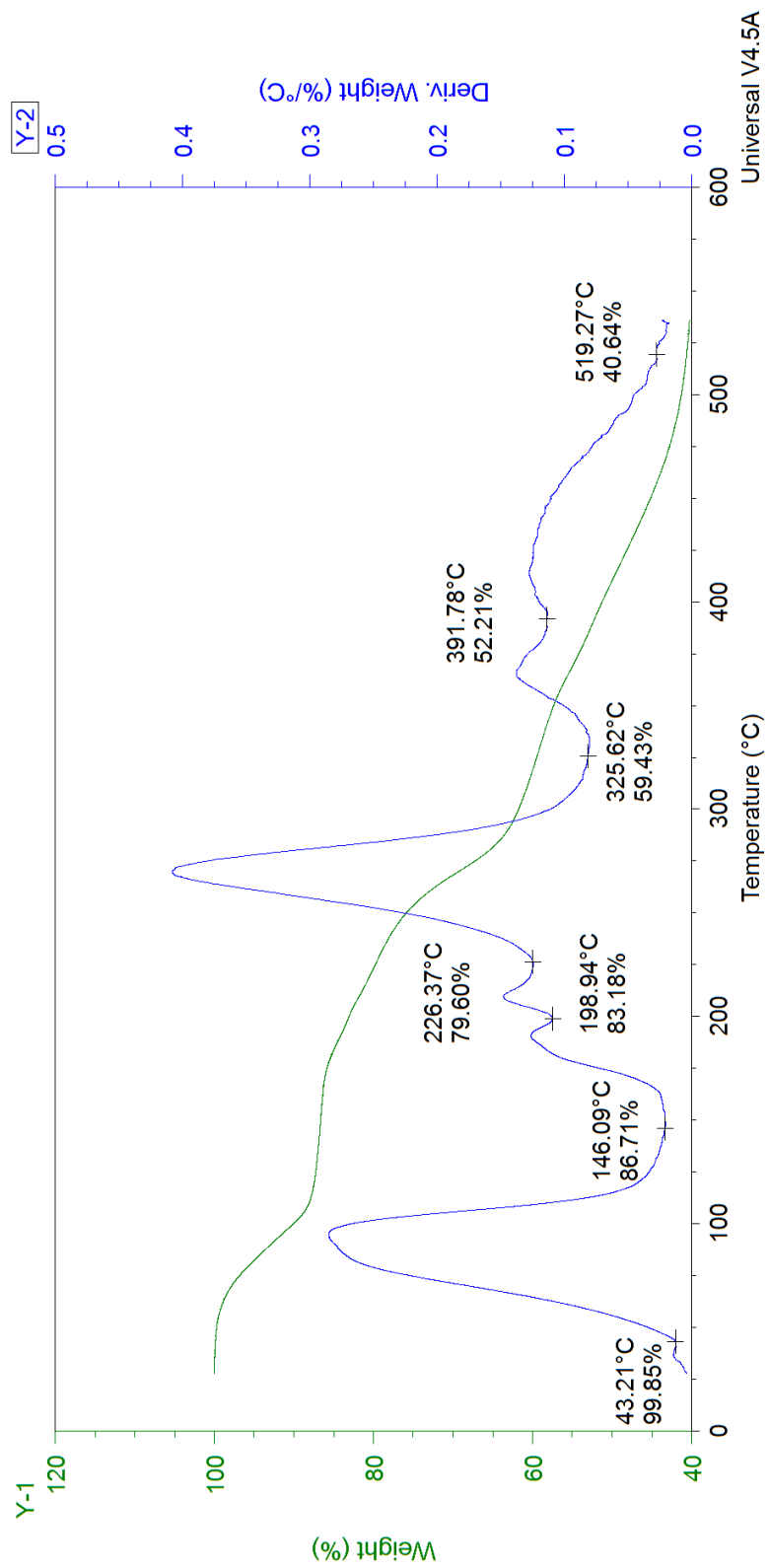


Figure II.7 Thermogravimetric analysis of ethylbenzene, heating rate of 4°C/min

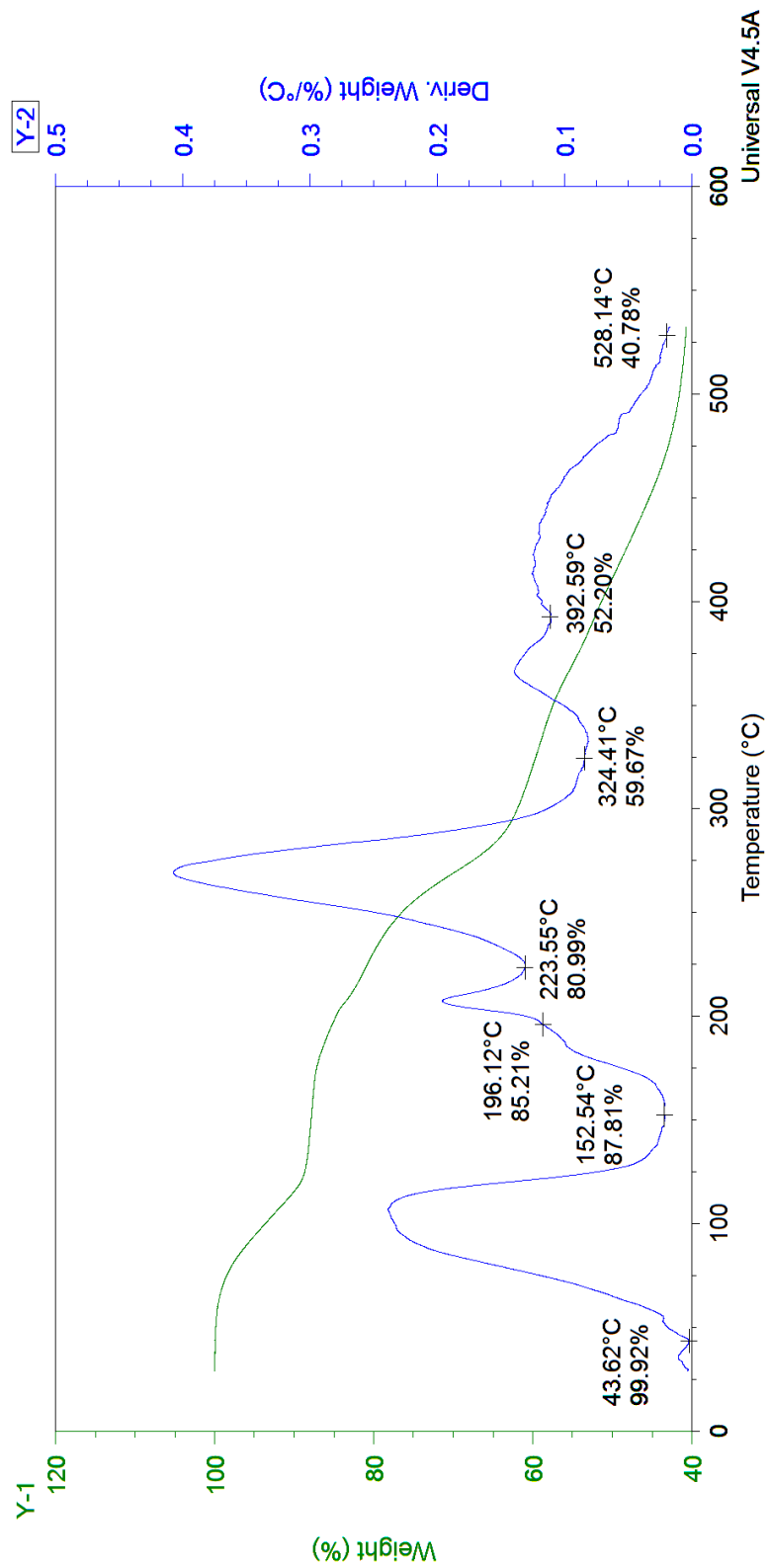


Figure II.8 Thermogravimetric analysis of ethylbenzene, heating rate of 8°C/min

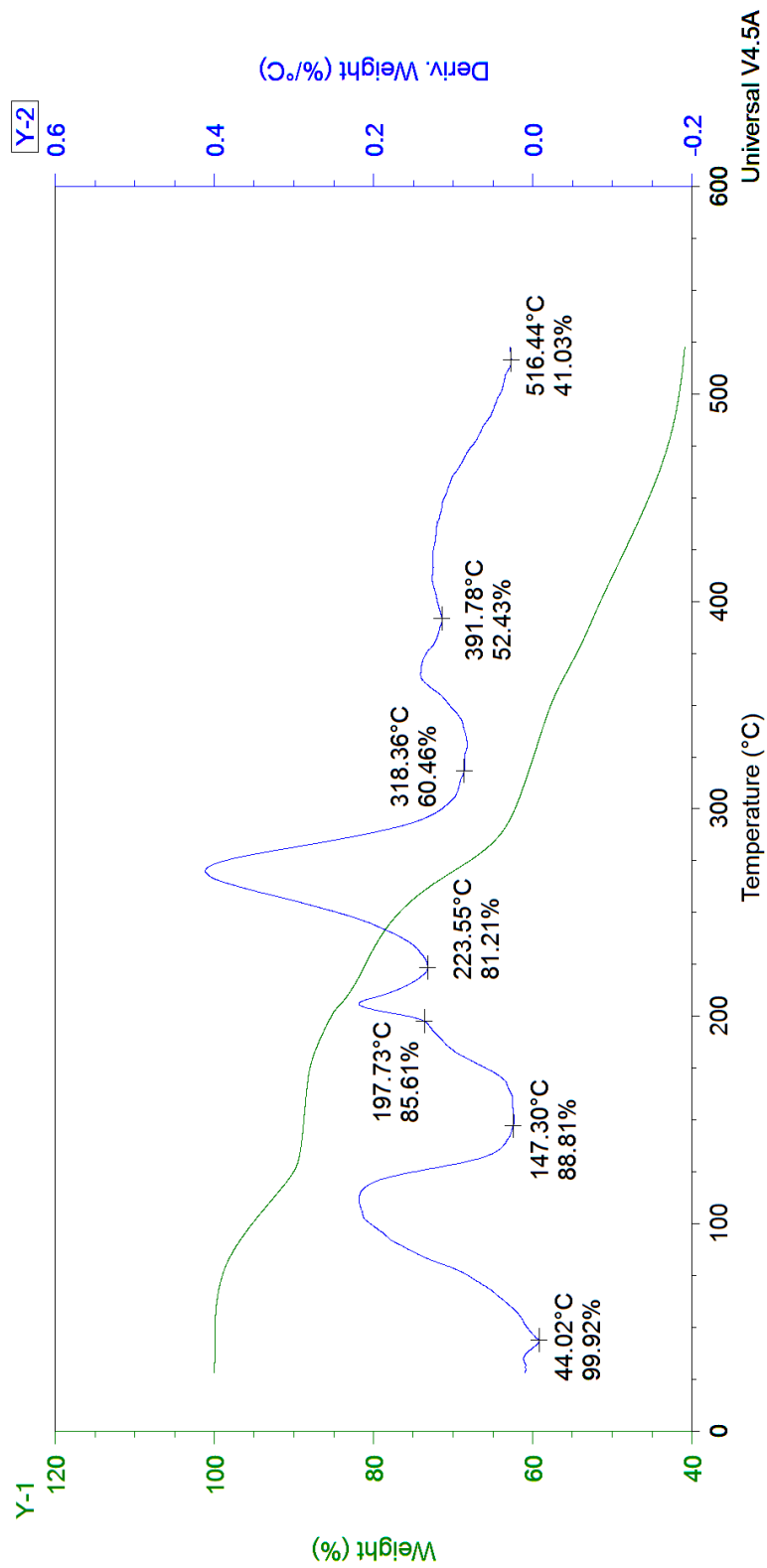


Figure II.9 Thermogravimetric analysis of ethylbenzene, heating rate of 16°C/min

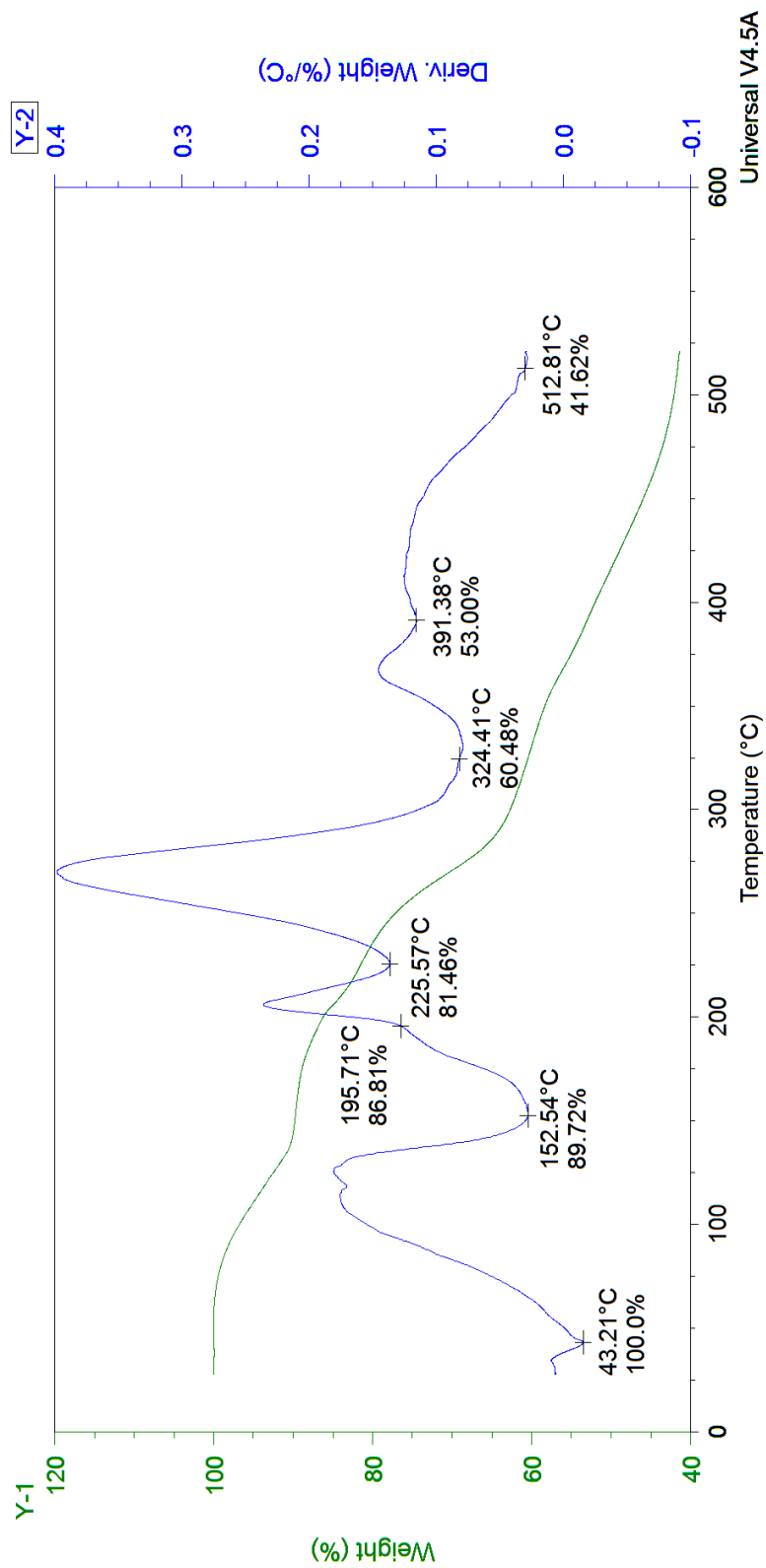


Figure II.10 Thermogravimetric analysis of ethylbenzene, heating rate of 32°C/min

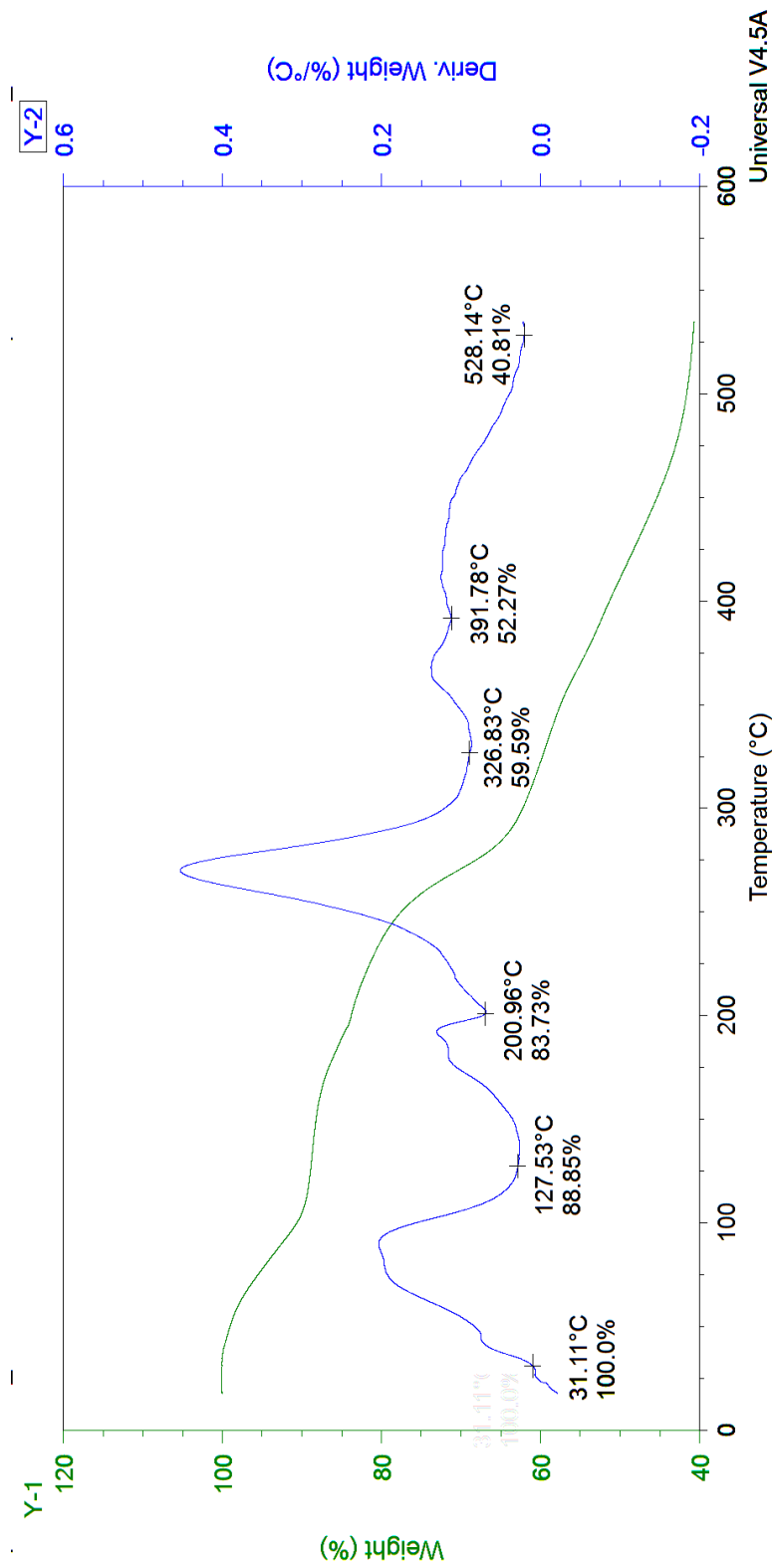


Figure II.11 Thermogravimetric analysis of toluene, heating rate of 2°C/min

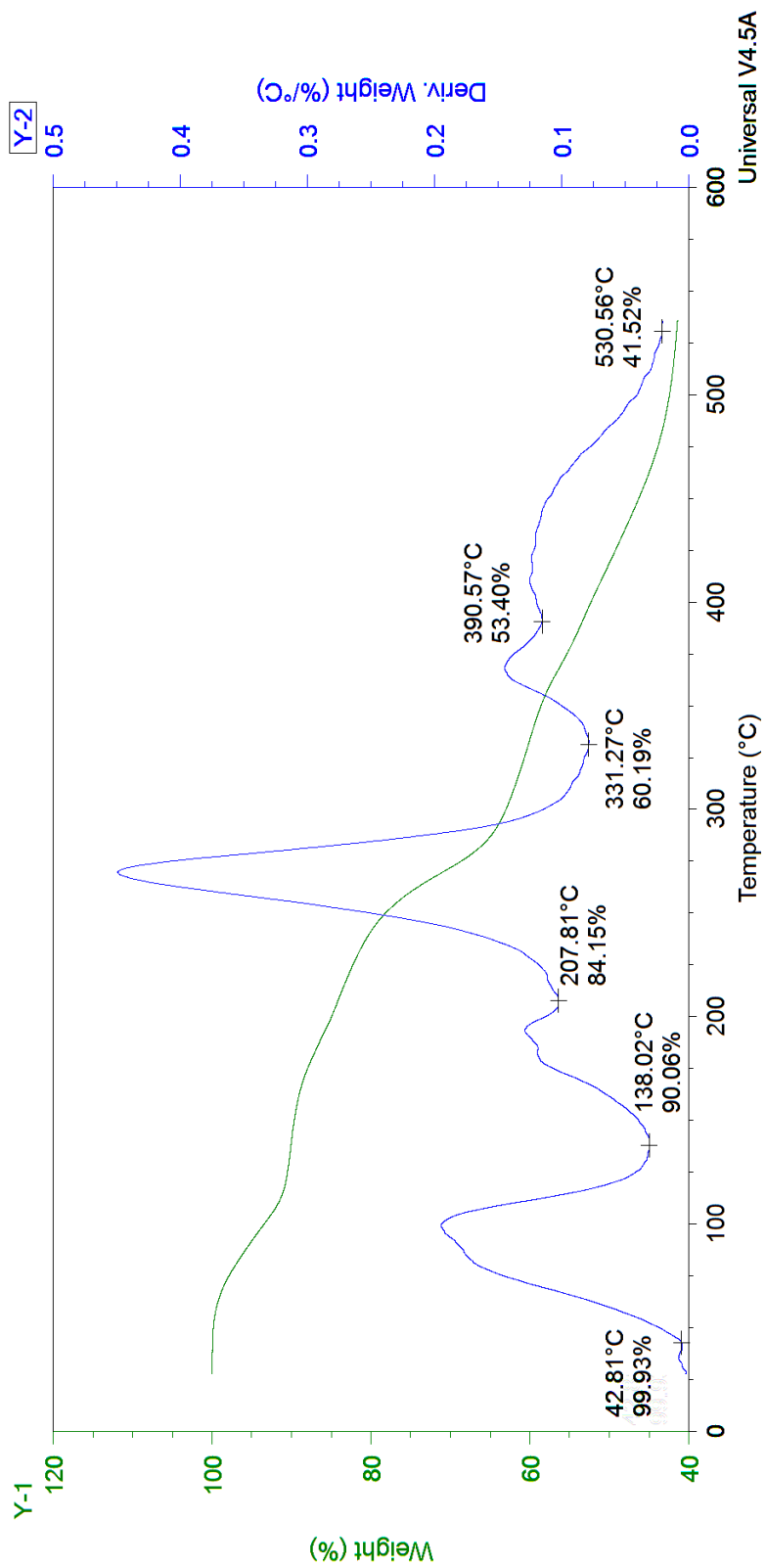


Figure II.12 Thermogravimetric analysis of toluene, heating rate of 4°C/min

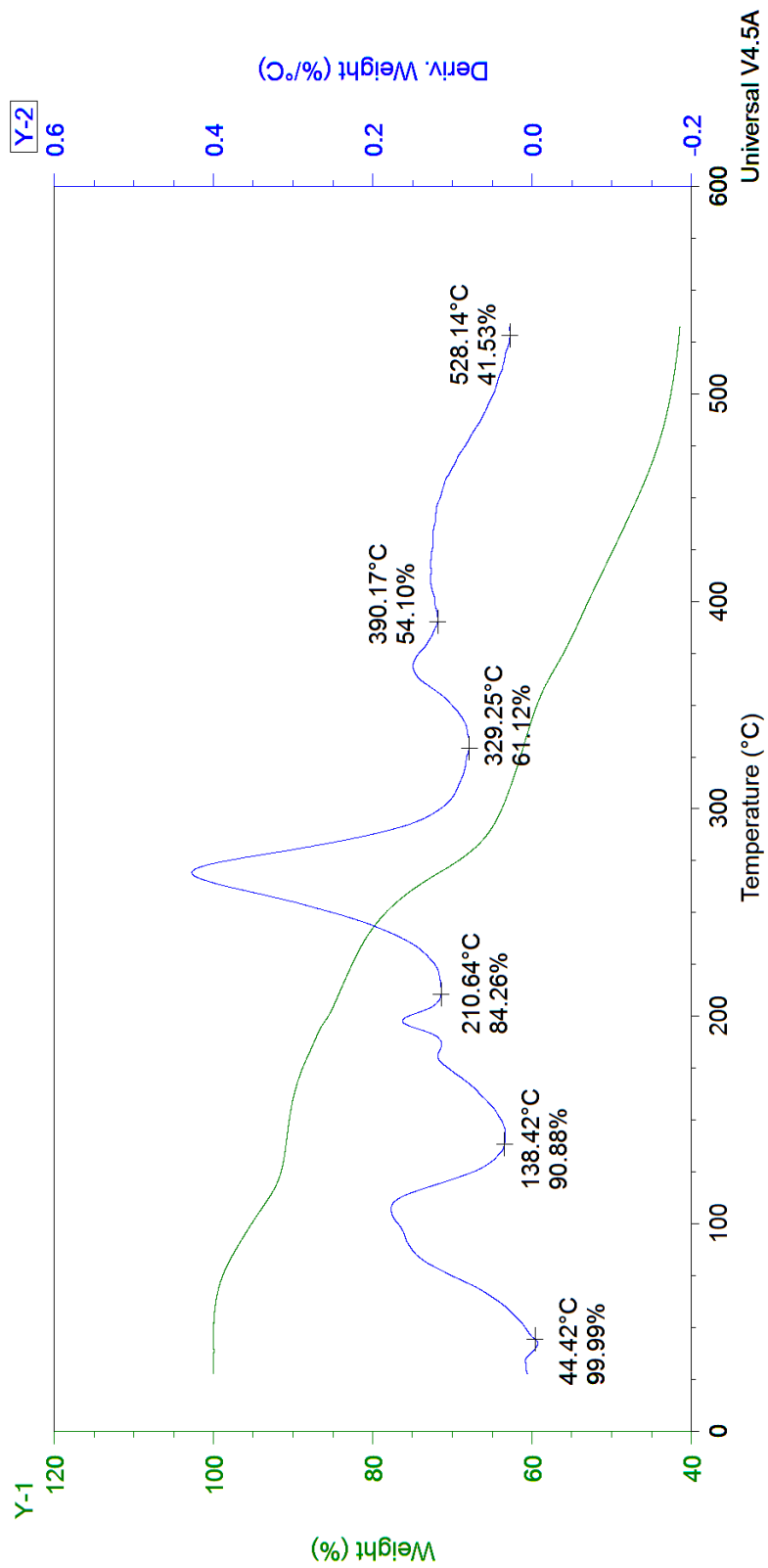


Figure II.13 Thermogravimetric analysis of toluene, heating rate of 8°C/min

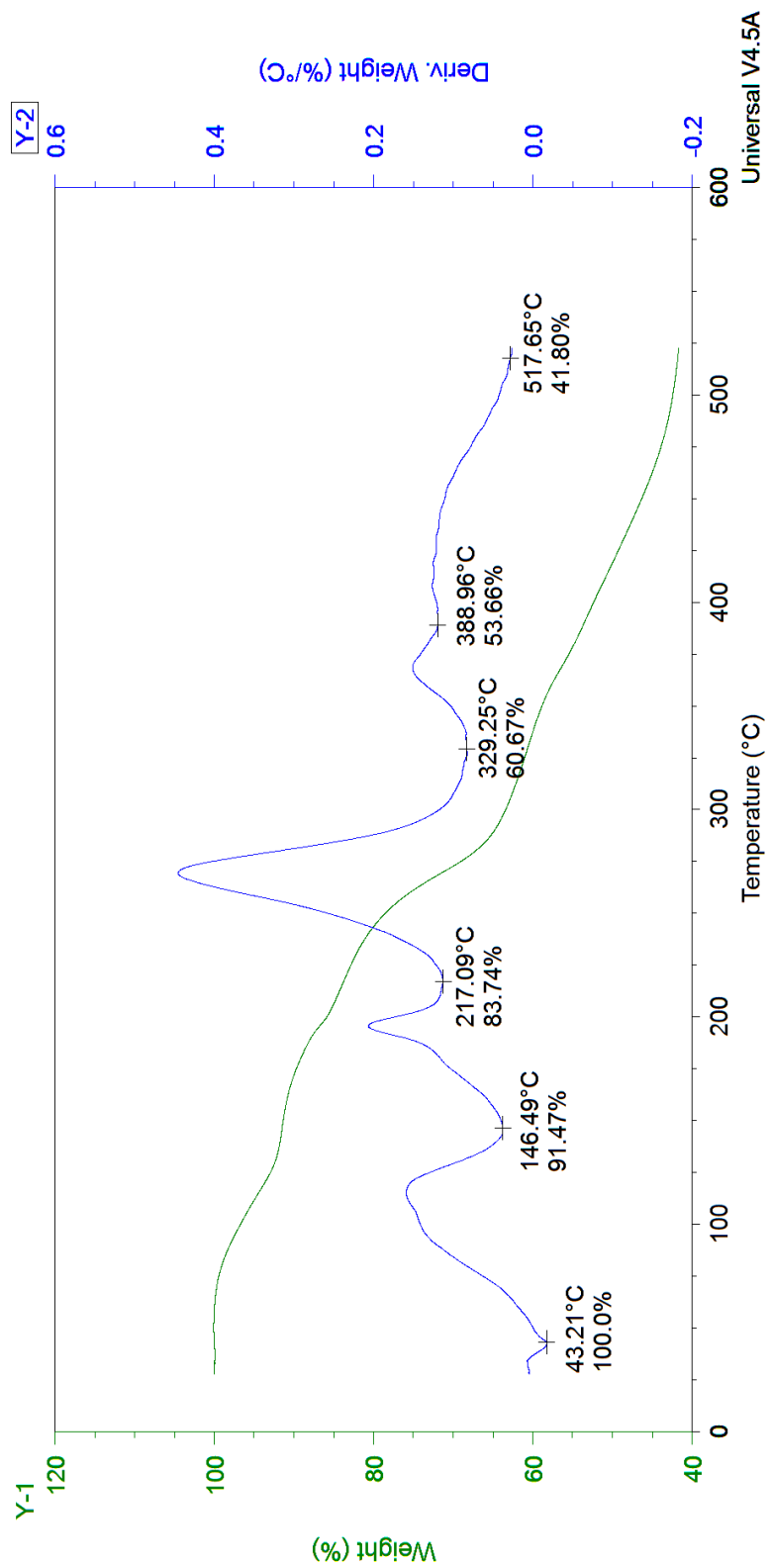


Figure II.14 Thermogravimetric analysis of toluene, heating rate of 16°C/min

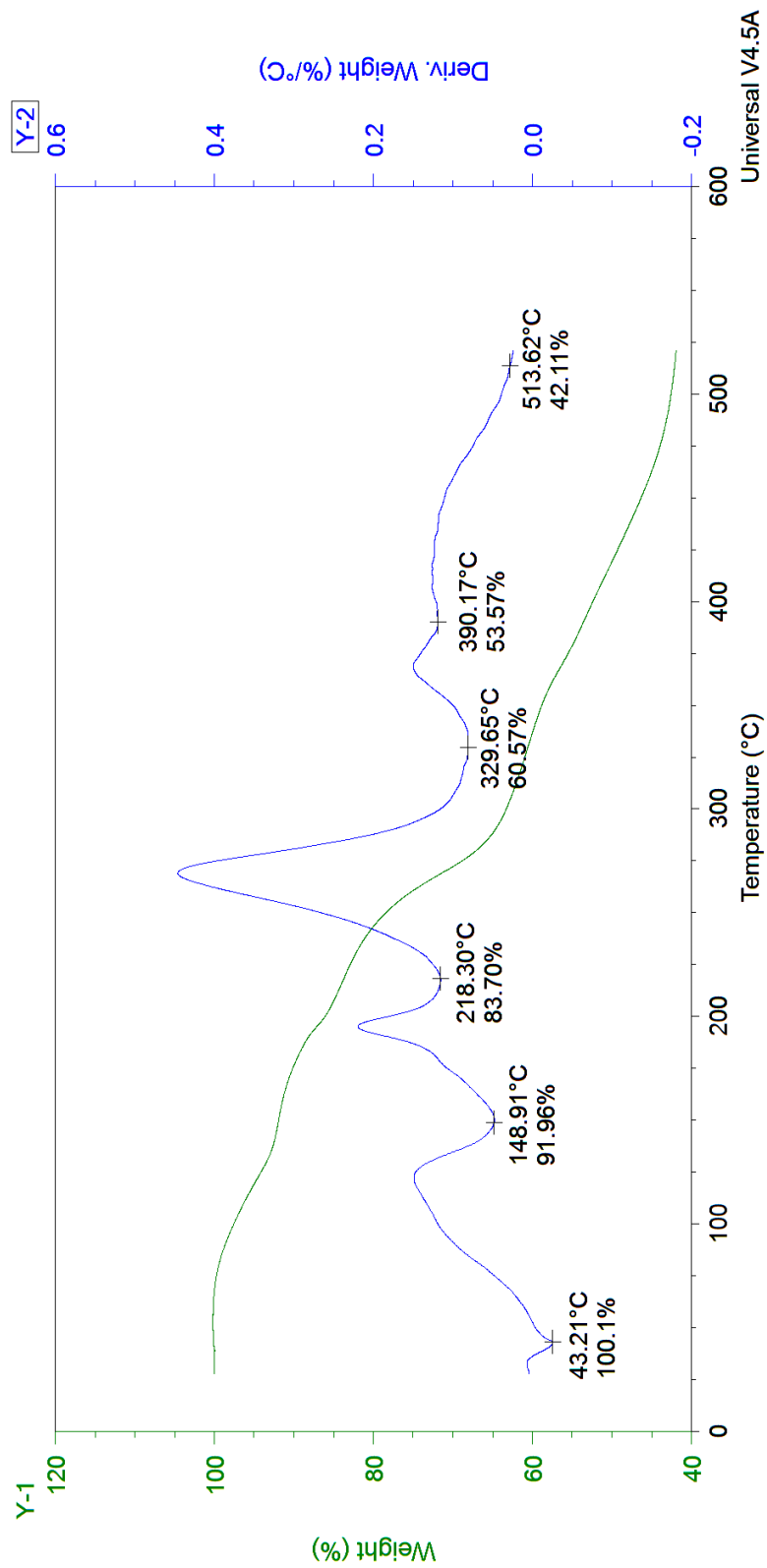


Figure II.15 Thermogravimetric analysis of toluene, heating rate of 32°C/min

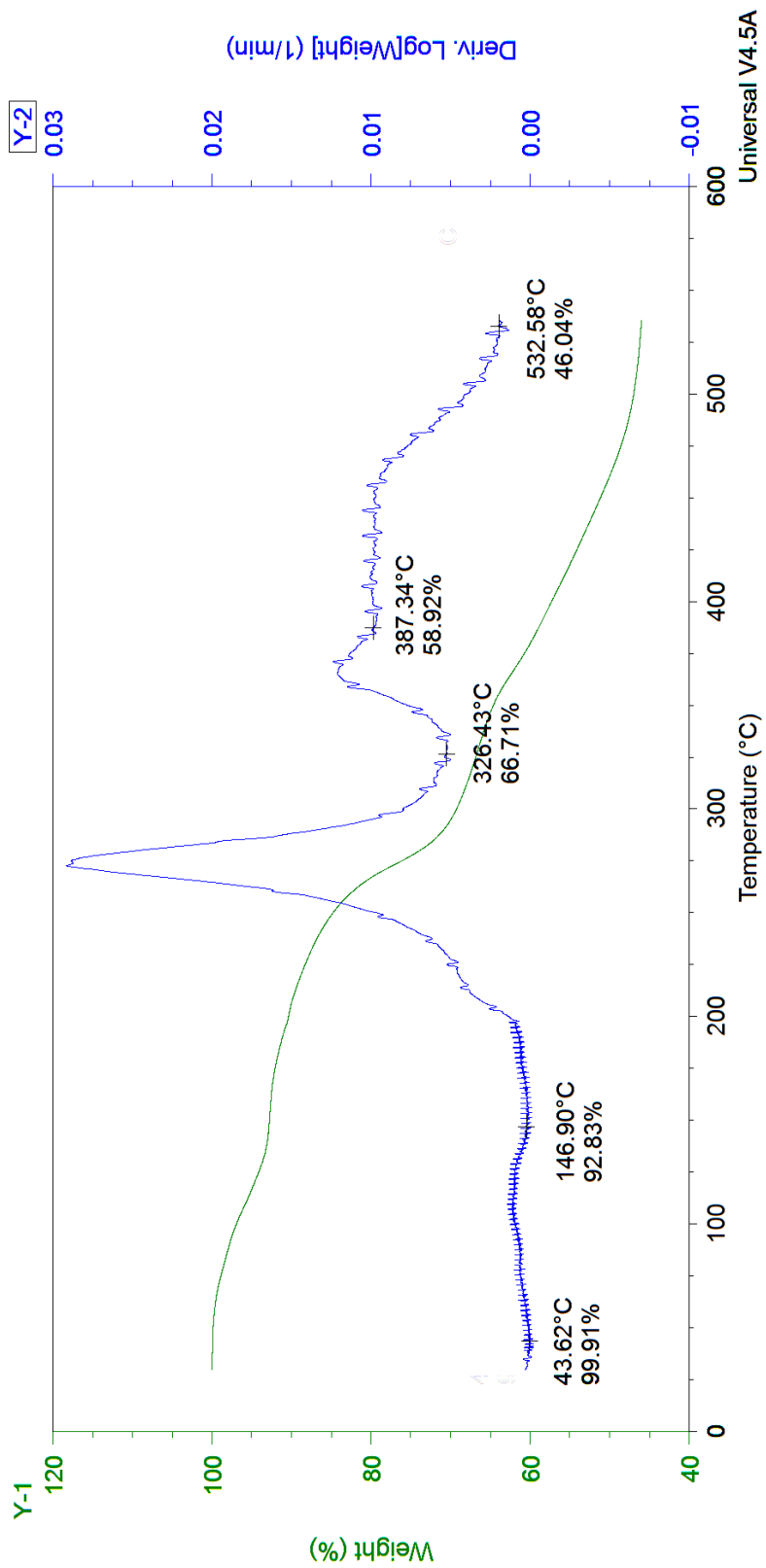


Figure II.16 Thermogravimetric analysis of benzene, heating rate of 2°C/min

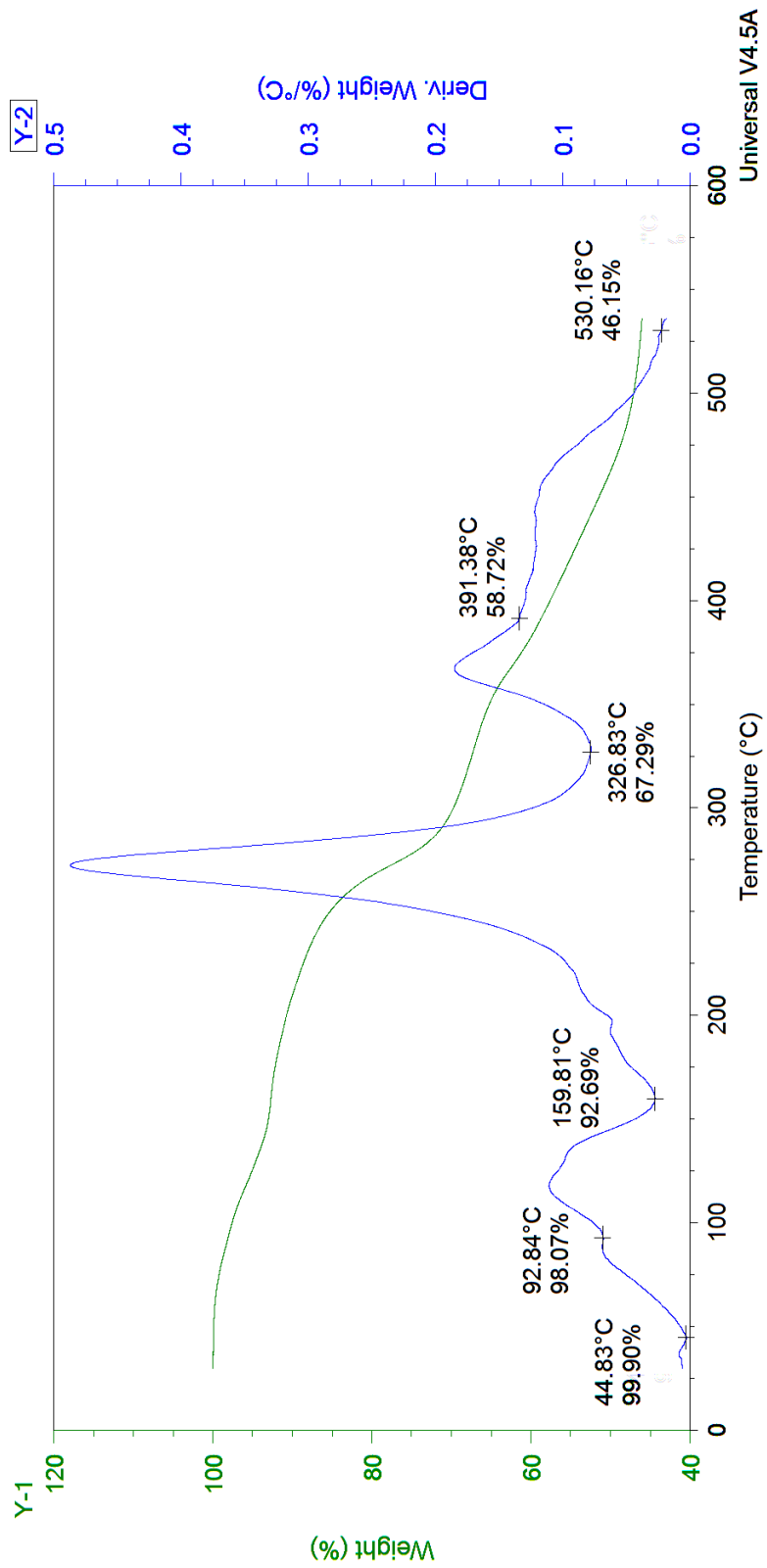


Figure II.17 Thermogravimetric analysis of benzene, heating rate of 4°C/min

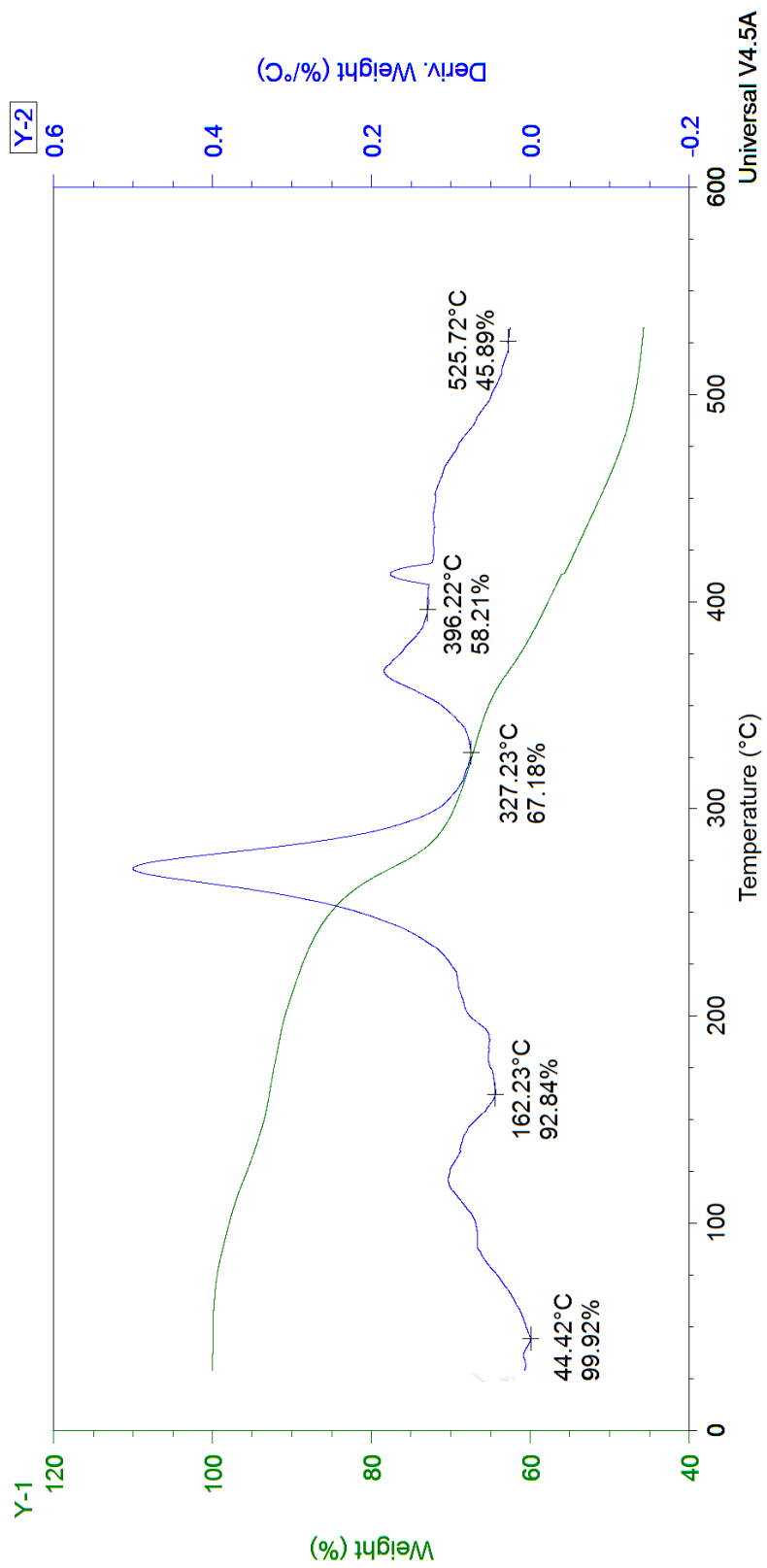


Figure II.18 Thermogravimetric analysis of benzene, heating rate of 8°C/min

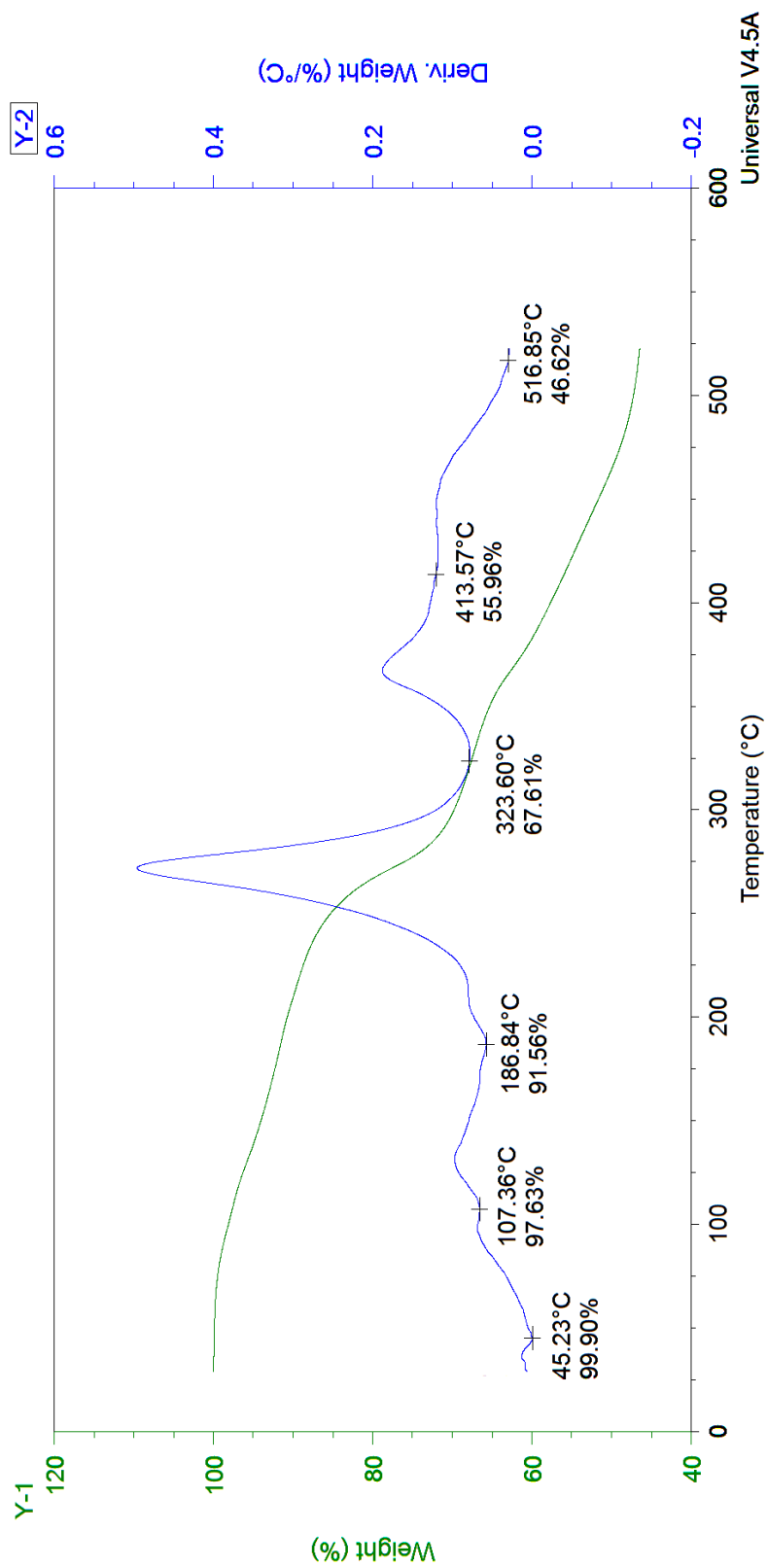


Figure II.19 Thermogravimetric analysis of benzene, heating rate of 16°C/min

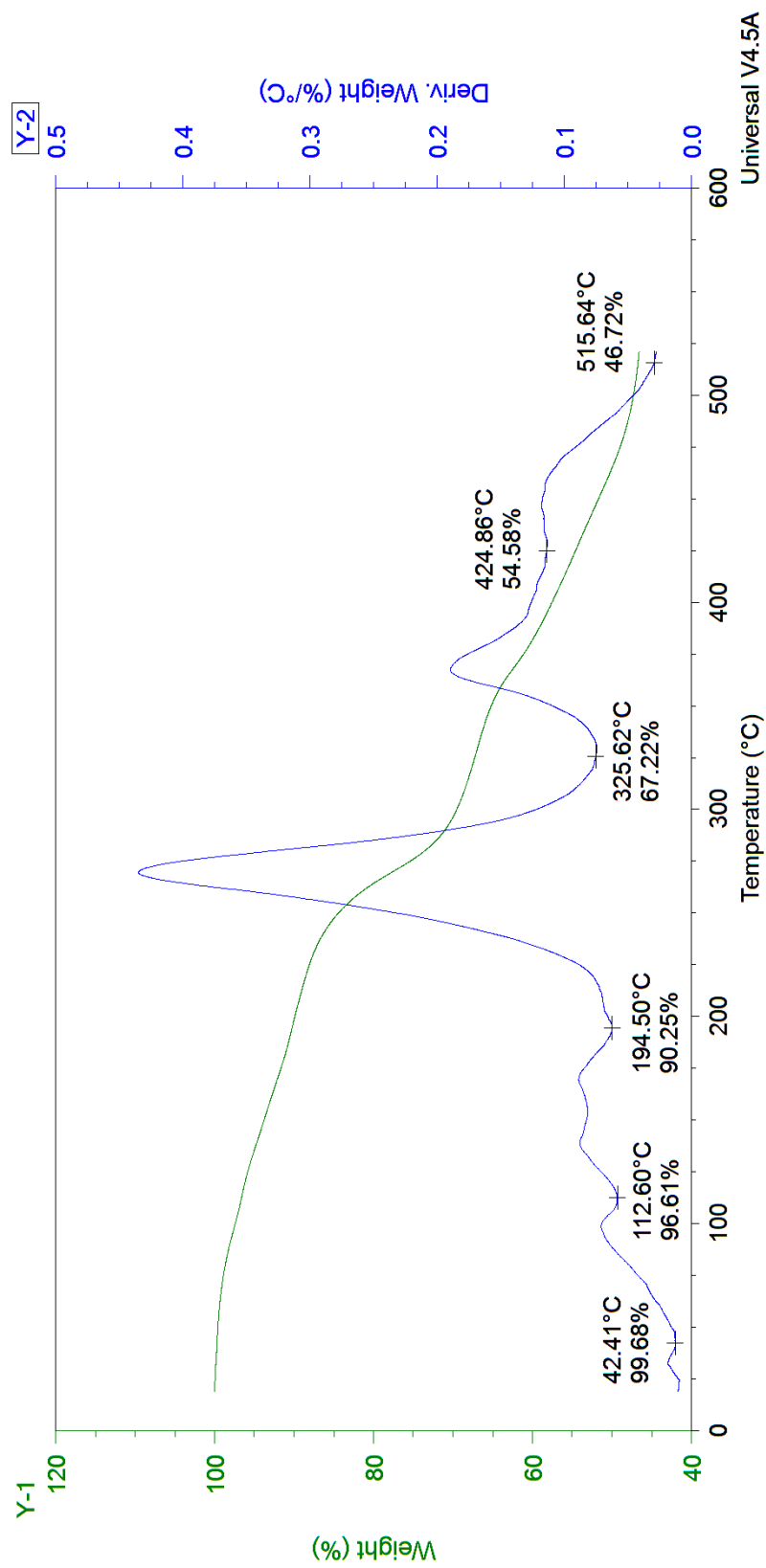


Figure II.20 Thermogravimetric analysis of benzene, heating rate of 32°C/min

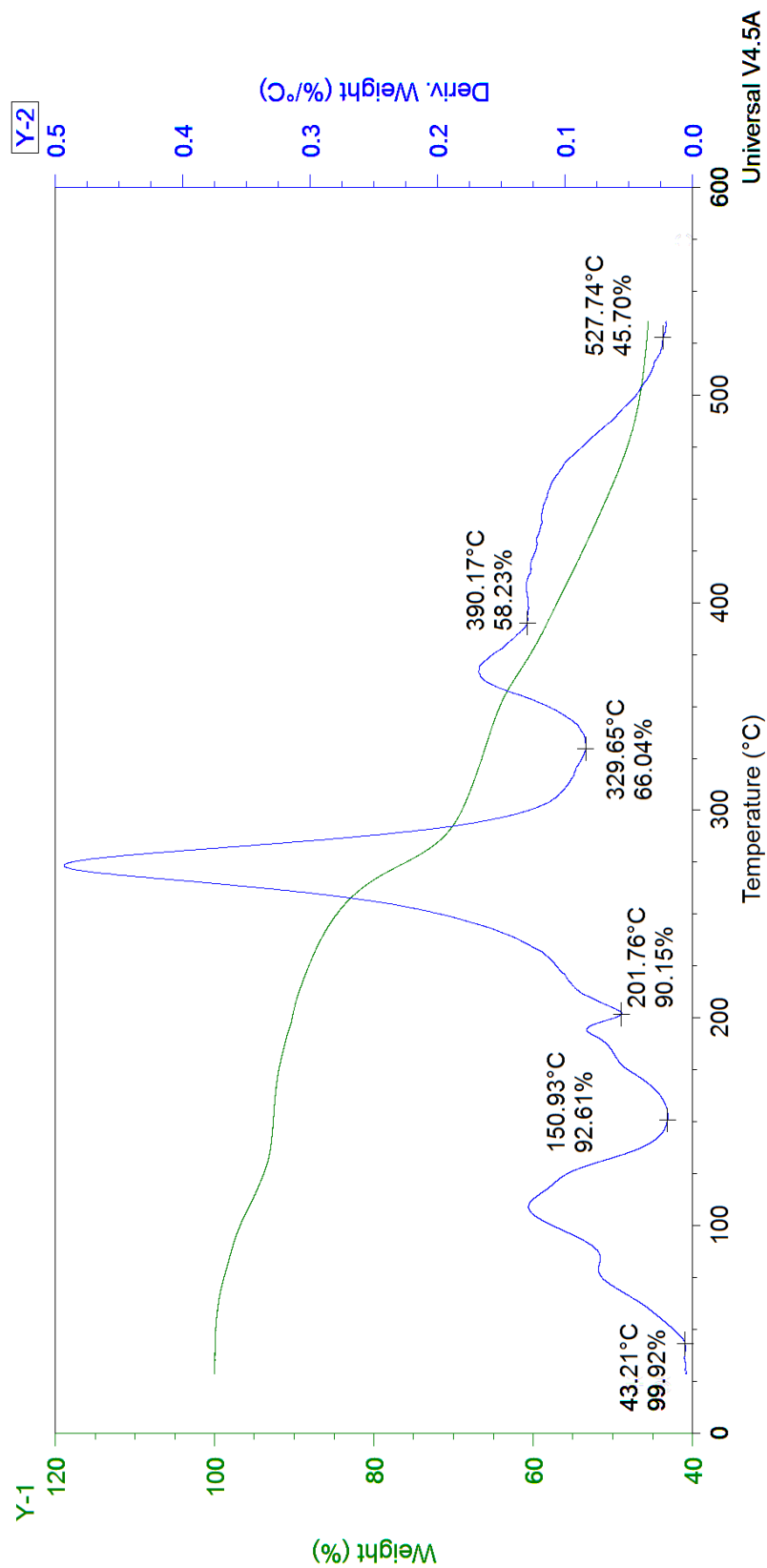


Figure II.21 Thermogravimetric analysis of fluorobenzene, heating rate of 2°C/min

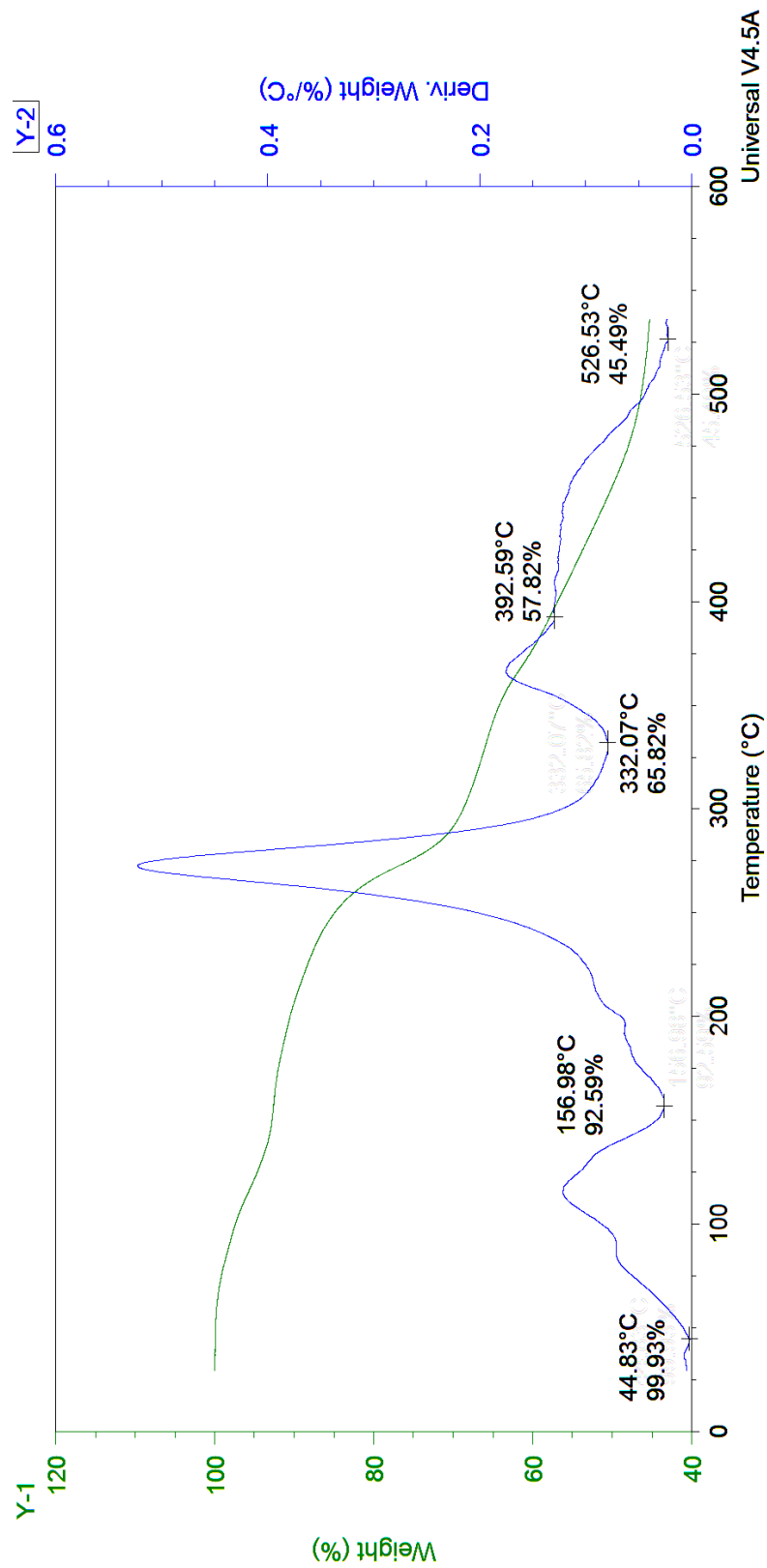


Figure II.22 Thermogravimetric analysis of fluorobenzene, heating rate of 4°C/min

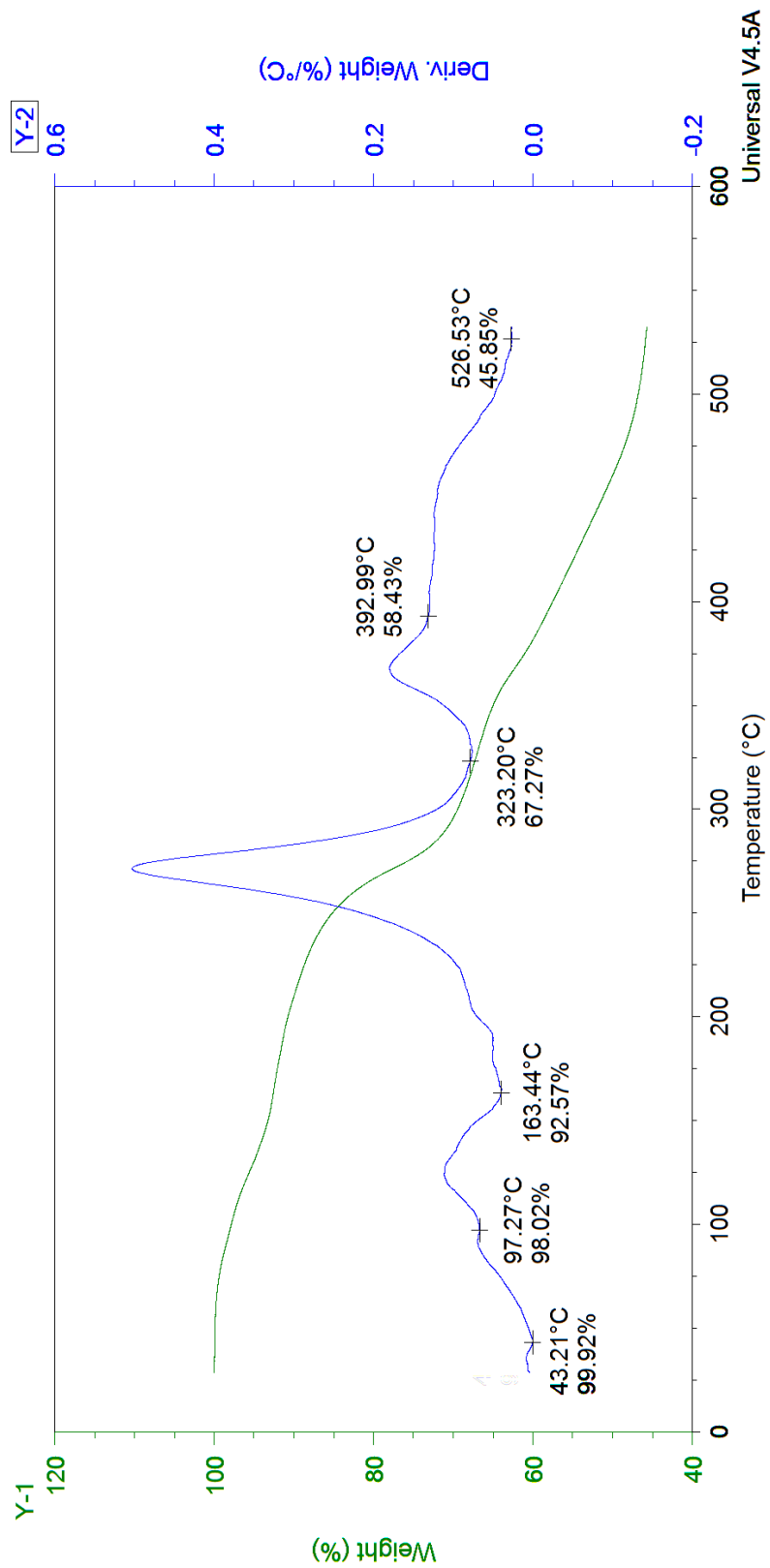


Figure II.23 Thermogravimetric analysis of fluorobenzene, heating rate of 8°C/min

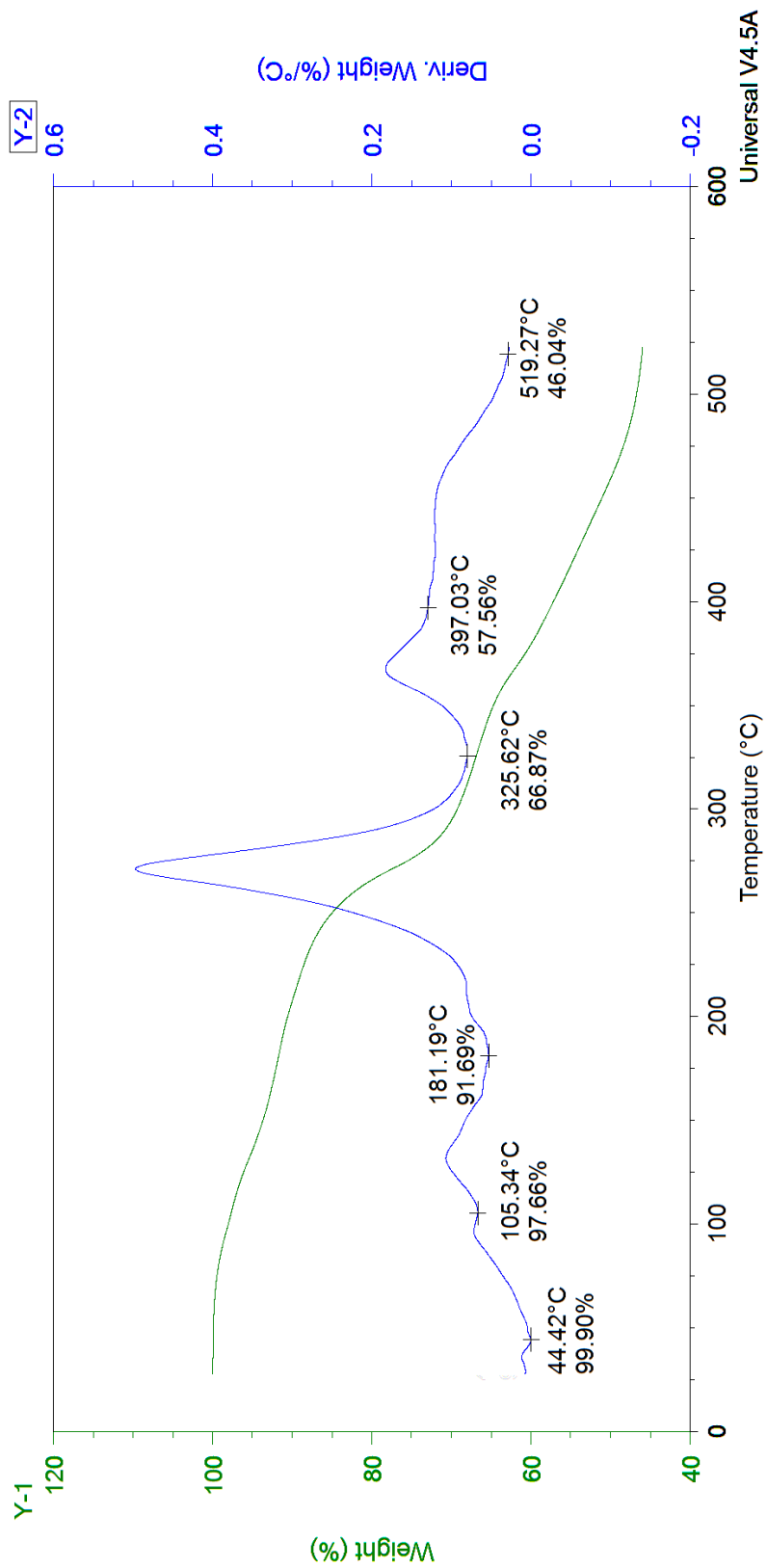


Figure II.24 Thermogravimetric analysis of fluorobenzene, heating rate of 16°C/min

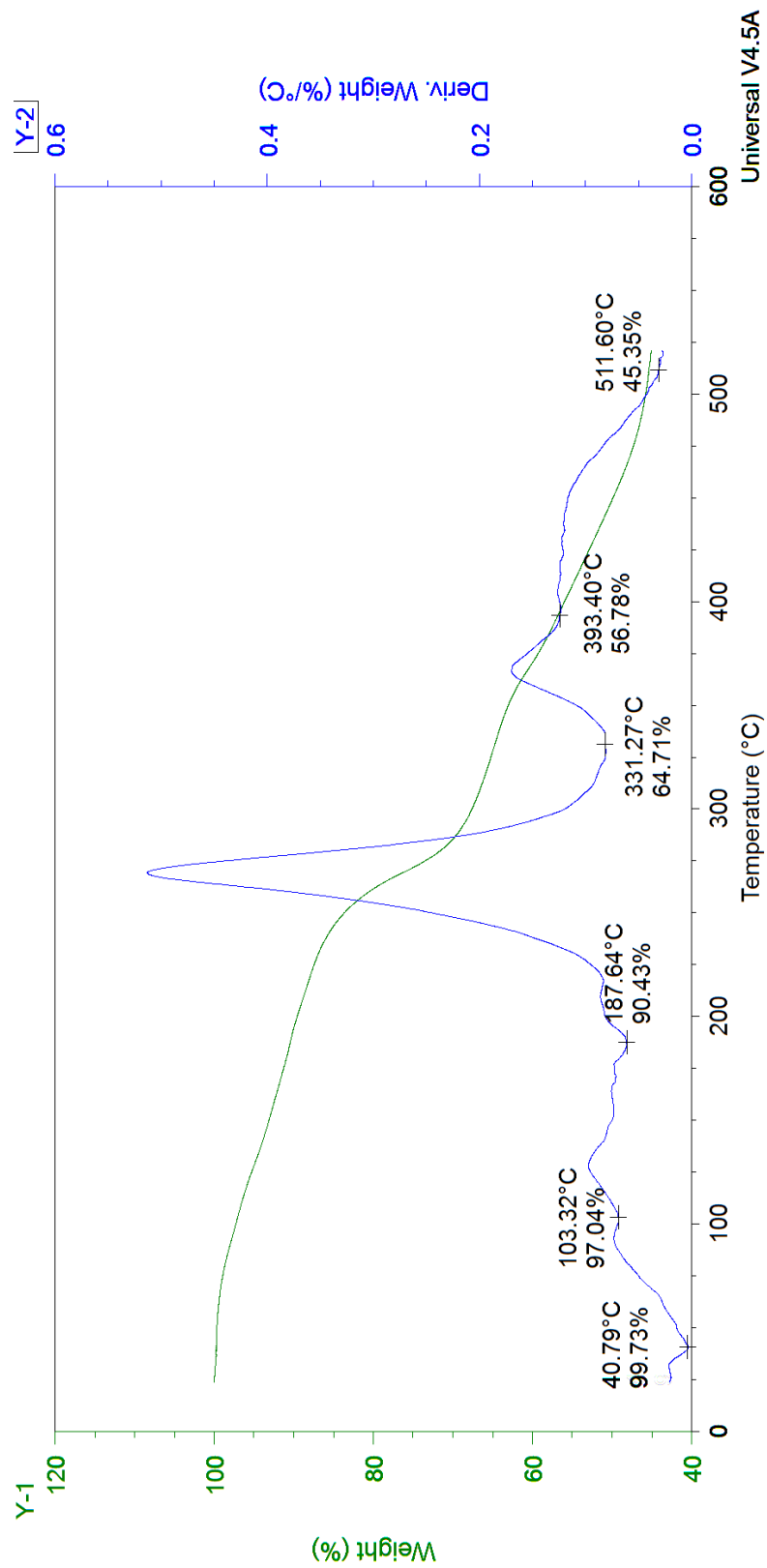


Figure II.25 Thermogravimetric analysis of fluorobenzene, heating rate of 32°C/min

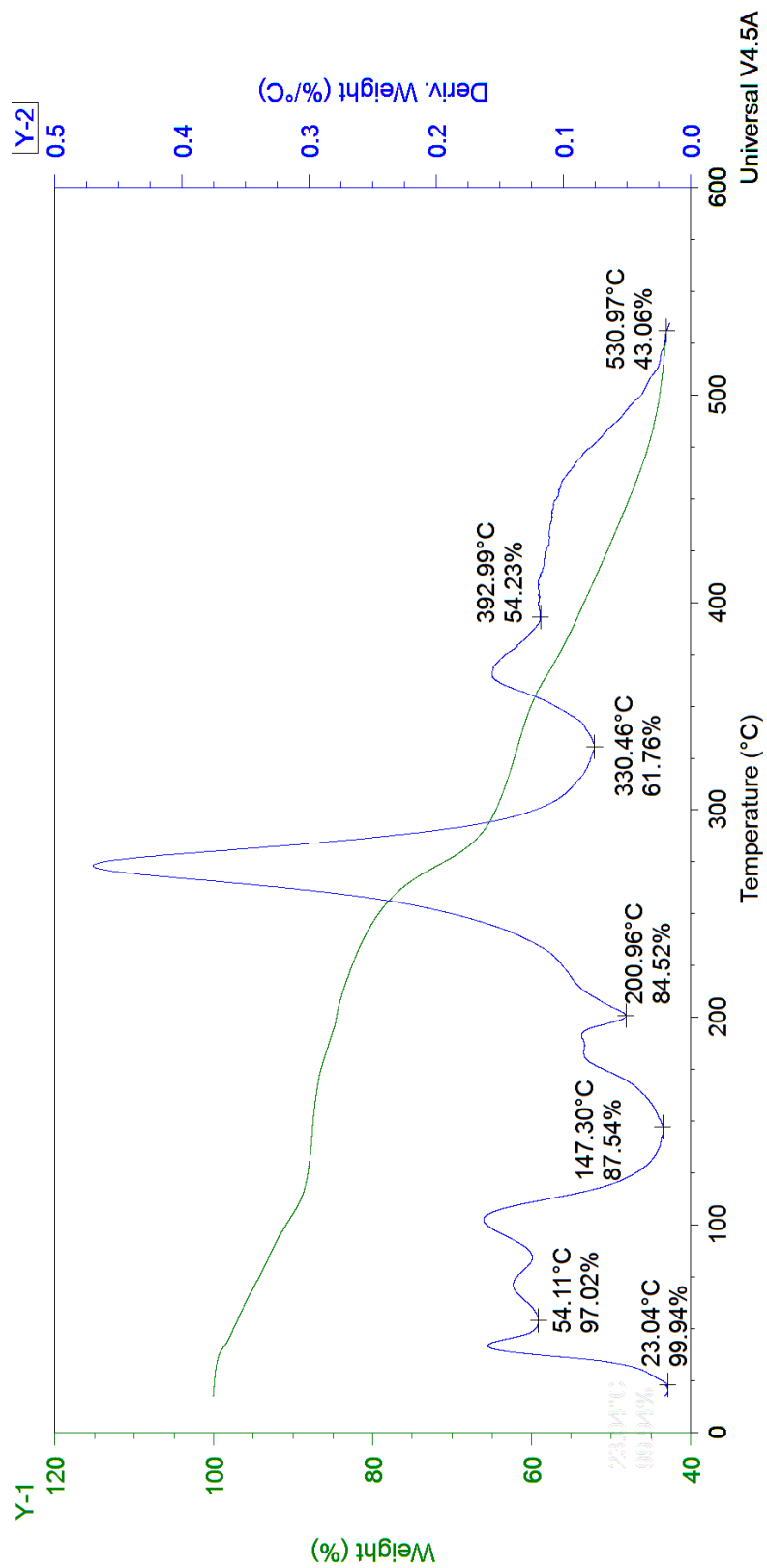


Figure II.26 Thermogravimetric analysis of chlorobenzene, heating rate of 2°C/min

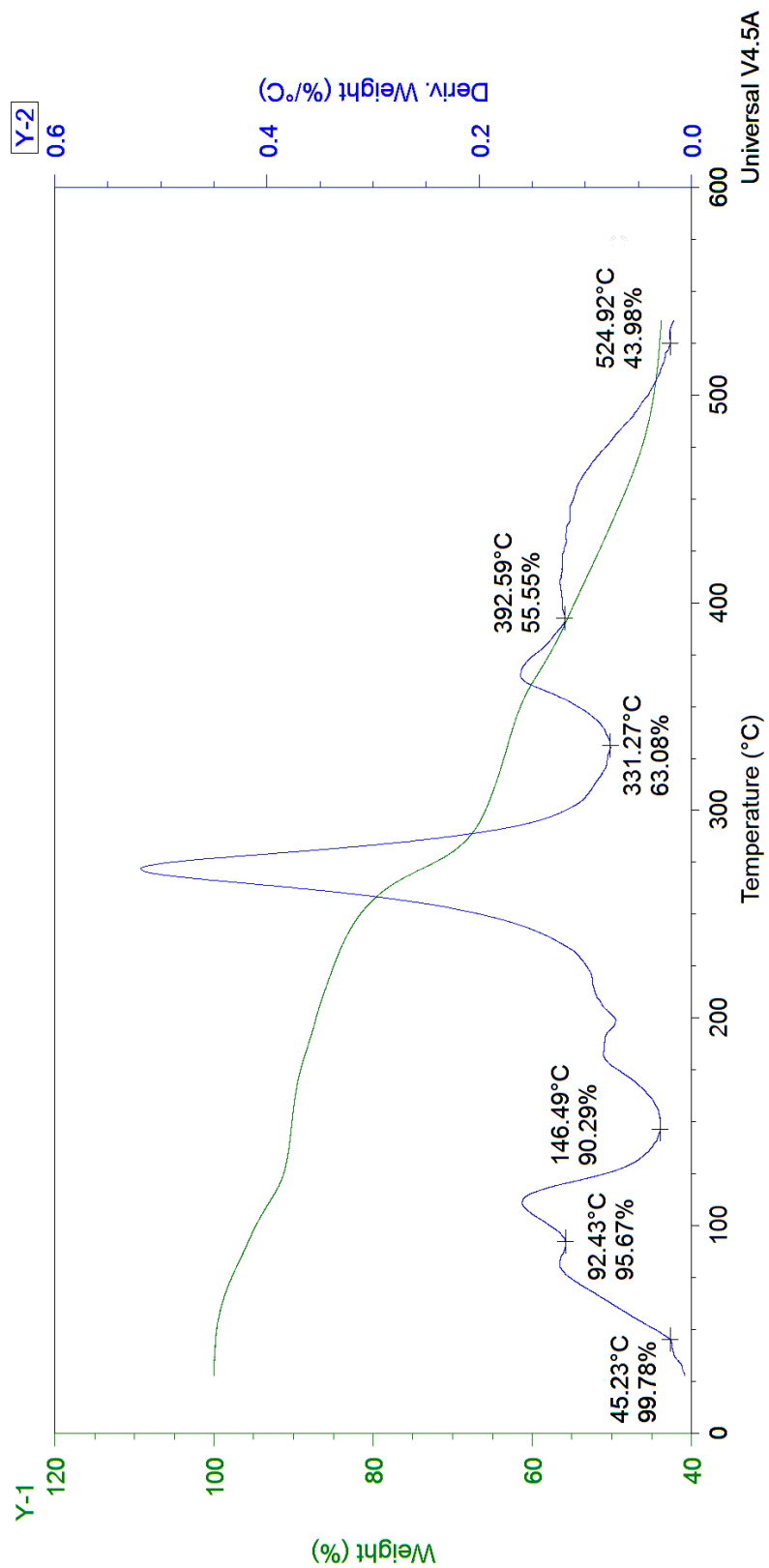


Figure II.27 Thermogravimetric analysis of chlorobenzene, heating rate of 4°C/min

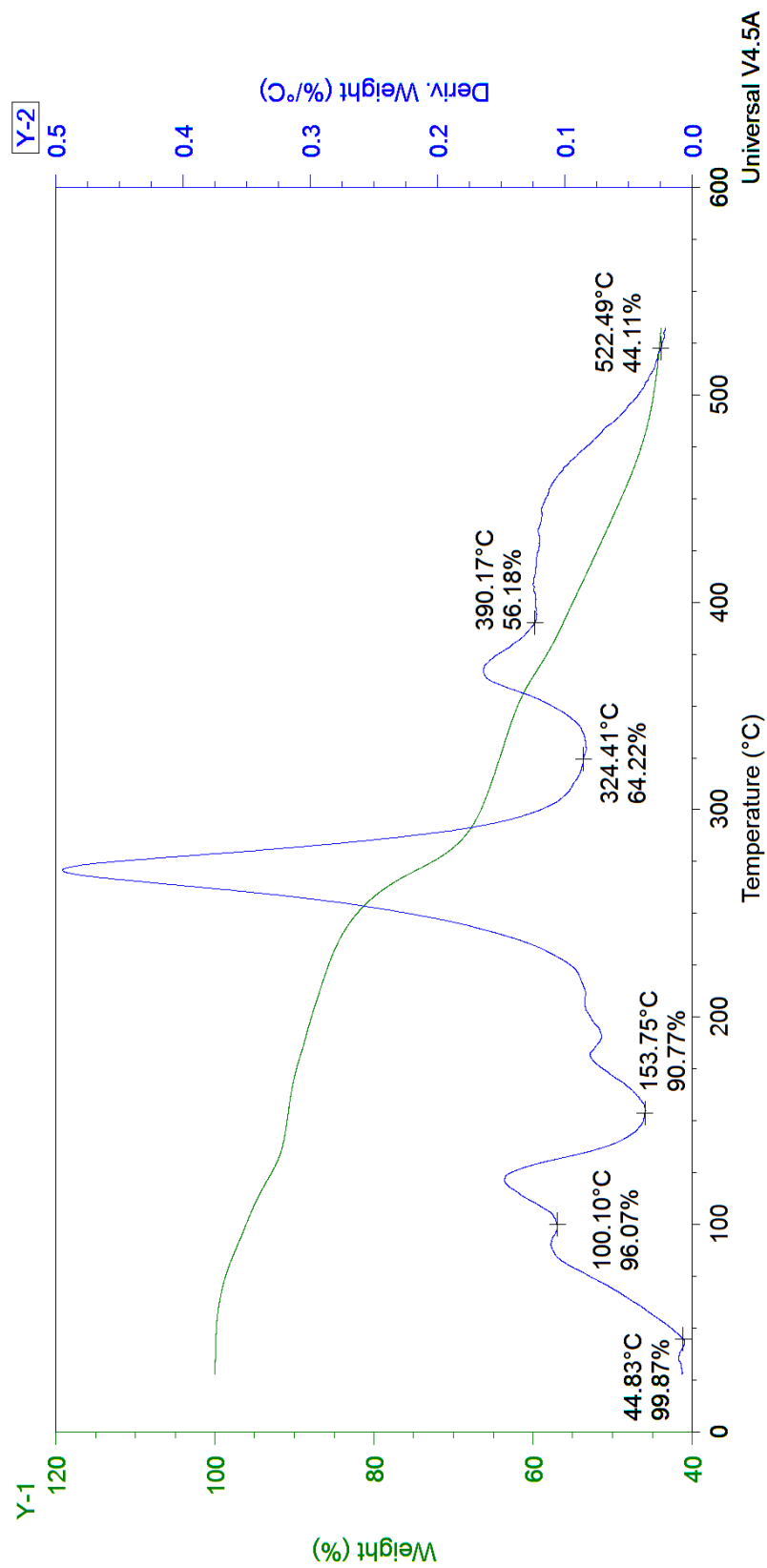


Figure II.28 Thermogravimetric analysis of chlorobenzene, heating rate of 8°C/min

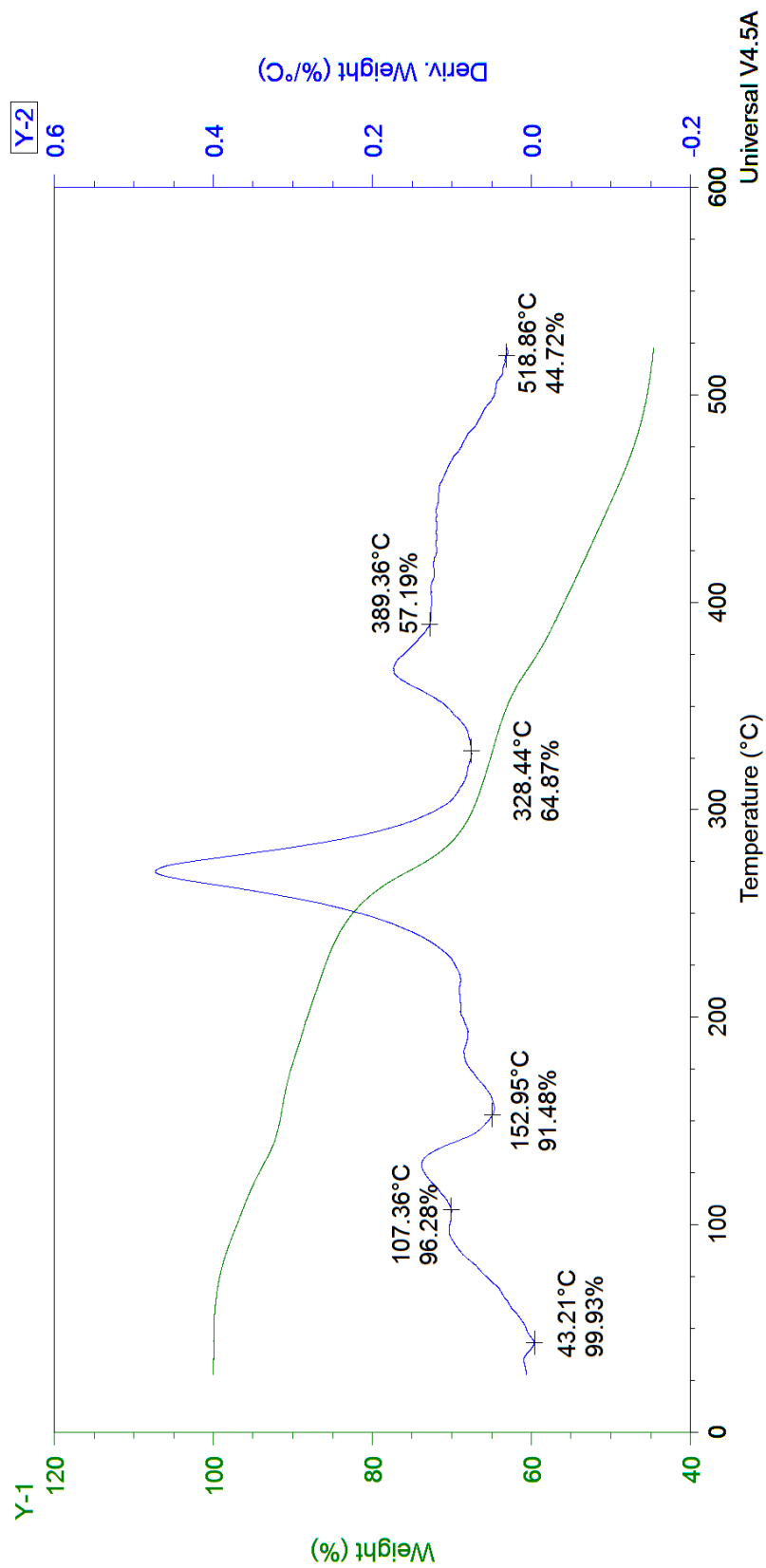


Figure II.29 Thermogravimetric analysis of chlorobenzene, heating rate of 16°C/min

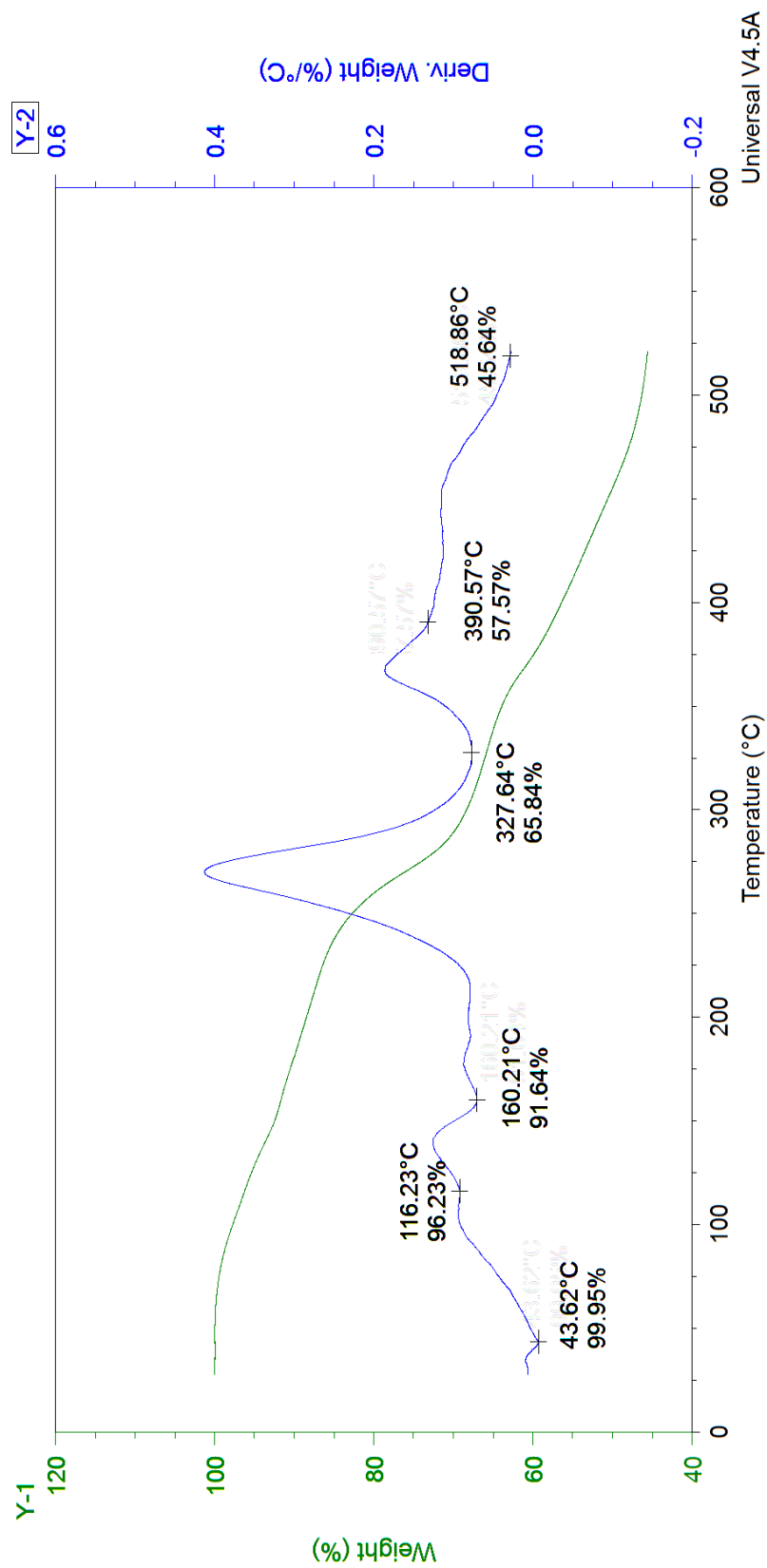


Figure II.30 Thermogravimetric analysis of chlorobenzene, heating rate of 32°C/min

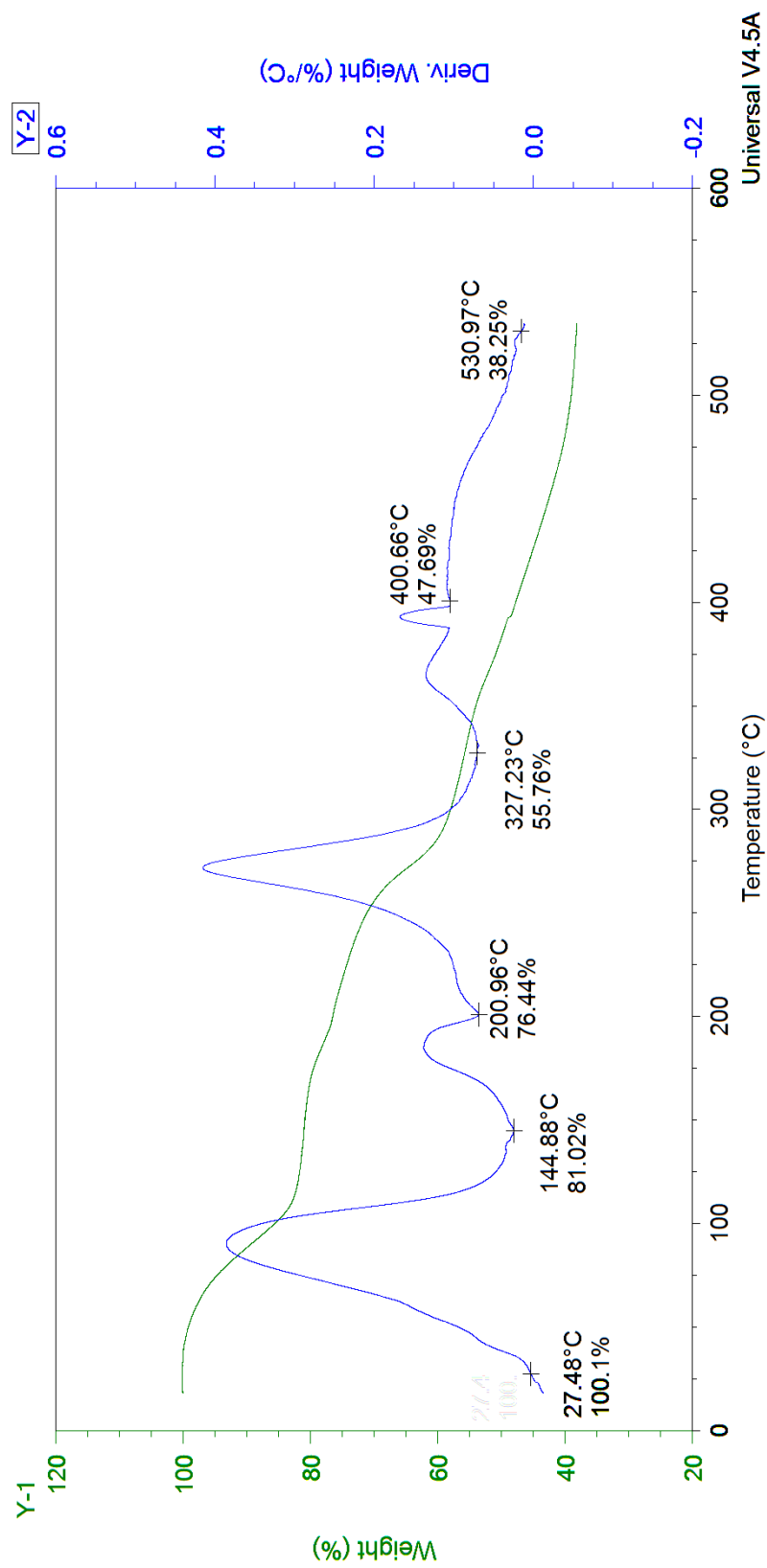


Figure II.31 Thermogravimetric analysis of bromobenzene, heating rate of 2°C/min

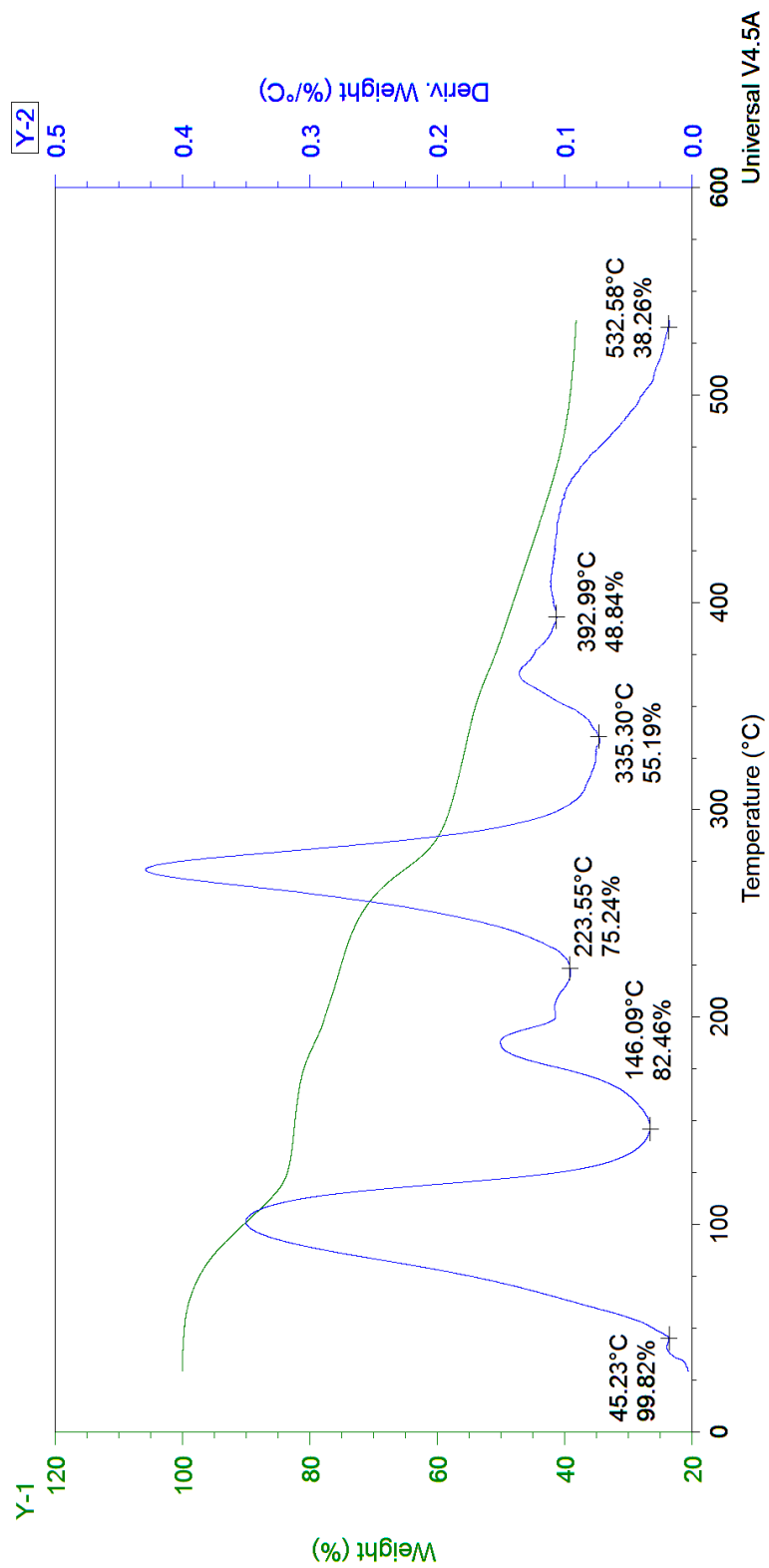


Figure II.32 Thermogravimetric analysis of bromobenzene, heating rate of 4°C/min

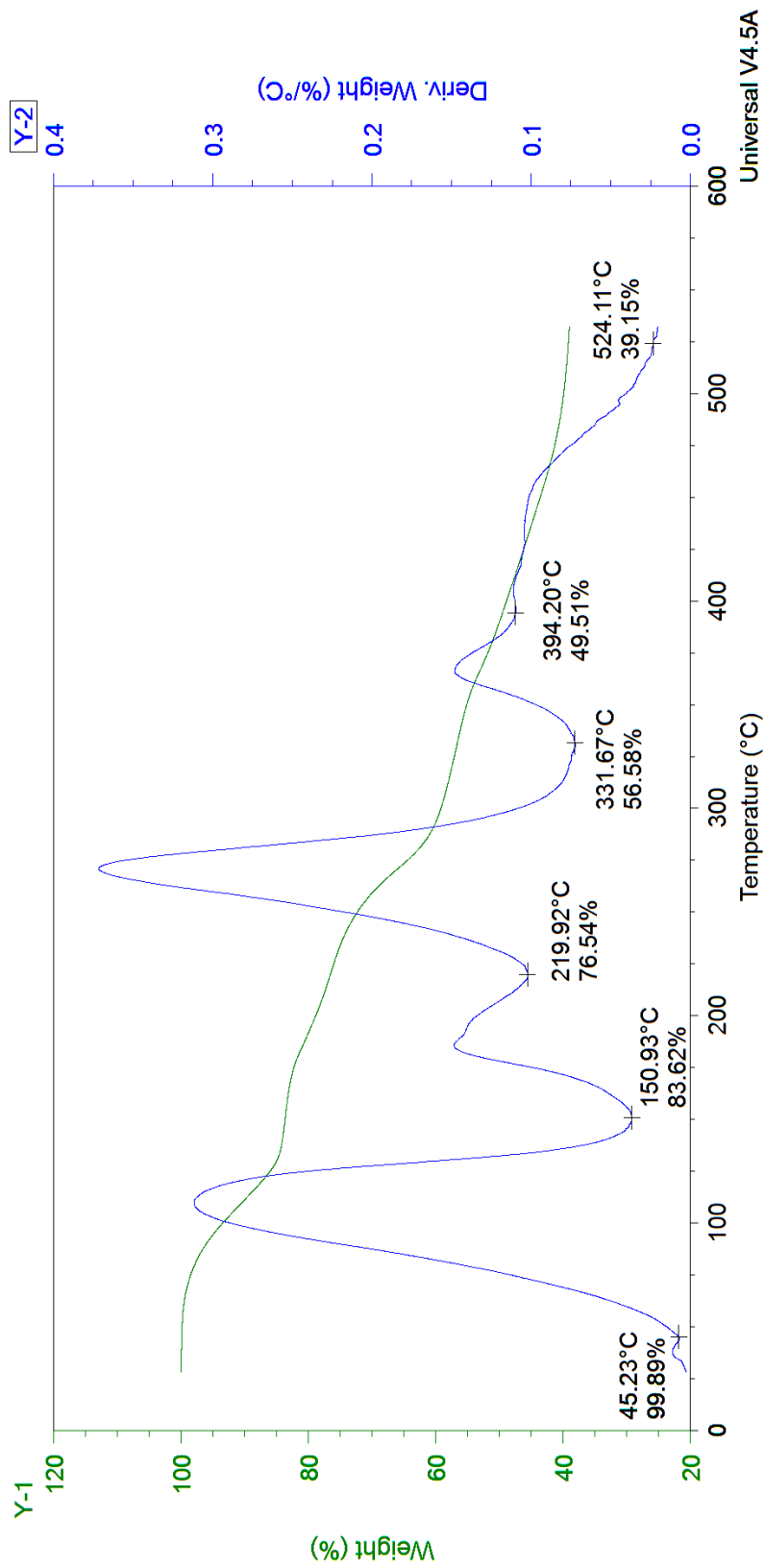


Figure II.33 Thermogravimetric analysis of bromobenzene, heating rate of 8°C/min

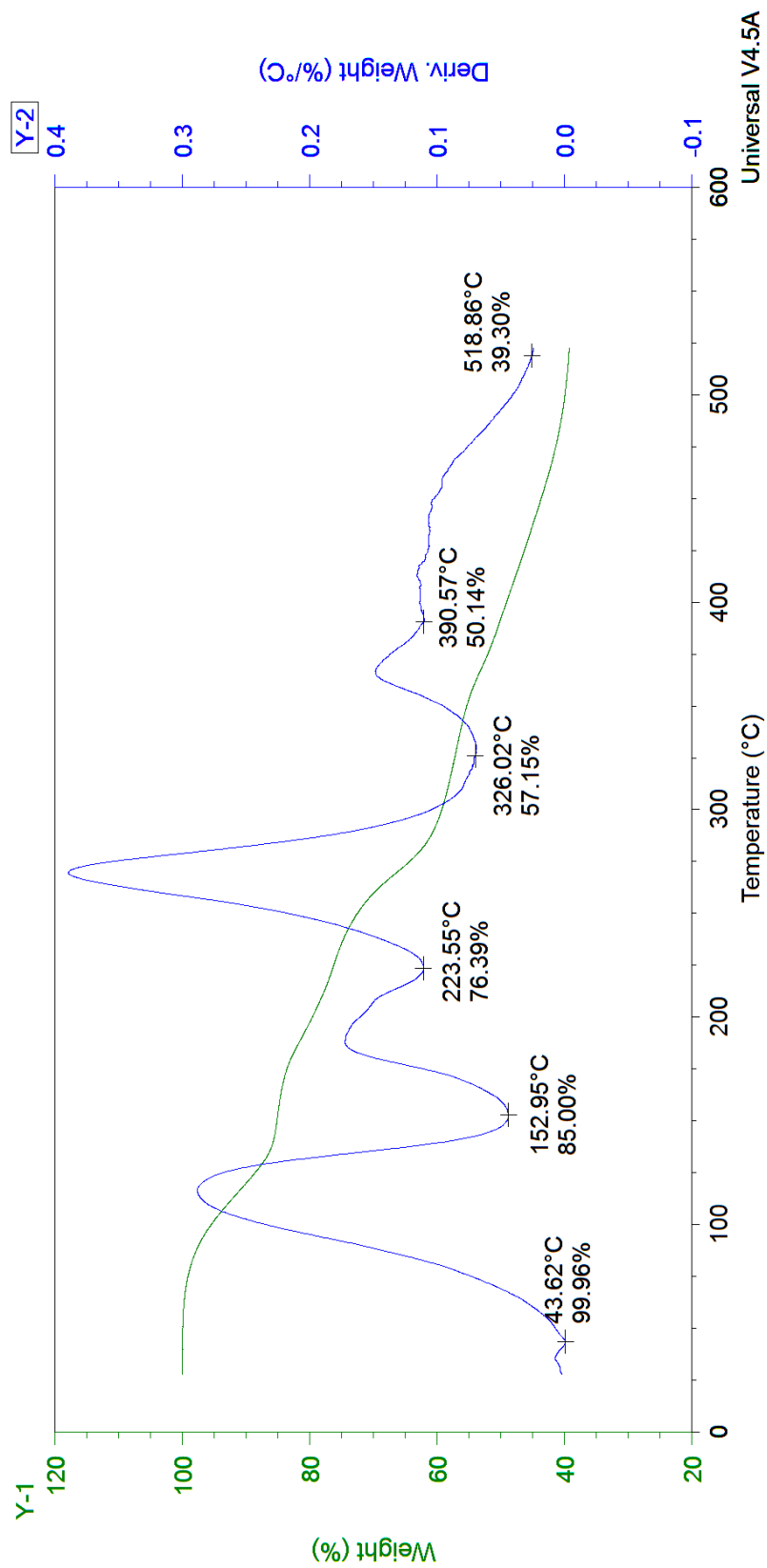


Figure II.34 Thermogravimetric analysis of bromobenzene, heating rate of 16°C/min

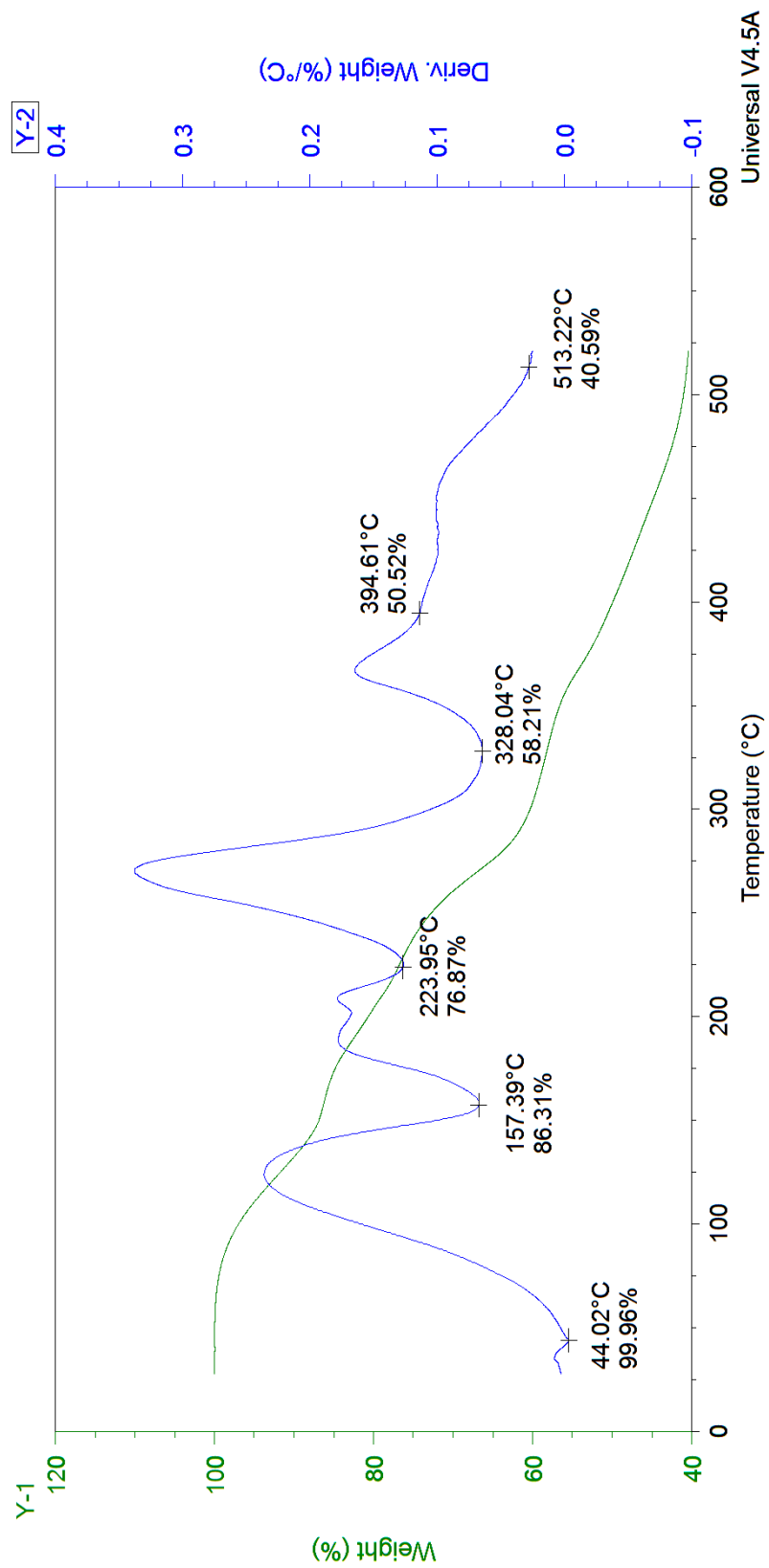


Figure II.35 Thermogravimetric analysis of bromobenzene, heating rate of 32°C/min

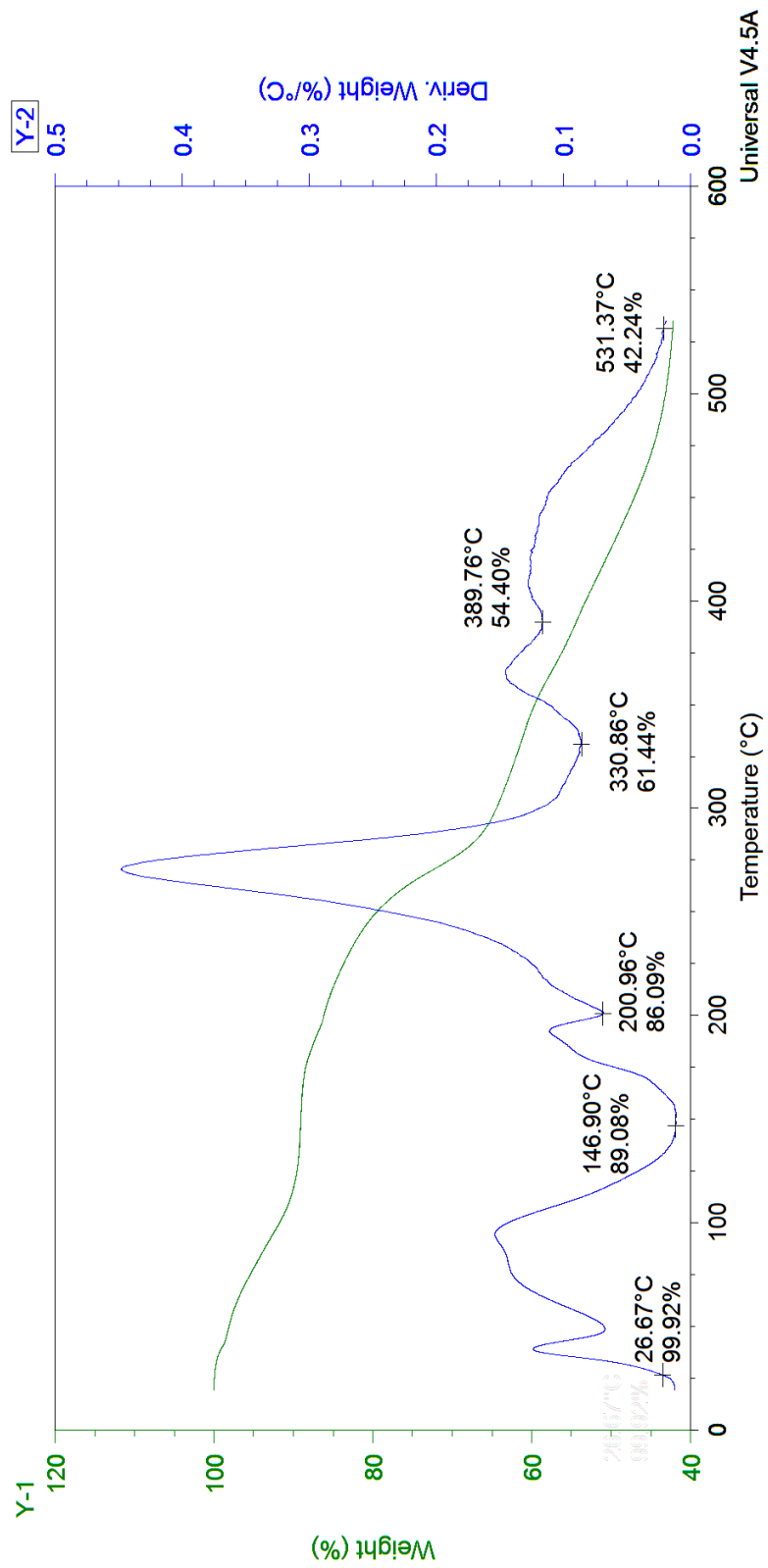


Figure II.36 Thermogravimetric analysis of iodobenzene, heating rate of 2°C/min

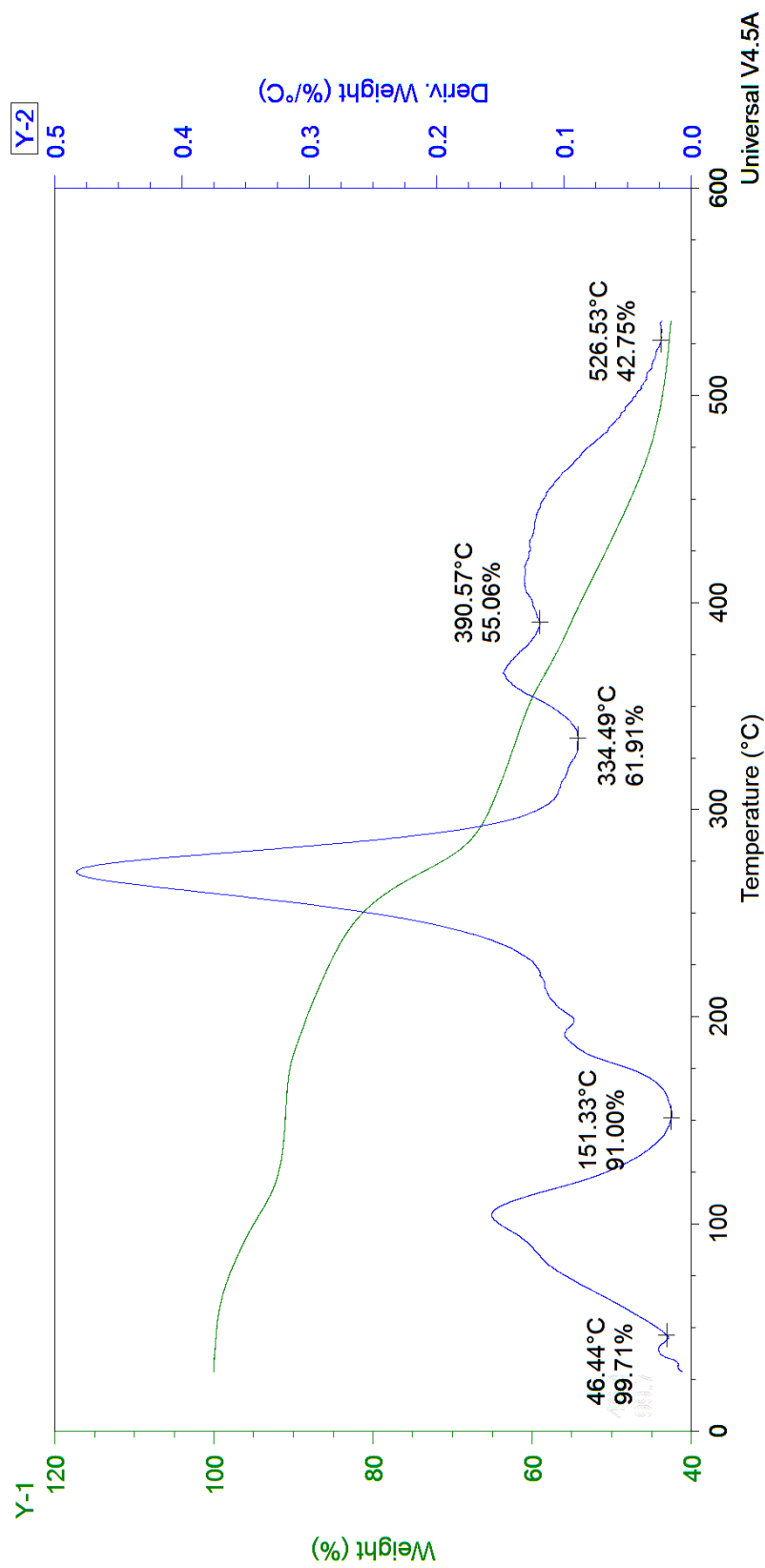


Figure II.37 Thermogravimetric analysis of iodobenzene, heating rate of 4°C/min

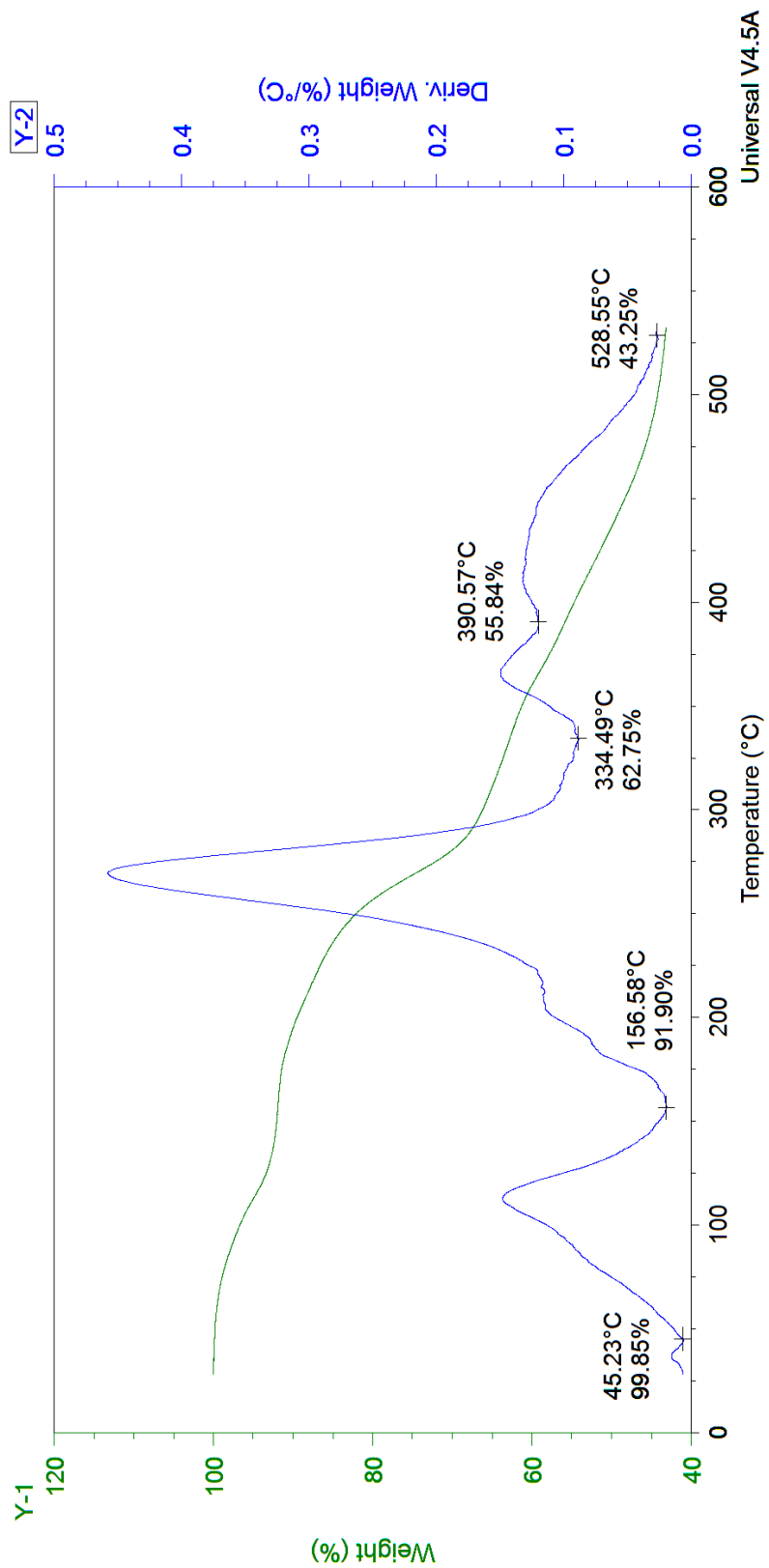


Figure II.38 Thermogravimetric analysis of iodobenzene, heating rate of 8°C/min

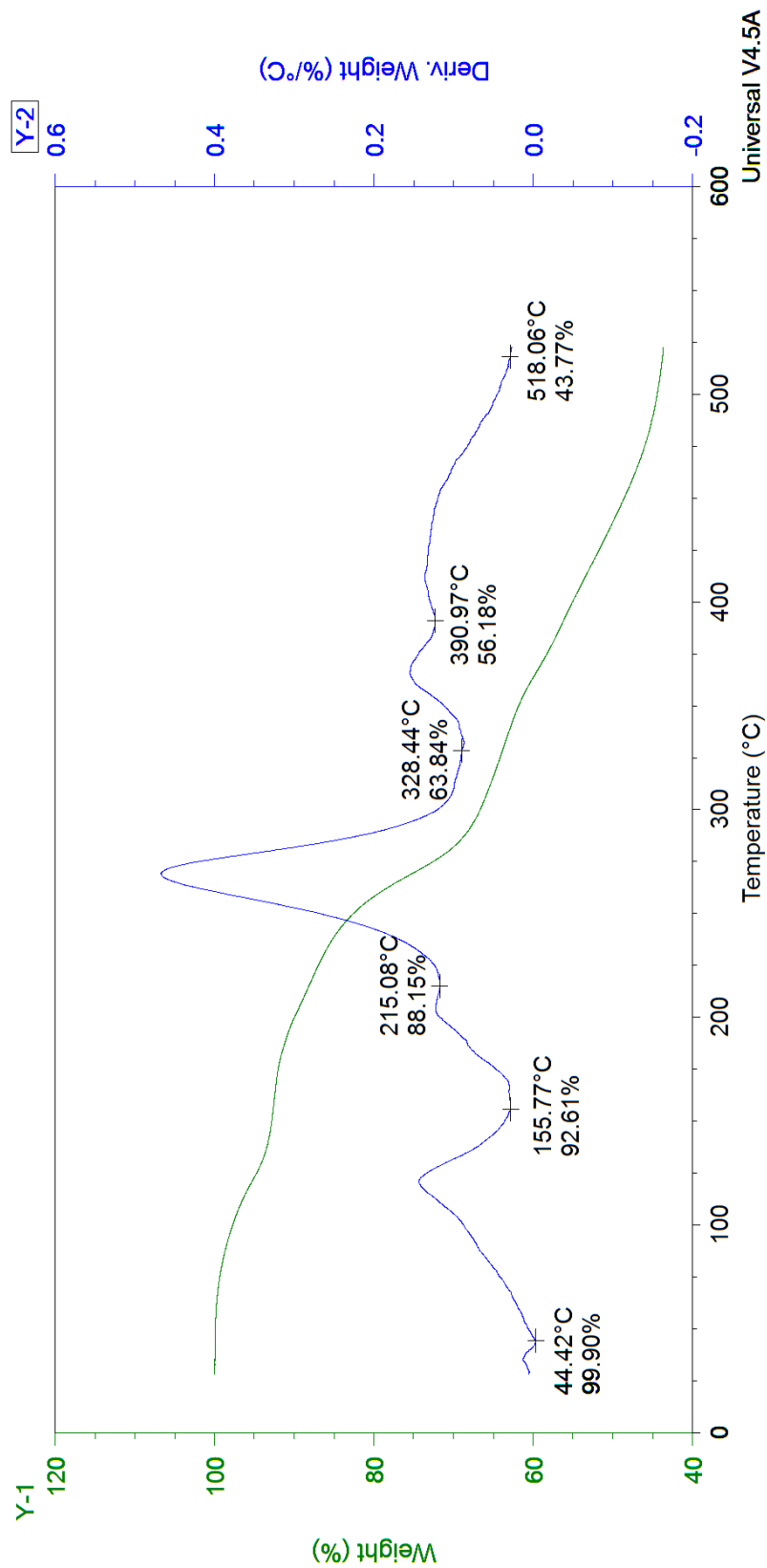


Figure II.39 Thermogravimetric analysis of iodobenzene, heating rate of 16°C/min

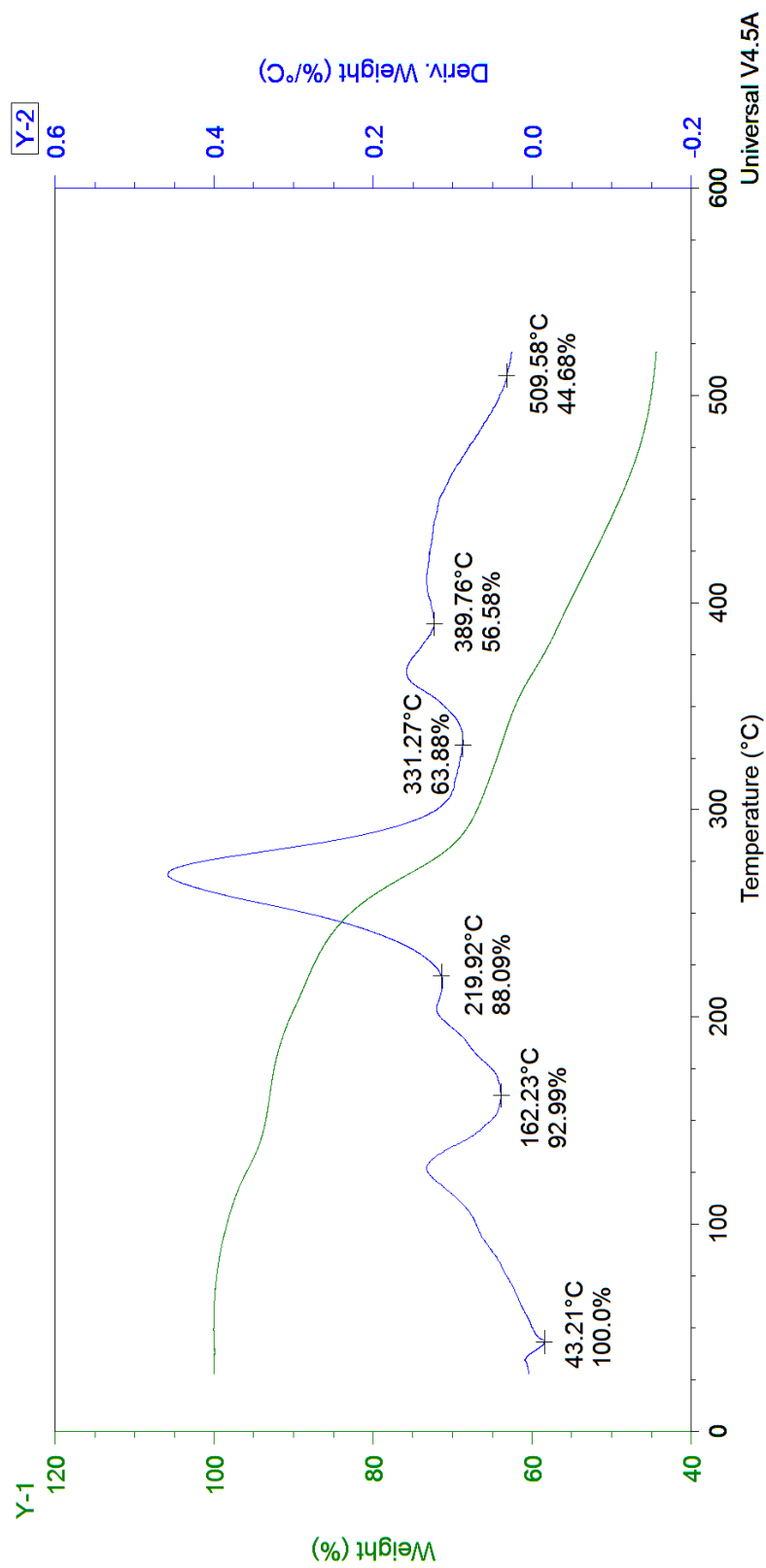


Figure II.40 Thermogravimetric analysis of iodobenzene, heating rate of 32°C/min

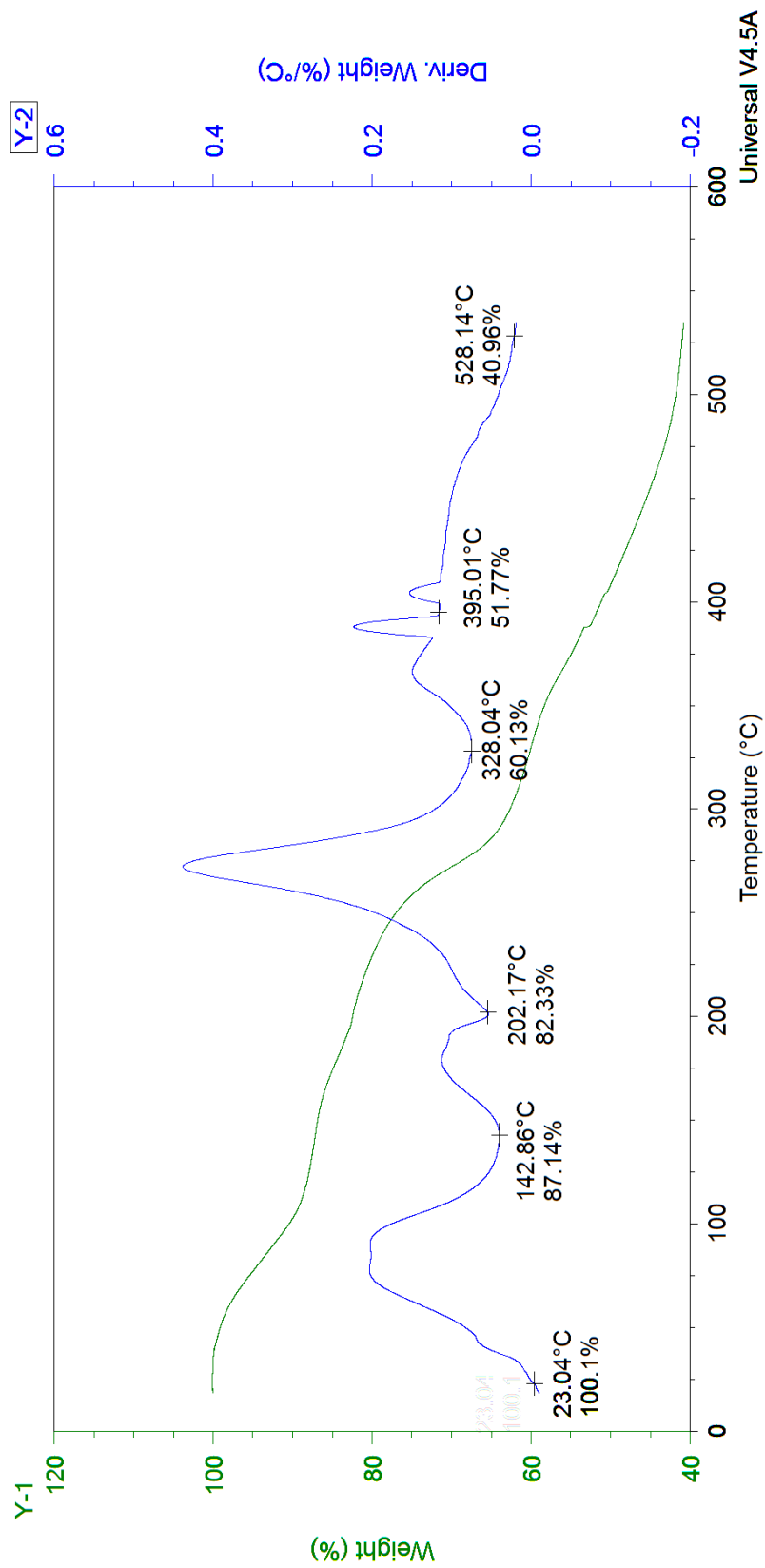


Figure II.41 Thermogravimetric analysis of nitrobenzene, heating rate of 2°C/min

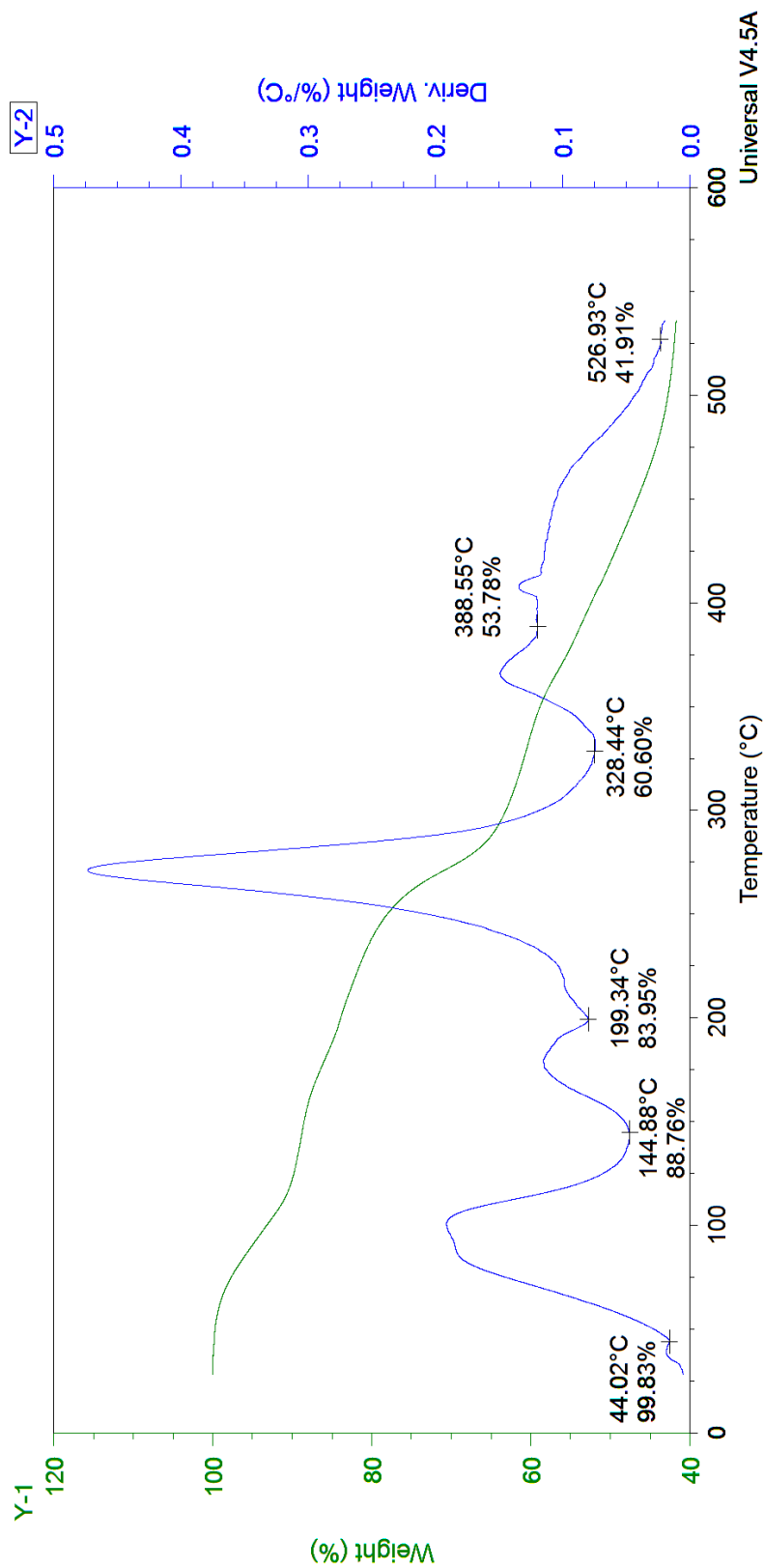


Figure II.42 Thermogravimetric analysis of nitrobenzene, heating rate of 4°C/min

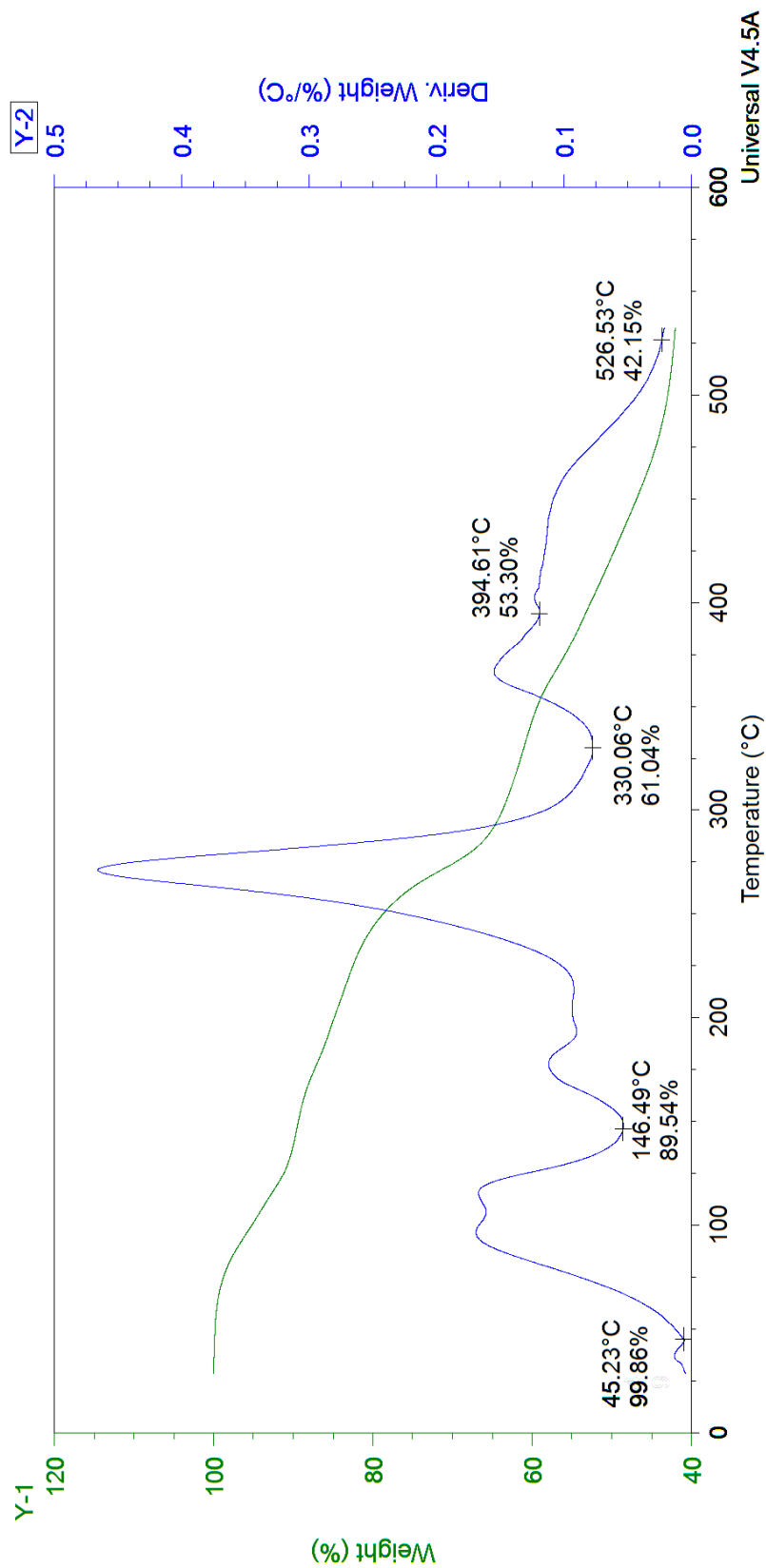


Figure II.43 Thermogravimetric analysis of nitrobenzene, heating rate of 8°C/min

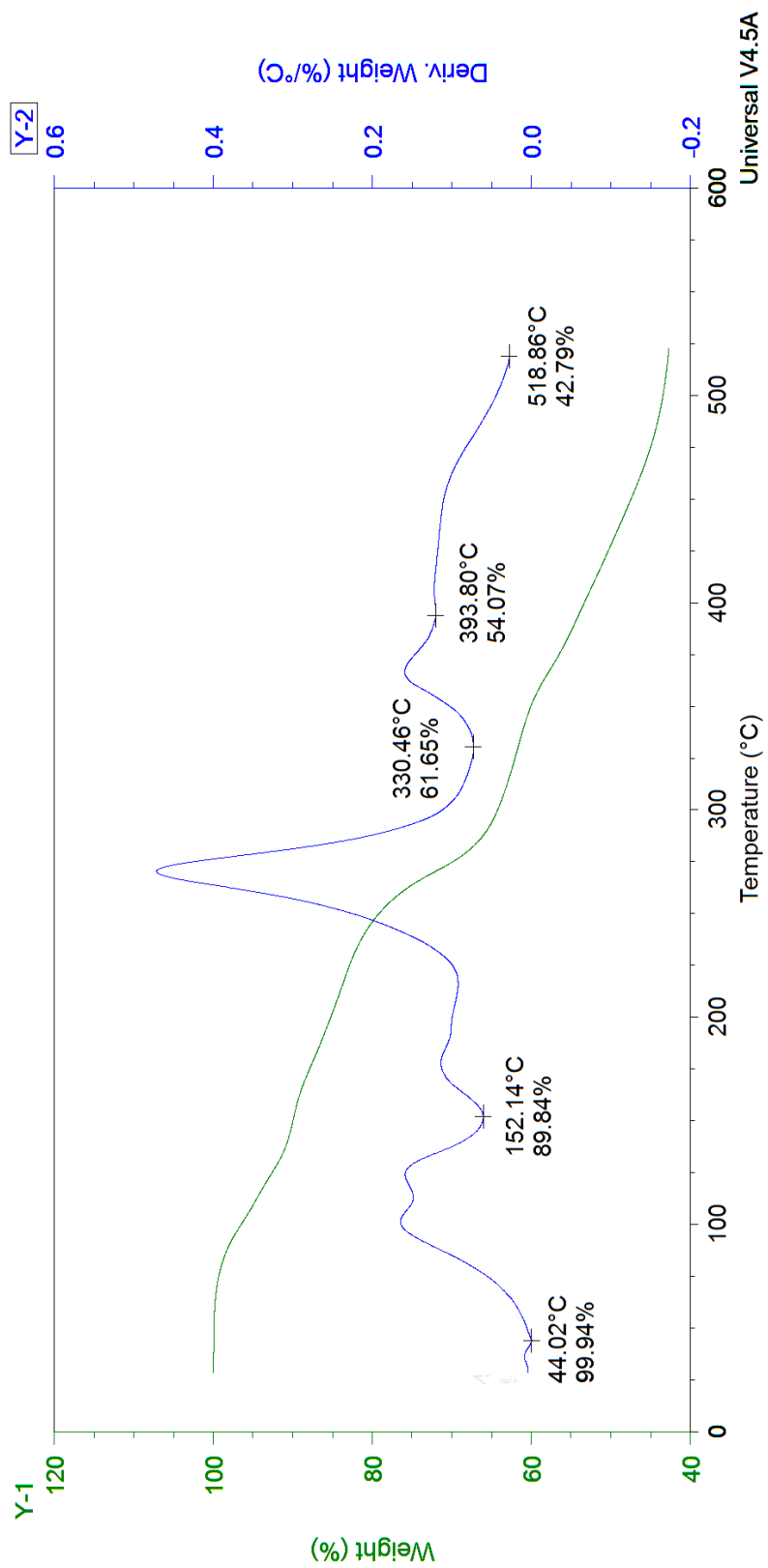


Figure II.44 Thermogravimetric analysis of nitrobenzene, heating rate of 16°C/min

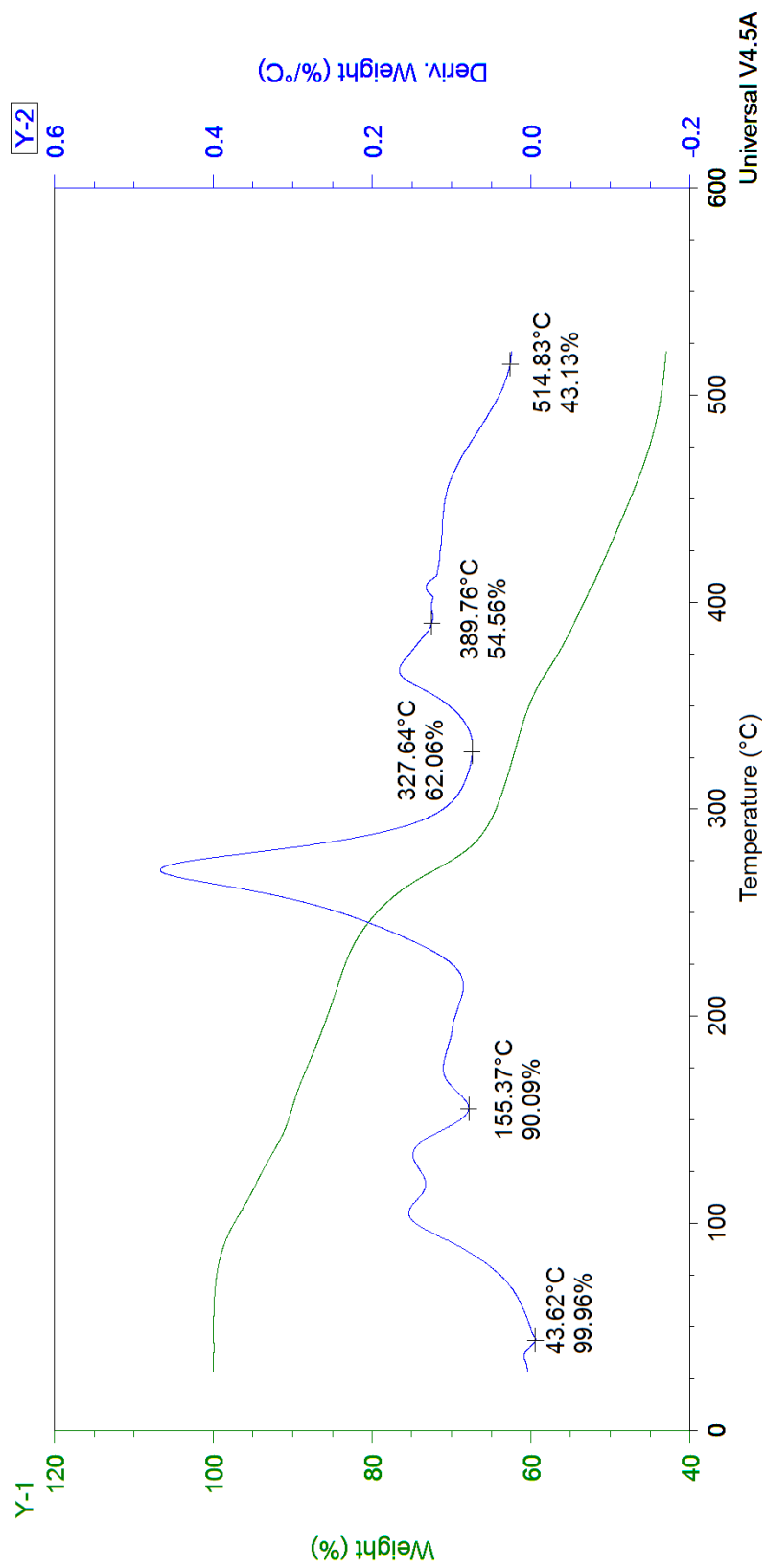


Figure II.45 Thermogravimetric analysis of nitrobenzene, heating rate of 32°C/min

Appendix III – Supplemental Figures for Chapter 5

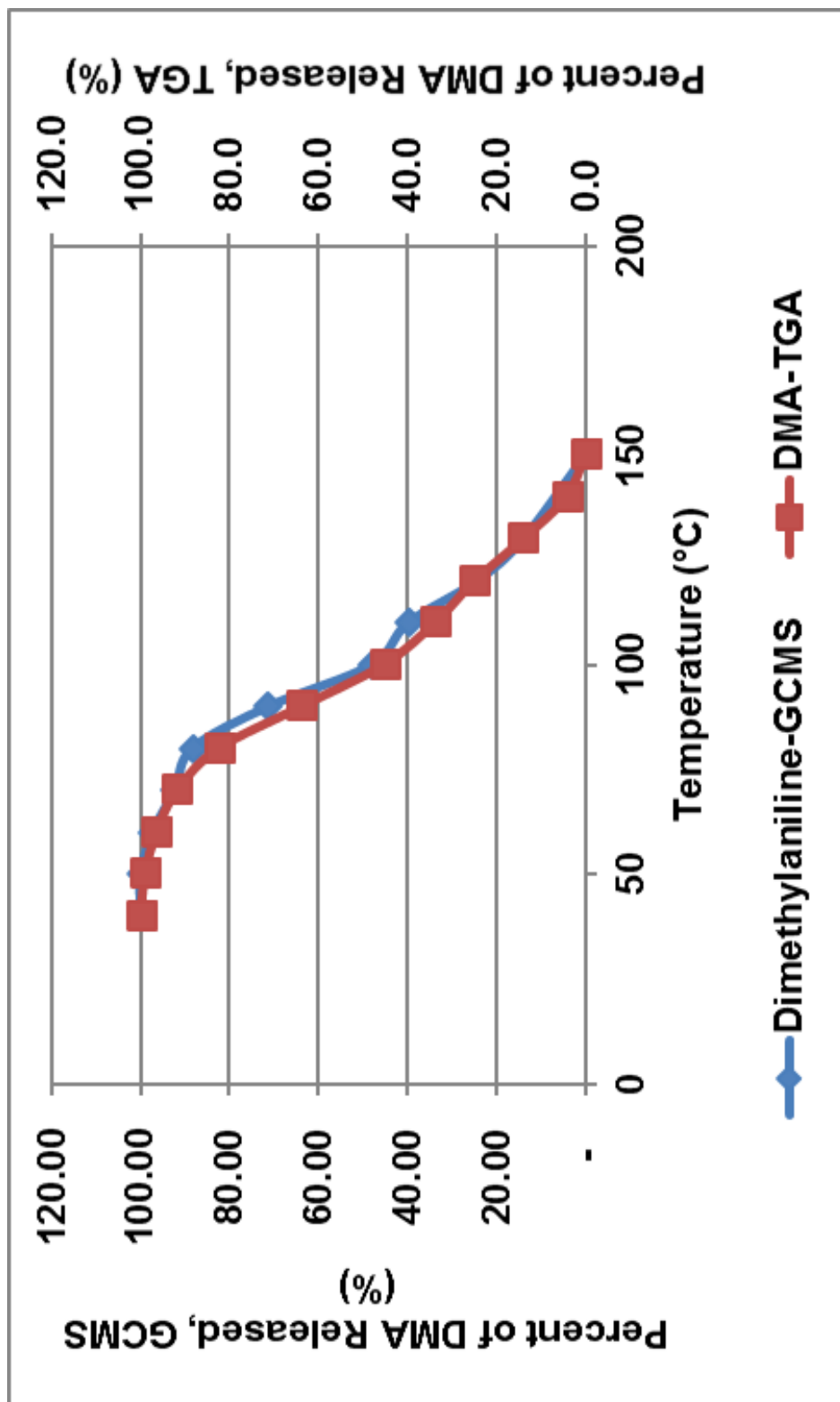


Figure IV.1 Evolution profile of N,N-dimethylaniline from 1•framework, TGA vs GCMS

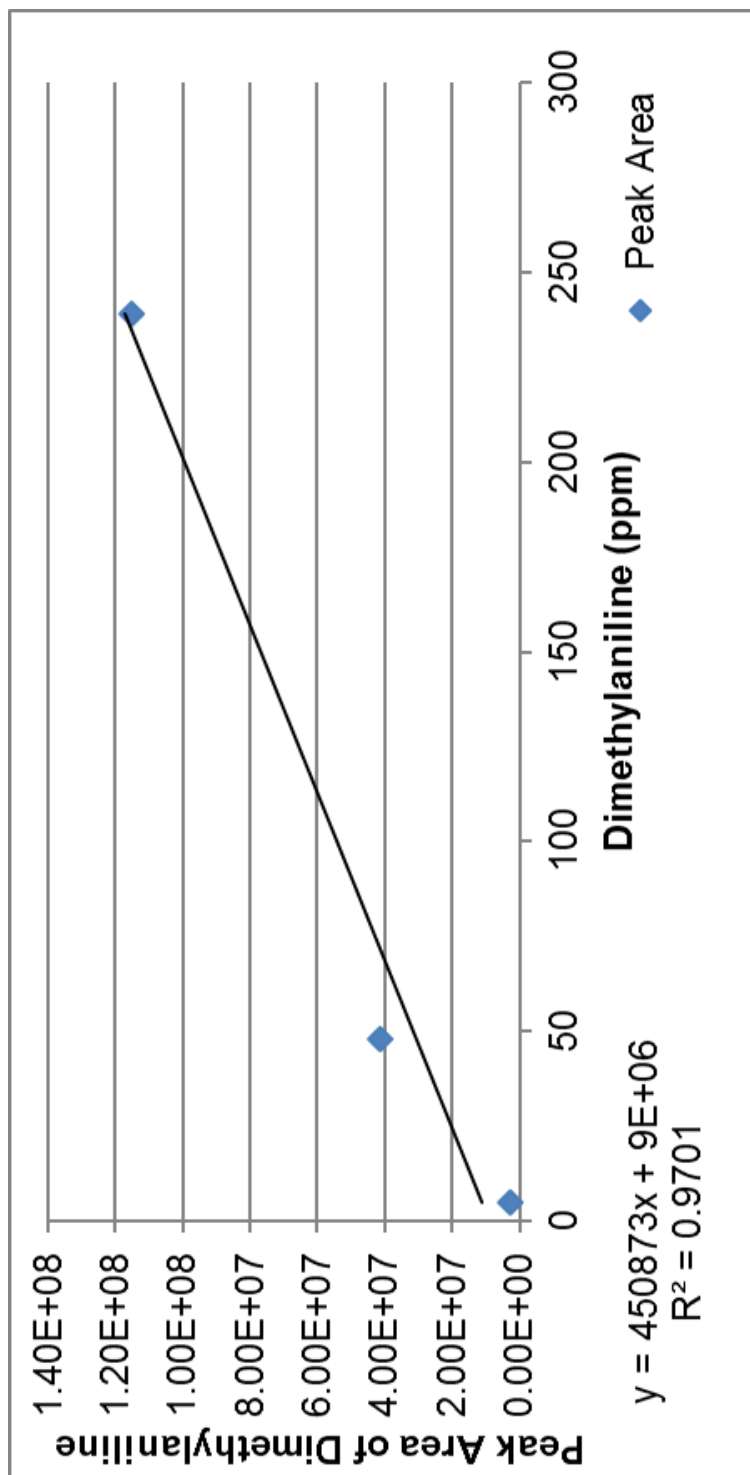


Figure IV.2 Calibration curve for N,N-dimethylaniline

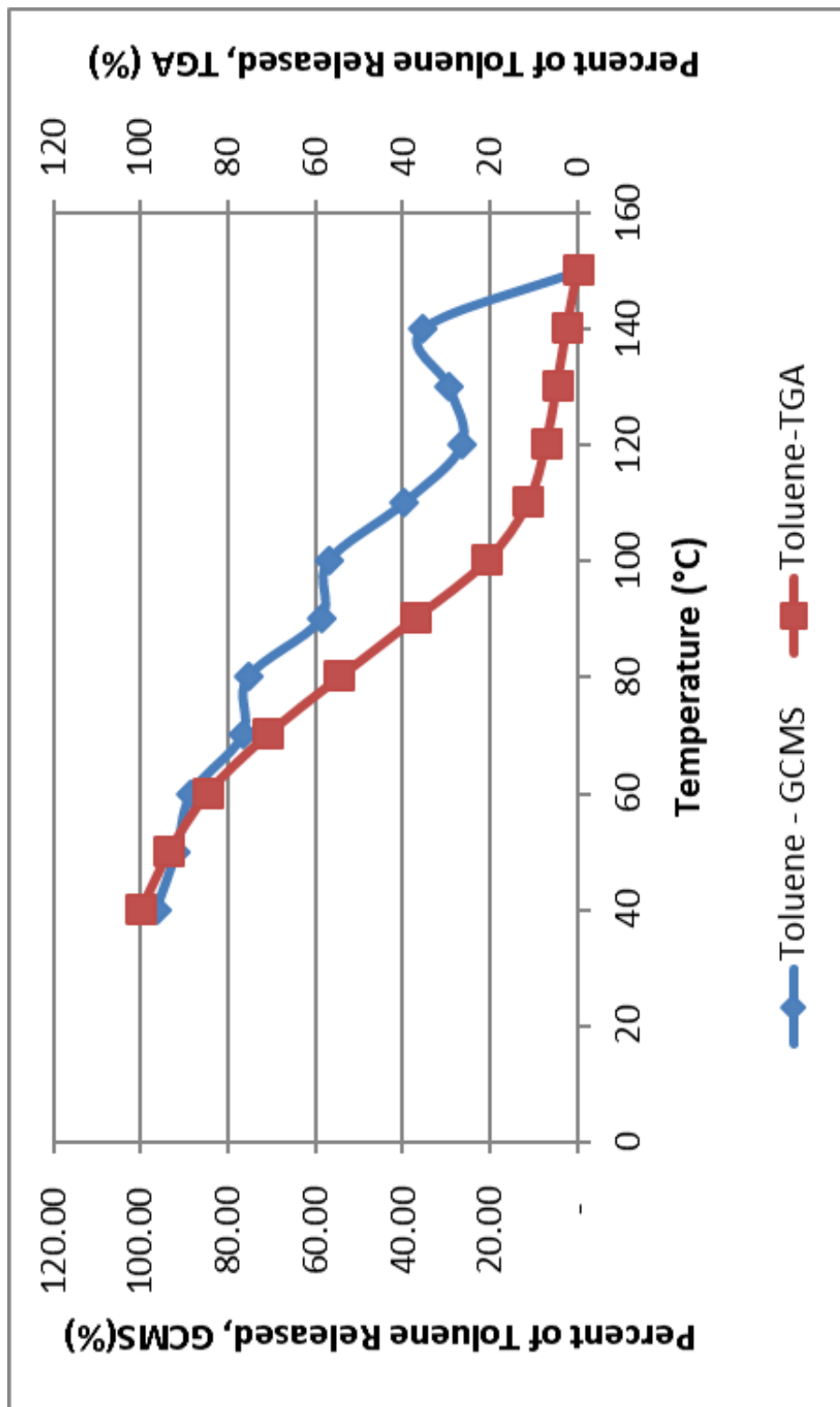


Figure IV.3 Evolution profile of Toluene from 1•framework, TGA vs GCMS

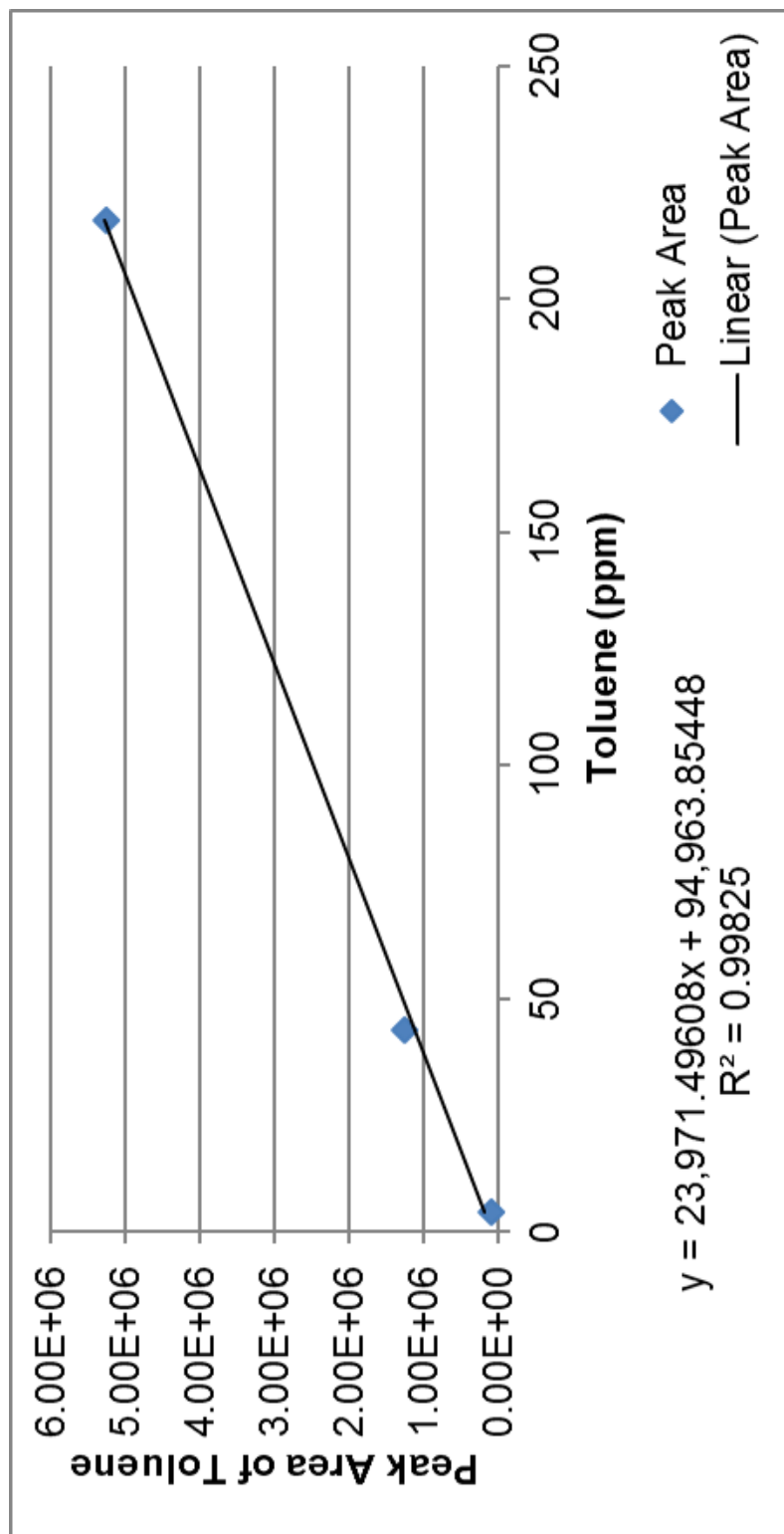


Figure IV.4 Calibration curve for Toluene, GC

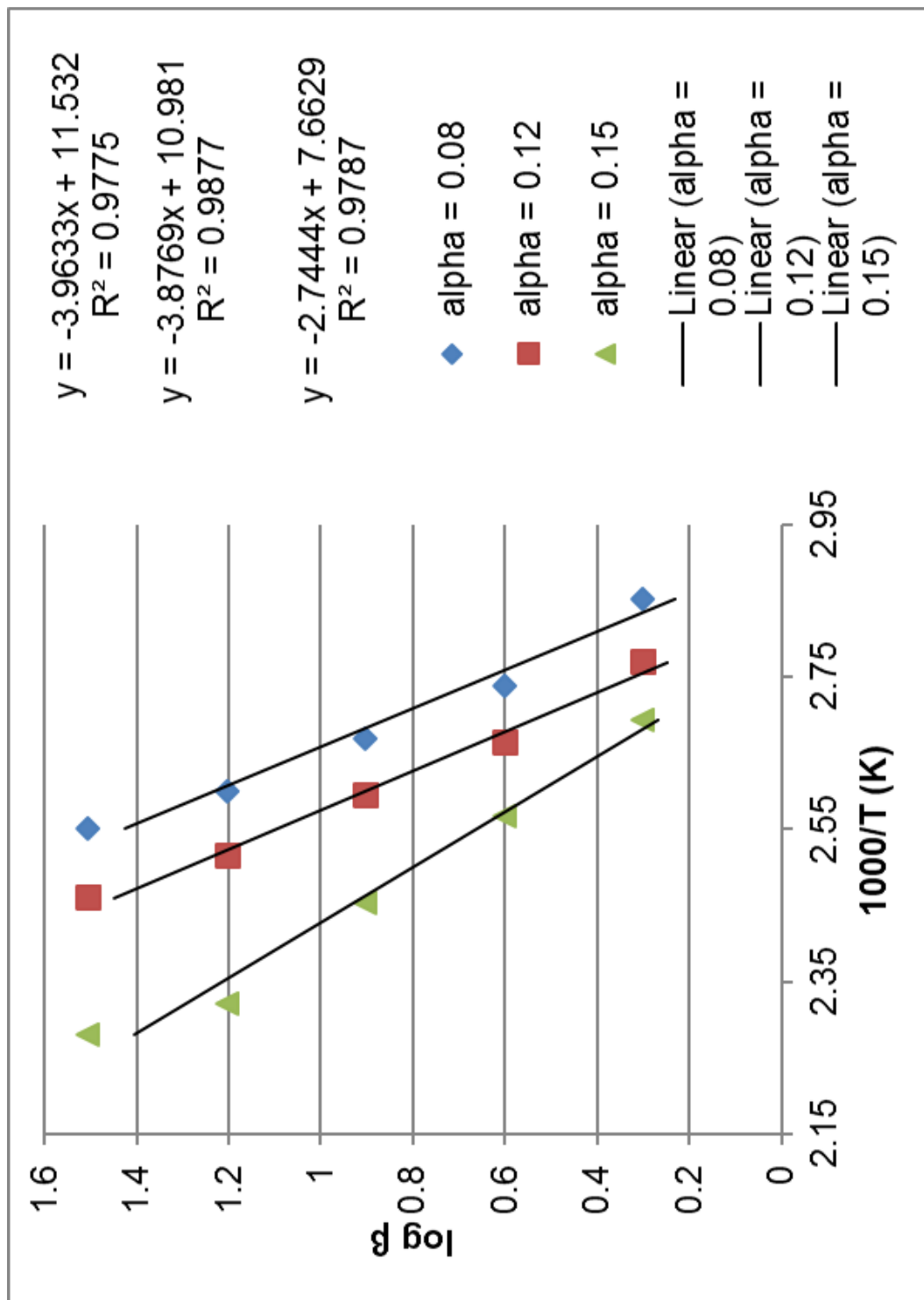


Figure IV.5 Estimate of activation energy for toluene loss, based on TGA using multiple heating rates

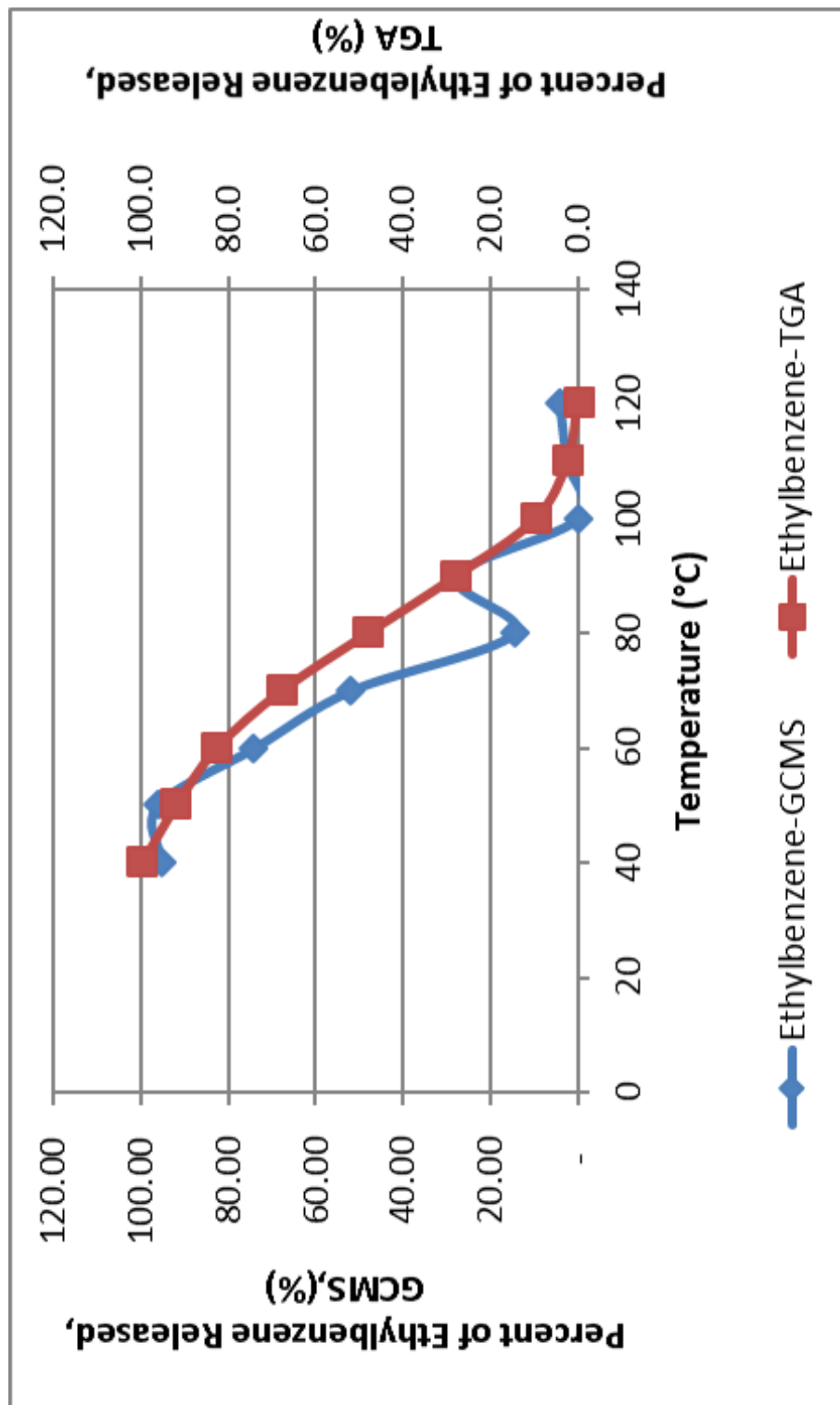


Figure IV.6 Evolution profile of thylbenzene from 1•framework, TGA vs GCMS

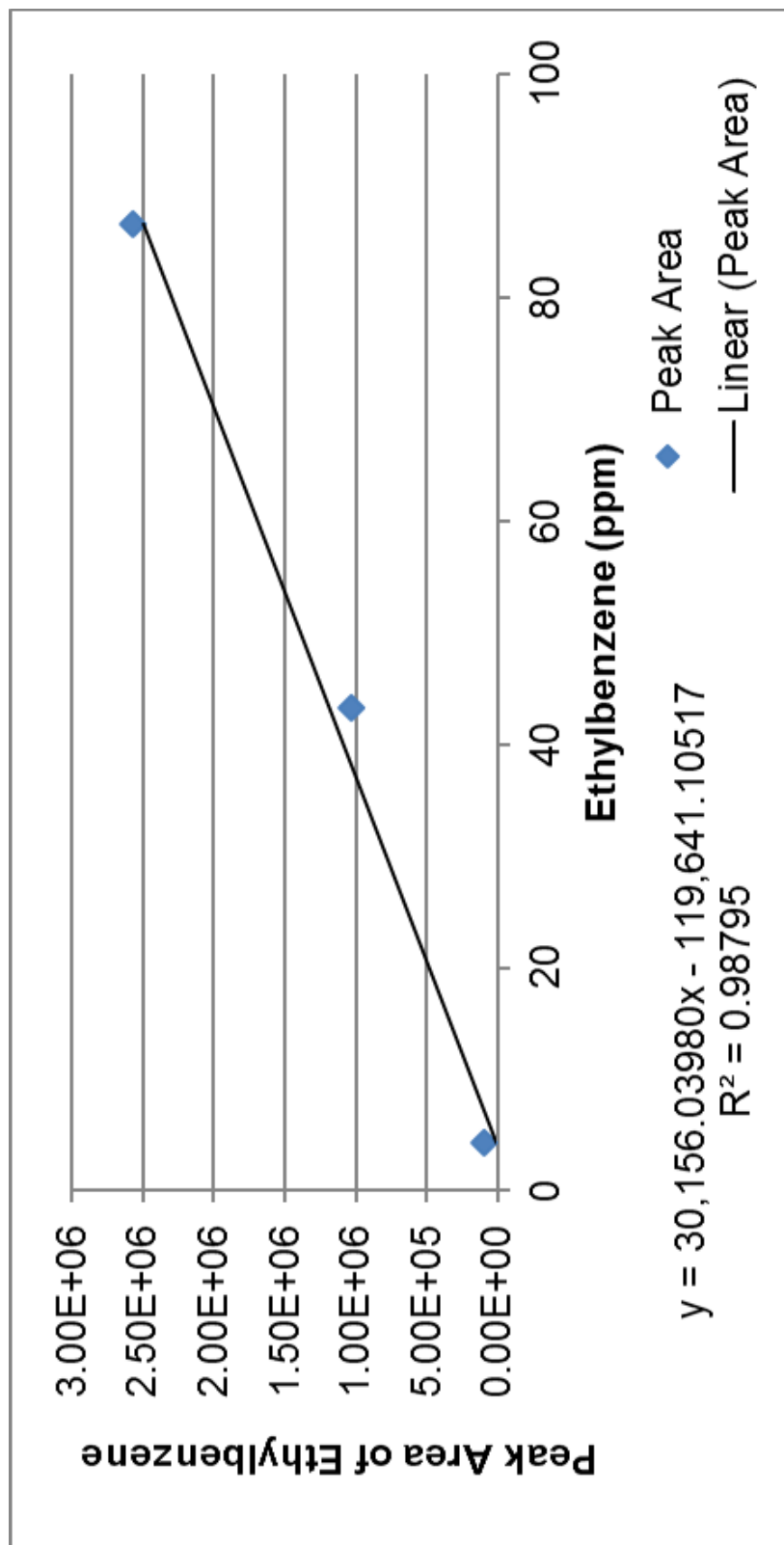


Figure IV.7 Calibration curve for ethylbenzene, GC

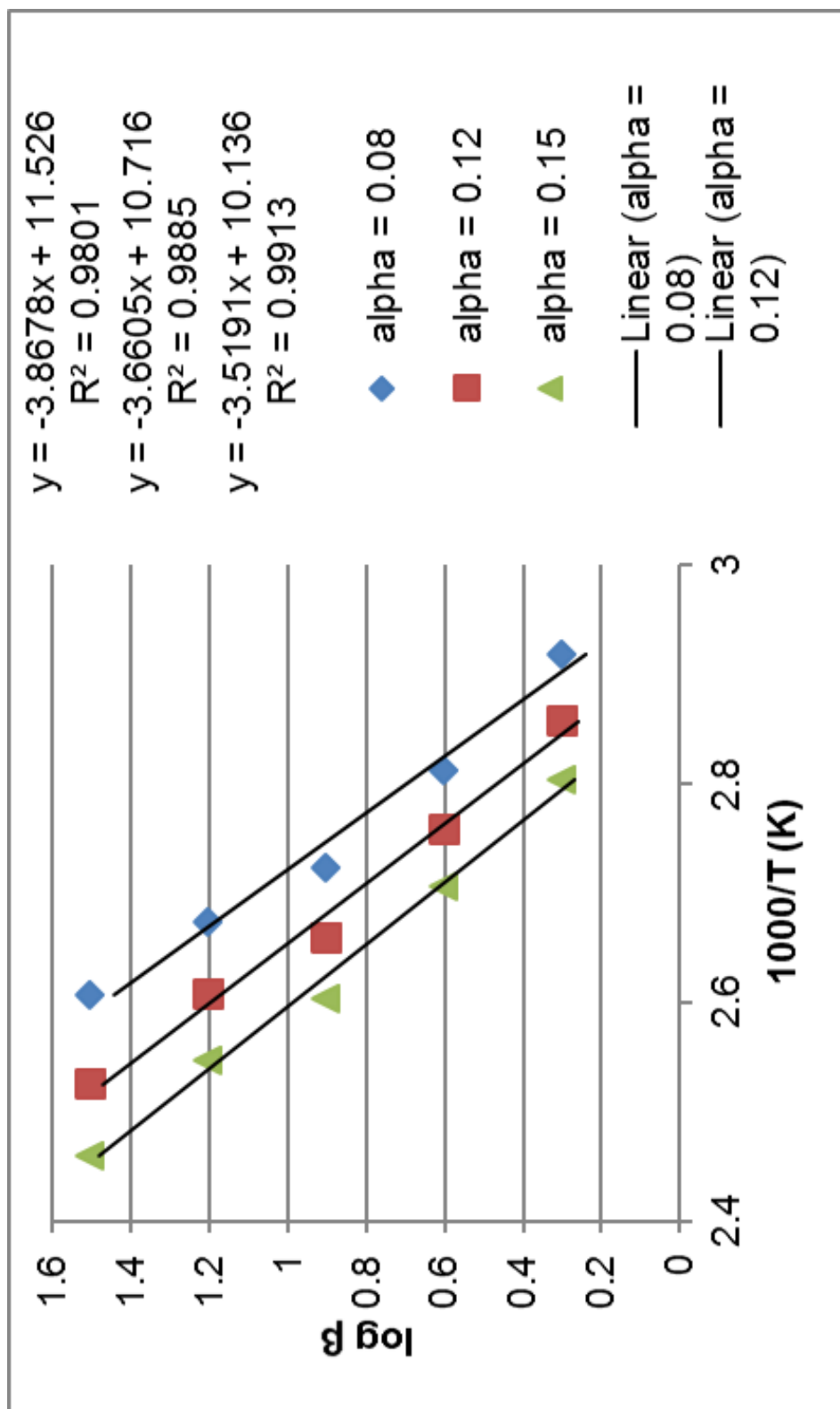


Figure IV.8 Estimate of activation energy for ethylbenzene loss, based on TGA using multiple heating rates

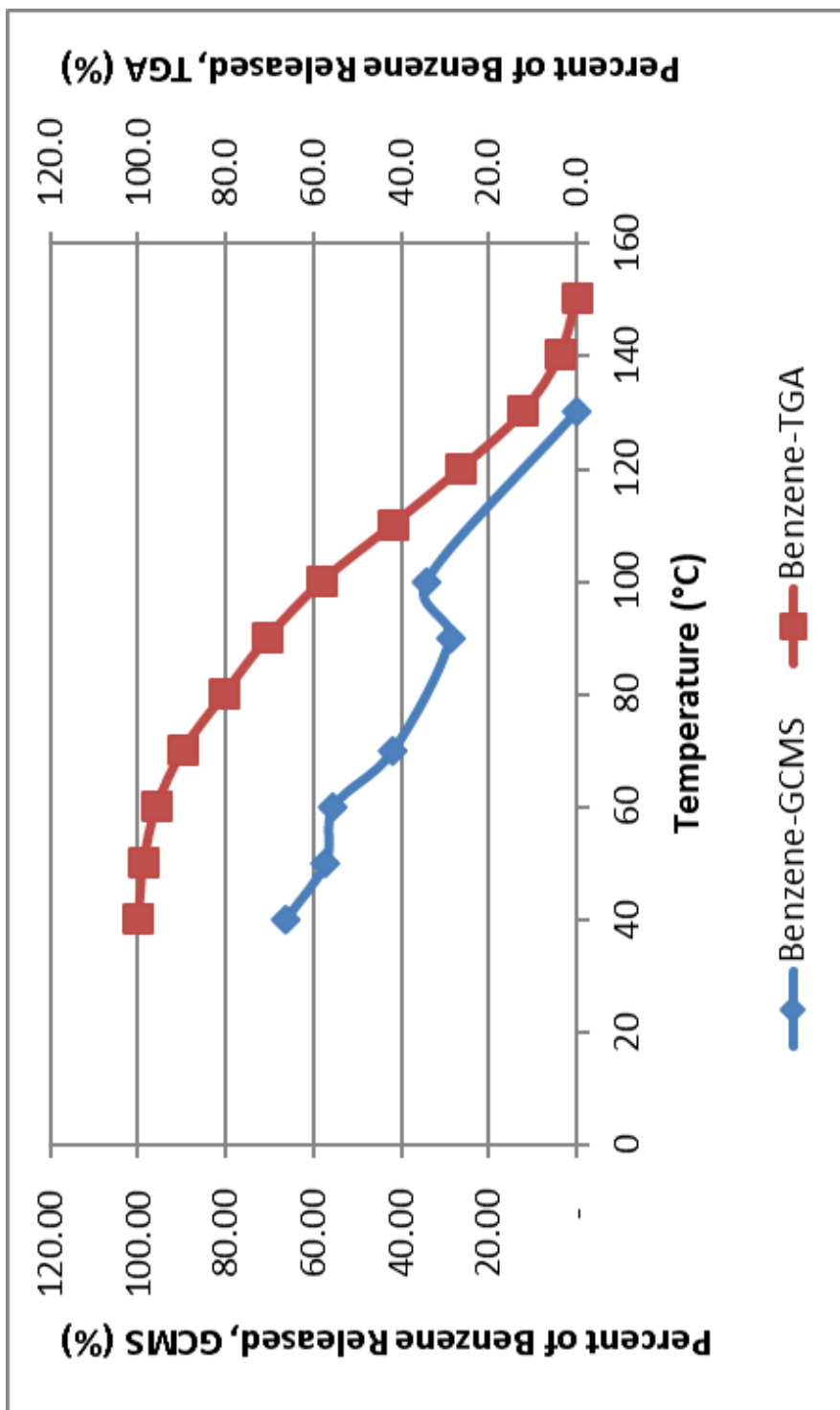


Figure IV.9 Evolution profile of benzene from 1, TGA vs GCMS

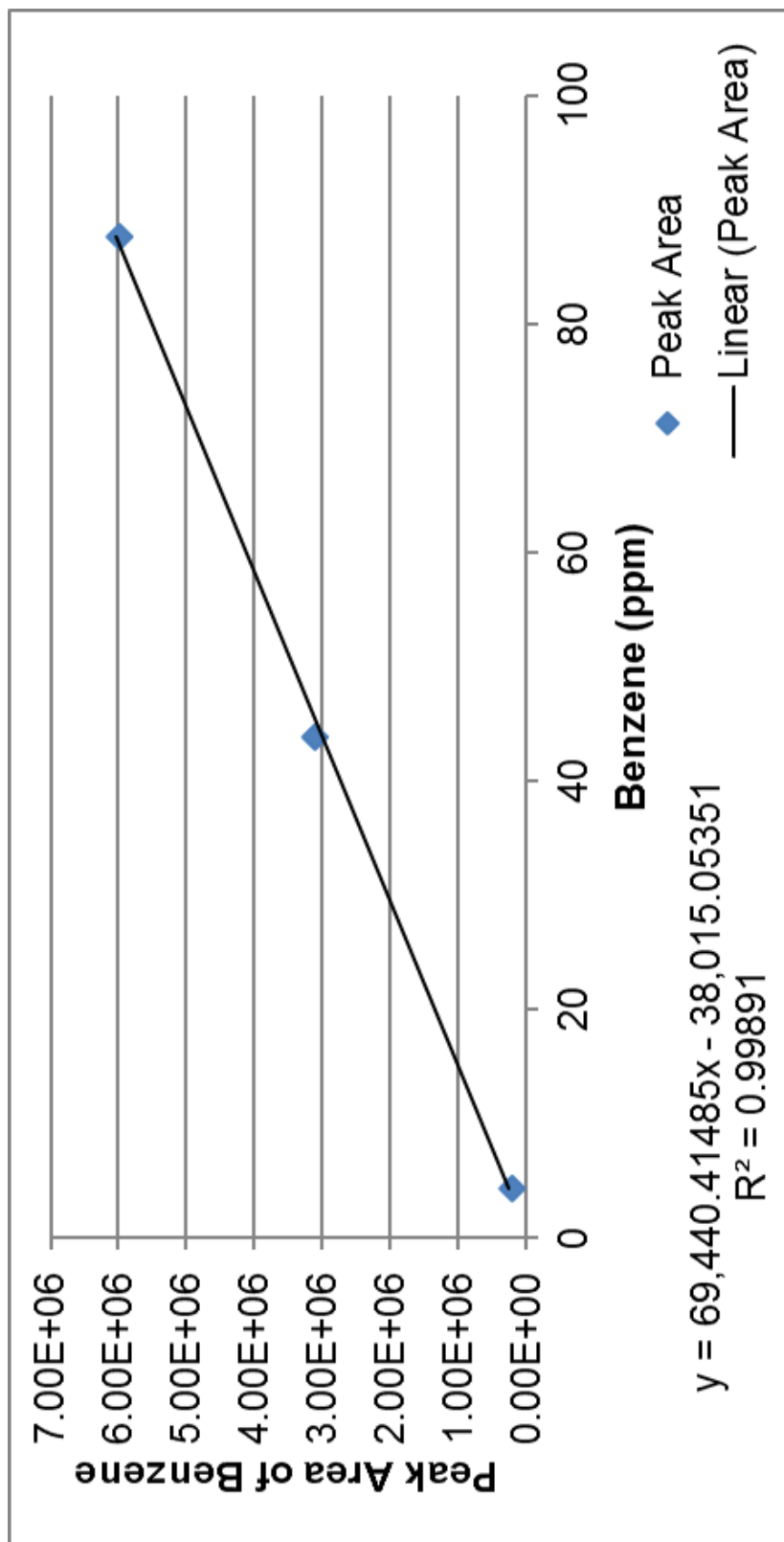


Figure IV.10 Calibration curve for benzene, GC

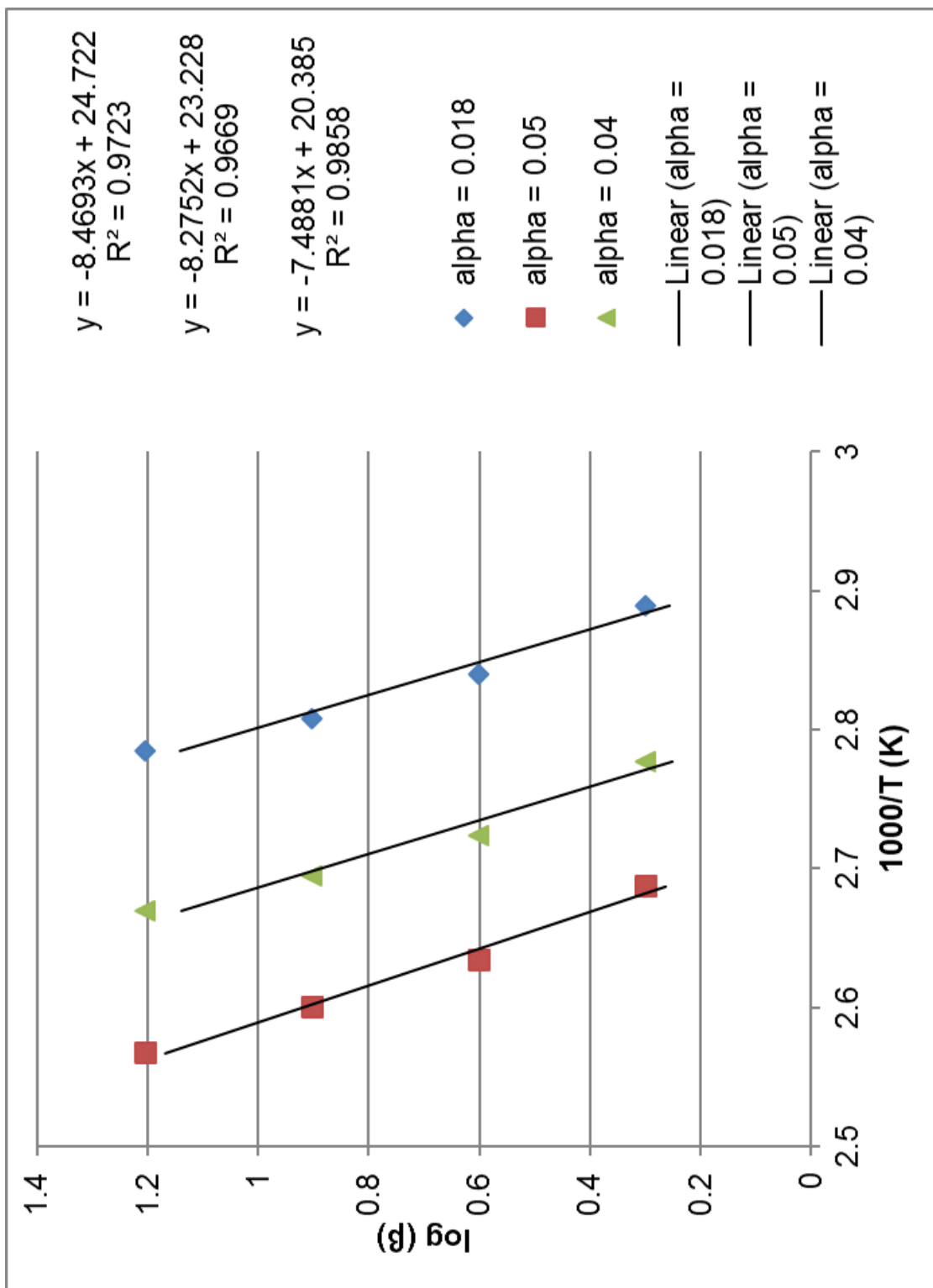


Figure IV.11 Estimate of activation energy for benzene loss, based on TGA using multiple heating rates

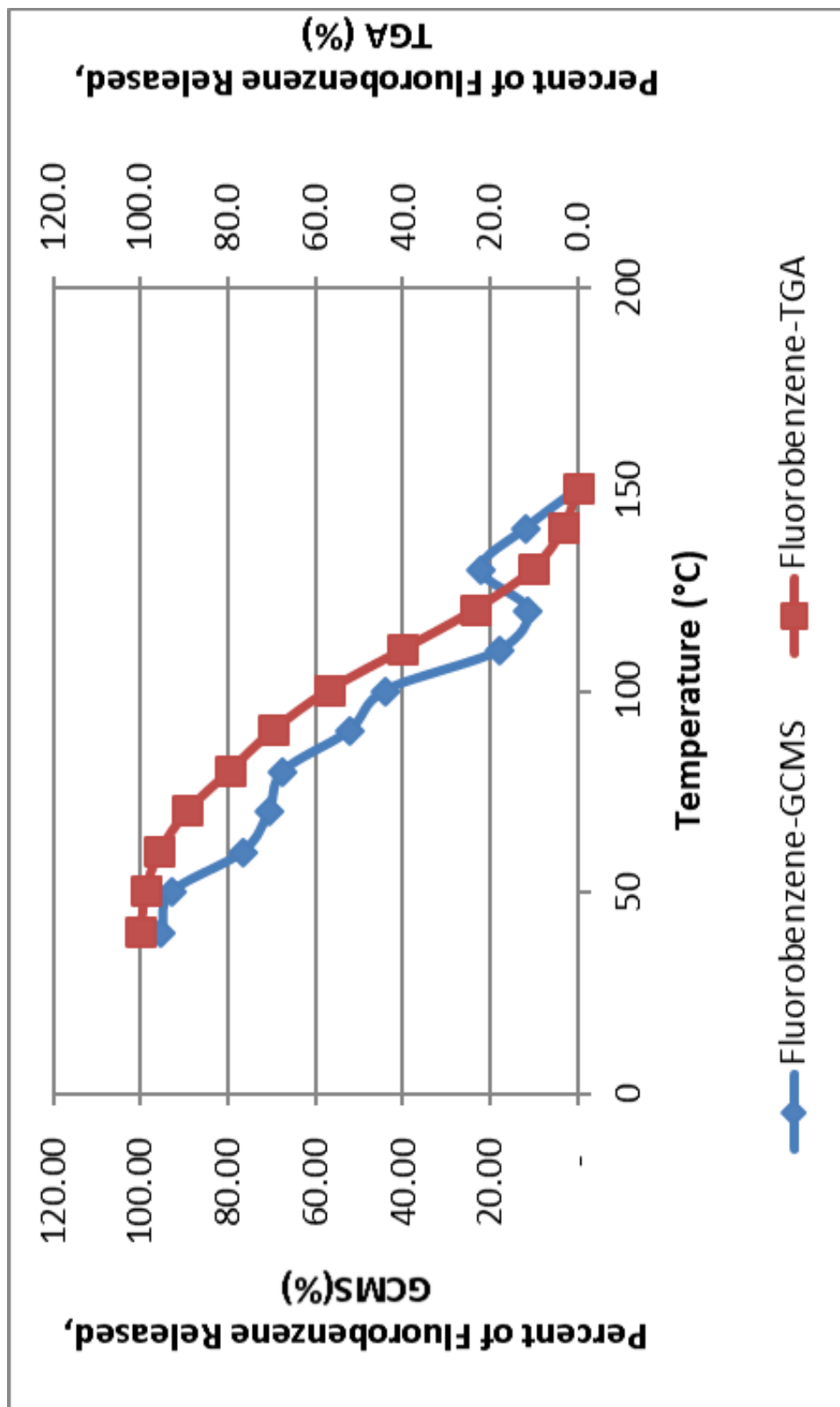


Figure IV.12 Evolution profile of fluorobenzene from 1, TGA vs GCMS

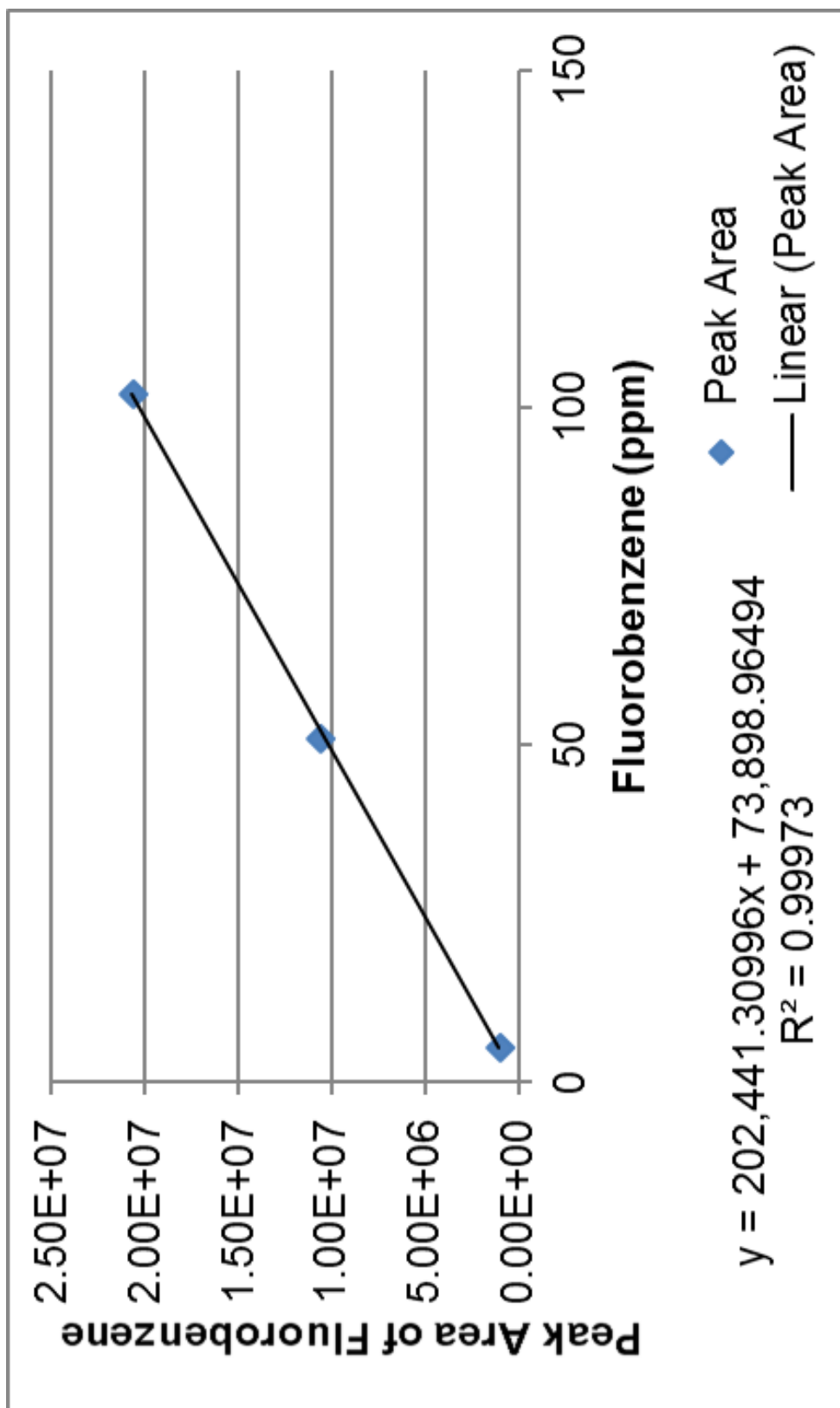


Figure IV.13 Calibration curve for fluorobenzene, GC

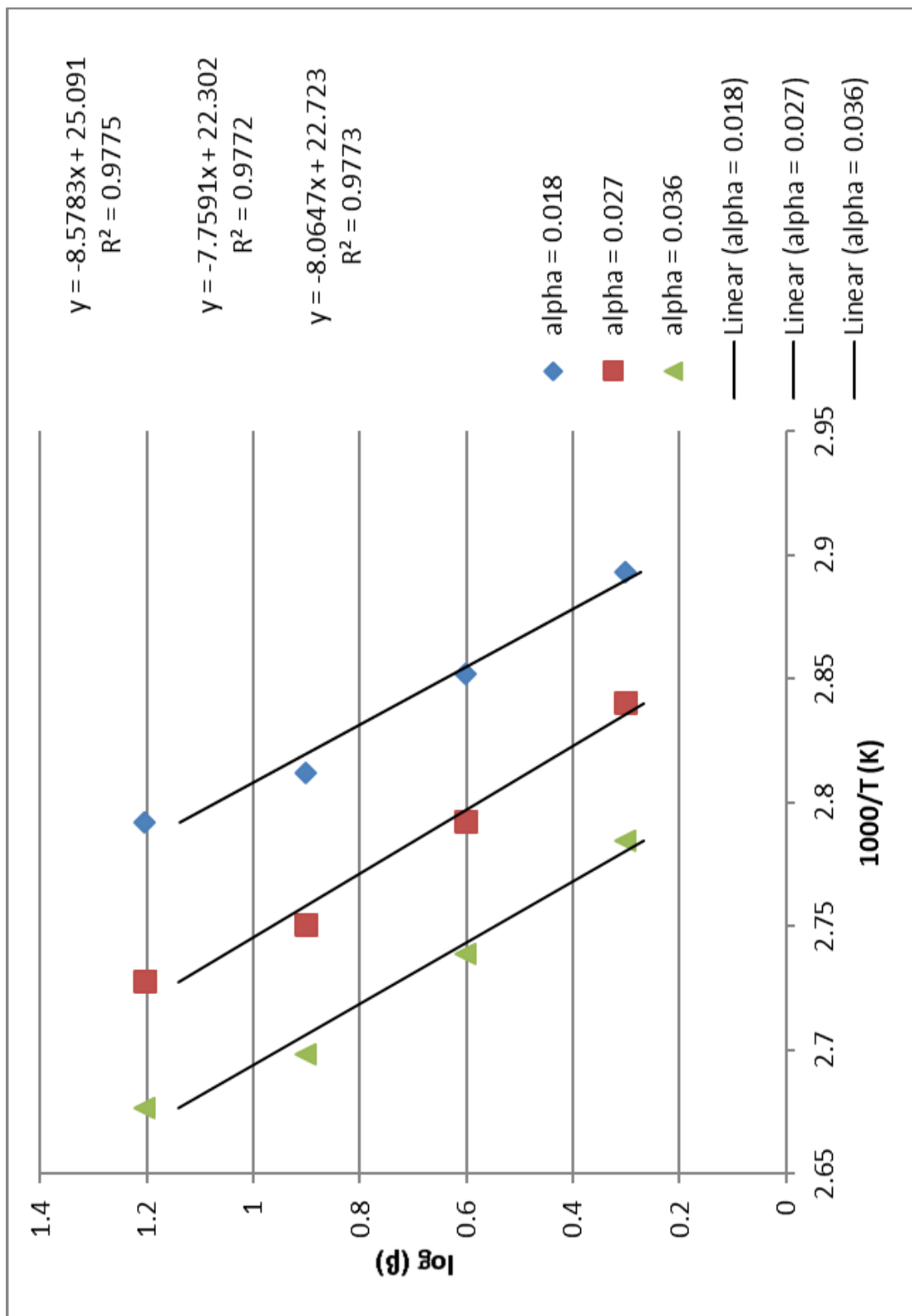


Figure IV.14 Estimate of activation energy for fluorobenzene loss, based on TGA using multiple heating rates

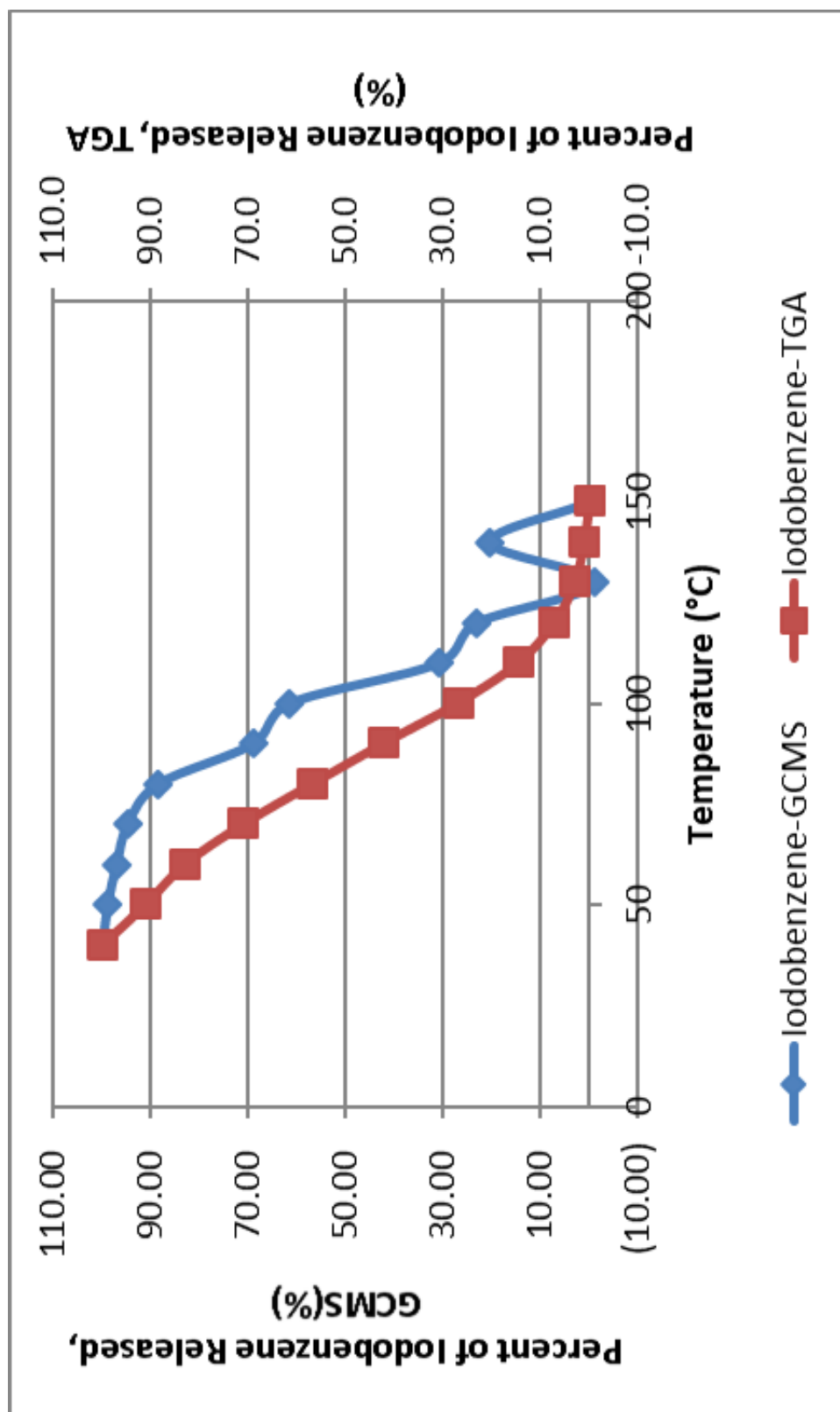


Figure IV.15. Evolution profile of iodobenzene from 1, TGA vs GCMS

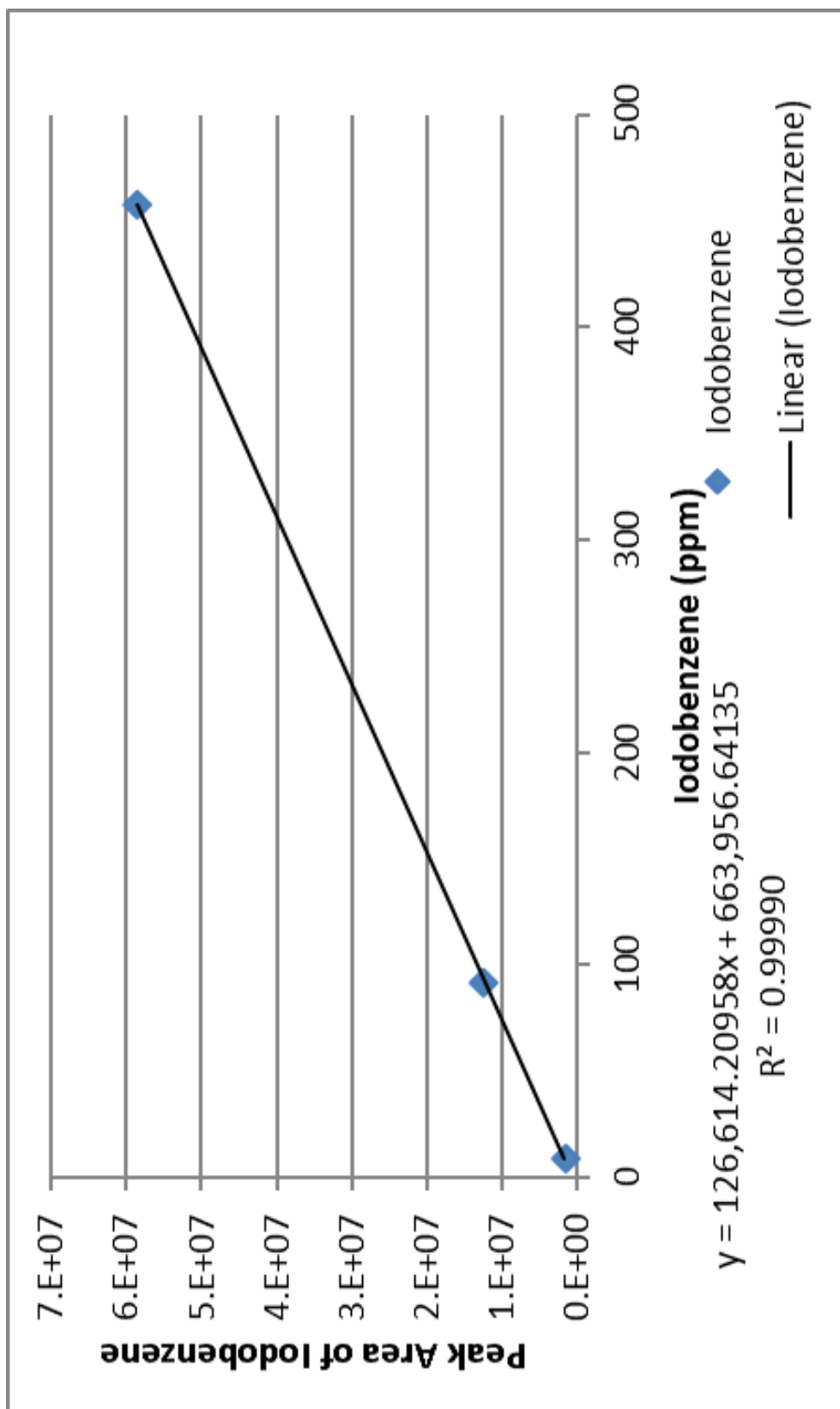


Figure IV.16 Calibration curve for iodobenzene, GC

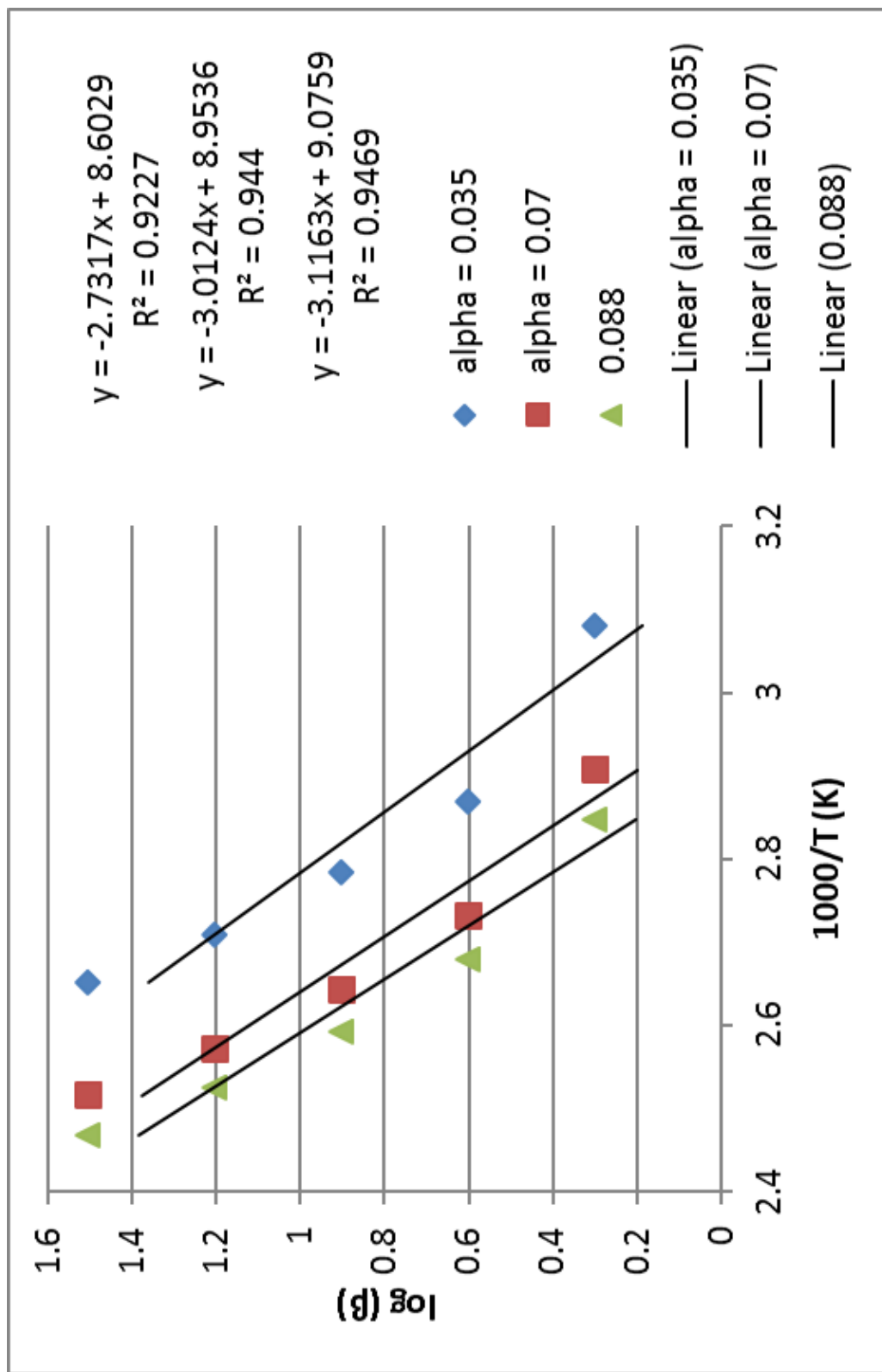


Figure IV.17 Estimate of activation energy for iodobenzene loss, based on TGA using multiple heating rates

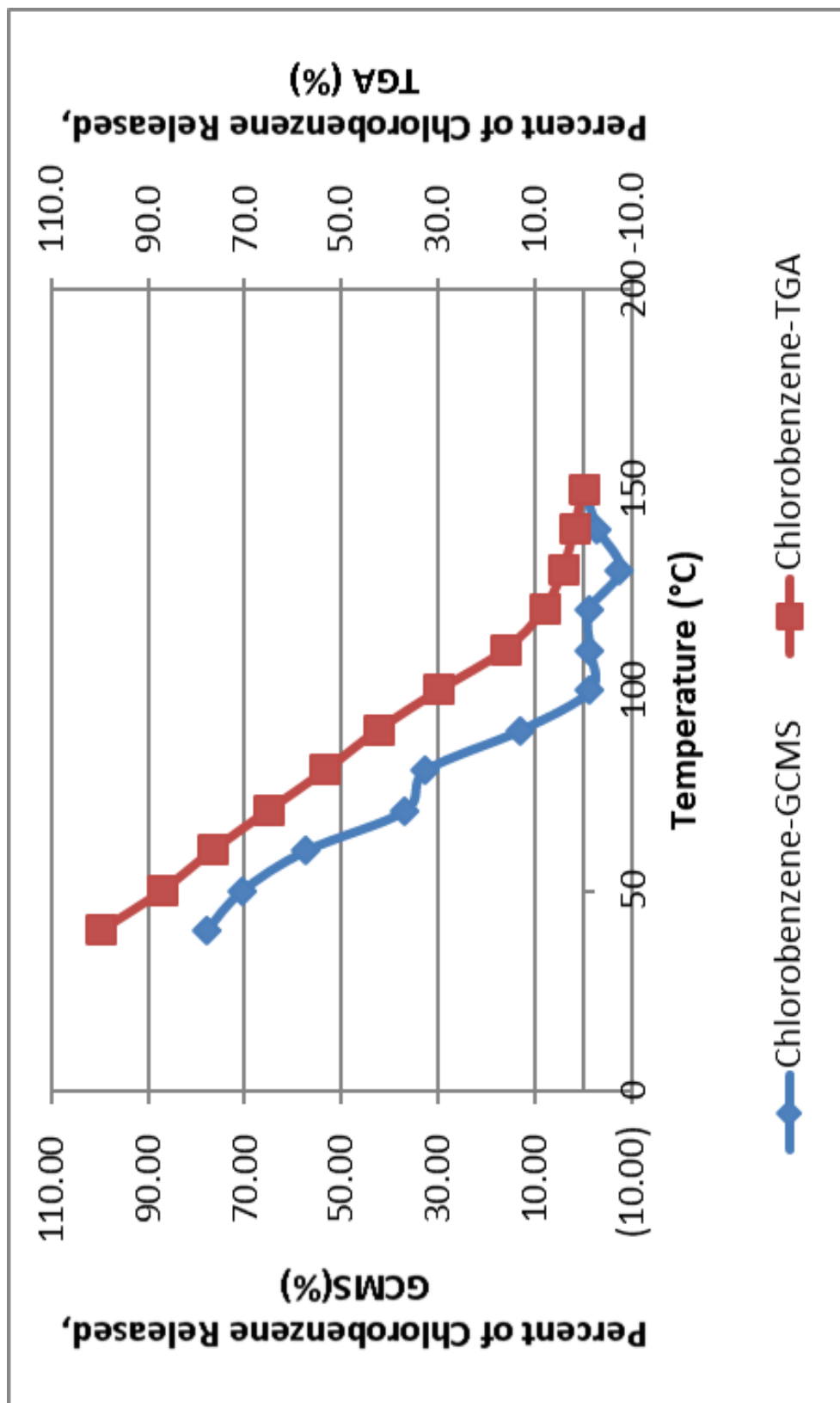


Figure IV.18 Evolution profile of chlorobenzene from 1, TGA vs GCMS

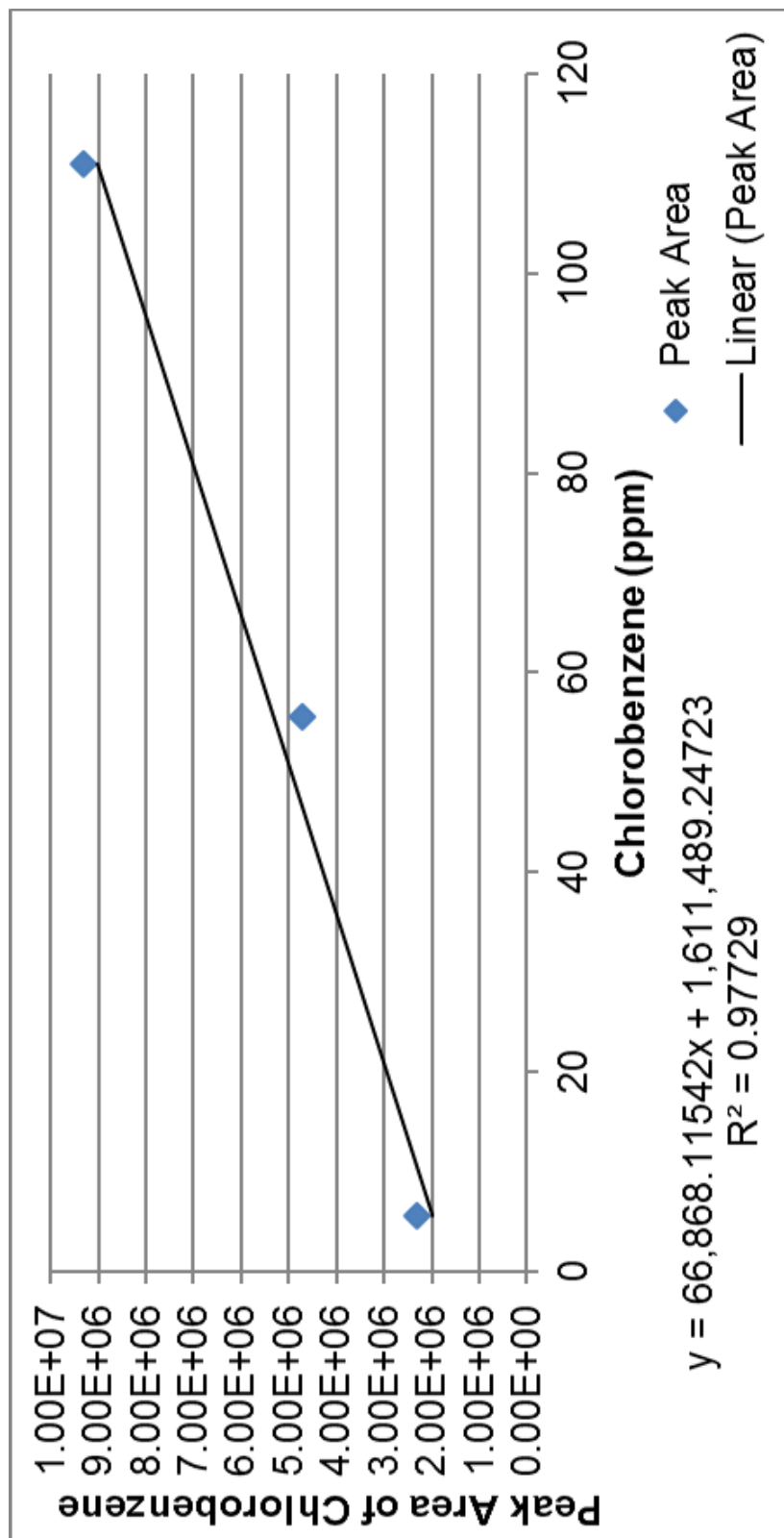


Figure IV.19 Calibration curve for chlorobenzene, GC

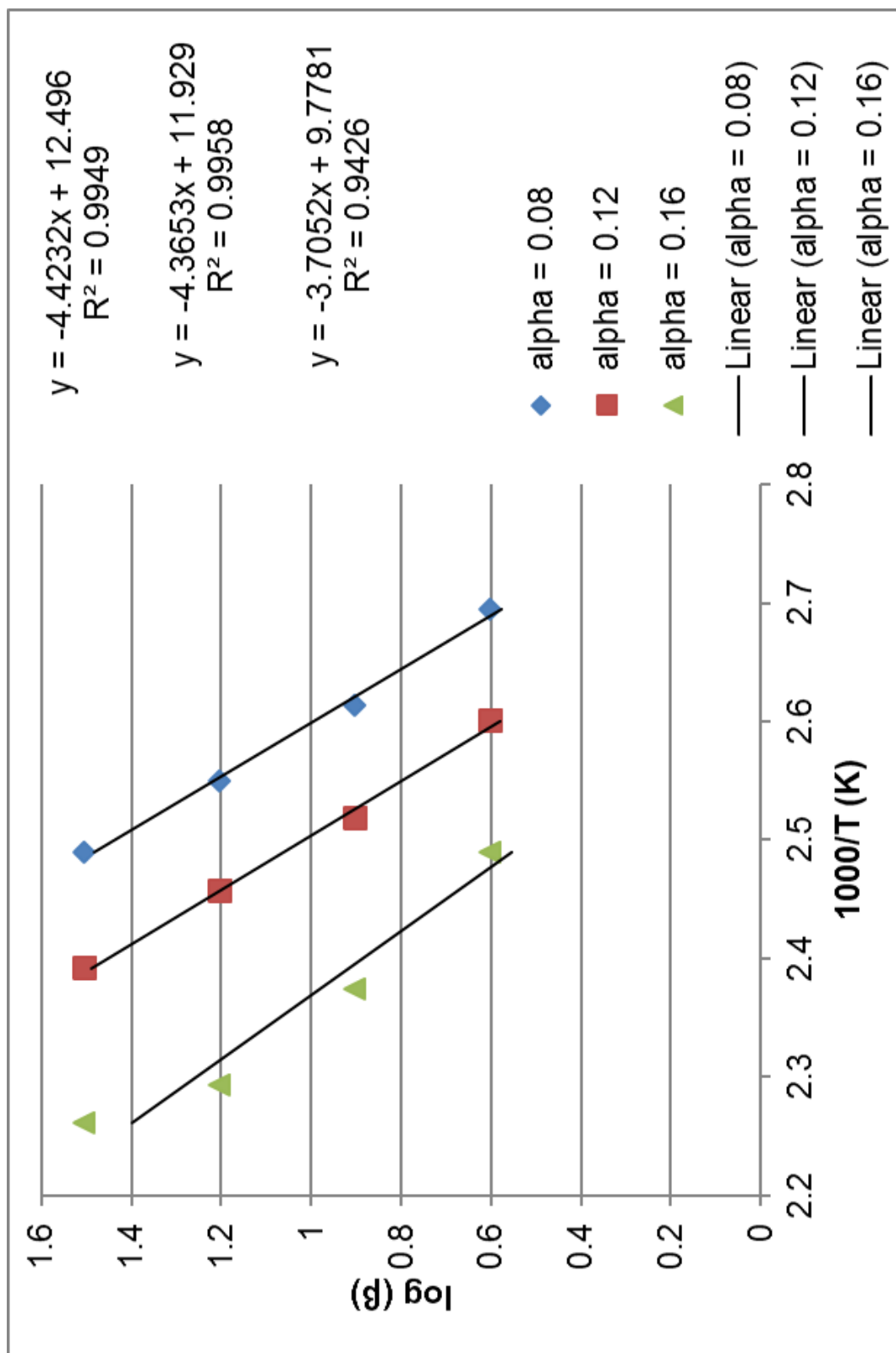


Figure IV.20 Estimate of activation energy for chlorobenzene loss, based on TGA using multiple heating rates

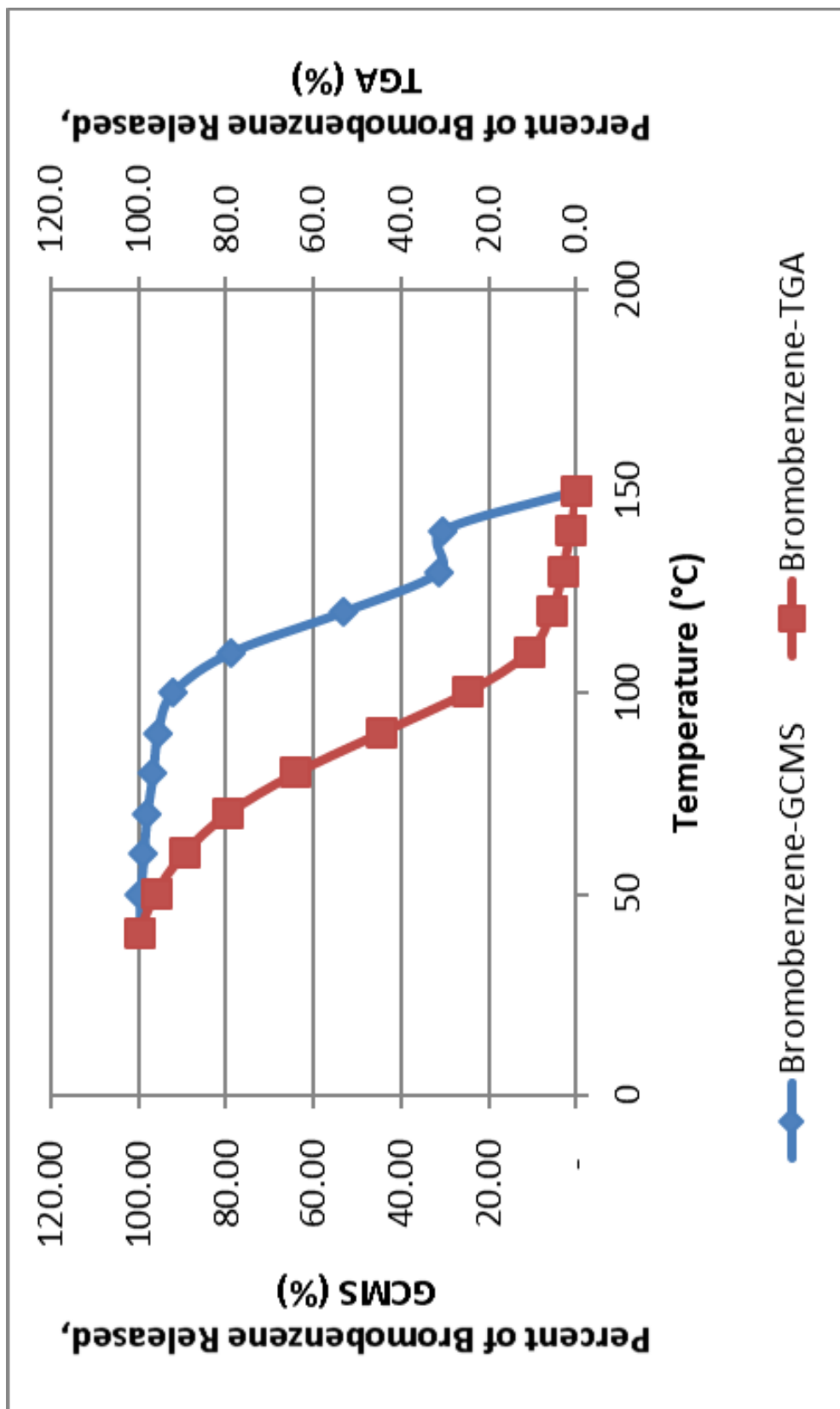


Figure IV.21 Evolution profile of bromobenzene from 1, TGA vs GCMS

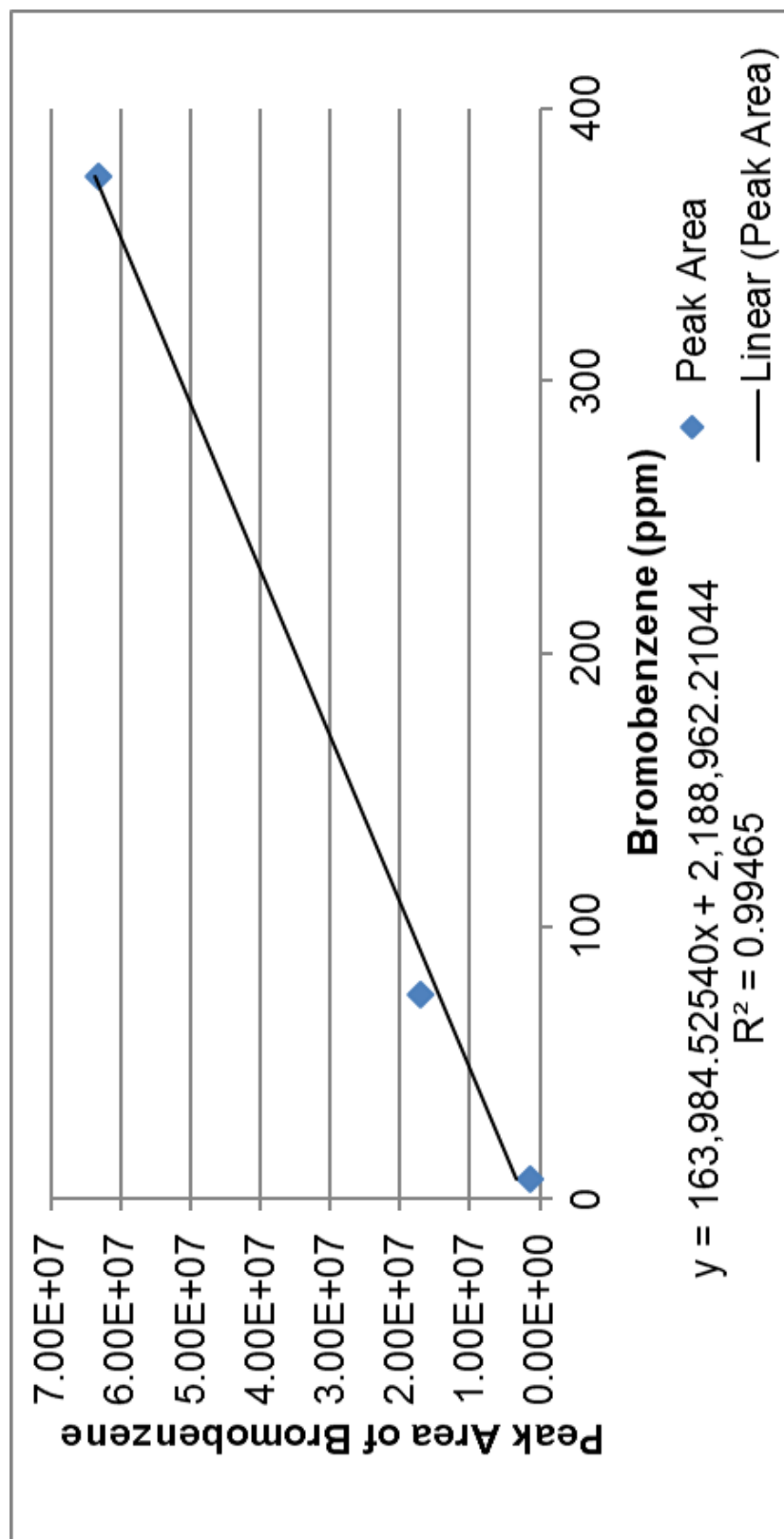


Figure IV.22 Calibration curve for bromobenzene, GC

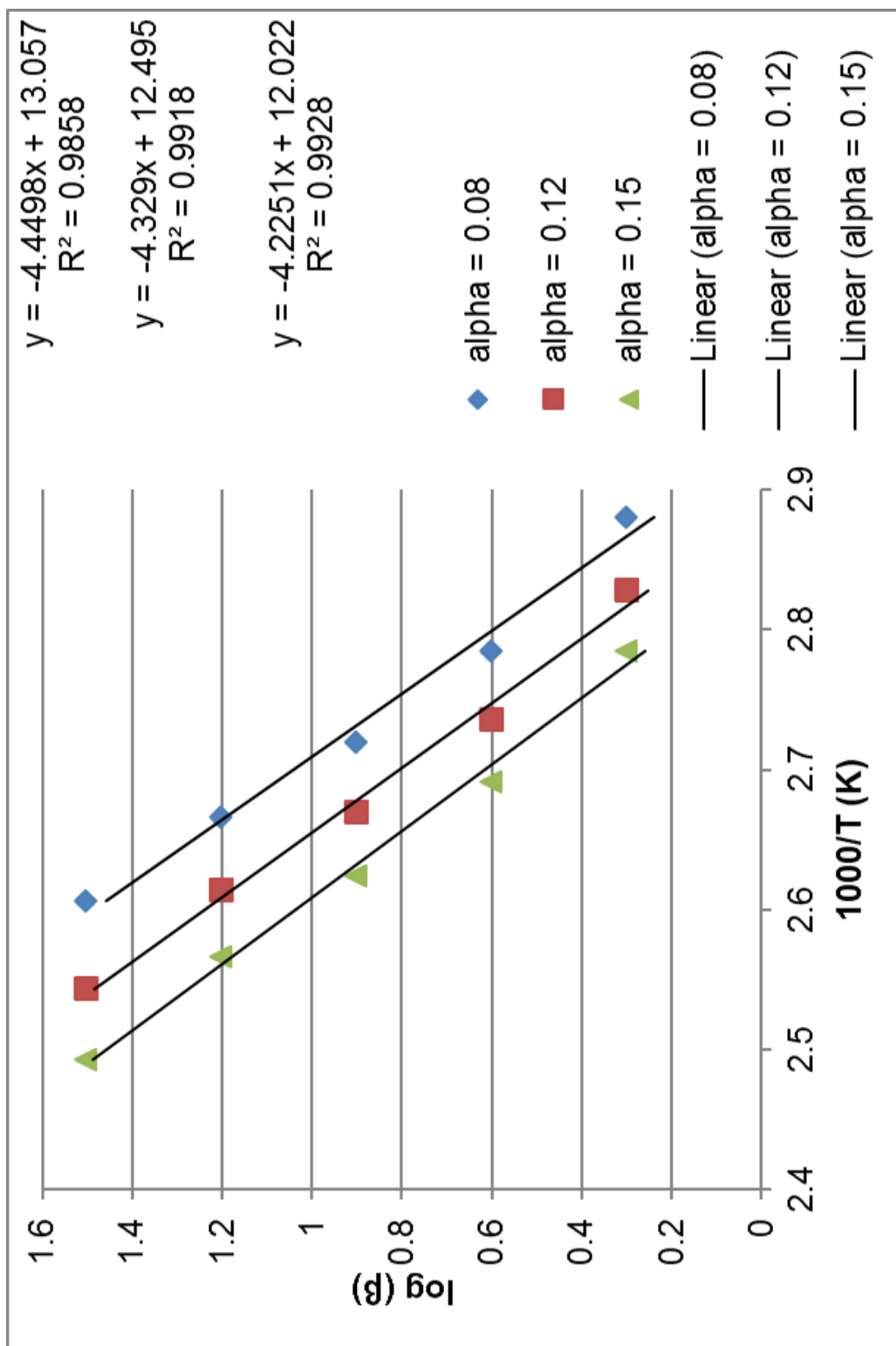


Figure IV.23 Estimate of activation energy for bromobenzene loss, based on TGA using multiple heating rates

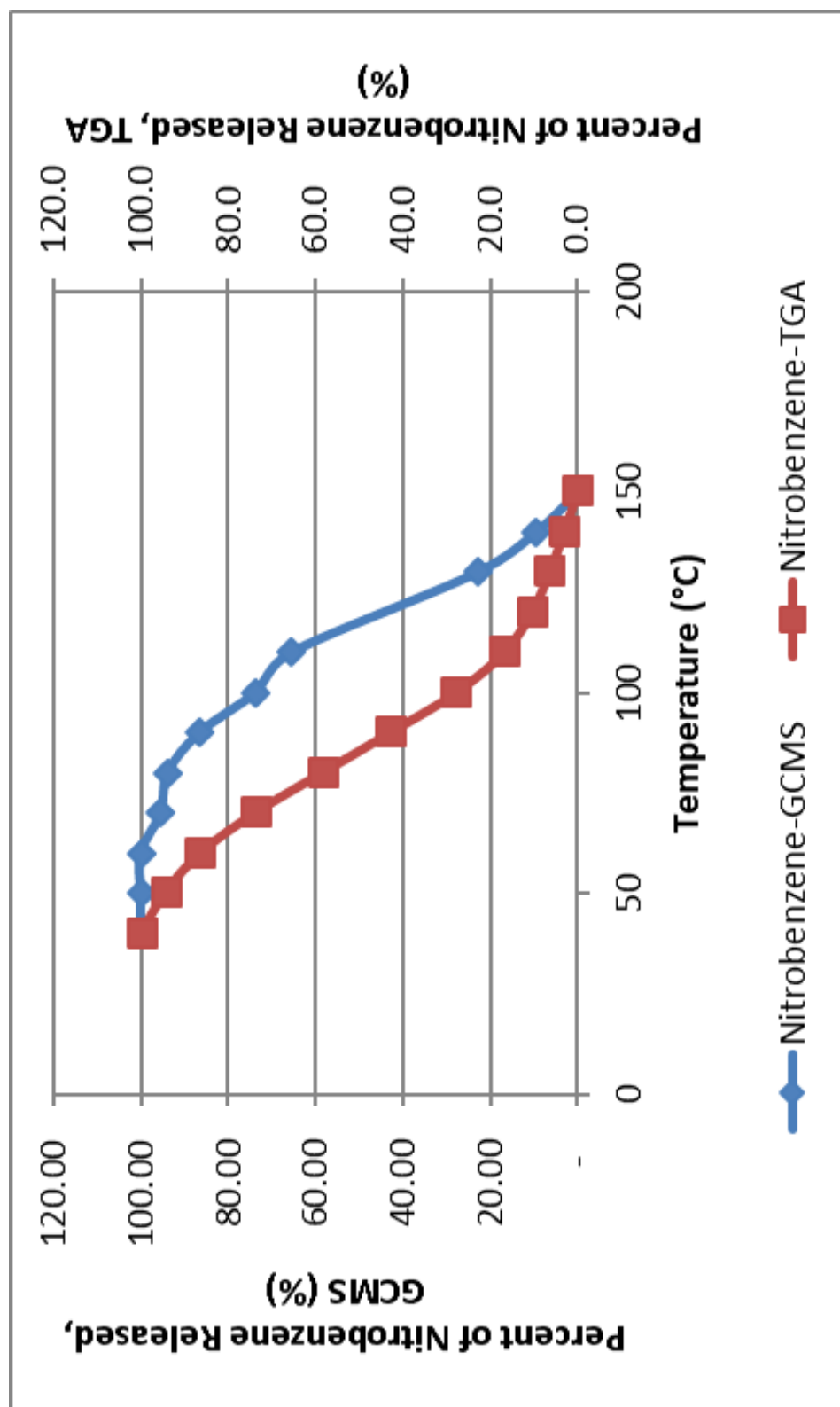


Figure IV.24. Evolution profile of nitrobenzene from 1, TGA vs GCMS

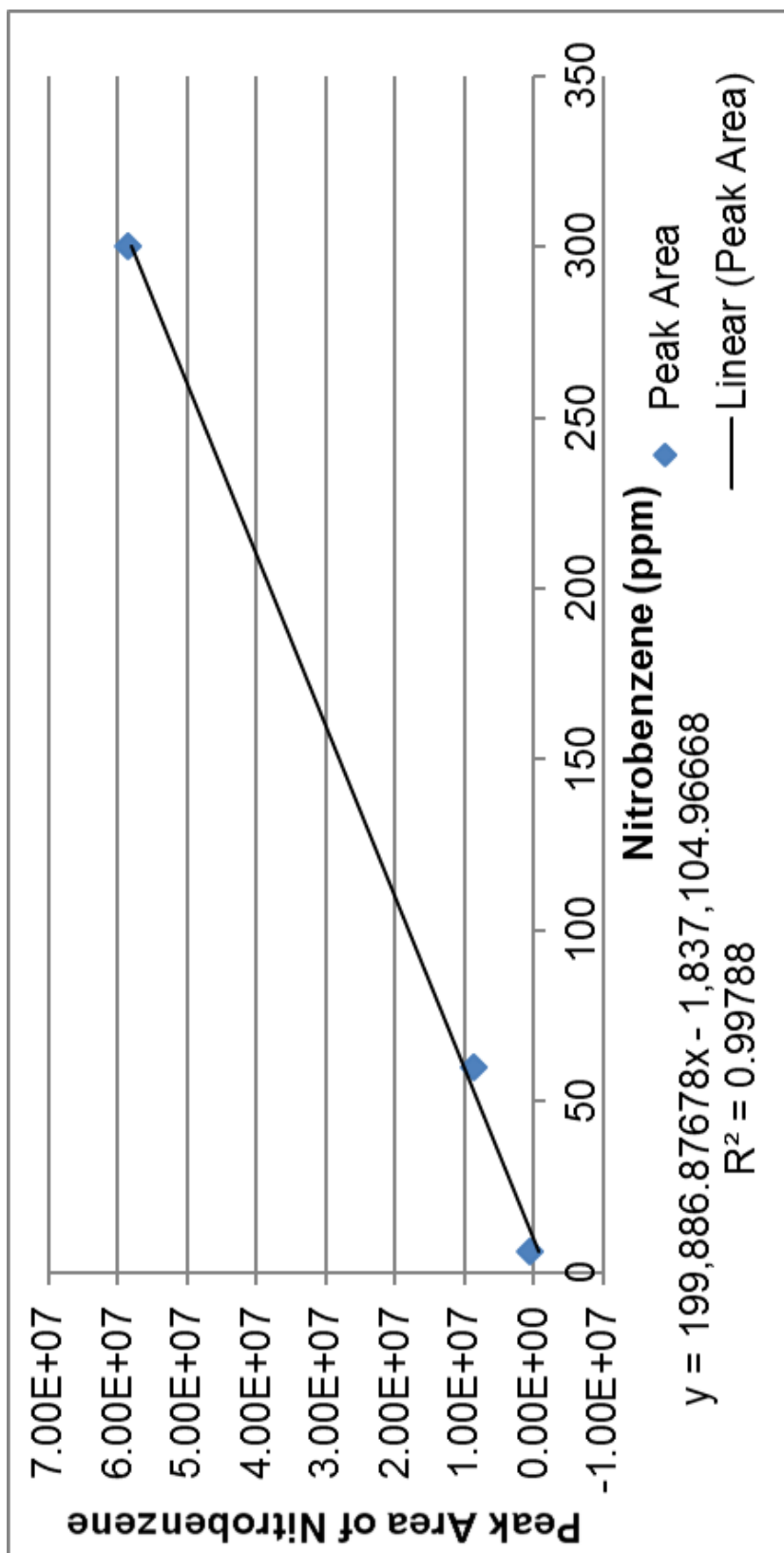


Figure IV.25 Calibration curve for nitrobenzene, GC

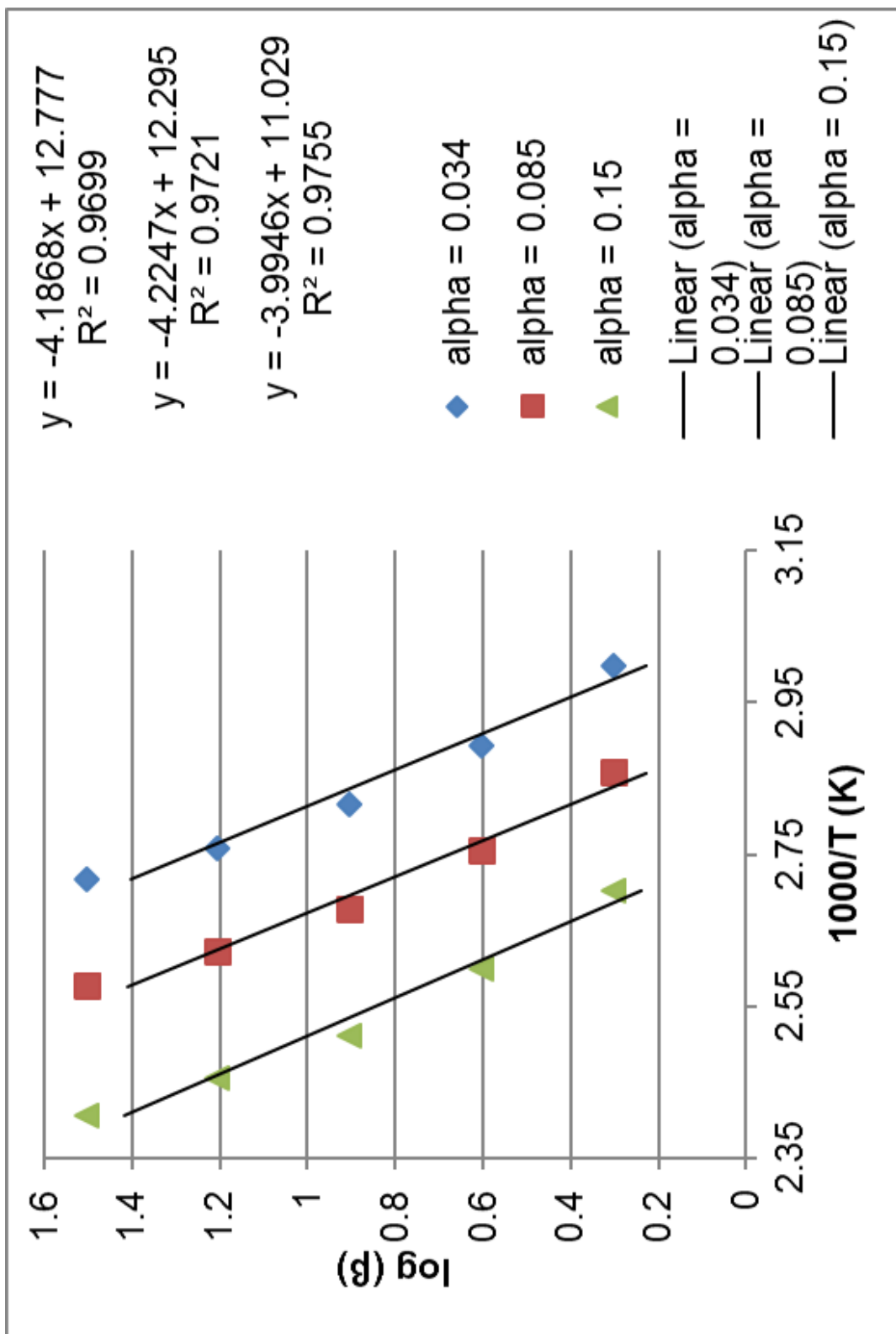


Figure IV.26 Estimate of activation energy for nitrobenzene loss, based on TGA using multiple heating rates